

3. Mode Functions in Closed and Open Waveguides

3.1 INTRODUCTION

By the modal analysis and synthesis procedure of Chapter 2, electromagnetic fields in isotropically filled uniform waveguide regions are representable as superpositions of modal fields. The latter have z -dependent amplitudes described by transmission-line voltages and currents, and transverse vector characteristics determined by the shape of the guide cross section. Solutions of the transmission-line equations in media piecewise homogeneous along the waveguide axis z have been given in Sec. 2.4, and their network interpretation has been emphasized. The present chapter deals with evaluation of the transverse vector eigenfunction characteristics. As noted in Sec. 2.3a, the solution of the vector eigenvalue problem is facilitated by introduction of scalar eigenfunctions satisfying appropriate scalar eigenvalue problems in the cross-sectional domain. This scalarization, equivalent to a field decomposition into E and H modes, is possible for homogeneously filled cross sections but fails when the medium properties depend on the cross-sectional vector coordinate, p . Nevertheless, for p -dependent medium parameters, the vector-field problem may still be scalarized if the waveguide region admits a transmission-line analysis along one of the transverse coordinates. This procedure is illustrated in Sec. 3.2d. Section 3.2d also contains a generalized derivation of the transverse field equations and modal representations of the electromagnetic field in transversely *inhomogeneous* regions.

Scalarization permits evaluation of vector-mode functions by solution of scalar eigenvalue problems in the transverse domain.[†] Little analytical progress

[†]It should be emphasized that scalarization is automatic in an acoustic field whose properties are derivable from a scalar pressure p . While solutions of scalar eigenvalue problems in this chapter are phrased in electromagnetic terms, they are applicable to the acoustic field on simple reinterpretation of relevant variables.

can be made unless the geometry is separable, in which event a two-dimensional eigenvalue problem can be reduced to two one-dimensional problems. Treatment of the one-dimensional case is thus of fundamental importance and is of primary concern in this chapter. The relevant eigenvalue equation is of the Sturm-Liouville type and exhibits certain general features that are reviewed in Sec. 3.2a. Eigenfunctions for closed and open regions describable in rectangular and circular cylindrical coordinates are derived in Secs. 3.2b and 3.2c by classical techniques, and orthonormality and completeness are expressed succinctly by spectral representations of the (unit operator) delta function $\delta(\rho - \rho')$. Anticipating subsequent function-theoretic applications to the construction of alternative field representations, some attention is given in Secs 3.2b and 3.2c to analytic continuation of modal representations into the complex plane of the spectral variable.

The classical procedure for solving eigenvalue problems leads to difficulties in open regions (one or both domain endpoints at infinity) since the mode spectra may then be continuous and the eigenfunctions improper. To normalize the mode set under these circumstances, one may pass to the infinite limit from an originally bounded domain, as illustrated in Secs. 3.2b and 3.2c for rectangular and circular geometries, respectively. A more powerful and direct technique is provided by the characteristic Green's function (resolvent) procedure of Sec. 3.3, based on the intimate relation between resonant solutions (eigenfunctions) and the response to point-source excitation already noted in Sec. 2.4e. This method, formulated in Secs. 3.3.1 and 3.3.2 for the Sturm-Liouville differential operator describing propagation on a general non-uniform transmission line, is relevant not only for one-dimensional eigenvalue problems but also for source problems in inhomogeneous media. Questions of mode completeness and normalization for both discrete and continuous eigenfunctions are answered systematically by exploring the singularities of the characteristic Green's function in the complex plane. The above-mentioned analytic continuation of spectral representations forms an integral part of this procedure, thereby facilitating the construction of alternative field representations as is shown in Sec. 3.3c. Detailed applications of the method to eigenvalue problems in various geometrical configurations are given in Sec. 3.4.

Although the theory of the Sturm-Liouville differential equation or, equivalently, propagation on a non-uniform transmission line, can be discussed in some generality, explicit solutions in terms of known functions are possible only for special inhomogeneity profiles. A variety of such special solutions is presented in Secs. 3.2 and 3.4. Under more general conditions, explicit construction of the field behavior requires approximation procedures whose success relies on the ability to represent the solution to the given problem as a weak perturbation of a known solution to a related problem. If the unperturbed problem is described by a differential equation that exhibits in certain critical regions (near turning points, singularities, etc.) the same analytical behavior as the desired

problem, solution of the latter can be constructed by systematic techniques detailed in Sec. 3.5. One aspect of this procedure involves reformulation of the differential equation problem as an integral equation whose kernel constitutes an unperturbed (“comparison”) Green’s function, and subsequent solution by iteration. Various techniques are illustrated by discussion of specific examples.

3.2 CLASSICAL EVALUATION OF MODE FUNCTIONS

3.2a General One-Dimensional Eigenvalue Problem

Before proceeding with the calculation of scalar two-dimensional eigenfunctions for various separable geometries encompassed by Eqs. (2.3.2), we consider briefly some characteristics of one-dimensional eigenfunctions and the associated eigenvalues. The determination of the eigenfunctions f_m and the eigenvalues λ_m in the domain $x_1 \leq x \leq x_2$ poses a problem of the Sturm–Liouville type:¹

$$\left[\frac{d}{dx} p(x) \frac{d}{dx} - q(x) + \lambda_m w(x) \right] f_m(x) = 0, \quad x_1 \leq x \leq x_2, \quad (1)$$

subject to the homogeneous boundary conditions

$$p \frac{df_m}{dx} + \alpha_{1,2} f_m = 0, \quad x = x_{1,2}, \quad (1a)$$

where p , q , and the weight function w are assumed to be piecewise continuous functions of x in $x_1 \leq x \leq x_2$. The boundary condition in Eq. (1a) is of the “impedance” type, as may be noted from the discussion relating to Eqs. (2.3.41) [see also Eqs. (3.3.5)].

We show first that the eigenvalues λ_m are real for real p , q , w , and $\alpha_{1,2}$, the so-called Hermitian case corresponding to a non-dissipative medium. Upon multiplying Eq. (1) by f_m^* , where * denotes the complex conjugate, integrating over x between the limits of x_1 and x_2 , and using integration by parts and the boundary conditions in Eq. (1a) on the first integral, one finds

$$\lambda_m = \frac{\int_{x_1}^{x_2} dx p |(df_m/dx)|^2 + \int_{x_1}^{x_2} dx q |f_m|^2 - \alpha_1 |f_m(x_1)|^2 + \alpha_2 |f_m(x_2)|^2}{\int_{x_1}^{x_2} dx w |f_m|^2}. \quad (2)$$

Since the right-hand side of Eq. (2) is real for real values of p , q , w , $\alpha_{1,2}$, it follows that λ_m is real in this case.

To deduce the orthogonality property of the eigenfunctions for the Hermitian case, one multiplies Eq. (1) by the eigenfunction f_n^* belonging to the eigenvalue $\lambda_n^* = \lambda_n$ and integrates over the x domain to obtain

$$\int_{x_1}^{x_2} dx f_n^* \frac{d}{dx} \left(p \frac{df_m}{dx} \right) - \int_{x_1}^{x_2} dx q f_n^* f_m + \lambda_m \int_{x_1}^{x_2} dx w f_n^* f_m = 0. \quad (3)$$

Similarly, starting from the defining equation for f_n^* , multiplying by f_m and integrating, one obtains Eq. (3) except for the interchange of m and n . Upon subtracting the second equation from the first, rearranging the terms and carrying out a simple integration by parts, one finds

$$(\lambda_m - \lambda_n) \int_{x_1}^{x_2} dx w f_n^* f_m = \left[p \left(f_m \frac{df_n^*}{dx} - f_n^* \frac{df_m}{dx} \right) \right]_{x_1}^{x_2}. \quad (4)$$

In view of the boundary conditions (1a), the right-hand side of Eq. (4) vanishes, leading to the orthogonality property of the eigenfunctions f_m and f_n^* relative to the weight factor w :

$$\int_{x_1}^{x_2} dx w f_m f_n^* = 0, \quad m \neq n. \quad (5a)$$

The eigenfunctions are normalized to unity by the requirement that

$$\int_{x_1}^{x_2} dx w |f_m|^2 = 1. \quad (5b)$$

The set of eigenfunctions f_m comprising all possible solutions of Eq. (1) constitutes a complete set that can be employed to represent a permissible function $F(x)$ in the interval $x_1 < x < x_2$ [a permissible function is one for which the representations below exist; i.e., the sums or integrals in Eqs. (6) converge]:

$$F(x) = \sum_m F_m f_m(x), \quad (6a)$$

where the sum extends over all eigenfunctions f_m . From the orthonormality property of the f_m functions in Eqs. (5) one evaluates the transform F_m as

$$F_m = \int_{x_1}^{x_2} d\xi w(\xi) F(\xi) f_m^*(\xi). \quad (6b)$$

The completeness and orthonormality of the set f_m can be expressed concisely in a symbolic manner by choosing for $F(x)$ the delta function $\delta(x - x')$. Then

$$F_m = \int_{x_1}^{x_2} d\xi w(\xi) \delta(\xi - x') f_m^*(\xi) = w(x') f_m^*(x'), \quad (7a)$$

so that from Eq. (6a) one infers the completeness relation

$$\frac{\delta(x - x')}{w(x')} = \sum_m f_m(x) f_m^*(x'), \quad x_1 < x' < x_2. \quad (7b)$$

The representation of a permissible function $F(x)$ as in Eq. (6a) follows from Eq. (7b) upon multiplication by $F(x')w(x')$ and integration over x' between the limits x_1 and x_2 .

The considerations above are based on the assumption that the eigenvalue spectrum is simple and discrete. Continuous spectra, when applicable, can be derived therefrom by the limiting procedure of Secs. 3.2b (semiinfinite region) and 3.2c (open angular sector). A more direct treatment in terms of characteristic Green's functions is given in Sec. 3.3.

3.2b Homogeneously Filled Rectangular Cross Sections

Finite rectangular region

The cross-sectional geometry is bounded by perfectly conducting walls and illustrated in Fig. 3.2.1. The transverse operator ∇_t^2 is represented in this case by

$$\nabla_t^2 = \frac{\partial^2}{\partial x^2} + \frac{\partial^2}{\partial y^2}. \quad (8)$$

Upon assuming a solution of the form

$$\Phi_i(\rho) = \Phi_p(x)\Phi_q(y), \quad \Phi_i(\rho) = 0 \quad \text{on } s, \quad (9)$$

where Φ_p and Φ_q are functions of x and y , respectively, one reduces Eqs. (2.3.2a) and (2.3.2b) to the two one-dimensional equations

$$\left(\frac{d^2}{dx^2} + p^2 \right) \Phi_p(x) = 0, \quad \Phi_p(0) = \Phi_p(a) = 0, \quad (10a)$$

$$\left(\frac{d^2}{dy^2} + q^2 \right) \Phi_q(y) = 0, \quad \Phi_q(0) = \Phi_q(b) = 0, \quad (10b)$$

where p^2 and q^2 are “separation” constants in terms of which the transverse wave-number k_{ii}' of Eq. (2.3.2a) is given by

$$k_{ii}'^2 = p^2 + q^2. \quad (10c)$$

Similarly, one assumes for the H -mode functions defined in Eqs. (2.3.2c) and (2.3.2d),

$$\psi_i(\rho) = \psi_p(x)\psi_q(y), \quad \frac{\partial \psi_i}{\partial \nu} = 0 \quad \text{on } s, \quad (11)$$

from which it follows that ψ_p and ψ_q satisfy one-dimensional equations as in Eqs. (10) with the boundary conditions

$$\frac{\partial \psi_p}{\partial x} = 0 \quad \text{at } x = 0, a; \quad \frac{\partial \psi_q}{\partial y} = 0 \quad \text{at } y = 0, b. \quad (12)$$

The solution of the eigenvalue problems posed in Eqs. (10) is readily found to be

$$\Phi_p(x) = \sqrt{\frac{2}{a}} \sin px, \quad p = \frac{m\pi}{a}, \quad m = 1, 2, 3, \dots, \quad (13a)$$

$$\Phi_q(y) = \sqrt{\frac{2}{b}} \sin qy, \quad q = \frac{n\pi}{b}, \quad n = 1, 2, 3, \dots, \quad (13b)$$

where the multiplicative constants have been so chosen as to normalize the mode sets to unity, i.e.,

$$\int_0^a \Phi_p^2(x) dx = 1 = \int_0^b \Phi_q^2(y) dy. \quad (14a)$$

One readily verifies the orthogonality of the eigenfunctions from the relation

$$\int_0^a \sin \frac{m\pi x}{a} \sin \frac{m'\pi x}{a} dx = 0, \quad m \neq m'; \quad m, m' = 1, 2, 3, \dots, \quad (14b)$$

and similarly for the $\Phi_q(y)$, so Eqs. (14a) and (14b) can be subsumed into the single orthonormality relation

$$\int_0^a \Phi_p(x) \Phi_{p'}(x) dx = \delta_{pp'} = \begin{cases} 1, & p = p' \\ 0, & p \neq p'. \end{cases} \quad (14c)$$

Since Eqs. (10) and (12) are evident specializations of Eqs. (1), the orthonormality properties of the one-dimensional eigenfunctions could have been anticipated from Eqs. (5) without the explicit calculation in Eqs. (14). As in Eq. (7b), completeness and orthonormality can be expressed concisely as

$$\delta(x - x') = \sum_{m=1}^{\infty} \Phi_p(x) \Phi_p(x') = \frac{2}{a} \sum_{m=1}^{\infty} \sin \frac{m\pi x}{a} \sin \frac{m\pi x'}{a}, \quad 0 < \frac{x}{x'} < a \quad (15)$$

whence the representation of a permissible function $F(x)$ follows from Eq. (15) upon multiplication by $F(x')$ and integration over x' between the limits 0 and a , while the orthonormality relation (14) is deduced upon choosing for $F(x)$ the eigenfunction $\Phi_p(x)$. In a directly analogous manner, one has for the y domain,

$$\delta(y - y') = \sum_{n=1}^{\infty} \Phi_q(y) \Phi_q(y') = \frac{2}{b} \sum_{n=1}^{\infty} \sin \frac{n\pi y}{b} \sin \frac{n\pi y'}{b}, \quad 0 < \frac{y}{y'} < b. \quad (16)$$

The representation of the two-dimensional delta function $\delta(\mathbf{p} - \mathbf{p}') = \delta(x - x')\delta(y - y')$ for the rectangular domain in Fig. 1 follows directly from the knowledge of the two one-dimensional representations above as

$$\delta(\mathbf{p} - \mathbf{p}') = \sum_i \Phi_i(\mathbf{p}) \Phi_i(\mathbf{p}'), \quad 0 < \frac{x}{x'} < a, 0 < \frac{y}{y'} < b, \quad (17a)$$

$$\frac{4}{ab} \sum_{m=1}^{\infty} \sum_{n=1}^{\infty} \sin \frac{m\pi x}{a} \sin \frac{n\pi y}{b} \sin \frac{m\pi x'}{a} \sin \frac{n\pi y'}{b}, \quad (17b)$$

from which the desired two-dimensional mode functions in Eqs. (2.3.2) are

$$\Phi_i(\mathbf{p}) = \frac{2}{\sqrt{ab}} \sin \frac{m\pi x}{a} \sin \frac{n\pi y}{b}, \quad m, n = 1, 2, 3, \dots, \quad (18a)$$

and the transverse wavenumbers

$$k_i'^2 = \left(\frac{m\pi}{a}\right)^2 + \left(\frac{n\pi}{b}\right)^2. \quad (18b)$$

\sum_i in this instance represents the double sum $\sum_{m=1}^{\infty} \sum_{n=1}^{\infty}$. The product representation of the delta function in Eq. (17a) is obtained from the requirement

$$1 = \iint_S \delta(\mathbf{p} - \mathbf{p}') dS = \int_0^a dx \int_0^b dy \delta(x - x') \delta(y - y'), \quad \mathbf{p}' \text{ in } S. \quad (19)$$

The orthonormality of the two-dimensional set $\Phi_i(\mathbf{p})$ is assured from that of $\Phi_p(x)$ and $\Phi_q(y)$ since for $i = (p, q), j = (p', q')$,

$$\iint_S \Phi_i(\mathbf{p})\Phi_j(\mathbf{p}) dS = \int_0^a dx \int_0^b dy \Phi_p(x)\Phi_q(y)\Phi_{p'}(x)\Phi_{q'}(y) = \delta_{pp'}\delta_{qq'} = \delta_{ij}. \quad (20)$$

A permissible function $F(\mathbf{p})$ in the rectangular domain can now be represented via Eq. (17a) as

$$F(\mathbf{p}) = \iint_S F(\mathbf{p}')\delta(\mathbf{p} - \mathbf{p}') dS' = \sum_i F_i \Phi_i(\mathbf{p}), \quad (21a)$$

$$F_i = \iint_S F(\mathbf{p}')\Phi_i(\mathbf{p}') dS'. \quad (21b)$$

Similarly, one deduces the mode functions ψ_i appropriate to the rectangular cross section in Fig. 3.2.1 and to the boundary conditions in Eq. (11). The orthonormal functions $\psi_p(x)$ and $\psi_q(y)$ are given by

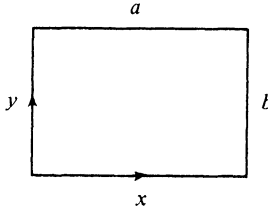


FIG. 3.2.1 Finite rectangular region.

$$\psi_p(x) = \sqrt{\frac{2}{a}} \cos px, \quad p = \frac{m\pi}{a}, \quad m = 1, 2, \dots; \quad \psi_0(x) = \frac{1}{\sqrt{a}}; \quad (22a)$$

$$\psi_q(y) = \sqrt{\frac{2}{b}} \cos qy, \quad q = \frac{n\pi}{b}, \quad n = 1, 2, \dots; \quad \psi_0(y) = \frac{1}{\sqrt{b}}. \quad (22b)$$

As in Eq. (15), the completeness and orthonormality of the mode set $\psi_p(x)$ is conveniently expressed via the delta-function representation

$$\delta(x - x') = \sum_{m=0}^{\infty} \psi_p(x)\psi_p(x') = \frac{1}{a} \sum_{m=0}^{\infty} \epsilon_m \cos px \cos px', \quad 0 < \frac{x}{x'} < a, \quad (23)$$

with $\epsilon_0 = 1, \epsilon_m = 2, m \geq 1$, while for the two-dimensional mode set $\psi_i(\mathbf{p})$,

$$\begin{aligned} \delta(\mathbf{p} - \mathbf{p}') &= \sum_i \psi_i(\mathbf{p})\psi_i(\mathbf{p}'), \quad 0 < \frac{x}{x'} < a, \quad 0 < \frac{y}{y'} < b, \\ &= \frac{1}{ab} \sum_{m=0}^{\infty} \sum_{n=0}^{\infty} \epsilon_m \epsilon_n \cos \frac{m\pi x}{a} \cos \frac{n\pi y}{b} \cos \frac{m\pi x'}{a} \cos \frac{n\pi y'}{b}. \end{aligned} \quad (24)$$

Thus,

$$\psi_r(\mathbf{p}) = \sqrt{\frac{\epsilon_m \epsilon_n}{ab}} \cos \frac{m\pi x}{a} \cos \frac{n\pi y}{b}, \quad m, n = 0, 1, 2, \dots, \quad (25a)$$

and

$$k''^2 = \left(\frac{m\pi}{a}\right)^2 + \left(\frac{n\pi}{b}\right)^2. \quad (25b)$$

Semiinfinite rectangular region

If the a dimension of the waveguide in Fig. 3.2.1 is allowed to become infinite, the rectangular waveguide configuration goes over into the semiinfinite rectangular trough shown in Fig. 3.2.2. The transition to the open region is traced out by defining

$$p \equiv \xi_m = \frac{m\pi}{a}, \quad \Delta\xi_m = \xi_{m+1} - \xi_m = \frac{\pi}{a}. \quad (26)$$

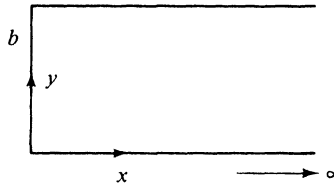


FIG. 3.2.2 Semi-infinite rectangular region.

As a becomes very large, one notes that the eigenvalues $p = m\pi/a$, $m = 1, 2, \dots$, fall closer and closer together until they coalesce in the limit into a continuous spectrum. Upon substituting Eq. (26) into Eq. (15), and letting $a \rightarrow \infty$ (i.e., $\Delta\xi_m \rightarrow 0$), one obtains

$$\delta(x - x') = \lim_{\Delta\xi_m \rightarrow 0} \frac{2}{\pi} \sum_{\xi_m=\Delta\xi_m}^{\infty} \sin(\xi_m x) \sin(\xi_m x') \Delta\xi_m \quad (27a)$$

$$= \frac{2}{\pi} \int_0^{\infty} \sin \xi x \sin \xi x' d\xi, \quad 0 < \frac{x}{x'} < \infty, \quad (27b)$$

so

$$\Phi_\xi(x) \equiv \Phi(\xi, x) = \sqrt{\frac{2}{\pi}} \sin \xi x, \quad 0 < \xi < \infty. \quad (27c)$$

The sum $\sum_{m=1}^{\infty}$ in Eq. (15) is replaced here by the integral $\int_0^{\infty} d\xi$, since the eigenvalues are continuous.

The continuous eigenfunctions in Eq. (27c) are improper [i.e., the normalizing integral $(2/\pi) \int_0^{\infty} dx \sin^2 \xi x$ does not exist (is infinite)]. The normalization constant $\delta_{pp'}$ in Eqs. (14) is replaced in this case by the delta function $\delta(\xi - \xi')$, as is verified upon multiplying Eq. (27b) by $\sin \xi' x'$, integrating from $x' = 0$ to $x' = \infty$, and interchanging the order of integration on the right-hand side

(the interchange of the order of integration is essential for the deduction of a transform theorem and is assumed valid for the class of permissible functions):

$$\begin{aligned}\sin \xi' x &= \int_0^\infty \sin \xi x \left(\frac{2}{\pi} \int_0^\infty \sin \xi' x' \sin \xi x' dx' \right) d\xi \\ &= \int_0^\infty \sin \xi x \delta(\xi - \xi') d\xi,\end{aligned}\quad (28a)$$

i.e.,

$$\frac{2}{\pi} \int_0^\infty \sin \xi' x' \sin \xi x' dx' = \delta(\xi - \xi'), \quad (28b)$$

which relation is evidently of the same form as Eq. (27b). $\Phi_\xi(x)$ in Eq. (27c) is seen to satisfy the required boundary condition $\Phi_\xi(0) = 0$. The lack of a boundary condition at $x = \infty$ is a consequence of the singular (limit point) character of the endpoint at infinity² [see the footnote to Eq. (3.3.21)].

The two-dimensional completeness statement for *E modes* in the semiinfinite region of Fig. 3.2.2 can be written as

$$\delta(\mathbf{p} - \mathbf{p}') = \begin{cases} \sum_i \Phi_i(\mathbf{p}) \Phi_i(\mathbf{p}'), & 0 < \frac{x}{x'} < \infty, \quad 0 < \frac{y}{y'} < b, \\ \frac{4}{\pi b} \int_0^\infty d\xi \sum_{n=1}^\infty \sin \xi x \sin \frac{n\pi y}{b} \sin \xi x' \sin \frac{n\pi y'}{b}, & \end{cases} \quad (29a)$$

$$(29b)$$

i.e.,

$$\begin{aligned}\Phi_i(\mathbf{p}) &= \frac{2}{\sqrt{\pi b}} \sin \xi x \sin \frac{n\pi y}{b}, \quad 0 < \xi < \infty, \quad n = 1, 2, 3, \dots, \\ k_i'^2 &= \xi^2 + \left(\frac{n\pi}{b} \right)^2.\end{aligned}\quad (29c)$$

It is noted that \sum_i in Eq. (29a) stands in this instance for $\int_0^\infty d\xi \sum_{n=1}^\infty$ since the mode set in the x domain is continuous.

For the *H-mode functions* one obtains, by a similar limiting process,

$$\delta(x - x') = \frac{2}{\pi} \int_0^\infty \cos \xi x \cos \xi x' d\xi, \quad 0 < \frac{x}{x'} < \infty, \quad (30a)$$

so

$$\psi_\xi(x) = \sqrt{\frac{2}{\pi}} \cos \xi x, \quad 0 < \xi < \infty. \quad (30b)$$

Thus,

$$\delta(\mathbf{p} - \mathbf{p}') = \begin{cases} \sum_i \psi_i(\mathbf{p}) \psi_i(\mathbf{p}'), & 0 < \frac{x}{x'} < \infty, \quad 0 < \frac{y}{y'} < b, \\ \frac{2}{\pi b} \int_0^\infty d\xi \sum_{n=0}^\infty \epsilon_n \cos \xi x \cos \frac{n\pi y}{b} \cos \xi x' \cos \frac{n\pi y'}{b}, & \end{cases} \quad (31a)$$

$$(31b)$$

i.e.,

$$\psi_i(\mathbf{p}) = \sqrt{\frac{2\epsilon_n}{\pi b}} \cos \xi x \cos \frac{n\pi y}{b}, \quad 0 < \xi < \infty, \quad n = 0, 1, 2, \dots,$$

$$k_{ii}''^2 = \xi^2 + \left(\frac{n\pi}{b}\right)^2. \quad (31c)$$

Quarter-space region

Upon letting the b dimension in Fig. 3.2.2 increase indefinitely, one obtains the quarter-space region in Fig. 3.2.3 and, from the preceding section, the following completeness statements (the continuously variable index q is denoted by η):

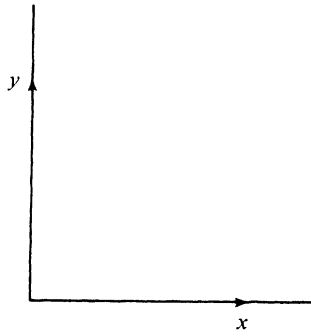


FIG. 3.2.3 Quarter-space region.

E modes:

$$\delta(\mathbf{p} - \mathbf{p}') = \begin{cases} \sum_i \Phi_i(\mathbf{p}) \Phi_i(\mathbf{p}'), & 0 < \frac{x}{x'} < \infty, \quad 0 < \frac{y}{y'} < \infty, \\ \frac{4}{\pi^2} \int_0^\infty d\xi \int_0^\infty d\eta \sin \xi x \sin \eta y \sin \xi x' \sin \eta y', & \end{cases} \quad (32a)$$

$$(32b)$$

i.e.,

$$\Phi_i(\mathbf{p}) = \frac{2}{\pi} \sin \xi x \sin \eta y, \quad 0 < \xi < \infty, \quad 0 < \eta < \infty; \quad k_{ii}''^2 = \xi^2 + \eta^2. \quad (32c)$$

The symbol \sum_i denotes in this case the double integral $\int_0^\infty d\xi \int_0^\infty d\eta$.

H modes:

$$\delta(\mathbf{p} - \mathbf{p}') = \begin{cases} \sum_i \psi_i(\mathbf{p}) \psi_i(\mathbf{p}'), & 0 < \frac{x}{x'} < \infty, \quad 0 < \frac{y}{y'} < \infty, \\ \frac{4}{\pi^2} \int_0^\infty d\xi \int_0^\infty d\eta \cos \xi x \cos \eta y \cos \xi x' \cos \eta y', & \end{cases} \quad (33a)$$

$$(33b)$$

i.e.,

$$\psi_i(\mathbf{p}) = \frac{2}{\pi} \cos \xi x \cos \eta y, \quad 0 < \xi < \infty, \quad 0 < \eta < \infty; \quad k_{ii}''^2 = \xi^2 + \eta^2. \quad (33c)$$

Half-space region

A half-space region $x > 0$ is shown in Fig. 3.2.4. Eigenfunctions for the infinite interval $-\infty < y < \infty$ are deduced most simply by considering not the bounded domain $0 < y < b$ as above, but instead $-b/2 < y < b/2$, and

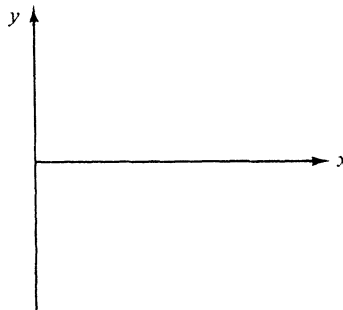


FIG. 3.2.4 Half-space region.

then letting $b \rightarrow \infty$. One finds the delta-function representation for the latter range directly from Eq. (16) upon introducing the change of variable $y \rightarrow y - b/2, y' \rightarrow y' - b/2$:

$$\delta(y - y') = \frac{2}{b} \sum_{n=1}^{\infty} \cos \frac{(2n-1)\pi y}{b} \cos \frac{(2n-1)\pi y'}{b} + \frac{2}{b} \sum_{n=1}^{\infty} \sin \frac{2n\pi y}{b} \sin \frac{2n\pi y'}{b}, \quad -\frac{b}{2} < y < \frac{b}{2} \quad (34a)$$

i.e., the eigenfunctions Φ_q in this case comprise the two mutually orthogonal sets

$$\Phi_q(y) = \sqrt{\frac{2}{b}} \begin{cases} \cos \frac{(2n-1)\pi y}{b} \\ \sin \frac{2n\pi y}{b} \end{cases}, \quad n = 1, 2, 3, \dots, \quad -\frac{b}{2} < y < \frac{b}{2}, \quad (34b)$$

which are even and odd in y , respectively. Upon defining in the first sum in Eq. (34a),

$$\eta_n = \frac{(2n-1)\pi}{b}, \quad \Delta\eta_n = \eta_{n+1} - \eta_n = \frac{2\pi}{b}, \quad (35a)$$

and in the second sum,

$$\eta_n = \frac{2n\pi}{b}, \quad \Delta\eta_n = \frac{2\pi}{b}, \quad (35b)$$

and going to the limit $b \rightarrow \infty$, one obtains

$$\delta(y - y') = \frac{1}{\pi} \int_0^\infty \cos \eta y \cos \eta y' d\eta + \frac{1}{\pi} \int_0^\infty \sin \eta y \sin \eta y' d\eta, \quad (36a)$$

$$\delta(y - y') = \begin{cases} \frac{1}{\pi} \int_0^\infty \cos \eta(y - y') d\eta, & -\infty < y' < \infty. \end{cases} \quad (36b)$$

For the H -mode functions, a similar result is obtained if the transition $b \rightarrow \infty$ is carried out for the $\psi_n(y)$ in Eq. (22b) after defining the latter over the interval $-b/2 < y < b/2$ as above. The lack of dependence of the infinite interval eigenfunctions $\Phi_\eta(y) = \psi_\eta(y)$ on the boundary conditions for the finite interval is a consequence of the limit-point type of singularity at $y = \pm\infty$ [see the footnote to Eq. (3.3.21)]. Thus we have, from Eq. (36a),

$$\Phi_\eta(y) = \psi_\eta(y) = \sqrt{\frac{1}{\pi}} \begin{Bmatrix} \sin \eta y \\ \cos \eta y \end{Bmatrix}, \quad -\infty < y < \infty, \quad 0 < \eta < \infty. \quad (36c)$$

An alternative and frequently more useful representation of the delta function is obtained upon expressing the cosine terms in Eq. (36b) as the sum of two exponentials:[†]

$$\begin{aligned} \delta(y - y') &= \frac{1}{2\pi} \int_0^\infty e^{j\eta(y-y')} d\eta + \frac{1}{2\pi} \int_0^\infty e^{-j\eta(y-y')} d\eta \\ &= \frac{1}{2\pi} \int_{-\infty}^\infty e^{j\eta(y-y')} d\eta = \frac{1}{2\pi} \int_{-\infty}^\infty e^{j\eta(y'-y)} d\eta \\ &= \sum_\eta \Phi_\eta(y)\Phi_\eta^*(y') = \sum_\eta \psi_\eta(y)\psi_\eta^*(y'). \end{aligned} \quad (37a)$$

In this Fourier integral representation, the eigenfunctions are complex and the delta-function representation involves the complex conjugate [see Eq. (7b)]. The eigenvalue parameter η ranges from $-\infty$ to $+\infty$. Thus,

$$\Phi_\eta(y) = \psi_\eta(y) = \frac{1}{\sqrt{2\pi}} e^{-j\eta y}, \quad -\infty < y < \infty, \quad -\infty < \eta < \infty. \quad (37b)$$

The orthogonality condition analogous to Eq. (28b) is now, with respect to the complex conjugate,

$$\frac{1}{2\pi} \int_{-\infty}^\infty e^{j\eta'y'} e^{-j\eta y'} dy' = \delta(\eta - \eta'). \quad (37c)$$

An advantage of the representation in Eq. (37a) is the simple deformability of the contour of integration into the complex η plane. If $y > y'$, the integrand in the first integral in Eq. (37a) decays exponentially in the upper half of the complex η plane ($\text{Im } \eta > 0$), so the endpoints of the integration contour can be shifted from the real η axis to $\eta = -\infty + j\epsilon$ and $\eta = +\infty + j\delta$, with $\epsilon, \delta > 0$. Similarly, if $y < y'$, the contour of integration in the second integral

[†]Note that the use of $j = \sqrt{-1}$ does not imply a preferred time dependence at this stage.

representation in Eq. (37a) can be deformed into the upper half of the η plane. The utility of these formulations in the complex plane for transformation of a given field representation into an alternative one will be emphasized in Sec. 3.3.

In summary, two-dimensional delta-function representations for the half-space region are as follows:

E modes

$$\begin{aligned}\delta(\mathbf{p} - \mathbf{p}') &= \sum_i \Phi_i(\mathbf{p}) \Phi_i^*(\mathbf{p}'), \quad 0 > \frac{x}{x'} < \infty, \quad -\infty < \frac{y}{y'} < \infty, \\ &= \frac{1}{\pi^2} \int_0^\infty d\xi \int_{-\infty}^\infty d\eta \sin \xi x e^{-j\eta y} \sin \xi x' e^{+j\eta y'},\end{aligned}\quad (38a)$$

i.e.,

$$\Phi_i(\mathbf{p}) = \frac{1}{\pi} \sin \xi x e^{-j\eta y}, \quad 0 < \xi < \infty, \quad -\infty < \eta < \infty; \quad k_{ii}'^2 = \xi^2 + \eta^2. \quad (38b)$$

H modes

$$\begin{aligned}\delta(\mathbf{p} - \mathbf{p}') &= \sum_i \psi_i(\mathbf{p}) \psi_i^*(\mathbf{p}'), \quad 0 < \frac{x}{x'} < \infty, \quad -\infty < \frac{y}{y'} < \infty, \\ &= \frac{1}{\pi^2} \int_0^\infty d\xi \int_{-\infty}^\infty d\eta \cos \xi x e^{-j\eta y} \cos \xi x' e^{+j\eta y'},\end{aligned}\quad (39a)$$

i.e.,

$$\psi_i(\mathbf{p}) = \frac{1}{\pi} \cos \xi x e^{-j\eta y}, \quad 0 < \xi < \infty, \quad -\infty < \eta < \infty, \quad k_{ii}''^2 = \xi^2 + \eta^2. \quad (39b)$$

Free-space region

For the free-space region shown in Fig. 3.2.5, the *E*- and *H*-mode scalar eigenfunctions $\Phi_i(\mathbf{p})$ and $\psi_i(\mathbf{p})$ are seen to be identical. The eigenvalue problem in x leads to the same Fourier integral representation as in Eq. (37a), so the two-dimensional free-space representation constitutes the two-dimensional Fourier integral theorem:

$$\begin{aligned}\delta(\mathbf{p} - \mathbf{p}') &= \sum_i \Phi_i(\mathbf{p}) \Phi_i^*(\mathbf{p}') = \sum_i \psi_i(\mathbf{p}) \psi_i^*(\mathbf{p}'), \quad -\infty < \frac{x}{x'} < \infty, \\ &\quad -\infty < \frac{y}{y'} < \infty, \\ &= \frac{1}{4\pi^2} \int_{-\infty}^\infty d\xi \int_{-\infty}^\infty d\eta e^{-j(\xi x + \eta y)} e^{+j(\xi x' + \eta y')},\end{aligned}\quad (40a)$$

i.e.,

$$\begin{aligned}\Phi_i(\mathbf{p}) &= \psi_i(\mathbf{p}) = \frac{1}{2\pi} e^{-j(\xi x + \eta y)}, \quad -\infty < \xi < \infty, \quad -\infty < \eta < \infty; \\ &\quad k_{ii}^2 = \xi^2 + \eta^2.\end{aligned}\quad (40b)$$

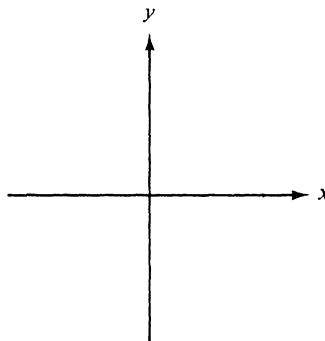


FIG. 3.2.5 Free-space region.

Parallel-plate region

For the parallel-plate region shown in Fig. 3.2.6, the y -dependent eigenfunctions are those in Eq. (37b), while those for the finite x domain are given in Eqs. (13a) and (22a), respectively. Thus, for E modes,

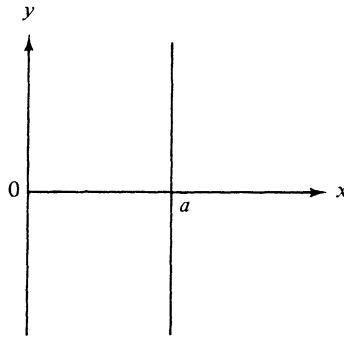


FIG. 3.2.6 Parallel-plate region.

$$\begin{aligned}\delta(\mathbf{p} - \mathbf{p}') &= \sum_i \Phi_i(\mathbf{p}) \Phi_i^*(\mathbf{p}'), \quad 0 < \frac{x}{x'} < a, \quad -\infty < \frac{y}{y'} < \infty, \\ &= \frac{1}{\pi a} \sum_{m=1}^{\infty} \int_{-\infty}^{\infty} d\eta \sin \frac{m\pi x}{a} e^{-j\eta y} \sin \frac{m\pi x'}{a} e^{j\eta y'},\end{aligned}\quad (41a)$$

i.e.,

$$\begin{aligned}\Phi_i(\mathbf{p}) &= \frac{1}{\sqrt{\pi a}} \sin \frac{m\pi x}{a} e^{-j\eta y}, \quad m = 1, 2, 3, \dots, \quad -\infty < \eta < \infty; \\ k_{ii}^2 &= \left(\frac{m\pi}{a}\right)^2 + \eta^2;\end{aligned}\quad (41b)$$

for H modes,

$$\begin{aligned}\delta(\mathbf{p} - \mathbf{p}') &= \sum_i \psi_i(\mathbf{p}) \psi_i^*(\mathbf{p}'), \quad 0 < \frac{x}{x'} < a, \quad -\infty < \frac{y}{y'} < \infty, \\ &= \frac{1}{2\pi a} \sum_{m=0}^{\infty} \int_{-\infty}^{\infty} d\eta \epsilon_m \cos \frac{m\pi x}{a} e^{-j\eta y} \cos \frac{m\pi x'}{a} e^{j\eta y'},\end{aligned}\quad (42a)$$

i.e.,

$$\begin{aligned}\psi_i(\mathbf{p}) &= \sqrt{\frac{\epsilon_m}{2\pi a}} \cos \frac{m\pi x}{a} e^{-j\eta y}, \quad m = 0, 1, 2, \dots, \quad -\infty < \eta < \infty; \\ k_i'^2 &= \left(\frac{m\pi}{a}\right)^2 + \eta^2, \quad \epsilon_0 = 1, \quad \epsilon_m = 2, \quad m \geq 1.\end{aligned}\quad (42b)$$

Transmission-line interpretation of one-dimensional eigenvalue problem

The one-dimensional eigenvalue problems in the preceding sections can be interpreted in transmission-line terms as defining resonant voltage or current solutions on an appropriately terminated source-free transmission line. Consider, for example, the eigenvalue problem in the x domain as stated in Eq. (10a). If x is taken as the transmission coordinate, the equivalent transmission-line configuration is that shown in Fig. 2.4.10 with $z_1 \equiv x_1 = 0$, $z_2 \equiv x_2 = a$, $\overleftarrow{Z}_T = 0 = \overrightarrow{Z}_T$. The source-free voltage solutions on such a transmission line are defined by the homogeneous second-order differential equation (2.4.2), which is identical with Eq. (10a), provided that $z \equiv x$, $\kappa \equiv p$. In view of the requirement that $\Phi_p(0) = \Phi_p(a) = 0$ in Eq. (10a) (i.e., the vanishing of the transmission-line solutions at the short-circuit terminations), one identifies $\Phi_p(x)$ as the resonant voltage $V(x)$. Equation (2.4.7a), with $z' \equiv x' = 0$, leads upon imposition of the boundary conditions $V(0) = V(a) = 0$ to the resonant solutions in Eq. (13a), to within an arbitrary multiplying constant. Similarly, from the source-free transmission-line equations, V is proportional to dI/dx [see Eq. (2.4.1)]. Hence, the eigenfunction $\psi_p(x)$ satisfying the boundary conditions in Eq. (12) can be identified as the current $I(x)$ on a short-circuited transmission line. The eigensolutions in Eq. (22a) then follow directly from Eq. (2.4.7b). Alternatively, one may employ the dual configuration of a transmission line terminated in open circuits at $x = 0, a$ (i.e., $\overleftarrow{Z}_T = \overrightarrow{Z}_T = \infty$). In this instance, the currents vanish at $x = 0, a$, so $\Phi_p(x)$ and $\psi_p(x)$ can be identified as the resonant current and voltage solutions, respectively.

As emphasized in Sec. 2.4e, the source-free solutions on a terminated transmission line are intimately related to the singularities of the modal Green's function $Z(x, x')$ or $Y(x, x')$ defined in Eqs. (2.4.28) and (2.4.29) (with z, z' replaced by x, x'). This connection is highlighted further by an examination of the voltage and current solutions $V(x, x')$ and $I(x, x')$ in Eqs. (2.4.22) excited by voltage and current sources v and i at x' . To obtain a finite response in the absence of excitation (i.e., when $v = i = 0$), one requires via Eqs. (2.4.22) the vanishing of the total impedance $\overleftrightarrow{Z}(x')$ and admittance $\overleftrightarrow{Y}(x')$ [see also Eq. (2.4.36)]:

$$\vec{Z}(x') = 0 = \vec{Z}(x') + \vec{Z}(x'), \quad (43a)$$

or, equivalently,

$$\vec{Y}(x') = 0 = \vec{Y}(x') + \vec{Y}(x'), \quad (43b)$$

where the choice of x' is arbitrary. Equations (43) constitute “transverse resonance” relations that can be satisfied only for resonant values of the propagation constant $k_{xr} = p$. For the case of a simple transmission line of length a short-circuited at both ends, one chooses $x' = 0$ so that $\vec{Z}(0) = 0$; then one has, via Eqs. (2.4.24a) and (43a), $\vec{Z}(0) = jZ_0 \tan pa = 0$, i.e.,

$$p = \frac{m\pi}{a}, \quad m = 1, 2, \dots, \quad (43c)$$

as in Eq. (13a). The corresponding source-free solutions (eigenfunctions) are then given by the expressions inside the second set of brackets of Eqs. (2.4.22b). For eigenvalue problems of a general type, the above relation between the singularities (resonances) of the modal Green’s functions and the source-free solutions on a terminated transmission line will be elaborated in Sec. 3.3a.

3.2c Homogeneously Filled Cylindrical Cross Sections

Coaxial cross-sectional waveguide configurations of interest are the coaxial sector and annulus shown in Fig. 3.2.7. The sector is bounded by perfectly conducting cylindrical segments at $\rho = a, b$ and radial plane segments at $\phi = 0$

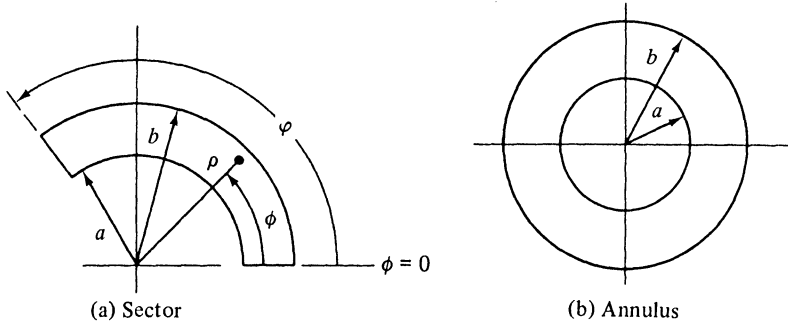


FIG. 3.2.7 Coaxial regions.

$0, \varphi$; the annulus is bounded by perfectly conducting cylinders at $\rho = a, b$. It is to be noted that a sector of angle $\varphi = 2\pi$ still contains a septum along the $\phi = 0$ axis and is not equivalent to the annular region.

The cylindrical ρ, ϕ coordinate representation for the transverse operator ∇_t^2 is

$$\nabla_t^2 = \frac{1}{\rho} \frac{\partial}{\partial \rho} \rho \frac{\partial}{\partial \rho} + \frac{1}{\rho^2} \frac{\partial^2}{\partial \phi^2}. \quad (44)$$

Assuming product solutions for E and H modes,

$$\Phi_i(\rho) = \Phi_p(\rho)\Phi_q(\phi), \quad \Phi_i(\rho) = 0 \quad \text{on } s, \quad (45a)$$

$$\psi_i(\rho) = \psi_p(\rho)\psi_q(\phi), \quad \frac{\partial\psi_i}{\partial\rho} = 0 \quad \text{on } s, \quad (45b)$$

one reduces Eqs. (2.3.2) to two one-dimensional equations:

$$\left(\frac{d^2}{d\phi^2} + q^2 \right) \psi_q(\phi) = 0, \quad \begin{cases} \Phi_q \\ \frac{\partial\psi_q}{\partial\phi} \end{cases} = 0 \quad \text{at } \phi = 0, \varphi, \quad (46a)$$

$$\left(\frac{d}{dp} p \frac{d}{dp} - \frac{q^2}{p} + p^2 \rho \right) \Phi_p(\rho) = 0, \quad \begin{cases} \Phi_p \\ \frac{\partial\Phi_p}{\partial\rho} \end{cases} = 0 \quad \text{at } \rho = a, b, \quad (46b)$$

where $p \equiv k_{ii}$; the eigenvalues p^2 and q^2 are, of course, different for E and H modes. For the annular region in Fig. 3.2.7(b), the boundary condition in the ϕ -domain is replaced by a periodicity requirement on Φ_q and $d\Phi_q/d\phi$ (similarly for ψ_q and $d\psi_q/d\phi$).

As for the rectangular-cross-section case, the two-dimensional eigenvalue problems in Eqs. (46) can be interpreted as resonant transmission-line problems for the ρ and ϕ domains. The eigenvalue problems in the ϕ domain in Eq. (46a) are identical in form to those encountered in the rectangular geometry in Eqs. (10)–(12), so the corresponding solutions $\Phi_q(\phi)$ and $\psi_q(\phi)$, are representative of the resonances on a uniform angular transmission line of length $\phi = \varphi$, with the eigenvalue parameter q distinguishing the resonant values of the propagation constant. In the radial eigenvalue problem (46b), distinguished by the Bessel differential operator, p is the eigenvalue parameter with q fixed by Eq. (46a). Upon comparison with Eqs. (2.3.41) (see also Sec. 3.3a), one notes that the resonant transmission line of length $b - a$, representative of the radial domain, is non-uniform, since both the characteristic impedance and propagation constant are functions of the transmission coordinate.

If the ϕ domain is bounded by radial planes at $\phi = 0, \varphi$, the complete set of eigenfunctions Φ_q and ψ_q can be employed as in Eqs. (15) and (23), to represent the delta function $\delta(\phi - \phi')$:

E modes

$$\delta(\phi - \phi') = \sum_q \Phi_q(\phi)\Phi_q(\phi') = \frac{2}{\varphi} \sum_{m=1}^{\infty} \sin \frac{m\pi\phi}{\varphi} \sin \frac{m\pi\phi'}{\varphi}, \quad 0 < \frac{\phi}{\phi'} < \varphi, \quad (47a)$$

i.e.,

$$\Phi_q(\phi) = \sqrt{\frac{2}{\varphi}} \sin q\phi, \quad q = \frac{m\pi}{\varphi}, \quad m = 1, 2, \dots \quad (47b)$$

H modes

$$\delta(\phi - \phi') = \sum_q \psi_q(\phi) \psi_q(\phi') = \frac{1}{\varphi} \sum_{m=0}^{\infty} \epsilon_m \cos \frac{m\pi\phi}{\varphi} \cos \frac{m\pi\phi'}{\varphi}, \quad 0 < \frac{\phi}{\varphi} < \varphi, \quad (48a)$$

i.e.,

$$\psi_q(\phi) = \sqrt{\frac{\epsilon_m}{\varphi}} \cos q\phi, \quad q = \frac{m\pi}{\varphi}, \quad m = 0, 1, 2, \dots, \quad \epsilon_m = \begin{cases} 1, & m = 0, \\ 2, & m \geq 1. \end{cases} \quad (48b)$$

For the complete annular region, $0 \leq \phi \leq 2\pi$, the eigenfunctions and their derivatives must be periodic with period 2π , i.e.,

$$\Phi_q(\phi) \Big|_{\phi}^{\phi+2\pi} = 0, \quad \frac{d}{d\phi} \Phi_q(\phi) \Big|_{\phi}^{\phi+2\pi} = 0, \quad (49)$$

and similarly for $\psi_q(\phi)$. The *E*- and *H*-mode functions are identical in this case and can be inferred from the delta-function representation

$$\frac{1}{2\pi} \sum_{m=0}^{\infty} \epsilon_m \cos m\phi \cos m\phi' + \frac{1}{\pi} \sum_{m=1}^{\infty} \sin m\phi \sin m\phi', \quad (50a)$$

$$\delta(\phi - \phi') = \begin{cases} \frac{1}{2\pi} \sum_{m=0}^{\infty} \epsilon_m \cos m(\phi - \phi'), \\ \frac{1}{2\pi} \sum_{m=-\infty}^{\infty} e^{-jm(\phi - \phi')}, \quad 0 \leq \phi \leq 2\pi. \end{cases} \quad (50b) \quad (50c)$$

The eigenfunctions can therefore be given either in the real form,

$$\Phi_q(\phi) = \psi_q(\phi) = \sqrt{\frac{\epsilon_m}{2\pi}} \begin{cases} \cos q\phi \\ \sin q\phi \end{cases}, \quad q = m = 0, 1, 2, \dots, \quad (51a)$$

or in the complex form [see Eq. (37b)],

$$\Phi_q(\phi) = \psi_q(\phi) = \frac{1}{\sqrt{2\pi}} e^{-jq\phi}, \quad q = m = 0, \pm 1, \pm 2, \dots \quad (51b)$$

The radial equation (46b) is satisfied by Bessel functions $Z_q(p\rho)$, where q and $(p\rho)$ denote the order and argument, respectively, and Z stands for the Bessel function J , the Neumann function N , or the Hankel functions $H^{(1)}$ and $H^{(2)}$. Two linearly independent solutions must generally be employed to satisfy the required boundary conditions at $\rho = a$ and $\rho = b$. Detailed calculations for various geometrical configurations are given in the examples below.

Finite angular sector

E modes. The angular sector configuration shown in Fig. 3.2.8 is obtained from Fig. 3.2.7(a) by letting $a \rightarrow 0$. The eigenfunctions for the ϕ domain are those listed in Eq. (47b). Concerning the radial domain $0 \leq \rho \leq b$, the eigenfunctions $\Phi_p(\rho)$ satisfy the differential equation and boundary conditions specified in Eq. (46b). At the singular endpoint $\rho = 0$, the boundary con-

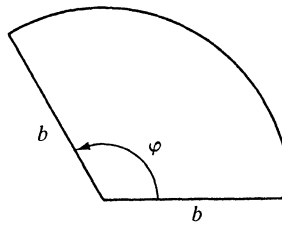


FIG. 3.2.8 Finite angular sector.

dition $\Phi_p(0) = 0$ is replaced by a finiteness condition. This requirement is satisfied by the Bessel functions J_q :

$$\Phi_p(\rho) = A_p J_q(p\rho); \quad J_q(x_{nq}) = 0, \quad x_{nq} \equiv pb, \quad (52)$$

where A_p is an as-yet-undetermined normalization constant and x_{nq} is the n th positive root of the Bessel function $J_q(x)$, satisfying the boundary condition $\Phi_p(b) = 0$. Finiteness at $\rho = 0$ follows from the small-argument behavior of the Bessel function $J_q(x) \sim x^q$ for $x \rightarrow 0$, where $q > 0$ from Eq. (47b). Since Eq. (46b) is a special case of Eq. (1) with $x \rightarrow \rho$, $p(x) = w(x) \rightarrow \rho$, $q(x) \rightarrow q^2/\rho$, $\lambda_m \rightarrow p^2$, it follows from Eq. (2) that p is real and that $\Phi_p(\rho)$ satisfies the orthogonality condition (5a). Indeed, proceeding as in Eq. (4),

$$(p^2 - p'^2) \int_{\rho_1}^{\rho_2} d\rho \rho J_q(p\rho) J_q(p'\rho) \\ = [pp' J'_q(p\rho) J'_q(p'\rho) - pp J'_q(p'\rho) J'_q(p\rho)]_{\rho_1}^{\rho_2}, \quad (53)$$

where $J'_q(x) \equiv (d/dx)J_q(x)$, and recalling the behavior of $J_q(x)$ near $x \rightarrow 0$, one affirms, for two unequal eigenvalues p and p' , that

$$\int_0^b \rho J_q(p\rho) J_q(p'\rho) d\rho = 0, \quad p \neq p'. \quad (54)$$

The normalization constant A_p can be determined from Eq. (53) by letting p be an eigenvalue satisfying Eq. (52) and treating p' as a variable parameter that approaches p . The resulting indeterminate form is evaluated by L'Hopital's rule to yield

$$\begin{aligned} \int_0^b \rho J_q^2(p\rho) d\rho &= \lim_{p' \rightarrow p} \frac{[pp' J'_q(p\rho) J'_q(p'\rho) - pp J'_q(p'\rho) J'_q(p\rho)]_0^b}{p^2 - p'^2} \\ &= -b \left. \frac{(d/dp')[p J_q(p'b) J'_q(pb)]}{(d/dp')(p^2 - p'^2)} \right|_{p'=p} \\ &= \frac{b^2}{2} J_q^2(pb) = \frac{b^2}{2} J_{q+1}^2(pb), \end{aligned}$$

so the identification

$$A_p = \frac{\sqrt{2}}{b} \frac{1}{J'_q(x_{nq})} = \frac{\sqrt{2}}{b} \frac{-1}{J_{q+1}(x_{nq})} \quad (55a)$$

assures the desired orthonormality

$$\int_0^b \rho \Phi_p(\rho) \Phi_{p'}(\rho) d\rho = \delta_{pp'}. \quad (55b)$$

The relation

$$J_q'(x_{nq}) = J_{q+1}^2(x_{nq}), \quad \text{when } J_q(x_{nq}) = 0, \quad n = 1, 2, 3, \dots, \quad (55c)$$

is a consequence of the recurrence formula³

$$J_{q+1}(x) = \frac{q}{x} J_q(x) - J_q'(x). \quad (55d)$$

It then follows from Eq. (7b) that we may represent the delta function $\delta(\rho - \rho')$ with weight factor ρ' as

$$\frac{\delta(\rho - \rho')}{\rho'} = \sum_p \Phi_p(\rho) \Phi_p(\rho') = \frac{2}{b^2} \sum_{n=1}^{\infty} \frac{J_q(pp) J_q(pp')}{J_{q+1}^2(pb)}, \quad 0 \leq \rho \leq b, \quad (56a)$$

where

$$p = \frac{x_{nq}}{b}; \quad J_q(x_{nq}) = 0, \quad n = 1, 2, 3, \dots, \quad q \text{ fixed.} \quad (56b)$$

The two-dimensional delta function $\delta(\rho - \rho')$ can be represented in cylindrical coordinates as the product of $\delta(\rho - \rho')/\rho'$ and $\delta(\phi - \phi')$ since

$$1 = \int_S \delta(\rho - \rho') dS' = \int_0^\pi d\phi' \int_0^b d\rho' \rho' \frac{\delta(\rho - \rho')}{\rho'} \delta(\phi - \phi'), \quad \rho \text{ in } S. \quad (57)$$

Thus, for $0 \leq \phi \leq \varphi$, $0 \leq \rho \leq b$,

$$\begin{aligned} \delta(\rho - \rho') &= \sum_i \Phi_i(\rho) \Phi_i(\rho') \\ &= \frac{4}{\varphi b^2} \sum_{m=1}^{\infty} \sum_{n=1}^{\infty} \frac{\sin q\phi J_q(pp) \sin q\phi' J_q(pp')}{J_{q+1}^2(pb)}, \quad q = \frac{m\pi}{\varphi}, \quad p = \frac{x_{nq}}{b} \end{aligned} \quad (58a)$$

i.e.,

$$\Phi_i(\rho) = \frac{2}{b \sqrt{\varphi J_{q+1}(pb)}} \sin q\phi J_q(pp), \quad k_i'^2 = \left(\frac{x_{nq}}{b} \right)^2. \quad (58b)$$

H modes. The angular eigenfunctions for the H-mode problem are given in Eqs. (48). Upon following the same procedure as in Eqs. (52)–(55), one obtains, for the radial eigenfunctions,

$$\psi_p(\rho) = p \sqrt{\frac{2}{(pb)^2 - q^2}} \frac{J_q(pp)}{J_q(pb)}, \quad (59a)$$

where for q fixed,

$$p = \frac{x'_{nq}}{b}; \quad J_q'(x'_{nq}) = 0, \quad n = 1, 2, \dots, \quad (59b)$$

x'_{nq} being the n th positive zero of $J_q'(x)$. Thus, one may represent the two-dimensional delta function as

$$\begin{aligned}\delta(\mathbf{p} - \mathbf{p}') &= \sum_i \psi_i(\mathbf{p})\psi_i(\mathbf{p}'), \quad 0 \leq \frac{\rho}{\rho'} \leq b, \quad 0 \leq \frac{\phi}{\phi'} \leq \varphi, \\ &= \frac{2}{\varphi} \sum_{m=0}^{\infty} \sum_{n=1}^{\infty} \epsilon_m \frac{p^2}{[(pb)^2 - q^2]J_q^2(pb)} \cos q\phi J_q(pp) \cos q\phi' J_q(pp'), \\ q &= \frac{m\pi}{\varphi}, \quad p = \frac{x'_{nq}}{b},\end{aligned}\tag{60a}$$

i.e.,

$$\psi_i(\mathbf{p}) = \left[\frac{2\epsilon_m}{\varphi[(pb)^2 - q^2]} \right]^{1/2} \frac{p}{J_q(pb)} \cos q\phi J_q(pp), \quad k'^{1/2} = \left(\frac{x'_{nq}}{b} \right)^2,\tag{60b}$$

with $\epsilon_0 = 1$, $\epsilon_m = 2$ for $m \geq 1$.

Open angular sector

E modes. If the b dimension in Fig. 3.2.8 is allowed to become infinite, one approaches in the limit the wedge geometry of Fig. 3.2.9. To obtain the radial spectrum from that for the finite sector, we introduce into Eqs. (56) the change of variable

$$p \equiv \xi_n = \frac{x_{nq}}{b}.\tag{61a}$$

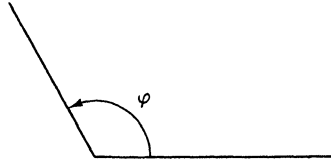


FIG. 3.2.9 Open angular sector.

As $b \rightarrow \infty$, the contributing terms in Eq. (56a) are those for which x_{nq} is large so that the asymptotic form for the Bessel function of large argument can be employed [see Eq. (4.2.22b)]:³

$$J_q(\xi_n b) \sim \sqrt{\frac{2}{\pi \xi_n b}} \cos \left(\xi_n b - \frac{q\pi}{2} - \frac{\pi}{4} \right), \quad b \rightarrow \infty,\tag{61b}$$

from which one obtains for the zeros $(\xi_n b)$ in Eq. (56b),

$$\xi_n b \sim \left(n + \frac{3}{4} \right) \pi + \frac{q\pi}{2}, \quad n = \text{large positive integer}.\tag{61c}$$

One notes that as $b \rightarrow \infty$, the discrete eigenvalues ξ_n coalesce into a continuum along the positive real axis. Also,

$$J_{q+1}(\xi_n b) \sim \sqrt{\frac{2}{\pi \xi_n b}} (-1)^n.\tag{61d}$$

If one defines the increment

$$\Delta\xi_n = \xi_{n+1} - \xi_n \sim \frac{\pi}{b}, \quad b \rightarrow \infty, \quad (61e)$$

then the radial delta function in Eq. (56a) transforms into

$$\begin{aligned} \frac{\delta(\rho - \rho')}{\rho'} &= \lim_{\Delta\xi_n \rightarrow 0} \sum_{\xi_n=0}^{\infty} \xi_n J_q(\xi_n \rho) J_q(\xi_n \rho') \Delta\xi_n = \int_0^{\infty} \xi J_q(\xi \rho) J_q(\xi \rho') d\xi, \\ 0 < \frac{\rho}{\rho'} &< \infty. \end{aligned} \quad (62)$$

The transform theorem associated with Eq. (62) is referred to as the Fourier-Bessel or Hankel transformation.³ The lack of a definite boundary condition on the eigenfunctions $\Phi_\xi(\rho) = \sqrt{\xi} J_q(\xi \rho)$ at $\rho \rightarrow \infty$ is a consequence of the limit-point singularity of the Bessel differential equation at this endpoint² [see the footnote to Eq. (3.3.21)].

The two-dimensional scalar representation theorem for the wedge-shaped region in Fig. 3.2.9 then becomes

$$\begin{aligned} \delta(\rho - \rho') &= \sum_i \Phi_i(\rho) \Phi_i(\rho'), \quad 0 < \frac{\rho}{\rho'} < \infty, \quad 0 < \frac{\phi}{\phi'} < \phi, \\ &= \frac{2}{\phi} \sum_{m=1}^{\infty} \int_0^{\infty} \xi \sin q\phi J_q(\xi \rho) \sin q\phi' J_q(\xi \rho') d\xi, \end{aligned} \quad (63a)$$

i.e.,

$$\begin{aligned} \Phi_i(\rho) &= \sqrt{\frac{2\xi}{\phi}} \sin q\phi J_q(\xi \rho), \quad q = \frac{m\pi}{\phi}, \quad m = 1, 2, \dots, \quad 0 < \xi < \infty; \\ k_{ii}^2 &= \xi^2. \end{aligned} \quad (63b)$$

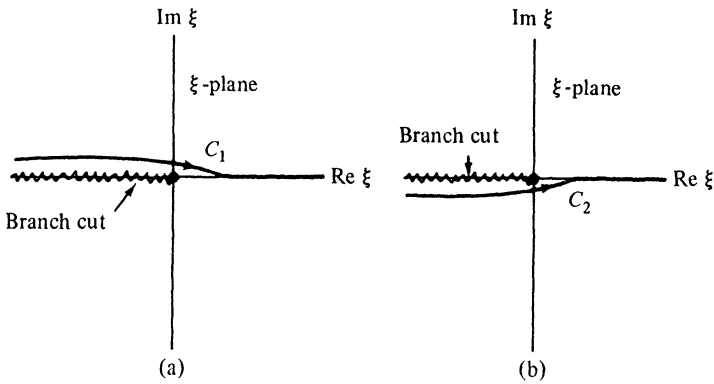
As in the transition from Eq. (36a) to the Fourier integral representation in Eq. (37a), it is often desirable to cast the Fourier-Bessel transform theorem in Eq. (62) into an alternative form in which the integration over ξ extends from $-\infty$ to $+\infty$. Upon introducing

$$J_q(\xi \rho) = \frac{1}{2} [H_q^{(1)}(\xi \rho) + H_q^{(2)}(\xi \rho)], \quad (64)$$

where $H_q^{(1,2)}(x)$ is the Hankel function of the first (second) kind of order q and argument x , one may write Eq. (62) as

$$\begin{aligned} \frac{\delta(\rho - \rho')}{\rho'} &= I_1 + I_2, \\ I_1 &= \frac{1}{2} \int_0^{\infty} \xi H_q^{(1)}(\xi \rho) J_q(\xi \rho') d\xi, \quad I_2 = \frac{1}{2} \int_0^{\infty} \xi H_q^{(2)}(\xi \rho) J_q(\xi \rho') d\xi. \end{aligned} \quad (65)$$

If the range of ξ is to be extended to $\xi = -\infty$, account must be taken in the integrands of I_1 and I_2 of the $\xi = 0$ branch-point singularity arising from the presence of the Hankel function [and also of the Bessel function in Eq. (62), since q is not integral]. To assure single-valuedness of the integrands when continued into the complex ξ plane, we introduce a branch cut along the negative real ξ axis (see Fig. 3.2.10). The following circuitual relations³ then provide the means for changing ξ into $-\xi$ ($0 < \xi < \infty$):

FIG. 3.2.10 Contours of integration in the complex ξ plane.

$$J_q(xe^{\pm j\pi}) = e^{\pm jq\pi} J_q(x), \quad (66a)$$

$$H_q^{(1)}(xe^{j\pi}) = -e^{-jq\pi} H_q^{(2)}(x), \quad H_q^{(2)}(xe^{-j\pi}) = -e^{jq\pi} H_q^{(1)}(x). \quad (66b)$$

Suppose we introduce the change of variable $\tilde{\xi} = \xi \exp(j\pi)$ in the integrand of I_2 in Eq. (65). Then

$$I_2 = \frac{1}{2} \int_0^{\infty e^{j\pi}} \tilde{\xi} H_q^{(2)}(\tilde{\xi} \rho e^{-j\pi}) J_q(\tilde{\xi} \rho' e^{-j\pi}) d\tilde{\xi}, \quad (67a)$$

$$= \frac{1}{2} \int_{-\infty e^{j\pi}}^0 \tilde{\xi} H_q^{(1)}(\tilde{\xi} \rho) J_q(\tilde{\xi} \rho') d\tilde{\xi}, \quad (67b)$$

where Eq. (67b) follows from Eq. (67a) upon use of Eqs. (66). Thus, Eq. (65) may be written as

$$\frac{\delta(\rho - \rho')}{\rho'} = \frac{1}{2} \int_{-\infty e^{j\pi}}^0 \tilde{\xi} H_q^{(1)}(\tilde{\xi} \rho) J_q(\tilde{\xi} \rho') d\tilde{\xi} = \frac{1}{2} \int_{-\infty e^{j\pi}}^0 \tilde{\xi} H_q^{(1)}(\tilde{\xi} \rho') J_q(\tilde{\xi} \rho) d\tilde{\xi}. \quad (68)$$

The contour of integration extends along the upper shore of the branch cut and the positive real axis as shown in Fig. (3.2.10a). The alternative expression, with ρ and ρ' interchanged, given by the second integral in Eq. (68), is deduced by representing $J_q(\xi \rho')$ in Eq. (62) in terms of the Hankel function combination in Eq. (64), and proceeding as above. It is noted that the spectral representation for the weighted delta function in Eq. (68) is not given in the Hermitean (complex-conjugate) form as in Eq. (7b), but rather in the “biorthogonal” form

$$\frac{\delta(\rho - \rho')}{\rho'} = \int_{-\infty e^{j\pi}}^0 \Phi_\xi(\rho) \bar{\Phi}_\xi(\rho') d\tilde{\xi}, \quad (68a)$$

$$\Phi_\xi(\rho) = \sqrt{\frac{\xi}{2}} J_q(\xi \rho), \quad \bar{\Phi}_\xi(\rho) = \sqrt{\frac{\xi}{2}} H_q^{(1)}(\xi \rho), \quad (68b)$$

where $\bar{\Phi}_\xi(\rho)$ represents an “adjoint” function.

In a completely analogous manner, one may proceed by introducing the new variable $\tilde{\xi} = \xi \exp(-j\pi)$ into I_1 of Eq. (65) and simplifying in accordance

with the circuital formulas in Eqs. (66) to obtain the representation

$$\frac{\delta(\rho - \rho')}{\rho'} = \frac{1}{2} \int_{-\infty e^{-j\pi}}^{\infty} \xi H_q^{(2)}(\xi\rho) J_q(\xi\rho') d\xi = \frac{1}{2} \int_{-\infty e^{-j\pi}}^{\infty} \xi H_q^{(2)}(\xi\rho') J_q(\xi\rho) d\xi \quad (69)$$

with the path of integration as shown in Fig. (3.2.10b).

The integral representations in Eqs. (68) and (69) permit deformation of the contours of integration into the complex ξ plane, results of which will be useful for subsequent function-theoretic manipulations. To show this, we examine the asymptotic behavior of the Bessel and Hankel functions for large values of their argument.³

$$J_q(w) \sim \sqrt{\frac{2}{\pi w}} \cos \left(w - \frac{q\pi}{2} - \frac{\pi}{4} \right), \quad |w| \rightarrow \infty, \quad -\pi < \arg w < \pi, \quad (70a)$$

$$H_q^{(1,2)}(w) \sim \sqrt{\frac{2}{\pi w}} \exp \left[\pm j \left(w - \frac{q\pi}{2} - \frac{\pi}{4} \right) \right], \quad |w| \rightarrow \infty, \quad -\pi < \arg w < \pi, \quad (70b)$$

where w is a complex variable whose argument lies between $-\pi$ and $+\pi$. If $\text{Im } w > 0$, the magnitude of $H_q^{(1)}(w)$ decays like $\exp(-\text{Im } w)$, while that of $J_q(w)$ increases like $\exp(\text{Im } w)$, so

$$|H_q^{(1)}(\xi\rho) J_q(\xi\rho')| \sim \frac{1}{\pi \sqrt{\rho\rho' |\xi|}} e^{-(\text{Im } \xi)(\rho - \rho')}, \quad |\xi| \rightarrow \infty, \quad 0 < \arg \xi < \pi. \quad (71)$$

For $\rho > \rho'$, the integrand of the first integral in Eq. (68) therefore decays exponentially over an infinite semicircle in the upper half of the complex ξ plane, while for $\rho < \rho'$, the integrand of the second integral exhibits a similar behavior. For a suitable class of functions representable by the transform theorem in Eq. (69), the contour C_1 in Fig. 3.2.10a can thus be deformed away from the real axis at $|\xi| \rightarrow \infty$ into a path C'_1 in the upper half of the ξ plane; in consequence, the delta function in Eq. (68) can be represented as

$$\frac{\delta(\rho - \rho')}{\rho'} = \frac{1}{2} \int_{C'_1} \xi H_q^{(1)}(\xi\rho) J_q(\xi\rho') d\xi, \quad 0 < \frac{\rho}{\rho'} < \infty, \quad (72)$$

where $\rho_<$ and $\rho_>$ denote the lesser and greater, respectively, of the quantities ρ and ρ' .

It should be emphasized that the above deformation of the contour C_1 into the contour C'_1 must be examined in detail when a function $F(\rho)$ is being represented. The representation for $F(\rho)$ becomes, via Eq. (68),

$$F(\rho) = \frac{1}{2} \int_{-\infty e^{j\pi}}^{\infty} \xi H_q^{(1)}(\xi\rho) \hat{\phi}(\xi) d\xi, \quad \hat{\phi}(\xi) = \int_0^{\infty} \rho' F(\rho') J_q(\xi\rho') d\rho'. \quad (72a)$$

Although it is assumed that the representation exists (integrals converge) and that $\hat{\phi}(\xi)$ is a regular function of ξ on the contour C_1 , $\hat{\phi}(\xi)$ may have singulari-

ties in the upper half of the ξ plane. The presence of such singularities (whether poles or branch points) must be taken into account in any path deformation. This aspect is given further attention in Sec. 3.3.

In a directly analogous manner, one may show that the delta-function representation in Eq. (69) involving the contour C_2 in Fig. (3.2.10b) can be expressed in terms of an integral over the contour C'_2 in the lower half of the ξ plane as

$$\frac{\delta(\rho - \rho')}{\rho'} = \frac{1}{2} \int_{C'_2} \xi H_q^{(2)}(\xi \rho_>) J_q(\xi \rho_<) d\xi, \quad 0 < \frac{\rho}{\rho'} < \infty, \quad (73)$$

with similar remarks applying to contour deformation when a function $F(\rho)$ is being represented.

H modes. Upon going to the limit $b \rightarrow \infty$ in Eq. (60a) in a manner analogous to that employed in Eqs. (61) and (62), one finds that the radial eigenfunctions $\psi_\xi(\rho)$ become identical with $\Phi_\xi(\rho)$ so that the delta-function representation in Eq. (62) applies here as well. This lack of dependence of the eigenfunctions for the infinite interval $b \rightarrow \infty$ on the boundary conditions at the finite endpoint b is a consequence of the limit-point type of singularity at $\rho \rightarrow \infty$. Thus, one obtains

$$\begin{aligned} \delta(\rho - \rho') &= \sum_i \psi_i(\rho) \psi_i(\rho'), \quad 0 < \frac{\phi}{\phi'} < \varphi, \quad 0 < \frac{\rho}{\rho'} < \infty, \\ &= \frac{1}{\varphi} \sum_m^{\infty} \int_0^{\infty} \xi \epsilon_m \cos q\phi J_q(\xi \rho) \cos q\phi' J_q(\xi \rho') d\xi, \end{aligned} \quad (74a)$$

i.e.,

$$\begin{aligned} \psi_i(\rho) &= \sqrt{\frac{\epsilon_m \xi}{\varphi}} \cos q\phi J_q(\xi \rho), \quad q = \frac{m\pi}{\varphi}, \quad m = 0, 1, 2, \dots, \quad 0 < \xi < \infty; \\ k''_i &= \xi^2, \quad \epsilon_m = \begin{cases} 1, & m = 0, \\ 2, & m \geq 1. \end{cases} \end{aligned} \quad (74b)$$

Circular waveguide

The eigenfunctions for the circular waveguide region shown in Fig. 3.2.11 differ from those for the finite angular sector in Fig. 3.2.8 only in that the one-dimensional eigenfunctions for the ϕ domain are those given in Eqs. (50) instead of Eqs. (47) and (48). The results can then be written down directly from Eqs. (56) and (59) for E and H modes, respectively.

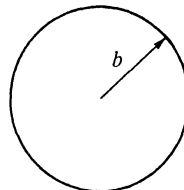


FIG. 3.2.11 Circular waveguide.

E modes

$$\begin{aligned}\delta(\rho - \rho') &= \sum_i \Phi_i(\rho) \Phi_i^*(\rho'), \quad 0 \leq \frac{\phi}{\phi'} \leq 2\pi, \quad 0 \leq \frac{\rho}{\rho'} \leq \infty, \\ &= \frac{1}{\pi b^2} \sum_{m=-\infty}^{\infty} \sum_{n=1}^{\infty} \frac{e^{-jm\phi} J_m(p\rho) e^{jm\phi'} J_m(p\rho')}{J_{m+1}^2(pb)},\end{aligned}\quad (75a)$$

where

$$p = \frac{x_{nm}}{b}; \quad J_m(x_{nm}) = 0, \quad n = 1, 2, \dots.$$

Thus,

$$\begin{aligned}\Phi_i(\rho) &= \frac{1}{b \sqrt{\pi} J_{m+1}(pb)} e^{-jm\phi} J_m(p\rho), \quad m = 0, \pm 1, \pm 2, \dots, \\ n &= 1, 2, \dots; \quad k_{ii}'^2 = \left(\frac{x_{nm}}{b}\right)^2.\end{aligned}\quad (75b)$$

H modes

$$\begin{aligned}\delta(\rho - \rho') &= \sum_i \psi_i(\rho) \psi_i^*(\rho') \\ &= \frac{1}{\pi} \sum_{m=-\infty}^{\infty} \sum_{n=1}^{\infty} \frac{p^2}{[(pb)^2 - m^2] J_m^2(pb)} e^{-jm\phi} J_m(p\rho) e^{jm\phi'} J_m(p\rho'),\end{aligned}\quad (76a)$$

where

$$p = \frac{x'_{nm}}{b}; \quad J'_m(x'_{nm}) = 0, \quad n = 1, 2, \dots.$$

Thus,

$$\begin{aligned}\psi_i(\rho) &= \frac{p}{\sqrt{\pi} [(pb)^2 - m^2] J_m(pb)} e^{-jm\phi} J_m(p\rho), \quad m = 0, \pm 1, \pm 2, \dots, \\ n &= 1, 2, \dots; \quad k_{ii}'^2 = \left(\frac{x'_{nm}}{b}\right)^2.\end{aligned}\quad (76b)$$

Although the radial eigenfunctions $\Phi_q(\rho)$ and $\psi_q(\rho)$ in Eqs. (56) and (59) were obtained on the assumption that $q > 0$, the extension of the above to negative integer values of q follows from the relation

$$J_m(x) = (-1)^m J_{-m}(x), \quad m = 0, 1, 2, \dots. \quad (77)$$

Free space

The free-space region in Fig. 3.2.5 can be analyzed in a polar-coordinate representation upon letting $b \rightarrow \infty$ in Fig. 3.2.11. The *E*- and *H*-mode problems become identical in this case, so

$$\begin{aligned}\delta(\rho - \rho') &= \sum_i \Phi_i(\rho) \Phi_i^*(\rho') = \sum_i \psi_i(\rho) \psi_i^*(\rho'), \quad 0 < \frac{\phi}{\phi'} \leq 2\pi, \quad 0 \leq \frac{\rho}{\rho'} < \infty, \\ &= \frac{1}{2\pi} \sum_{m=-\infty}^{\infty} \int_0^{\infty} \xi e^{-jm\phi} J_m(\xi\rho) e^{jm\phi'} J_m(\xi\rho') d\xi,\end{aligned}\quad (78a)$$

i.e.,

$$\Phi_i(\rho) = \psi_i(\rho) = \sqrt{\frac{\xi}{2\pi}} e^{-jm\phi} J_m(\xi\rho), \quad m = 0, \pm 1, \pm 2, \dots, \\ 0 < \xi < \infty, \quad k_{ii}^2 = \xi^2. \quad (78b)$$

Alternatively, one may employ the radial delta function representation in Eqs. (68) or (69) instead of the symmetric form (62) implied above.

3.2d Inhomogeneously Filled Cross Sections

Transverse field equations and modal representations

The representation of electromagnetic fields in uniform waveguide regions filled with a homogeneous medium has been discussed in Sec. 2.2 and has led to the eigenvalue problems in Secs. 3.2b and 3.2c. In this section we consider the more general problem wherein the cross-sectional medium is inhomogeneous (i.e., the dielectric constant ϵ and the permeability μ are functions of the cross-sectional variable ρ). To derive the transverse field equations for this case, one modifies the procedure of Sec. 2.2 since $\epsilon = \epsilon(\rho)$, $\mu = \mu(\rho)$. Instead of Eqs. (2.2.4) and (2.2.5), one has for a suppressed time dependence $\exp(j\omega t)$:

$$-\frac{\partial \mathbf{E}_t}{\partial z} = j\omega \left(\mu \mathbf{1} + \frac{1}{\omega^2} \nabla_t \cdot \frac{1}{\epsilon} \nabla_t \right) \cdot \mathbf{H}_t \times \mathbf{z}_0 + \mathbf{M}_{te} \times \mathbf{z}_0, \quad (79a)$$

$$\mathbf{M}_{te} = \mathbf{M}_t - \frac{1}{j\omega} \nabla_t \times \frac{\mathbf{J}_z}{\epsilon}, \quad (79b)$$

$$-\frac{\partial \mathbf{H}_t}{\partial z} = j\omega \left(\epsilon \mathbf{1} + \frac{1}{\omega^2} \nabla_t \cdot \frac{1}{\mu} \nabla_t \right) \cdot \mathbf{z}_0 \times \mathbf{E}_t + \mathbf{z}_0 \times \mathbf{J}_{te}, \quad (79c)$$

$$\mathbf{J}_{te} = \mathbf{J}_t + \frac{1}{j\omega} \nabla_t \times \frac{\mathbf{M}_z}{\mu}. \quad (79d)$$

Although Eqs. (79) are valid even in the general case $\epsilon = \epsilon(\rho, z)$, $\mu = \mu(\rho, z)$, the restriction to variation only in the cross section permits the use of simple field representations with z -independent vector-mode functions.

As in Sec. 2.2, it is assumed that the transverse electromagnetic fields defined by Eqs. (79) can be represented in terms of complete sets of transverse vector modes, characterizing the possible guided waves that can be propagated along the z direction:

$$\mathbf{E}_t(\mathbf{r}) = \sum_i V_i(z) \mathbf{e}_i(\rho), \quad (80a)$$

$$\mathbf{H}_t(\mathbf{r}) = \sum_i I_i(z) \mathbf{h}_i(\rho). \quad (80b)$$

In contrast to the homogeneous medium, the transverse vector-mode functions \mathbf{e}_i and \mathbf{h}_i , in general, are not related via $\mathbf{h}_i = \mathbf{z}_0 \times \mathbf{e}_i$ as in Eqs. (2.2.8e); moreover, no separability into E and H modes relative to the z direction exists (see Sec. 8.2 for a treatment of arbitrary media).

To determine vector modes $\mathbf{e}_i(\rho)$ and $\mathbf{h}_i(\rho)$, which constitute the transverse z -independent parts of the three-dimensional mode fields $\mathbf{E}_i(\mathbf{r})$ and $\mathbf{H}_i(\mathbf{r})$, we observe that the latter represent solutions of the source-free Maxwell field equations

$$\nabla \times \mathbf{E}_i(\mathbf{r}) = -j\omega\mu\mathbf{H}_i(\mathbf{r}), \quad \nabla \times \mathbf{H}_i(\mathbf{r}) = j\omega\epsilon\mathbf{E}_i(\mathbf{r}). \quad (81)$$

Since ϵ and μ are z independent, a typical mode field propagating in the $+z$ direction is characterized by a z -dependence $\exp(-jk_i z)$, so one may write

$$\mathbf{E}_i(\mathbf{r}) = \mathcal{E}_i(\rho)e^{-jk_i z}, \quad \mathbf{H}_i(\mathbf{r}) = \mathcal{H}_i(\rho)e^{-jk_i z}. \quad (82a)$$

The transverse mode functions \mathbf{e}_i and \mathbf{h}_i are then identified as

$$\mathbf{E}_i(\mathbf{r}) = \mathbf{e}_i(\rho)e^{-jk_i z}, \quad \mathbf{H}_i(\mathbf{r}) = Y_i \mathbf{h}_i(\rho)e^{-jk_i z}, \quad (82b)$$

where the characteristic admittance $Y_i = 1/Z_i$ is introduced as a convenient normalization parameter, to obtain the \mathbf{e}_i and \mathbf{h}_i relations previously derived in Sec. 2.2 for ϵ and μ constant. The defining equations for the eigenfunctions \mathbf{e}_i and \mathbf{h}_i and corresponding eigenvalue κ_i are obtained upon substituting Eqs. (82) into the source-free transverse field equations (79):

$$Z_i \kappa_i \mathbf{e}_i = \omega \left(\mu \mathbf{1} + \frac{1}{\omega^2} \nabla_t \cdot \frac{1}{\epsilon} \nabla_t \right) \cdot \mathbf{h}_i \times \mathbf{z}_0, \quad (83a)$$

$$Y_i \kappa_i \mathbf{h}_i = \omega \left(\epsilon \mathbf{1} + \frac{1}{\omega^2} \nabla_t \cdot \frac{1}{\mu} \nabla_t \right) \cdot \mathbf{z}_0 \times \mathbf{e}_i. \quad (83b)$$

On the perfectly conducting cross-section boundary s , \mathbf{e}_i and \mathbf{h}_i satisfy the boundary conditions

$$\mathbf{v} \times \mathbf{e}_i = 0 = \nabla_t \cdot (\mathbf{h}_i \times \mathbf{z}_0) \quad \text{on } s. \quad (83c)$$

In the previously considered case of constant ϵ and μ , Eqs. (83) were decoupled by letting $\mathbf{h}_i = \mathbf{z}_0 \times \mathbf{e}_i$; this choice leads to two separate and essentially scalar eigenvalue problems for E and H modes given in Eqs. (2.2.10) and (2.3.2), with Z_i and Y_i defined as in Eqs. (2.2.15). No such simplification obtains in this more general case. However, if the transverse cross-sectional configuration is describable by separable coordinates and the variability of ϵ and μ depends only on a single transverse coordinate, it is sometimes possible to decouple Eqs. (83) into two scalar eigenvalue problems. For the case of rectangular waveguide containing a dielectric stratified along one of the transverse coordinates, this procedure is illustrated below. It may be noted that Eqs. (83a) and (83b) and hence \mathbf{e}_i and \mathbf{h}_i are unchanged if Y_i and κ_i are replaced by $-Y_i$ and $-\kappa_i$, respectively; $-Y_i$ and $-\kappa_i$ describe a field traveling in the $-z$ direction [see Eq. (82b)].

Upon use of the transverse form of Green's theorem [see Eq. (2.2.11a)],

$$\begin{aligned} & \iint_s dS \left[\mathbf{A}_i \cdot \nabla_t \left(\frac{1}{\epsilon} \nabla_t \cdot \mathbf{A}_j^* \right) - \mathbf{A}_j^* \cdot \nabla_t \left(\frac{1}{\epsilon} \nabla_t \cdot \mathbf{A}_i \right) \right] \\ &= \oint_s ds \frac{1}{\epsilon} [(\mathbf{A}_i \cdot \mathbf{v})(\nabla_t \cdot \mathbf{A}_j^*) - (\mathbf{A}_j^* \cdot \mathbf{v})(\nabla_t \cdot \mathbf{A}_i)], \\ & \mathbf{A}_{i,j} = \mathbf{h}_{i,j} \times \mathbf{z}_0, \end{aligned} \quad (84)$$

and Eqs. (83a) and (83c), one deduces the following relation between the mode functions (ϵ and μ are assumed real so that the waveguide is non-dissipative):

$$Z_j^* \kappa_j^* \iint_S \mathbf{h}_i \times \mathbf{z}_0 \cdot \mathbf{e}_j^* dS = Z_i \kappa_i \iint_S \mathbf{h}_j^* \cdot \mathbf{z}_0 \times \mathbf{e}_i dS. \quad (85a)$$

By changing ϵ into μ and $\mathbf{h}_{i,j}$ into $-\mathbf{e}_{i,j}$ in Eq. (84), one obtains, via Eqs. (83b) and (83c), the dual relation

$$Y_j^* \kappa_j^* \iint_S \mathbf{z}_0 \times \mathbf{e}_i \cdot \mathbf{h}_j^* dS = Y_i \kappa_i \iint_S \mathbf{z}_0 \times \mathbf{e}_j^* \cdot \mathbf{h}_i dS, \quad (85b)$$

and, from combining Eqs. (85a) and (85b),

$$(\kappa_j^{*2} - \kappa_i^2) \iint_S \mathbf{h}_i \times \mathbf{z}_0 \cdot \mathbf{e}_j^* dS = 0. \quad (85c)$$

If $i = j$ in Eq. (85c), the integral is non-vanishing and represents the complex power carried by a typical mode. To satisfy the equation in this case, it is necessary that $\kappa_j^2 = \kappa_i^{*2}$ so that κ_j^2 is real. The appearance of κ_j^2 in Eq. (85c) implies the existence of propagation constants $\pm \kappa_j$ and is indicative of the z reflection symmetry in this configuration. Upon choosing an appropriate normalization, we may therefore write the biorthogonality relation between \mathbf{e}_i and \mathbf{h}_i for the non-degenerate case ($\kappa_i \neq \kappa_j$ when $i \neq j$) as

$$\iint_S \mathbf{h}_i \times \mathbf{z}_0 \cdot \mathbf{e}_j^* dS = \delta_{ij} \quad (\text{non-dissipative case}). \quad (86)$$

The orthogonality property in Eq. (86) permits the simple evaluation of the modal amplitudes in Eqs. (80) as

$$V_i(z) = \iint_S \mathbf{E}_i(\mathbf{r}) \cdot \mathbf{h}_i^*(\mathbf{p}) \times \mathbf{z}_0 dS, \quad (87a)$$

$$I_i(z) = \iint_S \mathbf{H}_i(\mathbf{r}) \cdot \mathbf{z}_0 \times \mathbf{e}_i^*(\mathbf{p}) dS. \quad (87b)$$

Multiplication of Eqs. (79a) and (79b) by $\mathbf{h}_i^* \times \mathbf{z}_0$ and $\mathbf{z}_0 \times \mathbf{e}_i^*$, respectively, integration over the cross-sectional domain S , reduction of the resulting integrals involving the gradient operators via Eqs. (83) and (84), and use of Eqs. (87) finally leads to transmission-line equations for the determination of V_i and I_i :

$$-\frac{dV_i}{dz} = j\kappa_i Z_i I_i + v_i, \quad (88a)$$

$$-\frac{dI_i}{dz} = j\kappa_i Y_i V_i + i_i, \quad (88b)$$

where

$$v_i(z) = \iint_S \mathbf{M}_{te}(\mathbf{r}) \cdot \mathbf{h}_i^*(\mathbf{p}) dS = \iint_S \mathbf{M}(\mathbf{r}) \cdot \mathbf{h}_i^*(\mathbf{p}) dS + Z_i^* \iint_S \mathbf{J}(\mathbf{r}) \cdot \mathbf{e}_{zi}^*(\mathbf{p}) dS, \quad (89a)$$

$$Z_i \mathbf{e}_{zi}(\mathbf{p}) = z_0 \frac{\nabla_t \cdot \mathbf{h}_t \times \mathbf{z}_0}{j\omega\epsilon}, \quad (89b)$$

and

$$i_i(z) = \iint_S \mathbf{J}_{te}(\mathbf{r}) \cdot \mathbf{e}_i^*(\mathbf{p}) dS = \iint_S \mathbf{J}(\mathbf{r}) \cdot \mathbf{e}_i^*(\mathbf{p}) dS + Y_i^* \iint_S \mathbf{M}(\mathbf{r}) \cdot \mathbf{h}_{zi}^*(\mathbf{p}) dS, \quad (89c)$$

$$Y_i \mathbf{h}_{zi}(\mathbf{p}) = z_0 \frac{\nabla_t \cdot \mathbf{z}_0 \times \mathbf{e}_i}{j\omega\mu}. \quad (89d)$$

The expressions for the source terms in Eqs. (89a) and (89c) are derived upon use of the integration-by-parts formula (2.2.13) and the specification $J_z = 0$ on the perfectly conducting boundary s . As in the analogous equations (2.2.14), no assumption concerning the differentiability of J_z/ϵ and M_z/μ , implied initially in Eqs. (79), is required. It is noted that the mode amplitudes V_i and I_i are determined from the solution of the uniform transmission-line equations (88) as for the case of homogeneously filled waveguide cross sections.

Evaluation of vector-mode functions by transverse transmission analysis

As for the homogeneously filled waveguide regions discussed in Chapter 2, field solutions in waveguides with inhomogeneously filled cross sections may be synthesized via Eqs. (80) from knowledge of the modal amplitudes $V_i(z)$ and $I_i(z)$ and the transverse vector-mode functions $\mathbf{e}_i(\mathbf{p})$ and $\mathbf{h}_i(\mathbf{p})$. The former satisfy the transmission-line equations (88), whereas the latter are defined by Eqs. (83). Solutions of vector field problems such as those in Eqs. (83) are facilitated if scalar potentials can be introduced; the vector partial differential field equations are transformed thereby into more easily treated scalar equations. Such a scalarization procedure has been employed in Sec. 2.3a for reduction of the vector eigenfunction equations (2.2.10) in homogeneously filled regions and has led to the decomposition of a general vector field into E and H modes with respect to z . As noted in connection with Eqs. (80), this procedure is inapplicable when the waveguide medium depends on the cross-sectional coordinates; in fact, it does not seem possible to scalarize the vector eigenvalue problem in the general case of inhomogeneously filled cross sections. Scalarization can, however, be achieved for special cross-sectional configurations, included among which are rectangular waveguides filled with a medium whose properties depend only on one of the cross-sectional coordinates, x . In this practical case one may decompose the field into E and H modes with respect to x ; although these modes are characterized by $H_x \equiv 0$ and $E_x \equiv 0$, respectively, they are in general “hybrid” with respect to z (i.e., they possess z components of both the electric and magnetic field).

In the solution of the constituent eigenvalue problems, it is convenient to view the cross-sectional region as a resonant transmission line, as was noted in Sec. 2.4e. To illustrate the “transverse transmission” method for determining

mode functions, we consider first the homogeneously filled rectangular cross section. Although this simple configuration is analyzed more easily by the conventional E - and H -mode decomposition with respect to z as in Secs. 2.3a and 3.2b, the transverse transmission analysis yields an alternative set of modes, hybrid with respect to z , comprised of a superposition of conventional E and H modes. The hybrid modes satisfy the orthogonality condition in Eq. (86) and are not characterized by the simple conventional relation $\mathbf{h}_i = \mathbf{z}_0 \times \mathbf{e}_i$. Considerations for the homogeneously filled cross section are then generalized to the inhomogeneous case for which scalarization cannot be achieved by the method of Sec. 2.2.

Homogeneous cross section

Referring to Fig. 3.2.12, we seek to evaluate mode fields characteristic of propagation along the z axis with a dependence $\exp(-jk_z z)$, with the wave-number k_z to be determined. Viewed in terms of transverse propagation, the configuration in Fig. 3.2.12 can be regarded as a parallel plate waveguide in the

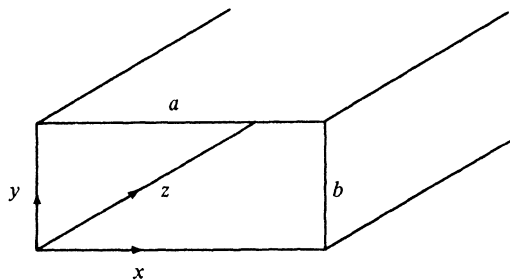


FIG. 3.2.12 Infinite rectangular waveguide.

x direction, terminated in short circuits at $x = 0$ and $x = a$. For a typical parallel-plate-guide mode, the transverse (to x) vector-mode functions (E modes and H modes with respect to x) have the form

$$\bar{\mathbf{e}}_T(y, z) = \bar{\mathbf{e}}_T(y)e^{-jk_z z} = [\mathbf{y}_0 \bar{e}_y(y) + \mathbf{z}_0 \bar{e}_z(y)]e^{-jk_z z}, \quad (90a)$$

$$\bar{\mathbf{h}}_T(y, z) = \bar{\mathbf{h}}_T(y)e^{-jk_z z} = [\mathbf{y}_0 \bar{h}_y(y) + \mathbf{z}_0 \bar{h}_z(y)]e^{-jk_z z}, \quad (90b)$$

$$\bar{\mathbf{h}}_T = \mathbf{x}_0 \times \bar{\mathbf{e}}_T, \quad (90c)$$

where the bar $\bar{}$ denotes quantities relating to the x transmission analysis, and the subscript T distinguishes vectors transverse to x ; the mode index i has been suppressed and \mathbf{x}_0 , \mathbf{y}_0 , and \mathbf{z}_0 are unit vectors along the x , y , and z directions. The mode functions $\bar{\mathbf{e}}_T$ and $\bar{\mathbf{h}}_T$ are derivable directly from Eqs. (41b) and (42b) (with x , a , y , η replaced by y , b , z , κ , respectively) and Eqs. (2.3.1) (with ∇_r , \mathbf{z}_0 replaced by ∇_r , \mathbf{x}_0). The transverse (to x) electric and magnetic mode fields can thus be represented as

$$\mathbf{E}_T(x, y, z) = \bar{V}(x)\bar{\mathbf{e}}_T(y)e^{-j\kappa z}, \quad (91a)$$

$$\mathbf{H}_T(x, y, z) = \bar{I}(x)\bar{\mathbf{h}}_T(y)e^{-j\kappa z}, \quad (91b)$$

while the x components of the fields are given by [see Eqs. (2.2.6)]

$$E_x(x, y, z) = \frac{1}{j\omega\epsilon} \nabla_T \cdot (\mathbf{H}_T \times \mathbf{x}_0) = \frac{\bar{I}(x)}{j\omega\epsilon} e^{-j\kappa z} \bar{\nabla}_T \cdot \bar{\mathbf{e}}_T(y), \quad (91c)$$

$$H_x(x, y, z) = \frac{1}{j\omega\mu} \nabla_T \cdot (\mathbf{x}_0 \times \mathbf{E}_T) = \frac{\bar{V}(x)}{j\omega\mu} e^{-j\kappa z} \bar{\nabla}_T \cdot \bar{\mathbf{h}}_T(y), \quad (91d)$$

where

$$\nabla_T = \mathbf{y}_0 \frac{\partial}{\partial y} + \mathbf{z}_0 \frac{\partial}{\partial z}, \quad \bar{\nabla}_T = \mathbf{y}_0 \frac{\partial}{\partial y} - j\kappa \mathbf{z}_0. \quad (91e)$$

$\bar{V}(x)$ and $\bar{I}(x)$ are the resonant transmission-line solutions discussed at the end of Sec. 3.2b.

The desired mode functions $\mathbf{e}(x, y)$ and $\mathbf{h}(x, y)$ corresponding to propagation in the z direction are obtained upon comparing Eqs. (91) with the alternative representation of the fields transverse to z :

$$\mathbf{E}_t(x, y, z) = V(z)\mathbf{e}(x, y) = \frac{1}{N} e^{-j\kappa z} \mathbf{e}(x, y), \quad (92a)$$

$$\mathbf{H}_t(x, y, z) = I(z)\mathbf{h}(x, y) = \frac{1}{NZ_0} e^{-j\kappa z} \mathbf{h}(x, y). \quad (92b)$$

Since we seek a traveling-wave solution in the z direction, the choice

$$V(z) = Z_0 I(z) = \frac{1}{N} e^{-j\kappa z}, \quad (92c)$$

has been made, with Z_0 representing the as yet unspecified characteristic impedance and N a normalization constant indicative of the arbitrary amplitude associated with the resonant solutions $\bar{V}(x)$ and $\bar{I}(x)$. Comparison of Eqs. (91) and (92) yields

$$\mathbf{e}(x, y) = N \left[\mathbf{x}_0 \frac{\bar{I}(x)}{j\omega\epsilon} \bar{\nabla}_T \cdot \bar{\mathbf{e}}_T(y) + \mathbf{y}_0 \bar{V}(x) \bar{e}_y(y) \right], \quad (93a)$$

$$\mathbf{h}(x, y) = NZ_0 \left[\mathbf{x}_0 \frac{\bar{V}(x)}{j\omega\mu} \bar{\nabla}_T \cdot \bar{\mathbf{h}}_T(y) + \mathbf{y}_0 \bar{I}(x) \bar{h}_y(y) \right]. \quad (93b)$$

Since all mode quantities (except N and Z_0) in Eqs. (93) are known, it is evident that the mode functions are solely dependent on the transmission-line solutions $\bar{V}(x)$ and $\bar{I}(x)$. In the simple example appropriate to the configuration in Fig. 3.2.12, the transverse transmission-line solutions are

$$\bar{V}(x) = \sin px, \quad p \equiv k_x \equiv \frac{m\pi}{a}, \quad (94a)$$

$$\bar{I}(x) = \frac{1}{-jk_x Z_0} \frac{d\bar{V}(x)}{dx} = j\bar{Y}_0 \cos px,$$

with

$$\bar{Y}_0 = \begin{cases} \frac{\omega\epsilon}{p} & \text{for } E \text{ modes in } x, \\ \frac{p}{\omega\mu} & \text{for } H \text{ modes in } x. \end{cases} \quad (94b)$$

The propagation constant κ of the mode propagating in the z direction is given by

$$\kappa = \sqrt{k^2 - k_t^2} = \sqrt{k^2 - k_x^2 - k_y^2}, \quad k_x = p = \frac{m\pi}{a}, \quad k_y = \frac{n\pi}{b}, \quad (94c)$$

where k_y is the originally given eigenvalue for the y domain of the parallel-plate configuration. It is noted that

$$\begin{aligned} \bar{\nabla}_T \cdot \bar{\mathbf{e}}_T(y) &= 0 && \text{for } H \text{ modes along } x, \\ \bar{\nabla}_T \cdot \bar{\mathbf{h}}_T(y) &= 0 && \text{for } E \text{ modes along } x, \end{aligned} \quad (94d)$$

while, from Eqs. (90) and (91),

$$\begin{aligned} E_z(x, y, z) &= \bar{V}(x)\bar{e}_z(y)e^{-j\kappa z}, \\ H_z(x, y, z) &= \bar{I}(x)\bar{h}_z(y)e^{-j\kappa z}. \end{aligned} \quad (94e)$$

The total vector-mode fields whose transverse parts are given by $\mathbf{e}(x, y)$ and $\mathbf{h}(x, y)$ in Eqs. (93) separate naturally into E and H modes along x but contain, in general, both E_z and H_z components. Moreover, $\mathbf{h} \neq \mathbf{z}_0 \times \mathbf{e}$, and the orthogonality properties are those given in Eq. (86). While N is chosen to achieve orthonormality of the mode set, the choice of Z_0 is a matter of convenience. If $\partial/\partial y \equiv 0$ in Eqs. (93) and $\bar{e}_z = 0 = \bar{h}_y$, then one notes that $\mathbf{h} = \mathbf{z}_0 \times \mathbf{e}$ provided that $Z_0\kappa/\omega\mu = 1$. The corresponding modes are H modes with respect to both the x and z directions, Z_0 is the conventional H mode characteristic impedance [see Eq. (2.2.15d)], and the \mathbf{e} - and \mathbf{h} -mode functions can be made identical with those in Eqs. (2.3.1).

Inhomogeneous cross section

To generalize the preceding results, we consider the evaluation of the vector-mode functions when the rectangular waveguide configuration in Fig. 3.2.1 is filled with a medium whose dielectric constant ϵ and permeability μ are x dependent [i.e., $\epsilon = \epsilon(x)$ and $\mu = \mu(x)$]. As mentioned previously, this structure cannot, in general, be described in terms of the conventional E and H modes with respect to the z direction. However, an analysis in terms of E and H modes with respect to the x coordinate can be carried out since the separability of the Maxwell field equations into transverse and longitudinal parts, and the subsequent derivation of the transmission-line equations, is not affected by a variability of the medium along the x transmission coordinate (see Sec. 2.2). Thus, the transverse (to x) and the x components of the electric and magnetic fields for a typical mode can be expressed as in Eqs. (91), leading to the transverse (to z) vector mode functions $\mathbf{e}(x, y)$ and $\mathbf{h}(x, y)$ in Eqs. (93), provided that $\bar{V}(x)$ and

$\tilde{I}(x)$ satisfy the source-free transmission-line equations (2.2.15) descriptive of a variable medium:

$$-\frac{dV(x)}{dx} = jk_x(x)Z(x)I(x), \quad (95a)$$

$$-\frac{dI(x)}{dx} = jk_x(x)Y(x)V(x), \quad Y(x) = \frac{1}{Z(x)}, \quad (95b)$$

where k_x denotes the propagation constant in the x direction. The bar $\bar{\cdot}$ has been omitted for convenience.

Second-order differential equations for either $V(x)$ or $I(x)$ are obtained from the two coupled first-order differential equations in Eq. (95) as

$$\frac{d}{dx} \left[\frac{1}{k_x(x)Z(x)} \frac{dV(x)}{dx} \right] + k_x(x)Y(x)V(x) = 0, \quad (96a)$$

$$\frac{d}{dx} \left[\frac{1}{k_x(x)Y(x)} \frac{dI(x)}{dx} \right] + k_x(x)Z(x)I(x) = 0. \quad (96b)$$

Since, from Eqs. (2.2.15),

$$k_x(x)Z(x) = \omega\mu(x) \quad \text{for } H \text{ modes in } x, \quad (97a)$$

$$k_x(x)Y(x) = \omega\epsilon(x) \quad \text{for } E \text{ modes in } x, \quad (97b)$$

the differential equations (96a) and (96b) have a simple form when applied, respectively, to H modes and E modes. Thus, the resonant transmission-line solutions are defined by:

H modes (along x)

$$\left[\mu(x) \frac{d}{dx} \frac{1}{\mu(x)} \frac{d}{dx} + k_x''(x) \right] V''(x) = 0, \quad k_x''(x) = \omega^2 \mu(x)\epsilon(x) - k_T''^2, \quad (98a)$$

$$V''(0) = V''(a) = 0. \quad (98b)$$

I'' is determined from a knowledge of V'' via

$$I''(x) = \frac{1}{-j\omega\mu(x)} \frac{dV''(x)}{dx}, \quad (98c)$$

E modes (along x)

$$\left[\epsilon(x) \frac{d}{dx} \frac{1}{\epsilon(x)} \frac{d}{dx} + k_x''(x) \right] I'(x) = 0, \quad k_x''(x) = \omega^2 \mu(x)\epsilon(x) - k_T''^2, \quad (99a)$$

$$\frac{dI'(x)}{dx} = 0 \quad \text{at } x = 0, a, \quad (99b)$$

with

$$V'(x) = \frac{1}{-j\omega\epsilon(x)} \frac{dI'(x)}{dx}. \quad (99c)$$

The primes and double primes distinguish E - and H -mode quantities on the

x -directed transmission line. The resonance (eigenvalue) problems above are of the general form discussed in Sec. 3.2a.

We note again that the vector-mode fields obtained on substitution of the above H - and E -mode resonance solutions from Eqs. (98) and (99) into Eqs. (91) are characterized by the vanishing of E_x and H_x , respectively, but they possess, in general, both E_z and H_z components.

3.3 CHARACTERISTIC GREEN'S FUNCTION (RESOLVENT) PROCEDURE AND ALTERNATIVE REPRESENTATIONS

For finite intervals and piecewise constant p , q , and w , the mode spectrum associated with the general Sturm-Liouville eigenvalue problem of Eqs. (3.2.1) is discrete.¹ Hence, the direct solution of these equations as well as the subsequent normalization of the eigenfunctions f_m in Eq. (3.2.5b) are straightforward. Moreover, the superposition of all possible discrete solutions constitutes a complete set of functions as noted in Eq. (3.2.7b). However, for open intervals and singular p , q , or w , which may admit continuous mode spectra, the direct solution of the eigenvalue problem offers difficulties; boundary conditions on f_m at singular endpoints are often ill defined, normalization of the now improper mode functions [see Eq. (3.2.28b)] may become formidable, and completeness of the modal set is not evident. To circumvent these problems, the normalized continuous mode spectra for a number of open configurations have been deduced in Sec. 3.2 as a limiting case of the known discrete spectra for corresponding finite domains in which one of the dimensions becomes infinite. In this section we examine an alternative and direct procedure for the determination of both discrete and continuous complete sets of modal representations.

The present method exploits an intimate relation between source-free (eigenvalue) solutions and the characteristic Green's function. In network terms, the eigenvalue problem defines the resonant voltage or current waves on a terminated non-uniform transmission line while the Green's function displays the similar resonant responses to excitation by a point voltage or current generator; these analogies are useful in subsequent discussion. After a description of the general procedure in Sec. 3.3a, construction of Green's functions for the Sturm-Liouville problem is given in Sec. 3.3b.

The theory of one-dimensional characteristic Green's functions facilitates consideration of alternative representations for two- and three-dimensional electromagnetic (or acoustic) fields. As noted in Sec. 2.3, electromagnetic field solutions for a variety of closed and open regions can be constructed via guided-wave representations along a preferred direction z . Such representations are predicated upon the availability of E - and H -mode eigenfunctions $\Phi_i(\rho)$ and $\psi_i(\rho)$ for separable cross sections transverse to z (Secs. 3.2 and 3.4) and the ability to determine the corresponding z -dependent modal amplitudes. For field calculations in certain parameter ranges, alternative representations are often desired since their convergence properties may be better than those for the z -

guided formulation. These observations have already been made in Sec. 1.5 and have been illustrated there for simple space- and time-dependent field representations either in space-guided or time-guided form. It has been shown that one representation may be derived from another by function-theoretic techniques involving analytic continuation and contour deformation in the complex plane. These function-theoretic aspects are treated naturally and concisely by use of one-dimensional characteristic Green's functions as shown in Sec. 3.3c. The method is illustrated in detail for three-dimensional scalar Green's functions in rectangular or cylindrical geometries, and more briefly for spherical regions.

3.3a Relation between Characteristic Green's Function and Eigenvalue Problems

The characteristic Green's function $g(x, x'; \lambda)$ for the Sturm-Liouville problem of Eqs. (3.2.1) is defined by the equation^{4,5}

$$\left[\frac{d}{dx} p(x) \frac{d}{dx} - q(x) + \lambda w(x) \right] g(x, x'; \lambda) = -\delta(x - x'), \quad x_1 < x' < x_2, \quad (1)$$

subject to the boundary conditions

$$\left(p \frac{d}{dx} + \alpha_{1,2} \right) g(x, x'; \lambda) = 0, \quad x = x_{1,2}. \quad (1a)$$

The parameter λ is arbitrary but so restricted as to assure a unique solution of Eqs. (1); discussion of these restrictions is deferred until later. The distinction between characteristic Green's functions and the modal Green's functions discussed in Sec. 2.4 is that the parameter λ is left unspecified for the former.

A network schematization of the characteristic Green's function problem

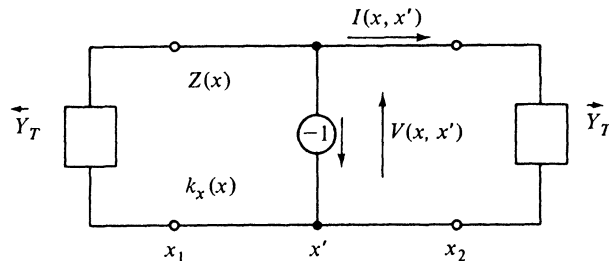


FIG. 3.3.1 Non-uniform transmission line excited with a unit current generator.

is shown in Fig. 3.3.1. The voltage and current on this transmission line satisfy the non-uniform transmission-line equations (3.2.95) with the addition of a current source term $i(x') = -\delta(x - x')$ [see Eqs. (2.3.10) or (2.4.15)].[†]

[†]When referring to wave solutions, a time-dependence $\exp(+j\omega t)$ will be used in this section.

$$-\frac{dV(x, x')}{dx} = jk_x(x)Z(x)I(x, x'), \quad (2a)$$

$$-\frac{dI(x, x')}{dx} = jk_x(x)Y(x)V(x, x') - \delta(x - x'), \quad (2b)$$

where $Z(x) = 1/Y(x)$ and $k_x(x)$ are the characteristic impedance and propagation constant. For an H -mode transmission line with distinguishing double-prime superscripts, $k''_x Z'' = \omega\mu$, so the corresponding second-order differential equation for $V''(x, x')$ has the form [see Eq. (3.2.98a)]

$$\left\{ \frac{d}{dx} \left[\frac{1}{\mu'(x)} \frac{d}{dx} \right] + k_0^2 \epsilon'(x) - \frac{k_T'^2}{\mu'(x)} \right\} V''(x, x') = -j\omega\mu_0 \delta(x - x'), \quad (3)$$

where $k_0^2 = \omega^2 \mu_0 \epsilon_0$ and

$$\mu'(x) = \frac{\mu(x)}{\mu_0}, \quad \epsilon'(x) = \frac{\epsilon(x)}{\epsilon_0}, \quad (3a)$$

μ_0 and ϵ_0 being convenient constant reference values for the permeability and dielectric constant, respectively. Upon comparing Eqs. (1) and (3) one makes the identifications:

$$\begin{aligned} p(x) &= w(x) = \frac{1}{\mu'(x)}, & q(x) &= -k_0^2 \epsilon'(x), & k_T'^2 &= -\lambda, \\ V''(x, x') &= j\omega\mu_0 g''(x, x'; \lambda). \end{aligned} \quad (4)$$

The boundary conditions in Eq. (1a) are rephrased by Eqs. (2a) and (4) in terms of

$$\frac{I''}{V''} = j \frac{p(dg''/dx)}{\omega\mu_0 g''}, \quad (5a)$$

and replaced by terminating admittances \vec{Y}_T'' and \overleftarrow{Y}_T'' at x_1 and x_2 :

$$\overleftarrow{Y}_T'' = -\frac{I''(x_1, x')}{V''(x_1, x')} = \frac{j\alpha_1}{\omega\mu_0}, \quad \vec{Y}_T'' = \frac{I''(x_2, x')}{V''(x_2, x')} = \frac{-j\alpha_2}{\omega\mu_0}. \quad (5b)$$

The behavior of g and dg/dx in the vicinity of the source at $x = x'$ is readily inferred from the network representation in Fig. 3.3.1. V'' is continuous across the current generator, i.e.,†

$$V''(x, x')|_{x' - \Delta}^{x' + \Delta} = 0, \quad \Delta \rightarrow 0, \quad (6a)$$

while the discontinuity in the current is given by

$$I''(x, x')|_{x' - \Delta}^{x' + \Delta} = 1. \quad (6b)$$

Thus, the corresponding conditions on g are

$$g''(x, x'; \lambda)|_{x' - \Delta}^{x' + \Delta} = 0, \quad p(x) \frac{d}{dx} g''(x, x'; \lambda)|_{x' - \Delta}^{x' + \Delta} = -1. \quad (6c)$$

†Note that $f(x)|_a^b = f(b) - f(a)$.

For the *E*-mode problem denoted by prime superscripts, $k'_x Y' = \omega\epsilon$, and the current $I'(x, x')$ is the most readily determined quantity [see Eqs. (3.2.99)]. The appropriate network problem, dual to that in Fig. 3.3.1, is shown in Fig. 3.3.2. Network equations and their connection with the characteristic Green's function are obtained upon making the following duality replacements in Eqs. (3)-(6):

$$V'' \rightarrow I', \quad I'' \rightarrow V', \quad \mu' \leftrightarrow \epsilon', \quad \mu_0 \leftrightarrow \epsilon_0, \quad k''_T \rightarrow k'_T, \quad Y''_T \rightarrow Z'_T, \quad g'' \rightarrow g'. \quad (7)$$

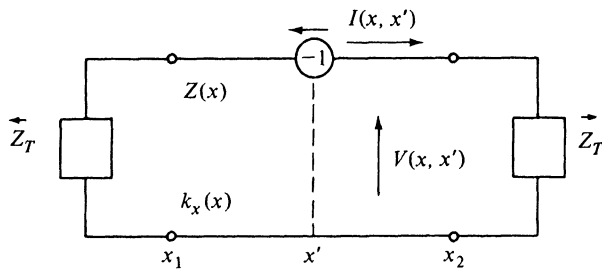


FIG. 3.3.2. Non-uniform transmission line excited with a unit voltage generator.

Since the configuration in Fig. 3.3.1 (or Fig. 3.3.2) can be viewed as a cavity (lossless if jY_T , jY_R , k_x^2 , and Z^2 are real), it is physically manifest that the voltage (or current) response g will be finite and well defined unless the choice of parameter λ is such that a resonance can exist. For fixed values of $\alpha_{1,2}$ and $x_{1,2}$, resonances will exist for parameter values λ_m at which the corresponding voltage or current will be infinite. To assure a unique solution of the network problem it is therefore necessary to restrict the parameter λ in Eq. (1) so that $\lambda \neq \lambda_m$. For the lossless situation, denoted mathematically as the Hermitian case wherein the resonant values λ_m are real [see Eq. (3.2.2)], this restriction can be stated more weakly as $\text{Im } \lambda \neq 0$. If λ in Eq. (1) is now regarded as a general complex parameter, $g(x, x'; \lambda)$ is a regular function of λ in the complex λ plane except at points $\lambda = \lambda_m$, where it becomes infinite and possesses simple pole singularities. Since the resonant condition $\lambda = \lambda_m$ implies the persistence of a response even when the source is removed, the functional form of the resonant solution satisfies the homogeneous equation (3.2.1). Thus, information about the desired eigensolutions of Eq. (3.2.1) is contained in the singularities of the characteristic Green's function g , and the problem of determining all possible resonances (i.e., a complete set of eigenfunctions) is directly related to the complete investigation of the singularities of $g(x, x'; \lambda)$ in the complex λ plane. In the above discussion it has been assumed that the dimensions x_1 and x_2 are finite so that cavity resonances, which occur for discrete values of λ_m , characterize simple pole singularities of g . If one of the dimensions becomes infinite, or if p , q , or w possesses a singularity, the discrete resonances may coalesce into a continuous spectrum;

in this instance, $g(x, x'; \lambda)$ possesses a branch-point singularity giving rise to the necessity of introducing a branch cut in the complex λ plane to ensure uniqueness of g .

To relate the complete eigenmode set f_m in Eq. (3.2.1) to the characteristic Green's function in Eq. (1), it will be assumed for the moment that the mode set is known so that any suitable function $F(x)$ can be represented as in Eqs. (3.2.6). In particular, $g(x, x'; \lambda)$ can be represented as

$$g(x, x'; \lambda) = \sum_m g_m(x'; \lambda) f_m(x), \quad x_1 < x < x_2, \quad (8a)$$

where

$$g_m(x', \lambda) = \int_{x_1}^{x_2} w(\xi) f_m^*(\xi) g(\xi, x'; \lambda) d\xi. \quad (8b)$$

Upon substituting Eq. (8a) into Eq. (1), utilizing the delta-function representation from Eq. (3.2.7b), interchanging the orders of summation and differentiation, employing Eq. (3.2.1), and equating like coefficients of the (linearly independent) eigenfunctions f_m on both sides of the equation, one obtains

$$g_m(x', \lambda) = -\frac{f_m^*(x')}{\lambda - \lambda_m}, \quad (9)$$

so, from Eq. (8a),

$$g(x, x'; \lambda) = -\sum_m \frac{f_m(x) f_m^*(x')}{\lambda - \lambda_m}. \quad (10)$$

This representation for g highlights the existence of singularities in the complex λ plane at the resonant (eigen) values λ_m .

If Eq. (10) is integrated in the complex λ plane about a contour C enclosing all the singularities of g , then an application of Cauchy's theorem yields the following formal relation [see Eq. (3.2.7b)]:

$$\begin{aligned} -\frac{1}{2\pi j} \oint_C g(x, x'; \lambda) d\lambda &= -\sum_m f_m(x) f_m^*(x') \left(-\frac{1}{2\pi j} \oint_C \frac{d\lambda}{\lambda - \lambda_m} \right) \\ &= \sum_m f_m(x) f_m^*(x') = \frac{\delta(x - x')}{w(x')}, \end{aligned} \quad (11a)$$

i.e.,[†]

$$\frac{\delta(x - x')}{w(x')} = -\frac{1}{2\pi j} \oint_C g(x, x'; \lambda) d\lambda. \quad (11b)$$

The integration is carried out in the positive (counterclockwise) sense. Although the restriction $\lambda \neq \lambda_m$ has been imposed to yield a unique solution of Eq. (1),

[†]An alternative proof of Eq. (11b) follows from Eq. (1) on multiplication by $1/\lambda$ and integration over a closed contour C such that

$$\oint_C \left[\frac{d}{dx} p \frac{d}{dx} - q \right] \frac{g(x, x', \lambda)}{\lambda} d\lambda$$

vanishes.⁶

this solution can be extended by analytic continuation to apply as $\lambda \rightarrow \lambda_m$. The procedure sketched above has assumed the presence of simple pole singularities of g (i.e., a discrete spectrum of eigenvalues). Equation (11b) can also be employed when g has branch-point singularities representative of a continuous spectrum; in this case, the integration contour must lie on the “spectral sheet” of the complex λ plane, whereon g decays as $|\lambda| \rightarrow \infty$.^{4,6} Moreover, the technique may apply to problems with dissipative media or boundaries (non-Hermitian case with p , q , w , or $\alpha_{1,2}$ not real) for which the eigenvalues λ_m may be complex. In this instance, $f_m^*(x')$ in the delta-function representation of Eq. (11) is generally replaced by an adjoint function $\bar{f}_m(x')$.

Thus, the problem of finding a complete orthonormal set of functions is reduced systematically to determining the solution of the corresponding inhomogeneous differential equation (1), completely investigating its singularities, and then inferring the desired representation theorem by carrying out the contour integration in Eq. (11) about all the singularities of the characteristic Green’s function in the complex λ plane. After discussing a general procedure for evaluation of g in the next section, the above technique will be illustrated in Sec. 3.4 by various examples.

3.3b Construction of the Characteristic Green’s Function

The characteristic H -mode Green’s function can be constructed from a knowledge of the two solutions $\vec{V}(x)$ and $\vec{\bar{V}}(x)$ of the homogeneous equation (1) satisfying the required boundary conditions at x_1 and x_2 , respectively:

$$\left(\frac{d}{dx} p \frac{d}{dx} - q + \lambda w \right) \vec{V}(x) = 0, \quad \left(p \frac{d}{dx} + \alpha_1 \right) \vec{V} = 0 \quad \text{at } x = x_1, \quad (12a)$$

$$\left(\frac{d}{dx} p \frac{d}{dx} - q + \lambda w \right) \vec{\bar{V}}(x) = 0, \quad \left(p \frac{d}{dx} + \alpha_2 \right) \vec{\bar{V}} = 0 \quad \text{at } x = x_2. \quad (12b)$$

The solution for g satisfying Eqs. (1) when $x \neq x'$ and the required continuity condition at $x = x'$ [see Eq. (6c)] is thus

$$g''(x, x'; \lambda) = A \vec{V}(x_<) \vec{\bar{V}}(x_>), \quad (13a)$$

The symbol V (voltage) has been retained to emphasize the network interpretation of the Green’s function, and $x_<$ or $x_>$ denote, respectively, the lesser and greater of the quantities x and x' ; the double prime on V , distinctive of an H -mode problem, has been omitted. The constant A must be so determined as to satisfy the jump condition (6c) on $p \, dg/dx$ (i.e., the current) at $x = x'$:

$$Ap(x') \left[\vec{V}(x') \frac{d}{dx'} \vec{\bar{V}}(x') - \vec{\bar{V}}(x') \frac{d}{dx'} \vec{V}(x') \right] = -1. \quad (13b)$$

Thus,

$$g''(x, x'; \lambda) = \frac{\vec{V}(x_<) \vec{\bar{V}}(x_>)}{-p W(\vec{V}, \vec{\bar{V}})}, \quad (14a)$$

where W is the Wronskian determinant,

$$W(\overleftarrow{V}, \overrightarrow{V}) = \left(\overleftarrow{V} \frac{d\overrightarrow{V}}{dx} - \overrightarrow{V} \frac{d\overleftarrow{V}}{dx} \right). \quad (14b)$$

If one multiplies Eq. (12a) by \overrightarrow{V} and Eq. (12b) by \overleftarrow{V} , and subtracts the resulting equations, one finds

$$0 = \overleftarrow{V} \frac{d}{dx} p \frac{d\overrightarrow{V}}{dx} - \overrightarrow{V} \frac{d}{dx} p \frac{d\overleftarrow{V}}{dx} = \frac{d}{dx} [pW(\overleftarrow{V}, \overrightarrow{V})], \quad (15a)$$

so

$$pW(\overleftarrow{V}, \overrightarrow{V}) = \text{constant for all } x, \quad (15b)$$

and can be evaluated at any convenient point x_0 in the interval $x_1 \leq x \leq x_2$. Upon introducing homogeneous solutions of Eqs. (12), $\overleftarrow{V}(x, x_0)$ and $\overrightarrow{V}(x, x_0)$, normalized to unity at x_0 ,

$$\overleftarrow{V}(x, x_0) = \frac{\overleftarrow{V}(x)}{\overleftarrow{V}(x_0)}, \quad \overrightarrow{V}(x, x_0) = \frac{\overrightarrow{V}(x)}{\overrightarrow{V}(x_0)}, \quad (15c)$$

and recalling Eqs. (5), one may write the Green's function solution in Eq. (14a) as

$$g''(x, x'; \lambda) = \frac{\overleftarrow{V}(x_<, x_0) \overrightarrow{V}(x_>, x_0)}{j\omega\mu_0 \overleftrightarrow{Y}(x_0)}, \quad (16)$$

where $\overleftrightarrow{Y}(x_0)$ denotes the sum of the admittances seen looking to the left and right from x_0 :

$$\overleftrightarrow{Y}(x_0) = \overrightarrow{Y}(x_0) + \overleftarrow{Y}(x_0) = \frac{\overrightarrow{I}(x_0)}{\overrightarrow{V}(x_0)} + \frac{\overleftarrow{I}(x_0)}{\overleftarrow{V}(x_0)}, \quad \overleftrightarrow{I}(x_0) = \pm \frac{p}{j\omega\mu_0} \frac{d\overleftrightarrow{V}}{dx} \Big|_{x_0}. \quad (16a)$$

Although we have employed network notation for the convenience of those familiar with such concepts, it should be noted that the network identifications in the derivation of $g(x, x'; \lambda)$ via Eqs. (12)–(16) et seq. are not essential.

The above considerations for non-uniform transmission lines are generalizations of those carried out in Sec. 2.4 for uniform transmission lines. It is noted that the resonant condition determining the singularities of g in the complex λ plane is given as in Eq. (2.4.36) by

$$\overleftrightarrow{Y}(x_0) \equiv \overleftrightarrow{Y}(x_0, \lambda_m) = 0, \quad (17)$$

where the dependence on λ has been indicated explicitly. The Green's function representation in Eq. (16) can be cast into a form analogous to that in Eq. (2.4.28) if one introduces standing-wave solutions $c(x, x_0)$ and $s(x, x_0)$ (regular in the complex λ plane) satisfying the homogeneous equation

$$\left(\frac{d}{dx} p \frac{d}{dx} - q + \lambda w \right) \frac{c(x, x_0)}{s(x, x_0)} = 0, \quad (18)$$

with the boundary conditions

$$\begin{aligned} c(x_0, x_0) &= 1, & s(x_0, x_0) &= 0, \\ p(x_0)c'(x_0, x_0) &= 0, & p(x_0)s'(x_0, x_0) &= 1, \end{aligned} \quad (18a)$$

where the prime denotes the derivative with respect to the first argument of c and s [i.e., $c'(x_0, x_0) \equiv (d/dx)c(x, x_0)|_{x=x_0}$]. For the uniform transmission line in Sec. 2.4, $\mu' = \epsilon' = 1$ [i.e., $p = w = 1$, $q = -k_0^2$, $c(x, x_0) = \cos k_{x_0}(x - x_0)$, $s(x, x_0) = (1/k_{x_0}) \sin k_{x_0}(x - x_0)$ with $k_{x_0}^2 = k_0^2 - \lambda = k_0^2 - k_T^2$]. In analogy to Eqs. (2.4.22a) and (2.4.22c) we may write

$$\vec{V}(x, x_0) = c(x, x_0) - j\omega\mu_0 \vec{Y}(x_0)s(x, x_0), \quad (19a)$$

whence, by Eq. (2a),

$$\omega\mu_0 \vec{I}(x, x_0) = jp(x)c'(x, x_0) + \omega\mu_0 p(x)\vec{Y}(x_0)s'(x, x_0). \quad (19b)$$

Equations (19) can be employed to deduce the relation between the admittance at x_0 and the terminal admittance \vec{Y}_T'' at x_2 in Eq. (5b):

$$\omega\mu_0 \vec{Y}(x_0) = \frac{jp(x_0)c'(x_0, x_2) + \omega\mu_0 p(x_0)\vec{Y}_T''s'(x_0, x_2)}{c(x_0, x_2) - j\omega\mu_0 \vec{Y}_T''s(x_0, x_2)}. \quad (20)$$

Similarly,[†]

$$\overleftarrow{V}(x, x_0) = c(x, x_0) + j\omega\mu_0 \overleftarrow{Y}(x_0)s(x, x_0), \quad (21a)$$

and

$$-\omega\mu_0 \overleftarrow{Y}(x_0) = \frac{jp(x_0)c'(x_0, x_1) - \omega\mu_0 p(x_0)\overleftarrow{Y}_T''s'(x_0, x_1)}{c(x_0, x_1) + j\omega\mu_0 \overleftarrow{Y}_T''s(x_0, x_1)}. \quad (21b)$$

The expression for the characteristic Green's function in Eq. (16) can now be written in the general form analogous to that in Eq. (2.4.28), which is particularly useful for the analysis of stratified regions:[‡]

$$\begin{aligned} g''(x, x'; \lambda) &= [c(x_<, x_0) + j\omega\mu_0 \overleftarrow{Y}(x_0)s(x_<, x_0)][c(x_>, x_0) - j\omega\mu_0 \vec{Y}(x_0)s(x_>, x_0)] \\ &\quad \overline{j\omega\mu_0 \vec{Y}(x_0)} \end{aligned} \quad (22)$$

[†]If x_1 or x_2 are singular points of the differential equations (12), the necessity or not, of specifying a boundary condition may be assessed from the dependence of $\vec{Y}(x_0)$ on \vec{Y}_T . If $\vec{Y}(x_0)$ is independent of the terminating admittance at the singular point ("limit-point" condition), requirement of a finite solution at x_1 or x_2 suffices.⁴

[‡]In the absence of stratification, it may be more convenient to use Eq. (14a) directly.

Since for the resonant values λ_m of λ one has

$$\overleftrightarrow{Y}(x_0, \lambda_m) = \overleftarrow{Y}(x_0, \lambda_m) + \overrightarrow{Y}(x_0, \lambda_m) = 0, \quad (23a)$$

the distinction between \overleftarrow{V} and \overrightarrow{V} in the expressions in the numerator of Eq. (22) can be suppressed so that each bracketed expression satisfies simultaneously the boundary conditions at x_1 and x_2 . Thus, the discrete H -mode eigenfunctions $\psi_m(x)$ (if they occur) have the form

$$\begin{aligned} \psi_m(x) &= A_m \overleftarrow{V}(x, x_0; \lambda_m) = A_m \overrightarrow{V}(x, x_0; \lambda_m) \\ &= A_m [c(x, x_0; \lambda_m) + j\omega\mu_0 \overleftarrow{Y}(x_0, \lambda_m) s(x, x_0; \lambda_m)], \quad x_1 \leq x \leq x_2 \end{aligned} \quad (23b)$$

where A_m is a normalization constant, and the dependence of all functions on λ_m has been exhibited explicitly.

A virtue of the characteristic Green's function procedure is that the mode set, obtained via the integration in Eq. (11b), is automatically normalized; the classical normalization procedure, as illustrated in Eq. (3.2.53) et seq., can become quite cumbersome if the eigenfunctions have a complicated form. If the only singularities of g in Eq. (16) [or Eq. (22)] in the complex λ plane are simple poles situated at the zeros λ_m of $\overleftrightarrow{Y}(x_0)$, then the behavior of the denominator in the neighborhood of a typical zero at λ_m is given by the Taylor series expansion

$$\overleftrightarrow{Y}(x_0, \lambda) = \overleftrightarrow{Y}(x_0, \lambda_m) + (\lambda - \lambda_m) \frac{\partial}{\partial \lambda_m} \overleftrightarrow{Y}(x_0, \lambda_m) + \dots, \quad (24a)$$

where

$$\frac{\partial}{\partial \lambda_m} \overleftrightarrow{Y}(x_0, \lambda_m) \equiv \frac{\partial}{\partial \lambda} \overleftrightarrow{Y}(x_0, \lambda)|_{\lambda=\lambda_m}. \quad (24b)$$

From Eqs. (11), (4), and (16), one thus has the following delta-function representation for the H -mode problem (in the non-dissipative case):

$$\mu'(x)\delta(x - x') = -\frac{1}{2\pi j} \oint_C g''(x, x'; \lambda) d\lambda = \sum_m \hat{\psi}_m(x) \hat{\psi}_m^*(x') \quad (25a)$$

$$= -\frac{1}{2\pi j} \oint_C \frac{\overleftarrow{V}(x_<, x_0; \lambda) \overrightarrow{V}(x_>, x_0; \lambda)}{j\omega\mu_0 \overleftrightarrow{Y}(x_0, \lambda)} d\lambda \quad (25b)$$

$$\begin{aligned} &= \sum_m \frac{\overleftarrow{V}(x_<, x_0; \lambda_m) \overleftarrow{V}^*(x_>, x_0; \lambda_m)}{-j\omega\mu_0(\partial/\partial \lambda_m) \overleftrightarrow{Y}(x_0, \lambda_m)} \frac{1}{2\pi j} \oint_C \frac{d\lambda}{\lambda - \lambda_m} \\ &= \sum_m \frac{\overleftarrow{V}(x, x_0; \lambda_m) \overleftarrow{V}^*(x', x_0; \lambda_m)}{\omega\mu_0(\partial/\partial \lambda_m) \overleftrightarrow{B}(x_0, \lambda_m)}, \quad \overleftrightarrow{Y} = j\overleftrightarrow{B}. \end{aligned} \quad (25c)$$

The normalized mode functions $\hat{\psi}_m(x)$ are therefore given by

$$\hat{\psi}_m(x) = \frac{1}{\sqrt{\omega\mu_0(\partial/\partial\lambda_m)\vec{B}(x_0, \lambda_m)}} \vec{V}(x, x_0; \lambda_m). \quad (25d)$$

A typical contour of integration in the complex λ plane is sketched in Fig. 3.3.3. The caret has been introduced to emphasize that the $\hat{\psi}_m$ are the scalar eigenfunctions appropriate to an H mode decomposition with respect to the transverse (x) coordinate. The vector eigenfunctions relative to the z direction are obtained as in Sec. 3.2d. For non-dissipative configurations, the eigenvalues

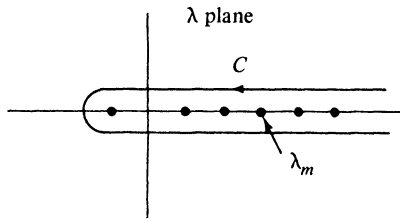


FIG. 3.3.3 Contour of integration.

λ_m and the susceptance function \vec{B} are real, so that, in view of Eq. (21a), the eigenfunctions $\hat{\psi}_m(x)$ are also real. However, an alternative representation employing the traveling-wave solutions in Eqs. (28), instead of the standing-wave functions in Eqs. (18), leads as in Eq. (25a) to a delta-function representation involving complex-conjugate functions $\hat{\psi}_m^*(x')$ [see Eqs. (3.2.76)]. These possibilities are illustrated by the examples in Sec. 3.4.

For the E -mode problem, a corresponding representation theorem is deduced upon use of the duality relations in Eq. (7). The E -mode characteristic Green's function $g'(x, x'; \lambda)$ is given by [see Eq. (16)]

$$g'(x, x'; \lambda) = \frac{\vec{I}(x_<, x_0) \vec{I}(x_>, x_0)}{j\omega\epsilon_0 \vec{Z}(x_0)}, \quad \vec{Z}(x_0) = \vec{Z}(x_0) + \vec{Z}(x_0), \quad (26)$$

where the primes, distinctive of the E -mode problem, have been omitted from \vec{I} and the total impedance function $\vec{Z}(x_0)$ [see the footnote for (Eq. 22)]. By duality with Eqs. (19)–(21),

$$\vec{I}(x, x_0) = c(x, x_0) \mp j\omega\epsilon_0 \vec{Z}(x_0) s(x, x_0) \quad (26a)$$

and

$$\pm \omega\epsilon_0 \vec{Z}(x_0) = \frac{j p(x_0) c'(x_0, x_{2,1}) \pm \omega\epsilon_0 p(x_0) \vec{Z}_T s'(x_0, x_{2,1})}{c(x_0, x_{2,1}) \mp j\omega\epsilon_0 \vec{Z}_T s(x_0, x_{2,1})}. \quad (26b)$$

The eigenvalues λ_m are specified implicitly by the resonance equation

$$\vec{Z}(x_0, \lambda_m) = 0, \quad (26c)$$

and the delta function can be represented in terms of the E -mode eigenfunctions $\hat{\Phi}_m$ as

$$\begin{aligned} \epsilon'(x)\delta(x - x') &= -\frac{1}{2\pi j} \oint_C g'(x, x'; \lambda) d\lambda = \sum_m \hat{\Phi}_m(x) \hat{\Phi}_m^*(x') \\ &= \sum_m \frac{\vec{I}(x, x_0; \lambda_m) \vec{I}^*(x, x_0; \lambda_m)}{\omega \epsilon_0 (\partial/\partial \lambda_m) \vec{X}(x_0, \lambda_m)}, \quad \vec{Z} = j \vec{X}. \end{aligned} \quad (27)$$

Thus, the discrete orthonormal E -mode eigenfunctions $\hat{\Phi}_m$ are given by

$$\hat{\Phi}_m(x) = \frac{1}{\sqrt{\omega \epsilon_0 (\partial/\partial \lambda_m) \vec{X}(x_0, \lambda_m)}} \vec{I}(x, x_0; \lambda_m), \quad x_1 \leq x \leq x_2, \quad (27a)$$

with \vec{I} taken from Eq. (26a).

It is sometimes convenient to deal with modal reflection coefficients instead of modal impedances. The appropriate generalizations of the uniform line relations (2.4.12) are obtained on writing

$$V(x) = V_+(x) + V_-(x) = V_+(1 + \vec{\Gamma}_v) = V_-(1 + \vec{\Gamma}_v), \quad (28a)$$

$$I(x) = I_+(x) + I_-(x) = I_+(1 + \vec{\Gamma}_i) = I_-(1 + \vec{\Gamma}_i), \quad (28b)$$

where the subscripts $+$ and $-$ on V or I denote wave components traveling in the $+x$ and $-x$ directions, respectively, and $\vec{\Gamma}_v(\vec{\Gamma}_i)$ are the voltage (current) reflection coefficients seen when looking along the $\pm x$ directions:

$$\vec{\Gamma}_v = \frac{V_{\mp}}{V_{\pm}}, \quad \vec{\Gamma}_i = \frac{I_{\mp}}{I_{\pm}}. \quad (28c)$$

If $\vec{\zeta} = V_+/I_+$ denotes the input impedance of a matched transmission line looking in the $+x$ direction, and $\vec{\zeta} = -V_-/I_-$ represents the corresponding quantity for the $-x$ direction, then

$$\vec{\Gamma}_i = -\frac{\vec{\zeta}}{\vec{\zeta}} \vec{\Gamma}_v, \quad \vec{\Gamma}_v = -\frac{\vec{\zeta}}{\vec{\zeta}} \vec{\Gamma}_i, \quad (29a)$$

and

$$\begin{aligned} \vec{Z}(x) &= \vec{\zeta}(x) \frac{1 + \vec{\Gamma}_v(x)}{1 - \frac{\vec{\zeta}(x)}{\vec{\zeta}(x)} \vec{\Gamma}_v(x)}, \quad \vec{Z}(x) = \vec{\zeta}(x) \frac{1 + \vec{\Gamma}_v(x)}{1 - \frac{\vec{\zeta}(x)}{\vec{\zeta}(x)} \vec{\Gamma}_v(x)}. \end{aligned} \quad (29b)$$

Conversely,

$$\vec{\Gamma}_v(x) = \frac{\vec{Z}(x)}{\frac{\vec{\zeta}(x)}{\vec{Z}(x)} + 1}, \quad \overleftarrow{\Gamma}_v(x) = \frac{\overleftarrow{Z}(x)}{\frac{\overleftarrow{\zeta}(x)}{\overleftarrow{Z}(x)} + 1}. \quad (29c)$$

The transverse resonance relation

$$\vec{Z}(x) + \overleftarrow{Z}(x) = 0$$

can then be expressed alternatively as

$$\vec{\Gamma}_v(x)\overleftarrow{\Gamma}_v(x) = 1 = \vec{\Gamma}_I(x)\overleftarrow{\Gamma}_I(x). \quad (30)$$

The above traveling-wave formulation leads to a set of eigenfunctions alternative to that in Eq. (27).

3.3c Alternative Representations

The theory of alternative Green's function representations, alluded to at the beginning of Sec. 3.3, is best discussed in conjunction with the one-dimensional characteristic Green's functions introduced in Sec. 3.3a. The starting point is provided by the completeness theorem in Eq. (11) relating the characteristic Green's function to a complete orthonormal set of eigenfunctions via an integration in the "characteristic" complex plane. We consider first uniform waveguide regions describable in a (ρ, z) coordinate system, and then summarize corresponding results for spherical waveguides. To extend the considerations of Sec. 3.3a to two-dimensional eigenfunctions $\Phi_i(\rho)$ of the form

$$\Phi_i(\rho) = \Phi_p(u)\Phi_q(v), \quad \rho = (u, v), \quad (31)$$

where $\Phi_p(u)$ and $\Phi_q(v)$ are one-dimensional orthonormal functions in separable u and v coordinate spaces transverse to z , we note from Sec. 3.2 that the completeness relation for the $\Phi_i(\rho)$ is as follows:

$$\delta(\rho - \rho') = \frac{\delta(u - u')\delta(v - v')}{h_u h_v} = \sum_i \Phi_i(\rho)\Phi_i^*(\rho') \quad (32a)$$

$$= \sum_p \Phi_p(u)\Phi_p^*(u') \sum_q \Phi_q(v)\Phi_q^*(v'), \quad (32b)$$

where the curvilinear metric parameters h_u and h_v in Eq. (32a) are defined via the relation $dS = h_u h_v du dv$, dS being an area element in the cross section. Then from Eq. (11) applied to the u -dependent functions,

$$\begin{aligned} \frac{\delta(u - u')}{h_u} &= \sum_p \Phi_p(u)\Phi_p^*(u') = \frac{1}{2\pi j} \sum_p \oint_{C_u} \frac{\Phi_{\lambda_p}(u)\Phi_{\lambda_p}^*(u')}{\lambda_u - \lambda_p} d\lambda_u \\ &= -\frac{1}{2\pi j} \oint_{C_u} g_u(u, u'; \lambda_u) d\lambda_u, \end{aligned} \quad (33)$$

where $\Phi_{\lambda_p} \equiv \Phi_p$, g_u is the characteristic Green's function associated with the

eigenvalue problem in the u domain, and the contour C_u in the complex λ_u plane encloses in the positive sense all the singularities (poles or branch points, with associated branch cuts) of g_u . The first representation in Eq. (33), involving the discrete or continuous sum over the eigenvalues λ_p , results on evaluation of the contour integral from the singularities of g_u , the contour integral being the more general form of the completeness relation. On employing the analogue of Eq. (33) for the v domain,

$$\frac{\delta(v - v')}{h_v} = \sum_q \Phi_q(v)\Phi_q^*(v') = -\frac{1}{2\pi j} \oint_{C_v} g_v(v, v'; \lambda_v) d\lambda_v \quad (34)$$

with C_v defined similarly to C_u , one has

$$\delta(\rho - \rho') = \left[-\frac{1}{2\pi j} \oint_{C_u} g_u(u, u'; \lambda_u) d\lambda_u \right] \left[-\frac{1}{2\pi j} \oint_{C_v} g_v(v, v'; \lambda_v) d\lambda_v \right] \quad (35a)$$

$$= \frac{1}{(-2\pi j)^2} \oint_{C_u} \oint_{C_v} g_u(u, u'; \lambda_u) g_v(v, v'; \lambda_v) d\lambda_u d\lambda_v. \quad (35b)$$

When the eigenfunctions in Eqs. (33) or (34) are used to represent a three-dimensional Green's function in (u, v, z) space, one obtains

$$G(\mathbf{r}, \mathbf{r}') = \sum_i \Phi_i(\rho)\Phi_i^*(\rho') g_z(z, z'; \lambda_{zi}). \quad (36)$$

The z -dependent modal Green's function g_z satisfies a one-dimensional equation resulting on elimination of the (u, v) dependence from the corresponding three-dimensional equation. Examples of a reduction of this kind have been given in Sec. 1.3, where Eq. (1.3.16) defines the one-dimensional time-dependent Green's function in terms of \mathbf{r} -dependent eigenfunctions; in Sec. 1.4, where Eq. (1.4.15) defines essentially the function g_z in Eq. (36)[†]; and in Sec. 2.3, where $(j\omega\epsilon)^{-1}Y'_i(z, z')$ in Eqs. (2.3.43a) and (2.3.41) can be identified with g_z . On comparing Eqs. (32), (35), and (36), one observes that the three-dimensional scalar Green's function G can be represented in terms of the one-dimensional characteristic Green's functions[‡] g_u and g_v , and the modal Green's function g_z as follows:

$$G(\mathbf{r}, \mathbf{r}') = \frac{1}{(-2\pi j)^2} \oint_{C_u} \oint_{C_v} g_u(u, u'; \lambda_u) g_v(v, v'; \lambda_v) g_z(z, z'; \lambda_z) d\lambda_u d\lambda_v d\lambda_z. \quad (37)$$

The contour C_u in the complex λ_u plane encloses in the positive sense all singularities of g_u *but no others*, while the contour C_v in the complex λ_v plane encloses in the positive sense all singularities of g_v *but no others*. Additional singularities in the λ_u and (or) λ_v planes arise due to $g_z(z, z'; \lambda_z)$; it is recognized that generally $\lambda_z = \lambda_z(\lambda_u, \lambda_v)$, where the detailed dependence of λ_z on λ_u and λ_v is dictated by the particular coordinate representation in the u, v domain. For example, from Eq. (3.2.10c), with $\lambda_z \equiv \kappa_i^2 = k^2 - k_u'^2$,

[†]Note use of a time-dependence $\exp(-i\omega t)$ in Sec. 1.4.

[‡]As pointed out in Sec. 3.3a, the modal and characteristic Green's functions differ only in that the parameter λ is specified for the former ($\lambda = \lambda_i$), but unspecified for the latter.

$$\lambda_z = k^2 - \lambda_u - \lambda_v \quad \text{for rectangular coordinates } u \equiv x, v \equiv y, \quad (38a)$$

and from Eq. (3.2.46b), with $k_{ii}^2 \equiv p^2 \rightarrow \lambda_u$,

$$\lambda_z = k^2 - \lambda_u \quad \text{for cylindrical coordinates } u \equiv \rho, v \equiv \varphi. \dagger \quad (38b)$$

The contour integral representation in Eq. (37), involving the one-dimensional Green's functions g_u , g_v , and g_z , can be considered as the most general separable representation for the three-dimensional Green's function G . Upon evaluating the contour integrals in Eq. (37) in terms of the discrete and (or) continuous spectra arising from the pole or branch-cut singularities, respectively, of g_u and g_v , and noting that g_z has no singularities inside the contours C_u and C_v , one recovers the original z -transmission formulation in Eq. (36). Different representations are also obtainable by contour deformations in the λ_u and λ_v planes. Typical examples wherein g_u , g_v , and g_z have singularities in the λ_u and λ_v planes are shown in Fig. 3.3.4. The functions g_u , g_v , and g_z are so defined as to vanish sufficiently rapidly at infinity in the λ_u and λ_v planes. This is achieved

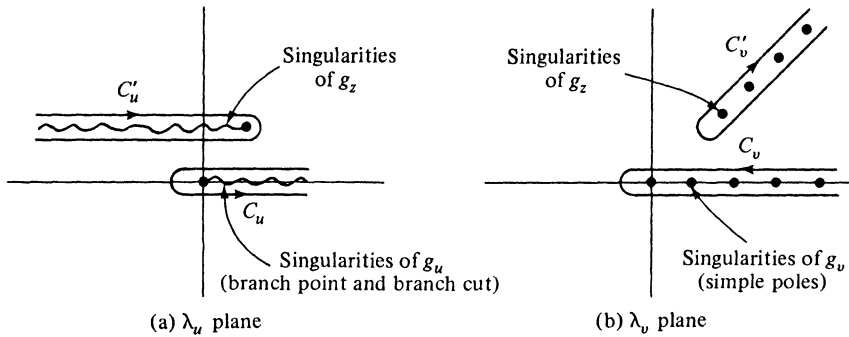


FIG. 3.3.4 Contours and singularities in λ_u and λ_v planes.

by an appropriate choice of branch cuts and Riemann surfaces, associated with any existing branch-point singularities of the g functions, so as to result in no contribution to the integral in Eq. (37) from closed contours as $|\lambda_u| \rightarrow \infty$ and $|\lambda_v| \rightarrow \infty$. The path C_u in Fig. 3.3.4(a) can therefore be deformed into the path C'_u enclosing the singularities of g_z in the λ_u plane, to yield

$$G(\mathbf{r}, \mathbf{r}') = \frac{1}{(-2\pi j)^2} \oint_{C'_u} \oint_{C_v} g_u(u, u'; \lambda_u) g_v(v, v'; \lambda_v) g_z(z, z'; \lambda_z) d\lambda_v d\lambda_u \quad (39a)$$

$$= \sum_q \Phi_q(v) \Phi_q^*(v') \sum_r \Phi_r(z) \Phi_r^*(z') g_u(u, u'; \lambda_{u,rq}), \quad (39b)$$

[†]In this case, $g_u \equiv g_\rho$ depends also on λ_v [see Eq. (3.2.46b)], so one should write $g_u \rightarrow g_u(u, u'; \lambda_u, \lambda_v)$. Thus, g_u has singularities in both the λ_u and λ_v planes, while g_z has singularities in the λ_u plane only. Only the singularities of g_u enclosed by the contour C_u in the complex λ_u plane contribute to the modal representation for G as in Eq. (36).

where the modal representation in Eq. (39b) is obtained upon evaluating the integrals over the contours C'_u and C_v in Eq. (39a). The $\Phi_r(z)$ denote the eigenfunctions in the z -domain arising from the eigenvalue problem associated with g_z, λ_u being the characteristic parameter.[†] In Eq. (39a), g_v and g_z are now characteristic Green's functions, while g_u is a modal Green's function wherein λ_u takes on the values specified along C'_u . Because of the explicit presence of $g_u(u, u'; \lambda_{u,v})$ in Eq. (39b), one identifies this representation as arising from a guided-wave analysis in which the transmission direction is taken along the u coordinate. The above procedure has evident similarities with that used in connection with Eqs. (1.5.55) and (1.5.59); with reference to Figs. 3.3.4(a) and (1.5.3), λ_u may be identified with ω^2 .

Alternatively, one may deform the contour C_v into the contour C'_v in the complex λ_v plane as shown in Fig. 3.3.4(b) to obtain

$$G(\mathbf{r}, \mathbf{r}') = \frac{1}{(-2\pi j)^2} \oint_{C_u} \oint_{C'_v} g_u(u, u'; \lambda_u) g_v(v, v'; \lambda_v) g_z(z, z'; \lambda_z) d\lambda_v d\lambda_u, \quad (40a)$$

$$= \sum_s \Phi_s(z) \Phi_s^*(z') \sum_p \Phi_p(u) \Phi_p^*(u') g'_v(v, v'; \lambda_{v,s,p}). \quad (40b)$$

The modal representation in Eq. (40b) is derived by considerations analogous to the above and is identified as a v -transmission formulation. The $\Phi_s(z)$ are the eigenfunctions in the z domain arising from the eigenvalue problem associated with g_z as the characteristic Green's function and λ_v as the characteristic parameter. Additional representations are possible wherein, say, only the integral C_u in Eq. (40a) is evaluated in terms of the mode spectrum in u while the integral C'_v remains unchanged. It is to be emphasized that all of the above alternative representations are to be considered as formal in that the deformability of contours must be verified in each case.

Equations (40) are valid for the case wherein g_z is a function of both λ_u and λ_v . For a radial transmission formulation, as in Eq. (38b), g_z is not a function of λ_v ; instead, g_u , as noted thereunder, is a function of both λ_u and λ_v . In this instance, the contour C'_v encloses the singularities of g_u in the λ_v plane, with λ_u treated as a fixed parameter. From Eqs. (3.2.46b) and (1) [see also Eq. (3.4.91)], one notes that

$$\left(\frac{d}{dp} p \frac{d}{dp} + \lambda_u p - \frac{\lambda_v}{p} \right) g_u(p, p'; \lambda_u, \lambda_v) = -\delta(p - p'). \quad (41)$$

Then one has, instead of Eq. (40a),

$$G(\mathbf{r}, \mathbf{r}') = \frac{1}{(-2\pi j)^2} \oint_{C'_u} \oint_{C'_v} g'_u(u, u'; \lambda_u; \lambda_v) g'_v(v, v'; \lambda_v) g'_z(z, z'; k^2 - \lambda_u) d\lambda_v d\lambda_u. \quad (42)$$

[†]For non-Hermitian problems with complex eigenvalues, the spectral representation involves the symmetric form wherein $\Phi_r^*(z')$ is replaced by $\Phi_r(z')$, or more generally by an "adjoint" function $\bar{\Phi}_r(z')$.

Equation (40b) still applies formally, except that $\Phi_s(z)$ are the eigenfunctions in the z domain arising now from the eigenvalue problem associated with g_z in the λ_u plane, while $\Phi_p(u)$ are eigenfunctions in the u domain arising from the eigenvalue problem associated with g_u in the λ_v plane (in the latter, λ_u is held fixed at the eigenvalues arising from the eigenvalue problem in the z domain). As for Eq. (39b), the remarks concerning the form of the spectral representation apply here as well.

Alternative representations for Green's functions in spherical regions are constructed in a similar manner. On defining radial and angular characteristic Green's functions g_r , g_ϕ , and g_θ as in Eqs. (3.4.92) and (3.4.64), respectively, one may rewrite the E -mode Green's function in Eq. (2.6.11a) in the following forms [see also Eq. (11)]⁵:

$$\left. -\frac{1}{2\pi j} \sum_q \Phi_q(\phi)\Phi_q^*(\phi') \oint_{C_\theta} g_\theta(\theta, \theta'; q^2; \lambda_\theta) g_r(r, r'; \lambda_\theta) d\lambda_\theta, \right. \quad (43a)$$

$$rr'G'(\mathbf{r}, \mathbf{r}') = \left. \left(-\frac{1}{2\pi j} \right)^2 \oint_{C_\phi} \oint_{C_\theta} g_\phi(\phi, \phi'; \lambda_\phi) g_\theta(\theta, \theta'; \lambda_\phi; \lambda_\theta) g_r(r, r'; \lambda_\theta) d\lambda_\phi d\lambda_\theta, \right. \quad (43b)$$

$$\left. + \frac{1}{2\pi j} \sum_q \Phi_q(\phi)\Phi_q^*(\phi') \oint_{C_r} g_\theta(\theta, \theta'; q^2; \lambda_\theta) g_r(r, r'; \lambda_\theta) d\lambda_\theta, \right. \quad (43c)$$

$$\left. \sum_q \Phi_q(\phi)\Phi_q^*(\phi') \sum_s R_s(r)\bar{R}_s(r') g_\theta(\theta, \theta'; q^2; \lambda_s), \quad \text{etc.} \right. \quad (43d)$$

The dependence of g_θ on the two parameters $\lambda_\phi = q^2$ and $\lambda_\theta = p(p+1)$ has been exhibited explicitly, and C_θ , C_r , and C_ϕ denote contours that enclose in the positive sense all of (and only) the singularities of g_θ , g_r , and g_ϕ in the complex λ_θ and λ_ϕ planes, respectively. Equation (43c) follows from Eq. (43a) by contour deformation about the singularities of g_r , and Eq. (43d) results by evaluating the integral in terms of the radial eigenfunctions $R_s(r)$ and the adjoint functions $\bar{R}_s(r)$ via [see Eqs. (3.4.100) and (3.4.101)]:

$$r'^2\delta(r - r') = \frac{1}{2\pi j} \oint_{C_r} g_r(r, r'; \lambda) d\lambda = \sum_s R_s(r)\bar{R}_s(r'). \quad (44)$$

In addition to Sec. 1.5, detailed applications of the characteristic Green's function method for construction of alternative representations for $G(\mathbf{r}, \mathbf{r}')$ may be found in Secs. 5.6a, 5.7b, 6.7, and 6.8. Directly analogous considerations can be applied to the scalar function \mathcal{S}' defined in Eqs. (2.3.24) or (2.3.39), in which case an additional pole singularity exists in the complex λ_u and (or) λ_v plane because of the presence of the $1/k_n^2$ factor. Although the examples above involve primarily the electromagnetic E -mode problem, construction of the electromagnetic H -mode Green's functions, or of the acoustic Green's function defined in Sec. 1.1a, proceeds similarly.

3.4 ONE-DIMENSIONAL CHARACTERISTIC GREEN'S FUNCTION AND EIGENFUNCTION SOLUTIONS

The characteristic Green's function method of Sec. 3.3a for solving eigenvalue problems in closed and open regions is applied in this section to rectangular, cylindrical, and spherical cross sections. To illustrate the method, we begin with a detailed discussion of closed rectangular geometries and then pass on to open regions, first by a limiting procedure and subsequently by a direct approach. Examples thereafter are treated more concisely, with the presentation comprising essentially the characteristic Green's functions, their analytic properties, and corresponding completeness relations.

3.4a Rectangular Cross Sections

Bounded x domains

We consider the composite cross sections shown in Fig. 3.4.1, which are all characterized by the same one-dimensional eigenvalue problem in the x domain. The various media contain a piecewise constant lossless dielectric with

$$\epsilon(x) = \begin{cases} \epsilon_1, & -d < x < 0 \\ \epsilon_2, & 0 < x < a \end{cases}, \quad \epsilon_1 > \epsilon_2, \quad (1)$$

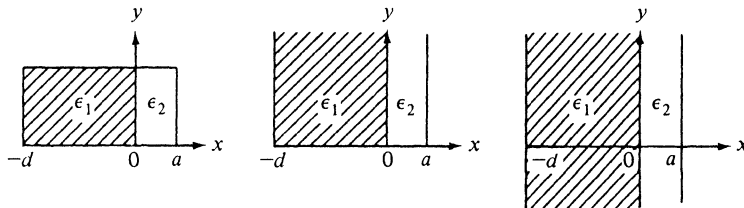
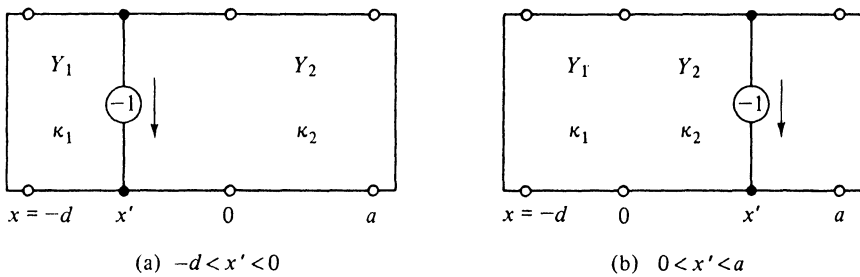


FIG. 3.4.1 Rectangular regions (bounded in x) partially filled with dielectric.

the discontinuous nature of which leads to a discontinuous representation of the eigenfunctions, as will be seen below. The eigenvalue problems in the y domain are those appropriate to a homogeneous medium and have been solved in Sec. 3.2b. A constant, free-space permeability μ_0 is assumed, so $\mu'(x) = 1$ in Eq. (3.3.3a), and the surfaces at $x = a$, $-d$ are assumed to be perfectly conducting.

H modes (in x)

The network configuration descriptive of the H -mode characteristic Green's function problem is shown in Fig. 3.4.2, where we distinguish between source locations in media 1 and 2, respectively. The relevant propagation constants and characteristic admittances are denoted, respectively, by $k_{x1} \equiv \kappa_1$, Y_1 , and

FIG. 3.4.2 Equivalent transmission-line problems (H modes along x).

$k_{x2} \equiv \kappa_2$, Y_2 . From Eq. (3.3.4) it is noted that the homogeneous equation (3.3.18) for the standing-wave functions c and s becomes

$$\left[\frac{d^2}{dx^2} + \kappa^2(x, \lambda) \right] s(x) = 0, \quad (2)$$

where

$$\kappa^2(x, \lambda) = \begin{cases} \kappa_1^2(\lambda) = k_1^2 + \lambda, & -d < x < 0 \\ \kappa_2^2(\lambda) = k_2^2 + \lambda, & 0 < x < a \end{cases}, \quad k_{1,2}^2 = \omega^2 \mu_0 \epsilon_{1,2} > 0. \quad (2a)$$

If one chooses $x_0 = 0$ in Eq. (3.3.18a), he finds that

$$\begin{aligned} c(x) &= \cos \kappa_1 x, & s(x) &= \frac{1}{\kappa_1} \sin \kappa_1 x, & -d < x < 0, \\ c(x) &= \cos \kappa_2 x, & s(x) &= \frac{1}{\kappa_2} \sin \kappa_2 x, & 0 < x < a, \end{aligned} \quad (3)$$

where the explicit dependence of the c and s functions on $x_0 = 0$ will not be exhibited henceforth. Since $\vec{Y}_T = \infty = \vec{Y}_T$ for the perfectly conducting terminations at $x = -d, a$, it follows from Eqs. (3.3.20) and (3.3.21b) that

$$\omega \mu_0 \vec{Y}(0) = -j \kappa_2 \cot \kappa_2 a, \quad \omega \mu_0 \vec{Y}(0) = -j \kappa_1 \cot \kappa_1 d, \quad (4)$$

$\kappa/\omega\mu_0$ being the H -mode characteristic admittance, whence from Eq. (3.3.19a) and (3.3.21a),

$$\vec{V}(x) = \begin{cases} \vec{V}_2(x) = \frac{\sin \kappa_2(a-x)}{\sin \kappa_2 a}, & 0 < x < a, \end{cases} \quad (5a)$$

$$\vec{V}(x) = \begin{cases} \vec{V}_1(x) = \cos \kappa_1 x - \frac{\kappa_2}{\kappa_1} \cot \kappa_2 a \sin \kappa_1 x, & -d < x < 0, \end{cases} \quad (5b)$$

$$\vec{V}(x) = \begin{cases} \vec{V}_2(x) = \cos \kappa_2 x + \frac{\kappa_1}{\kappa_2} \cot \kappa_1 d \sin \kappa_2 x, & 0 < x < a, \end{cases} \quad (5c)$$

$$\vec{V}(x) = \begin{cases} \vec{V}_1(x) = \frac{\sin \kappa_1(x+d)}{\sin \kappa_1 d}, & -d < x < 0. \end{cases} \quad (5d)$$

For subsequent application it will be convenient to employ, instead of Eq. (5c), the traveling-wave formulation:

$$\overleftarrow{V}_2(x) = \frac{1}{1 + \overleftarrow{\Gamma}_2(0)} [e^{j\kappa_2 x} + \overleftarrow{\Gamma}_2(0)e^{-j\kappa_2 x}], \quad 0 < x < a, \quad (6)$$

where the reflection coefficient $\overleftarrow{\Gamma}_2(0)$ looking to the left at $x = +0$ is given by

$$\overleftarrow{\Gamma}_2(0) = \frac{Y_{02} - \overleftarrow{Y}(0)}{Y_{02} + \overleftarrow{Y}(0)} = \frac{\kappa_2 + j\kappa_1 \cot \kappa_1 d}{\kappa_2 - j\kappa_1 \cot \kappa_1 d}, \quad Y_{02} = \frac{\kappa_2}{\omega \mu_0}. \quad (6a)$$

The H -mode characteristic Green's function $g''(x, x'; \lambda)$ can now be written down directly from Eq. (3.3.16).† In view of the discontinuous representation of $\overrightarrow{V}(x)$ for $x > 0$ and $x < 0$, g'' is represented discontinuously about $x = 0$. For a source location as in Fig. 3.4.2(a),

$$g''(x, x'; \lambda) = \begin{cases} \frac{\overleftarrow{V}_1(x_-) \overrightarrow{V}_1(x_+)}{j\omega \mu_0 \overleftrightarrow{Y}(0)}, & -d < x < 0, \quad -d < x' < 0, \\ \overleftarrow{V}_1(x') \overrightarrow{V}_2(x), & 0 < x < a, \quad -d < x' < 0; \end{cases} \quad (7a)$$

$$g''(x, x'; \lambda) = \begin{cases} \overleftarrow{V}_1(x') \overrightarrow{V}_2(x), & 0 < x < a, \quad -d < x' < 0; \end{cases} \quad (7b)$$

for the source location in Fig. 3.4.2(b),

$$g''(x, x'; \lambda) = \begin{cases} \frac{\overleftarrow{V}_1(x) \overrightarrow{V}_2(x')}{j\omega \mu_0 \overleftrightarrow{Y}(0)}, & -d < x < 0, \quad 0 < x' < a, \\ \overleftarrow{V}_2(x_-) \overrightarrow{V}_2(x_+), & 0 < x < a, \quad 0 < x' < a. \end{cases} \quad (7c)$$

$$g''(x, x'; \lambda) = \begin{cases} \overleftarrow{V}_2(x_-) \overrightarrow{V}_2(x_+), & 0 < x < a, \quad 0 < x' < a. \end{cases} \quad (7d)$$

Equations (7) can be subsumed under the single formula

$$g''(x, x'; \lambda) = \frac{\overleftarrow{V}_\beta(x_-) \overrightarrow{V}_\beta(x_+)}{j\omega \mu_0 \overleftrightarrow{Y}(0)}, \quad \overleftrightarrow{Y}(0) = \overleftarrow{Y}(0) + \overrightarrow{Y}(0), \quad (8)$$

where the subscript β stands for 1 or 2 if the corresponding variable x or x' lies in the range $-d$ to 0 or 0 to a , respectively. To assure that the solution for g'' is unique, the restriction $\text{Im } \lambda \neq 0$ (i.e., $\text{Im } \kappa_1^2 \neq 0$, $\text{Im } \kappa_2^2 \neq 0$) is implied.

The singularities of g'' in the complex λ plane consist of real simple poles at the zeros of $\overleftrightarrow{Y}(0)$. Although g'' is a function of $\kappa_{1,2}$, and, from Eq. (2a),

$$\kappa_{1,2} = \sqrt{\lambda + k_{1,2}^2}, \quad (9)$$

† $\overrightarrow{V}(x)$ and $\overleftarrow{V}(x)$, as given in Eqs. (5) and (6), are identically the normalized quantities defined in Eq. (3.3.15c). To simplify the present notation the dependence on $x_0 = 0$ has not been exhibited.

no branch-point singularities exist at $\lambda = -k_{1,2}^2$ since \vec{V}_β , $\vec{\bar{Y}}(0)$ and therefore g'' are even functions of $\kappa_{1,2}$ [see Eqs. (4)–(6)]. Thus, a power-series expansion about $\kappa_1 = 0$ or $\kappa_2 = 0$ comprises only integral powers of κ_1^2 or κ_2^2 and hence integral powers of λ , so the regularity of g'' in the neighborhood of the points $\lambda = -k_{1,2}^2$ is assured. From Eq. (4) the zeros λ_m of $\vec{\bar{Y}}(0, \lambda)$ are specified implicitly by the transcendental equation

$$\kappa_2 \cot \kappa_2 a = -\kappa_1 \cot \kappa_1 d, \quad (10)$$

$$\kappa_2^2 = \lambda + k_2^2 = \hat{\lambda}, \quad \kappa_1^2 = \lambda + k_1^2 = \hat{\lambda} + h, \quad h = k_1^2 - k_2^2 > 0. \quad (10a)$$

For real values of κ_1 and κ_2 (i.e., $\hat{\lambda} > 0$), Eq. (10) has an infinite number of solutions to be denoted by κ_{1m} , κ_{2m} (only positive roots κ_{1m} and κ_{2m} need be considered since negative values leads to the same λ_m). For imaginary values of κ_1 and κ_2 ($\hat{\lambda} < -h$), Eq. (10) becomes

$$|\kappa_2| \coth [|\kappa_2| a] = -|\kappa_1| \coth [|\kappa_1| d], \quad \kappa_1, \kappa_2 \text{ imaginary.} \quad (11a)$$

Since the left-hand side of Eq. (11a) is positive while the right-hand side is negative, no solution exists. However, for real κ_1 and imaginary κ_2 ($-h < \hat{\lambda} < 0$), Eq. (10) can have roots κ_{1v} , $|\kappa_{2v}|$:

$$r_v \cot r_v = -t_v \coth \left(\frac{a}{d} t_v \right), \quad r_v^2 + t_v^2 = hd^2 = \left(1 - \frac{\epsilon_2}{\epsilon_1} \right) (k_1 d)^2, \quad (11b)$$

where

$$\kappa_{1v} d \equiv r_v > 0; \quad |\kappa_{2v}| d \equiv t_v, \quad \kappa_{2v} \text{ imaginary.} \quad (11c)$$

Equation (11b) can be interpreted graphically as in Fig. 3.4.3. It is noted that N roots exist for $(2N - 1)\pi/2 < \sqrt{h}d < (2N + 1)\pi/2$, with no solution possible when $\sqrt{h}d < \pi/2$. These modes therefore possess a low-frequency cutoff.

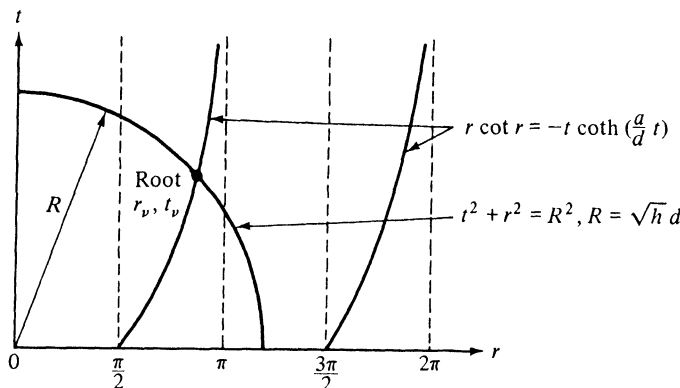


FIG. 3.4.3 Graphical solution of transcendental equation (11b).

The spectral representation of the delta function is now obtained, as in Eqs. (3.3.25), by integrating the characteristic Green's function g'' in Eq. (8) along the contour C shown in Fig. 3.4.4 enclosing all singularities:

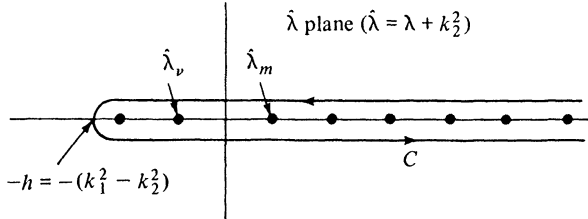


FIG. 3.4.4 Contour of integration and singularities in the λ plane.

$$\delta(x - x') = -\frac{1}{2\pi j} \oint_C g''(x, x'; \lambda) d\lambda, \quad (12a)$$

$$= \sum_v \hat{\psi}_{v\beta}(x) \hat{\psi}_{v\beta}^*(x') + \sum_m \hat{\psi}_{m\beta}(x) \hat{\psi}_{m\beta}^*(x'), \quad -d < \frac{x}{x'} < a, \quad (12b)$$

where the contributions for $-h < \hat{\lambda}_v < 0$ and $\hat{\lambda}_m > 0$ have been exhibited separately. From Eq. (3.3.25d) and Eqs. (5) and (6) one obtains, for the orthonormal eigenfunctions $\hat{\psi}_{v\beta}$ and $\hat{\psi}_{m\beta}$,

$$\hat{\psi}_{v1}(x) = \frac{1}{A_v} \frac{\sin [r_v(x/d + 1)]}{\sin r_v}, \quad 0 < r_v < \sqrt{h}d, \quad -d < x < 0, \quad (13a)$$

$$\hat{\psi}_{v2}(x) = \frac{1}{A_v} \frac{\sinh [t_v \alpha (1 - x/a)]}{\sinh (t_v \alpha)}, \quad \alpha = \frac{a}{d}, \quad 0 < x < a, \quad (13b)$$

where

$$A_v^2 = \omega \mu_0 \frac{\partial}{\partial \lambda_v} \vec{B}(0, \lambda_v) = \frac{d}{2} \left[\frac{\coth (t_v \alpha)}{t_v r_v^2} h d^2 + \csc^2 r_v - \alpha \operatorname{csch}^2 (t_v \alpha) \right]. \quad (13c)$$

Similarly,

$$\hat{\psi}_{m1}(x) = \frac{1}{A_m} \frac{\sin \kappa_{1m}(x + d)}{\sin \kappa_{1m} d}, \quad \kappa_{1m} > 0, \quad -d < x < 0, \quad (14a)$$

$$\hat{\psi}_{m2}(x) = \begin{cases} \frac{1}{A_m} \frac{\sin \kappa_{2m}(a - x)}{\sin \kappa_{2m} a}, & \kappa_{2m} > 0, \quad 0 < x < a, \\ \frac{1}{A_m [1 + \Gamma_m(0)]} [e^{j\kappa_{2m} x} + \vec{\Gamma}_m(0)^{-j\kappa_{2m} x}], & \end{cases} \quad (14b)$$

$$\hat{\psi}_{m2}(x) = \begin{cases} \frac{1}{A_m} \frac{\sin \kappa_{2m}(a - x)}{\sin \kappa_{2m} a}, & \kappa_{2m} > 0, \quad 0 < x < a, \\ \frac{1}{A_m [1 + \Gamma_m(0)]} [e^{j\kappa_{2m} x} + \vec{\Gamma}_m(0)^{-j\kappa_{2m} x}], & \end{cases} \quad (14c)$$

with

$$A_m^2 = \omega \mu_0 \frac{\partial}{\partial \lambda_m} \vec{B}(0, \lambda_m) = \begin{cases} \frac{a}{2} \left[\left(1 + \frac{1}{\alpha}\right) + \left(\frac{\kappa_{1m}^2}{\kappa_{2m}^2} + \frac{1}{\alpha}\right) \cot^2 \kappa_{1m} d \right. \\ \quad \left. + \frac{h}{a \kappa_{1m} \kappa_{2m}^2} \cot \kappa_{1m} d \right], & (14d) \\ \frac{d}{2} \left[(1 + \alpha) + \left(\frac{\kappa_{2m}^2}{\kappa_{1m}^2} + \alpha\right) \cot^2 \kappa_{2m} a \right. \\ \quad \left. - \frac{h}{d \kappa_{2m} \kappa_{1m}^2} \cot \kappa_{2m} a \right]. & (14e) \end{cases}$$

It is verified that Eqs. (13) and (14) reduce to the results obtained previously for a homogeneously filled waveguide [Sec. 3.2b] when (a) $h = 0$ ($\epsilon_1 = \epsilon_2$), (b) $d = 0$, or (c) $a = 0$. Attention should be called to the different behavior of the eigenfunctions $\hat{\psi}_v(x)$ in Eqs. (13) and $\hat{\psi}_m(x)$ in Eqs. (14). While $\hat{\psi}_m(x)$ is represented by an oscillating function over the entire region $-d < x < a$, $\hat{\psi}_v(x)$ behaves in this manner only in the dielectric ϵ_1 (note: $\epsilon_1 > \epsilon_2$). In the remaining interval $0 < x < a$, $\hat{\psi}_v$ decays away from the interface $x = 0$. Viewed in modal terms with respect to propagation along z , the fields corresponding to the $\hat{\psi}_v$ are essentially confined within the dielectric slab while the fields derived from the $\hat{\psi}_m$ fill the entire waveguide cross section. The former are termed “trapped” modes and their existence depends entirely on the presence of the dielectric; the latter may be regarded as perturbations about the dielectric-free case.

E modes (in x). The solution for the *E*-mode characteristic Green's function $g'(x, x'; \lambda)$ and the associated orthonormal eigenfunctions is similar to the above except for duality replacements [see Eqs. (3.3.26)–(3.3.30)]. The results are summarized below.

Characteristic Green's function

$$g'(x, x'; \lambda) = \frac{\vec{I}_\beta(x_<) \vec{I}_\beta(x_>)}{j \omega \epsilon_0 \vec{Z}(0)}, \quad \vec{Z}(0) = \vec{Z}(0) + \vec{Z}(0). \quad (15)$$

$$\begin{aligned} c(x) &= \cos \kappa_1 x, \quad s(x) = \frac{\epsilon'_1}{\kappa_1} \sin \kappa_1 x, \quad -d < x < 0, \\ c(x) &= \cos \kappa_2 x, \quad s(x) = \frac{\epsilon'_2}{\kappa_2} \sin \kappa_2 x, \quad 0 < x < a, \end{aligned} \quad (15a)$$

$$\omega \epsilon_0 \vec{Z}(0) = j \frac{\kappa_2}{\epsilon'_2} \tan \kappa_2 a, \quad \omega \epsilon_0 \vec{Z}(0) = j \frac{\kappa_1}{\epsilon'_1} \tan \kappa_1 d, \quad \epsilon'_{1,2} = \frac{\epsilon_{1,2}}{\epsilon_0},$$

$$\kappa_1^2 = k_1^2 + \lambda, \quad \kappa_2^2 = k_2^2 + \lambda. \quad (15b)$$

$$\left. \begin{aligned} \vec{I}_1(x) &= \cos \kappa_1 x + \frac{\epsilon'_1 \kappa_2}{\epsilon'_2 \kappa_1} \tan \kappa_2 a \sin \kappa_1 x \\ \vec{I}_1(x) &= \frac{\cos \kappa_1 (x + d)}{\cos \kappa_1 d} \end{aligned} \right\} -d < x < 0, \quad (15c)$$

$$\left. \begin{aligned} \vec{I}_2(x) &= \frac{\cos \kappa_2(a-x)}{\cos \kappa_2 a} \\ \leftarrow I_2(x) &= \cos \kappa_2 x - \frac{\epsilon'_2 \kappa_1}{\epsilon'_1 \kappa_2} \tan \kappa_1 d \sin \kappa_2 x \end{aligned} \right\} \quad 0 < x < a. \quad (15d)$$

Singularities of g' : Simple real poles at

$$\frac{\epsilon'_1}{\epsilon'_2} \kappa_{2m} \tan \kappa_{2m} a = -\kappa_{1m} \tan \kappa_{1m} d, \quad \kappa_{1m}, \kappa_{2m} > 0, \quad (16a)$$

and at

$$\begin{aligned} \frac{\epsilon'_1}{\epsilon'_2} r_v \tan r_v &= t_v \tanh(t_v \alpha), \quad r_v^2 + t_v^2 = hd^2, \quad \alpha = \frac{a}{d}, \quad h = k_1^2 - k_2^2, \\ \kappa_{1v} d &\equiv r_v > 0; \quad |\kappa_{2v}|d \equiv t_v, \quad \kappa_{2v} \text{ imaginary}. \end{aligned} \quad (16b)$$

Equation (16a) has an infinite number of solutions and Eq. (16b) has a finite number. The graphical representation of Eq. (16b) resembles that in Fig. 3.4.3, provided that all curves (except the circle) are shifted to the left through an interval $\pi/2$. The low-frequency cutoff found for the H -mode solutions ψ_v is therefore absent in the E -mode case.

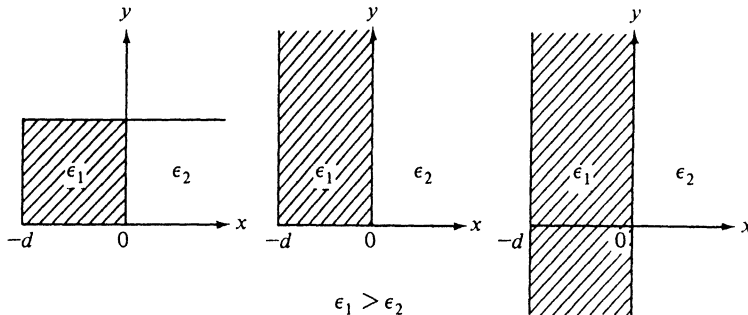


FIG. 3.4.5 Semi-infinite regions (in x) partially filled with dielectric.

Delta-function representation ($-d < x' < a$),

$$\begin{aligned} \epsilon'(x') \delta(x - x') &= -\frac{1}{2\pi j} \oint_C g'(x, x'; \lambda) d\lambda \\ &= \sum_v \hat{\Phi}_{v\beta}(x) \hat{\Phi}_{v\beta}^*(x') + \sum_m \hat{\Phi}_{m\beta}(x) \hat{\Phi}_{m\beta}^*(x'), \end{aligned} \quad (17)$$

with the subscript β defined as under Eq. (8), and

$$\hat{\Phi}_{v1}(x) = \frac{\cos [r_v(x/d + 1)]}{A_v \cos r_v}, \quad 0 < r_v < \sqrt{h}d, \quad -d < x < 0, \quad (17a)$$

$$\hat{\Phi}_{v2}(x) = \frac{\cosh [t_v \alpha (1 - x/a)]}{A_v \cosh t_v \alpha}, \quad 0 < x < a, \quad (17b)$$

$$A_v^2 = \omega \epsilon_0 \frac{\partial}{\partial \lambda_v} \vec{X}(0, \lambda_v) = \frac{d}{2} \left[\frac{\tanh(t_v \alpha)}{r_v^2 t_v \epsilon'_2} hd^2 + \frac{\sec^2 r_v}{\epsilon'_1} + \frac{\alpha}{\epsilon'_2} \operatorname{sech}^2(t_v \alpha) \right], \quad (17c)$$

while

$$\hat{\Phi}_{m1}(x) = \frac{\cos \kappa_{1m}(x+d)}{A_m \cos \kappa_{1m} d}, \quad \kappa_{1m} > 0, \quad -d < x < 0, \quad (17d)$$

$$\hat{\Phi}_{m2}(x) = \frac{\cos \kappa_{2m}(a-x)}{A_m \cos \kappa_{2m} a}, \quad \kappa_{2m} > 0, \quad 0 < x < a, \quad (17e)$$

$$A_m^2 = \frac{a}{2\epsilon'_1} \left[\frac{\epsilon'_1}{\epsilon'_2} + \frac{1}{\alpha} + \left(\frac{\kappa_{1m}^2 \epsilon'_2}{\kappa_{2m}^2 \epsilon'_1} + \frac{1}{\alpha} \right) \tan^2 \kappa_{1m} d - \frac{h}{a \kappa_{1m} \kappa_{2m}^2} \tan \kappa_{1m} d \right]. \quad (17f)$$

The physical distinction between the mode fields corresponding to the $\hat{\Phi}_v$ and $\hat{\Phi}_m$ is the same as discussed in connection with the H modes.

Employing Eq. (17), one may represent a suitable function $F(x)$ in the interval $-d < x < a$ as follows:

$$F(x) = \int_{-d}^a \frac{F(x')}{\epsilon'(x')} \epsilon'(x') \delta(x - x') dx' \\ = \begin{cases} \sum_v f_v \hat{\Phi}_{v1}(x) + \sum_m f_m \hat{\Phi}_{m1}(x), & -d < x \leq 0, \\ \sum_v f_v \hat{\Phi}_{v2}(x) + \sum_m f_m \hat{\Phi}_{m2}(x), & 0 \leq x < a, \end{cases} \quad (18)$$

where

$$f_v = \frac{1}{\epsilon'_1} \int_{-d}^0 F(x') \hat{\Phi}_{v1}^*(x') dx' + \frac{1}{\epsilon'_2} \int_0^a F(x') \hat{\Phi}_{v2}^*(x') dx', \quad (18a)$$

$$f_m = \frac{1}{\epsilon'_1} \int_{-d}^0 F(x') \hat{\Phi}_{m1}^*(x') dx' + \frac{1}{\epsilon'_2} \int_0^a F(x') \hat{\Phi}_{m2}^*(x') dx', \quad (18b)$$

and the asterisk denotes the complex conjugate.

Semiinfinite x domain

As $a \rightarrow \infty$ in Fig. 3.4.1, one obtains the open cross-section configurations in Fig. 3.4.5. The eigenfunctions appropriate to this case can be obtained as a limiting case of those for finite a .

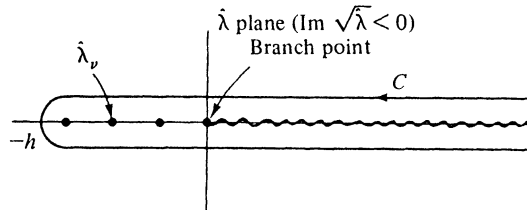


FIG. 3.4.6 Path of integration and singularities in a complex $\hat{\lambda}$ plane.

H modes (in x) ($a \rightarrow \infty$). As $a \rightarrow \infty$, the resonances κ_{1m} and κ_{2m} in Eq. (10), with $\kappa_{2m} > 0$, coalesce into a continuous spectrum, while those in Eq. (11) remain discrete and satisfy the equation

$$r_v \cot r_v = -t_v, \quad r_v^2 + t_v^2 = hd^2, \quad \text{as } a \rightarrow \infty. \quad (19a)$$

Moreover, from Eq. (13c),

$$A_v^2 \rightarrow \frac{d}{2} \frac{hd^2}{r_v^2} \left(1 + \frac{1}{t_v}\right), \quad (19b)$$

while, from Eq. (14d),

$$A_m^2 \rightarrow A_\xi^2 = \frac{a}{2} \left(1 + \frac{\xi_1^2}{\xi^2} \cot^2 \xi_1 d\right) = \frac{2a}{[1 + \tilde{\Gamma}_2(\xi, 0)][1 + \tilde{\Gamma}_2(\xi, 0)^*]}, \quad (19c)$$

where $\tilde{\Gamma}_2(\xi, 0)$ is given in Eq. (6). In the last equation the continuous variables ξ_1 and ξ have been defined as the limiting values of κ_{1m} and κ_{2m} as $a \rightarrow \infty$:

$$\kappa_{2m} \rightarrow \xi, \quad \kappa_{1m} \rightarrow \xi_1 = \sqrt{\xi^2 + h}, \quad 0 < \xi < \infty, \quad a \rightarrow \infty. \quad (19d)$$

Upon noting that the increment $\Delta\xi$ is given as in Eq. (3.2.26) by $\Delta\xi = \pi/a$, $a \rightarrow \infty$, one may write Eq. (12b) as

$$\delta(x - x') = \sum_v \hat{\psi}_{v\beta}(x) \hat{\psi}_{v\beta}^*(x') + \int_0^\infty \hat{\psi}_\beta(\xi, x) \hat{\psi}_\beta^*(\xi, x') d\xi, \\ -d < \frac{x}{x'} < \infty, \quad \beta = 1, 2, \quad (20)$$

where, in view of Eqs. (13), (14), and (19), one has, for the discrete spectrum,

$$\hat{\psi}_{v1}(x) = \frac{1}{A_v} \frac{\sin [r_v((x/d) + 1)]}{\sin r_v}, \quad 0 < r_v < \sqrt{h}d, \quad -d < x < 0, \quad (20a)$$

$$\hat{\psi}_{v2}(x) = \frac{1}{A_v} e^{-t_v x/d}, \quad 0 < x < \infty. \quad (20b)$$

As in Eq. (8), $\beta = 1$ for x or x' between $-d$ and 0, while $\beta = 2$ for x or x' between 0 and ∞ . Just as in the closed region, the magnitude of $\hat{\psi}_{v1}$ oscillates while that of $\hat{\psi}_{v2}$ decreases exponentially for $x > 0$. Thus, the field of such a mode is confined again to the region $-d < x < 0$ occupied by the dielectric ϵ_1 . Modes traveling in the z direction with this transverse field behavior are characterized as “trapped waves,” or “surface waves,” since the field appears to be trapped inside the dielectric with the larger permittivity and guided by the dielectric surface.

For the continuous spectrum,

$$\hat{\psi}_1(\xi, x) = \frac{\sin \xi_1(x + d)}{\sqrt{2\pi} \sin \xi_1 d} [1 + \tilde{\Gamma}_2(0, \xi)], \quad 0 < \xi < \infty, \quad -d < x < 0, \quad (20c)$$

$$\hat{\psi}_2(\xi, x) = \frac{1}{\sqrt{2\pi}} [e^{j\xi x} + \overleftarrow{\Gamma}_2(0, \xi) e^{-j\xi x}], \quad 0 < x < \infty, \quad (20d)$$

where

$$\overleftarrow{\Gamma}_2(0, \xi) = \frac{\xi + j\xi_1 \cot \xi_1 d}{\xi - j\xi_1 \cot \xi_1 d}, \quad \xi_1^2 = h + \xi^2 = (k_1^2 - k_2^2) + \xi^2. \quad (20e)$$

The traveling-wave representation for $\hat{\psi}_2$, derived as a limiting case of Eq. (14c), has a significant physical interpretation. For the assumed time dependence $\exp(+j\omega t)$, the contribution from the first term inside the brackets in Eq. (20d) constitutes a properly normalized (incident) free-space plane-wave mode traveling in the $-x$ direction [see Eq. (3.2.37b)], while the second term comprises the wave reflected at $x=0$ with reflection coefficient $\overleftarrow{\Gamma}_2(0, \xi)$. Thus, the continuous spectrum for $x>0$ is obtained by adding to a properly normalized incident wave a reflected wave so adjusted that the boundary conditions at $x=0$ are satisfied.

The delta-function representation in Eq. (20) could also have been deduced directly from the characteristic Green's function. As $a \rightarrow \infty$ and since $\text{Im } \kappa_2 \neq 0$, the standing wave in Eq. (5a) goes over into a traveling wave. In this transition, the restriction $\text{Im } \kappa_2 < 0$ appropriate to the assumed time dependence $\exp(+j\omega t)$ must be observed [see Eqs. (2.2.15)] and yields the following (bounded) result for $x > 0$:

$$\vec{V}_2(x) \rightarrow e^{-j\kappa_2 x}, \quad \kappa_2 = \sqrt{k_2^2 + \lambda} = \sqrt{\hat{\lambda}}, \quad \text{Im } \kappa_2 < 0, \quad (21a)$$

and

$$\vec{V}_1(x) \rightarrow \cos \kappa_1 x - j \frac{\kappa_2}{\kappa_1} \sin \kappa_1 x, \quad \kappa_1 = \sqrt{\hat{\lambda} + h}, \quad h = k_1^2 - k_2^2, \quad (21b)$$

Moreover, from Eq. (4),

$$\vec{Y}(0) \rightarrow \frac{\kappa_2}{\omega \mu_0}, \quad \text{i.e., } j\omega \mu_0 \overleftrightarrow{\vec{Y}}(0) = j\kappa_2 + \kappa_1 \cot \kappa_1 d. \quad (21c)$$

The $\overleftarrow{V}_{1,2}(x)$ are still given by Eqs. (5c) and (5d). \vec{V}_β and $\overleftrightarrow{\vec{Y}}(0)$ remain even functions of κ_1 but not of κ_2 . $\lambda = -k_1^2$ is therefore a regular point in the complex λ -plane. On the other hand, an expansion of $g''(x, x'; \lambda)$ about the point $\lambda = -k_1^2$ contains integral powers of κ_2 , so $\lambda + k_1^2 = \hat{\lambda} = 0$ is a branch point of order 1. If we define

$$\hat{\lambda} = |\hat{\lambda}| e^{j\gamma}, \quad \sqrt{\hat{\lambda}} = |\sqrt{\hat{\lambda}}| e^{j\gamma/2}, \quad (22)$$

the convergence requirement $\text{Im } \sqrt{\hat{\lambda}} < 0$ in Eq. (21a) restricts the argument γ to the range $0 > \gamma > -2\pi$. To impose this condition on the entire top sheet, the spectral sheet, of the two-sheeted complex $\hat{\lambda}$ plane, one chooses a branch cut along the positive real axis as shown in Fig. 3.4.6.

The Green's function g'' may also have relevant pole singularities at the zeros of $\overleftrightarrow{Y}(0)$, namely when

$$j\kappa_2 = -\kappa_1 \cot \kappa_1 d. \quad (23)$$

Solutions of Eq. (23) exist only for real values of κ_1 and imaginary values of $\kappa_2 = -j|\kappa_2|$ (i.e., $0 > \hat{\lambda} > -h$), leading to the transcendental equation (19a). The location of possible pole singularities is shown in Fig. 3.4.6. Upon performing an integration as in Eq. (12a) about the contour C in Fig. 3.4.6 enclosing all the singularities of g'' in the complex λ plane, one obtains after residue evaluation at the poles λ_v , the series in Eq. (20), with $g''(x, x'; \lambda)$ given by Eq. (8) and subject to the modifications in Eqs. (21). The remaining contour integral about the branch cut can be written as

$$I = -\frac{1}{2\pi j} \int_{\infty e^{-j2\pi}}^0 g''(x, x'; \lambda) d\hat{\lambda} - \frac{1}{2\pi j} \int_0^{\infty e^{-j0}} g''(x, x; \lambda) d\hat{\lambda} \quad (24a)$$

$$\begin{aligned} &= -\frac{1}{2\pi j} \int_0^{\infty e^{-j0}} [g''(x, x'; \hat{\lambda} - k_2^2) - g''(x, x'; \hat{\lambda} e^{-j2\pi} - k_2^2)] d\hat{\lambda} \\ &= -\frac{1}{\pi} \operatorname{Im} \int_0^{\infty e^{-j0}} g''(x, x'; \hat{\lambda} - k_2^2) d\hat{\lambda} \\ &= -\frac{2}{\pi} \operatorname{Im} \int_0^\infty \xi g''(x, x'; \xi^2 - k_2^2) d\xi, \quad \xi^2 = \hat{\lambda}. \end{aligned} \quad (24b)$$

The transition from Eq. (24a) to (24b) is based on the property

$$g''(x, x'; \hat{\lambda} e^{-j2\pi}) = g''(x, x'; \hat{\lambda}^*) = g''*(x, x'; \hat{\lambda}), \quad \hat{\lambda} = |\hat{\lambda}| e^{-j0}, \quad (24c)$$

satisfied by g'' . Upon substituting the appropriate representations for g'' into Eq. (24b), one obtains directly the continuous spectrum as in Eq. (20).

E modes (in x) ($a \rightarrow \infty$)

The results for the *E*-mode problem, obtained in direct analogy to those above, are summarized below:

$$\epsilon'(x')\delta(x - x') = -\frac{1}{2\pi j} \oint_C g'(x, x'; \lambda) d\lambda \quad (25a)$$

$$= \sum_v \hat{\Phi}_{v\beta}(x)\hat{\Phi}_{v\beta}^*(x') + \int_0^\infty \hat{\Phi}_\beta(\xi, x)\hat{\Phi}_\beta^*(\xi, x')d\xi, \quad (25b)$$

$$-d < \frac{x}{x'} < \infty, \quad \beta = 1, 2,$$

where, for the discrete spectrum [see Eq. (20) for definition of domains corresponding to $\beta = 1, 2$],

$$\hat{\Phi}_{v1}(x) = \frac{\cos[r_v((x/d) + 1)]}{A_v \cos r_v}, \quad 0 < r_v < \sqrt{h}d, \quad -d < x < 0, \quad (26a)$$

$$\hat{\Phi}_{\nu 2}(x) = \frac{e^{-t_v x/d}}{A_\nu}, \quad 0 < x < \infty, \quad (26b)$$

$$A_\nu^2 = \frac{d}{2} \left\{ \left[1 + \left(\frac{t_v}{r_v} \right)^2 \right] \frac{1}{t_v \epsilon_2'} + \left[1 + \left(\frac{t_v \epsilon_1'}{r_v \epsilon_2'} \right)^2 \right] \frac{1}{\epsilon_1'} \right\}. \quad (26c)$$

Also, r_v and t_v are the solutions of the transcendental equations

$$\frac{\epsilon_2'}{\epsilon_1'} r_v \tan r_v = t_v, \quad r_v^2 + t_v^2 = h d^2. \quad (26d)$$

The continuous spectrum is given by

$$\begin{aligned} \hat{\Phi}_1(\xi, x) &= \sqrt{\frac{\epsilon_2'}{2\pi}} \frac{\cos \xi(x+d)}{\cos \xi_1 d} [1 - \tilde{\Gamma}_2(0, \xi)], \quad \xi_1^2 = h + \xi^2, \\ 0 < \xi < \infty, \quad -d < x < 0, \end{aligned} \quad (27a)$$

$$\hat{\Phi}_2(\xi, x) = \sqrt{\frac{\epsilon_2'}{2\pi}} [e^{j\xi x} - \tilde{\Gamma}_2(0, \xi) e^{-j\xi x}], \quad 0 < x < \infty, \quad (27b)$$

$$\tilde{\Gamma}_2(0, \xi) = \frac{\tilde{Z}(0) - Z_{02}}{\tilde{Z}(0) + Z_{02}} = \frac{j\xi_1 \tan \xi_1 d - \xi(\epsilon_1'/\epsilon_2')}{j\xi_1 \tan \xi_1 d + \xi(\epsilon_1'/\epsilon_2')}. \quad (27c)$$

If $d \rightarrow \infty$ in Fig. 3.4.1, one obtains the semiinfinite configurations shown in Fig. 3.4.7, which differ from those in Fig. 3.4.5 in that the medium with the larger dielectric constant (ϵ_1) extends to infinity in the x direction.

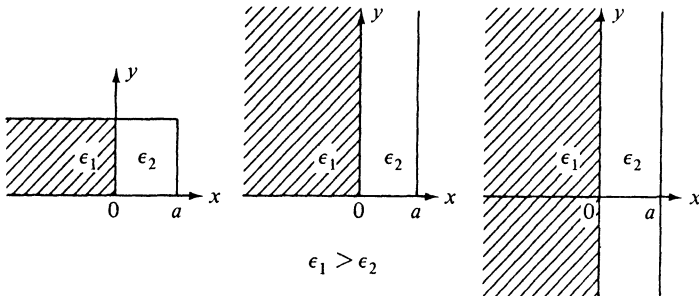


FIG. 3.4.7 Semi-infinite regions (in x) partially filled with dielectric.

H modes (in x) ($d \rightarrow \infty$)

As $d \rightarrow \infty$ in Eq. (10), the resonances $\kappa_{1m}, \kappa_{2m} > 0$, coalesce into a continuous spectrum and the second series in the delta-function representation (12b) transforms into an integral analogous to that in Eq. (20). However, in distinction to the case $a \rightarrow \infty$, the resonance parameters κ_{1v} and $|\kappa_{2v}|$ in Eq. (11b) become continuous as $d \rightarrow \infty$. In tracing out the transition $d \rightarrow \infty$, one employs instead of Eq. (5b) the traveling-wave formulation similar to that in Eq. (6):

$$\vec{V}_1(x) = \frac{1}{1 + \vec{\Gamma}_1(0)} [e^{-j\kappa_1 x} + \vec{\Gamma}_1(0)e^{j\kappa_1 x}], \quad -d < x < 0, \quad (28)$$

where the reflection coefficient $\vec{\Gamma}_1(0)$ seen to the right at $x = 0^-$ is given by

$$\vec{\Gamma}_1(0) = \frac{\kappa_1 + j\kappa_2 \cot \kappa_2 a}{\kappa_1 - j\kappa_2 \cot \kappa_2 a}. \quad (28a)$$

Since from Eqs. (13c) and (14e),

$$A_m^2 \rightarrow A_{\xi_1}^2 = \frac{2d}{[1 + \vec{\Gamma}_1(\xi_1, 0)][1 + \vec{\Gamma}_1(\xi_1, 0)^*]}, \quad d \rightarrow \infty, \quad \sqrt{h} < \xi_1 < \infty, \quad (29a)$$

with

$$\vec{\Gamma}_1(\xi_1, 0) = \frac{\xi_1 + j\xi \cot \xi a}{\xi_1 - j\xi \cot \xi a}, \quad \xi = \sqrt{\xi_1^2 - h}, \quad h = k_1^2 - k_2^2 > 0, \quad (29b)$$

and

$$A_v^2 \rightarrow A_{\xi_1}^2, \quad d \rightarrow \infty, \quad 0 < \xi_1 < \sqrt{h}, \quad (29c)$$

one obtains via Eqs. (12)–(14) and (28) the delta-function representation:

$$\delta(x - x') = \int_0^\infty \hat{\psi}_\beta(\xi_1, x)\hat{\psi}_\beta^*(\xi_1, x') d\xi_1, \quad -\infty < \frac{x}{x'} < a, \quad \beta = 1, 2, \quad (30)$$

where $-\infty < (x \text{ or } x') < 0$ for $\beta = 1$ and $0 < (x \text{ or } x') < a$ for $\beta = 2$, with

$$\hat{\psi}_1(\xi_1, x) = \frac{1}{\sqrt{2\pi}} [e^{-j\xi_1 x} + \vec{\Gamma}_1(\xi_1, 0)e^{j\xi_1 x}], \quad 0 < \xi_1 < \infty, \quad -\infty < x < a, \quad (30a)$$

$$\hat{\psi}_2(\xi_1, x) = \frac{\sin \xi(a - x)}{\sqrt{2\pi} \sin \xi a} [1 + \vec{\Gamma}_1(\xi_1, 0)], \quad 0 < x < a. \quad (30b)$$

It is noted that ξ is imaginary for $0 < \xi_1 < \sqrt{h}$.

To deduce Eqs. (30) directly from a characteristic Green's function analysis, one notes from Eqs. (5) that as $d \rightarrow \infty$, with $\text{Im } \kappa_1 < 0$ appropriate to an $\exp(j\omega t)$ time dependence,

$$\tilde{V}_1(x) \rightarrow e^{j\kappa_1 x}, \quad -\infty < x < 0, \quad (31a)$$

$$\tilde{V}_2(x) \rightarrow \cos \kappa_2 x + j \frac{\kappa_1}{\kappa_2} \sin \kappa_2 x, \quad 0 < x < a, \quad (31b)$$

$$\omega \mu_0 \tilde{Y}(0) \rightarrow \kappa_1. \quad (31c)$$

Since $g''(x, x'; \lambda)$, by Eqs. (8) and (31), is an even function of κ_2 but not of κ_1 , a branch-point singularity exists at $\kappa_1 = 0$ (i.e., $\lambda = -k_1^2$) in the complex λ

plane. In analogy to Eq. (22), the restriction on the argument of λ on the spectral sheet is

$$\operatorname{Im} \sqrt{\hat{\lambda} + h} < 0, \quad \text{i.e., } -2\pi < \arg(\hat{\lambda} + h) < 0, \quad \hat{\lambda} = \lambda + k_2^2 = \kappa_2^2, \quad (32)$$

so that the branch cut is drawn from $\hat{\lambda} = -h$ to ∞ along the positive real axis in the $\hat{\lambda}$ plane (see Fig. 3.4.8). To determine possible pole singularities we examine the resonance condition

$$j\omega\mu_0 \overleftrightarrow{Y}(0) = 0 = j\kappa_1 + \kappa_2 \cot \kappa_2 a. \quad (33)$$

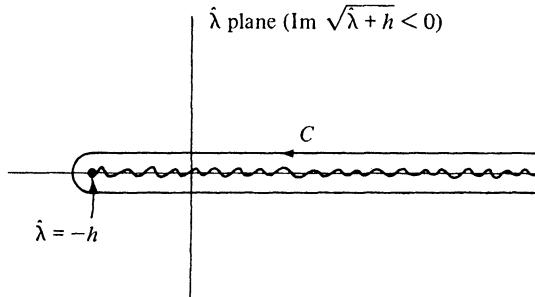


FIG. 3.4.8 Singularities and path of integration in $\hat{\lambda}$ plane.

Since Eq. (33) has no real solution λ , on the branch $\operatorname{Im} \kappa_1 < 0$ [†], no pole singularities exist, and the contour of integration is that shown in Fig. 3.4.8. Thus, in analogy with Eqs. (24),

$$\delta(x - x') = -\frac{1}{2\pi j} \oint_C g''(x, x'; \lambda) d\hat{\lambda} \quad (34a)$$

$$= -\frac{2}{\pi} \operatorname{Im} \int_0^\infty d\xi_1 \xi_1 g''(x, x'; \xi_1^2 - k_1^2), \quad -\infty < \frac{x}{x'} < a, \quad (34b)$$

which, upon insertion of g'' from Eqs. (8), (5), and (31), yields Eq. (30).

E modes (in x) ($d \rightarrow \infty$)

Spectral representation of delta function:

$$\epsilon'(x') \delta(x - x') = -\frac{1}{2\pi j} \oint_C g'(x, x'; \lambda) d\hat{\lambda}, \quad (35a)$$

$$= \int_0^\infty \hat{\Phi}_\beta(\xi_1, x) \hat{\Phi}_\beta^*(\xi_1, x') d\xi_1, \quad \beta = 1, 2, \quad (35b)$$

[†]The corresponding discrete eigenfunctions, if they exist, must be square integrable (i.e., vanish at $x \rightarrow -\infty$), so Sec. 3.2a applies. Since the problem is non-dissipative, any discrete eigenvalues must be real.

where $\beta = 1$ when $-\infty < (x \text{ or } x') < 0$ while $\beta = 2$ when $0 < (x \text{ or } x') < a$. The contour C in the complex $\hat{\lambda}$ plane is as shown in Fig. 3.4.8, and from Eqs. (17) as $d \rightarrow \infty$,

$$\hat{\Phi}_1(\xi_1, x) = \sqrt{\frac{\epsilon'_1}{2\pi}} [e^{-j\xi_1 x} - \vec{\Gamma}_1(\xi_1, 0)e^{j\xi_1 x}], \quad 0 < \xi_1 < \infty, \quad -\infty < x < 0, \quad (36a)$$

$$\hat{\Phi}_2(\xi_1, x) = \sqrt{\frac{\epsilon'_1}{2\pi}} [1 - \vec{\Gamma}_1(\xi_1, 0)] \frac{\cos \xi(a-x)}{\cos \xi a}, \quad 0 < x < a, \quad (36b)$$

$$\vec{\Gamma}_1(\xi_1, 0) = \frac{j\xi \tan \xi a - \xi_1(\epsilon'_2/\epsilon'_1)}{j\xi \tan \xi a + \xi_1(\epsilon'_2/\epsilon'_1)}, \quad \xi = \sqrt{\xi_1^2 - h}, \quad h = k_1^2 - k_2^2 > 0. \quad (36c)$$

Infinite x domain

Configurations comprising two dielectrics, semiinfinite in x , are shown in Fig. 3.4.9.

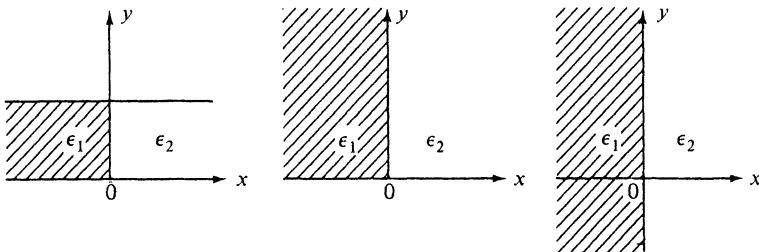


FIG. 3.4.9 Rectangular domains (infinite in x) partially filled with dielectric.

H modes (in x). The characteristic Green's function for this case is given by

$$g''(x, x'; \lambda) = \frac{\overleftarrow{V}_\beta(x_<) \overrightarrow{V}_\beta(x_>)}{j\omega \mu_0 \overleftrightarrow{Y}(0)}, \quad (37)$$

with

$$\overleftarrow{V}_1(x) = e^{j\kappa_1 x}, \quad \kappa_1^2 = k_1^2 + \lambda, \quad \text{Im } \kappa_1 < 0, \quad (37a)$$

$$\overrightarrow{V}_2(x) = e^{-j\kappa_2 x}, \quad \kappa_2^2 = k_2^2 + \lambda, \quad \text{Im } \kappa_2 < 0, \quad (37b)$$

$$\vec{V}_1(x) = \frac{1}{1 + \vec{\Gamma}_1(0)} [e^{-j\kappa_1 x} + \vec{\Gamma}_1(0)e^{j\kappa_1 x}], \quad \vec{\Gamma}_1(0) = \frac{\kappa_1 - \kappa_2}{\kappa_1 + \kappa_2}, \quad (38a)$$

$$\vec{V}_2(x) = \frac{1}{1 + \vec{\Gamma}_2(0)} [e^{j\kappa_2 x} + \vec{\Gamma}_2(0)e^{-j\kappa_2 x}], \quad \vec{\Gamma}_2(0) = -\vec{\Gamma}_1(0), \quad (38b)$$

$$j\omega \mu_0 \overleftrightarrow{Y} = j(\kappa_1 + \kappa_2). \quad (38c)$$

Since $g''(x, x'; \lambda)$ is not an even function of either κ_1 or κ_2 , branch points exist in the complex λ plane at $\lambda = -k_1^2$ and $\lambda = -k_2^2$. The argument of $\hat{\lambda} = \lambda + k_1^2$ is then restricted in accordance with $\text{Im } \kappa_1 < 0$, $\text{Im } \kappa_2 < 0$, as follows [see Eqs. (22) and (32)]:

$$0 > \arg \hat{\lambda} > -2\pi, \quad 0 > \arg (\hat{\lambda} + h) > -2\pi, \quad h = k_1^2 - k_2^2, \quad (39)$$

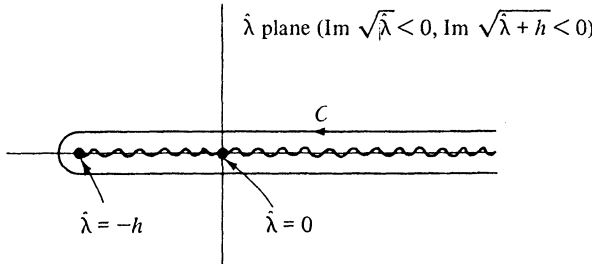


FIG. 3.4.10 Contour of integration and singularities in the complex $\hat{\lambda}$ -plane.

with corresponding branch cuts along the real $\hat{\lambda}$ axis shown in Fig. 3.4.10. Since g'' possesses no pole singularities on the branch of the Riemann surface for which $\text{Im } \kappa_1 < 0$ and $\text{Im } \kappa_2 < 0$, the contour of integration is drawn as in Fig. 3.4.10. Since the replacement of $\hat{\lambda}$ by $\hat{\lambda} e^{-j2\pi}$ in g'' yields g''^* [see Eq. (24c)], we may write

$$\begin{aligned} \delta(x - x') &= -\frac{1}{2\pi j} \oint_C g''(x, x'; \lambda) d\lambda \\ &= -\frac{2}{\pi} \text{Im} \int_0^{\sqrt{h}} \xi_1 g''(x, x'; \xi_1^2 - k_1^2) d\xi_1 - \frac{2}{\pi} \text{Im} \int_0^\infty \xi g''(x, x'; \xi^2 - k_2^2) d\xi \\ &\quad (40a) \end{aligned}$$

$$= \int_0^{\sqrt{h}} \hat{\psi}_\beta(\xi_1, x) \hat{\psi}_\beta^*(\xi_1, x') d\xi_1 + \int_0^\infty \hat{\psi}'_\beta(\xi, x) \hat{\psi}'_\beta^*(\xi, x') d\xi, \quad (40b)$$

$$-\infty < \frac{x}{x'} < \infty,$$

where $\beta = 1$ and $\beta = 2$ correspond to $-\infty < (x \text{ or } x') < 0$ and $0 < (x \text{ or } x') < \infty$, respectively. For $0 < \xi < \infty$, one has the two mutually orthogonal sets

$$\hat{\psi}'_1(\xi, x) = \sqrt{\frac{1 - \vec{\Gamma}_1(\xi, 0)}{\pi}} \begin{cases} \cos \xi_1 x \\ \sqrt{\frac{\xi}{\xi_1}} \sin \xi_1 x \end{cases}, \quad -\infty < x < 0, \quad (41a)$$

$$\hat{\psi}'_2(\xi, x) = \sqrt{\frac{1 - \vec{\Gamma}_1(\xi, 0)}{\pi}} \begin{cases} \cos \xi x \\ \sqrt{\frac{\xi_1}{\xi}} \sin \xi x \end{cases}, \quad 0 < x < \infty, \quad (41b)$$

with

$$\xi_1 = \sqrt{\xi^2 + h} > 0, \quad \vec{\Gamma}_1(\xi, 0) = \frac{\xi_1 - \xi}{\xi_1 + \xi}. \quad (41c)$$

For $0 < \xi_1 < \sqrt{h}$ (i.e., $\xi = -j|\xi|$), the reflection coefficient $\vec{\Gamma}_1$ is complex and of unit magnitude; one has

$$\hat{\psi}_1(\xi_1, x) = \frac{1}{\sqrt{2\pi}} [e^{-j\xi_1 x} + \vec{\Gamma}_1(-j|\xi|, 0)e^{j\xi_1 x}], \quad -\infty < x < 0, \quad (42a)$$

$$\hat{\psi}_2(\xi_1, x) = \frac{1}{\sqrt{2\pi}} [1 + \vec{\Gamma}_1(-j|\xi|, 0)]e^{-j\xi_1 x}, \quad 0 < x < \infty. \quad (42b)$$

E modes (in x)

Characteristic Green's function:

$$g'(x, x'; \lambda) = \frac{\overleftarrow{I}_\beta(x_<) \vec{I}_\beta(x_>)}{j\omega\epsilon_0 \vec{Z}(0)}, \quad (43)$$

with

$$\overleftarrow{I}_1(x) = e^{j\kappa_1 x}, \quad \text{Im } \kappa_1 < 0, \quad \kappa_1^2 \equiv \xi_1^2 = k_1^2 + \lambda, \quad (43a)$$

$$\vec{I}_2(x) = e^{-j\kappa_2 x}, \quad \text{Im } \kappa_2 < 0, \quad \kappa_2^2 \equiv \xi^2 = k_2^2 + \lambda = \hat{\lambda}, \quad (43b)$$

$$\vec{I}_1(x) = \cos \kappa_1 x - j \frac{\epsilon'_1 \kappa_2}{\epsilon'_2 \kappa_1} \sin \kappa_1 x, \quad (43c)$$

$$\overleftarrow{I}_2(x) = \cos \kappa_2 x + j \frac{\epsilon'_2 \kappa_1}{\epsilon'_1 \kappa_2} \sin \kappa_2 x, \quad (43d)$$

$$j\omega\epsilon_0 \vec{Z}(0) = j \left(\frac{\kappa_2}{\epsilon'_2} + \frac{\kappa_1}{\epsilon'_1} \right). \quad (43e)$$

Spectral representation of delta function for $-\infty < x' < \infty$:

$$\begin{aligned} \epsilon'(x') \delta(x - x') &= -\frac{1}{2\pi j} \oint_C d\hat{\lambda} g'(x, x'; \lambda) \\ &= \int_0^{\sqrt{h}} d\xi_1 \hat{\Phi}_\beta(\xi_1, x) \hat{\Phi}_\beta^*(\xi_1, x') + \int_0^\infty d\xi \hat{\Phi}_\beta(\xi, x) \hat{\Phi}_\beta^*(\xi, x'), \end{aligned} \quad (44)$$

where the contour C is given as in Fig. 3.4.10, and with $0 < \xi < \infty$,

$$\hat{\Phi}'_1(\xi, x) = \sqrt{\frac{\epsilon'_2}{\pi} [1 + \vec{\Gamma}_1(\xi, 0)]} \begin{cases} \cos \xi_1 x \\ \sqrt{\frac{\xi \epsilon'_1}{\xi_1 \epsilon'_2}} \sin \xi_1 x \end{cases}, \quad -\infty < x < 0, \quad (45a)$$

$$\hat{\Phi}'_2(\xi, x) = \sqrt{\frac{\epsilon'_2}{\pi} [1 + \vec{\Gamma}_1(\xi, 0)]} \begin{cases} \cos \xi x \\ \sqrt{\frac{\xi_1 \epsilon'_2}{\xi \epsilon'_1}} \sin \xi x \end{cases}, \quad 0 < x < \infty, \quad (45b)$$

with

$$\vec{\Gamma}_1(\xi, 0) = \frac{\xi - \xi_1(\epsilon'_2/\epsilon'_1)}{\xi + \xi_1(\epsilon'_2/\epsilon'_1)}, \quad \xi_1 = \sqrt{\xi^2 + h}. \quad (45c)$$

Also, with $0 < \xi_1 < \sqrt{h}$,

$$\hat{\Phi}_1(\xi_1, x) = \frac{1}{\sqrt{2\pi}} [e^{-j\xi_1 x} - \vec{\Gamma}_1(-j|\xi|, 0)e^{j\xi_1 x}], \quad -\infty < x < 0, \quad (46a)$$

$$\hat{\Phi}_2(\xi_1, x) = \frac{1}{\sqrt{2\pi}} [1 - \vec{\Gamma}_1(-j|\xi|, 0)]e^{-|\xi| x}, \quad 0 < x < \infty. \quad (46b)$$

3.4b Angular Transmission Lines

When waves propagate along an angular coordinate in a curvilinear coordinate system, their characteristics differ from those associated with rectilinear propagation. A distinguishing feature in angular regions is the invisibility of a source point from an observation point displaced far enough along the curved axis; the consequent division of an angular propagation region into illuminated and shadow zones is explored in detail in Chapter 6 for diffraction in cylindrical and spherical geometries. Despite these differences, some angular regions are described by one-dimensional angular transmission lines that are indistinguishable from uniform lines. Angular intervals are finite in extent, owing either to the presence of angular boundaries or to periodicity requirements in the absence of boundaries; corresponding angular transmission lines therefore have finite length and are terminated in impedances representative of boundary conditions at the endpoints of the interval. However, as in rectilinear regions, wave motion is analyzed most directly on an infinite reflectionless (bilaterally “matched”) transmission line. Reflective terminations are then accounted for by superposition of multiply reflected waves or, alternatively, by auxiliary (image) sources located outside the physical section of the infinite line. Because of their importance for cylindrical and spherical scattering problems, image representations on angular transmission lines are emphasized in this section; the ray-optical interpretation of image contributions is presented in Chapter 6.

Cylindrical regions

Angular boundary-value problems encountered in the analysis of scattering in cylindrical (ρ, ϕ, z) regions are schematized in Fig. 3.4.11; Fig. 3.4.11(a) shows a wedge-shaped domain with radial planes at $\phi = 0, \varphi$, while Fig. 3.4.11(b) indicates the angular periodicity required in the absence of ϕ -dependent boundaries. The radial coordinate ρ and the axial coordinate z are perpendicular to

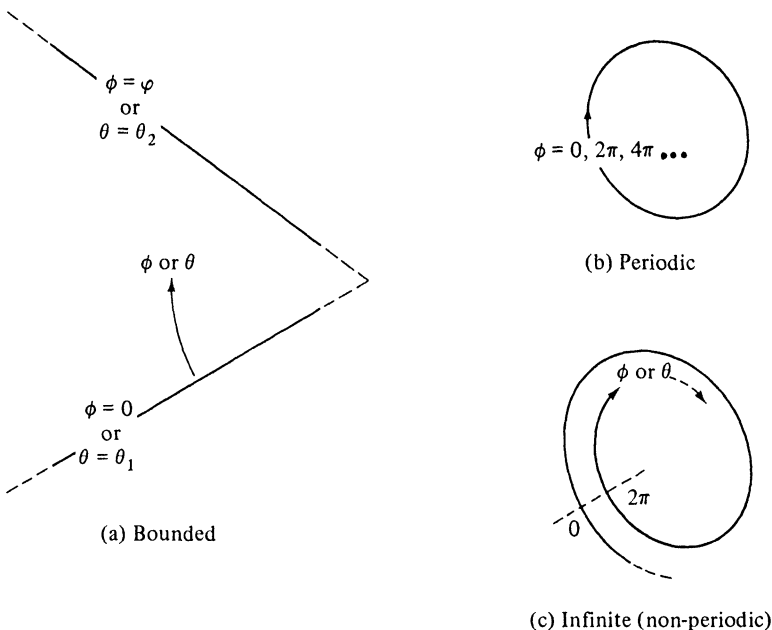


FIG. 3.4.11 Angular domains (ϕ =azimuthal coordinate, θ =latitudinal coordinate).

ϕ in the plane of each figure and perpendicular to that plane, respectively. As noted in Sec. 6.2, information relevant to angular transmission is obtained most simply by considering z -independent fields which decompose into E -mode and H -mode constituents with respect to z . The corresponding angular characteristic Green's functions are denoted, respectively, by $g'_\phi(\phi, \phi'; \lambda)$ and $g''_\phi(\phi, \phi'; \lambda)$, and are defined by the differential equation [see Eqs. (3.2.46a) and (3.3.1)]

$$\left(\frac{d^2}{d\phi^2} + \lambda \right) g_\phi(\phi, \phi'; \lambda) = -\delta(\phi - \phi'). \quad (47)$$

While Eq. (47) is of the same form as Eq. (2.4.30) for a uniform rectilinear region and the transmission-line solutions for the two systems are therefore identical, the physical attributes of angularly and rectilinearly propagating waves differ substantially. In the absence of angular boundaries [see Fig. 3.2.7(b)], g_ϕ must meet the periodicity requirements [Fig. 3.4.11(b)]

$$g_\phi(\phi + \pi, \phi'; \lambda) = g_\phi(\phi - \pi, \phi'; \lambda);$$

$$\frac{d}{d\phi} g_\phi(\phi + \pi, \phi'; \lambda) = \frac{d}{d\phi} g_\phi(\phi - \pi, \phi'; \lambda), \quad (48a)$$

with $-\pi \leq (\phi, \phi') \leq \pi$. The E - and H -mode functions are identical in this case, thereby making the distinguishing primes on g_ϕ unnecessary. If the ϕ interval is taken as $-\pi < (\phi - \phi') < \pi$ (i.e., symmetric about the source location), condition (48a) can be written in the simpler form

$$\frac{d}{d\phi} g_\phi(\phi, \phi'; \lambda) = 0 \quad \text{at } (\phi - \phi') = \pm\pi. \quad (48b)$$

If perfectly conducting plane boundaries are present at $\phi = 0$ and at $\phi = \varphi$, $0 < \varphi \leq 2\pi$ [see Figs. 3.2.7(a), 3.2.9, and 3.4.11(a)], the range of ϕ and ϕ' is restricted to $0 \leq (\phi, \phi') \leq \varphi$ and the corresponding boundary conditions on g_ϕ are

E modes (along z)

$$g'_\phi(\phi, \phi'; \lambda) = 0 \quad \text{at } \phi = 0, \varphi. \quad (49)$$

H modes (along z)

$$\frac{d}{d\phi} g''_\phi(\phi, \phi'; \lambda) = 0 \quad \text{at } \phi = 0, \varphi. \quad (50)$$

Equivalent network configurations representing the various boundary-value problems above are shown in Figs. 3.4.12 and 3.4.13 (see Figs. 3.3.1 and 3.3.2). For two-dimensional diffraction problems involving E modes along z , the source is an electric line current and the only electric field component, E_z , is proportional to the two-dimensional Green's function \bar{G}' (see Sec. 6.2). Hence, it is appropriate to treat g'_ϕ as a measure of E_z (i.e., as a voltage), leading via Fig. 3.3.1 and Eq. (3.3.4) to the equivalent networks in Fig. 3.4.12.[†] Analogous considerations apply to the H -mode problem and yield the network representations in Fig. 3.4.13. It is noted that the network problems in Figs. 3.4.12(a) and

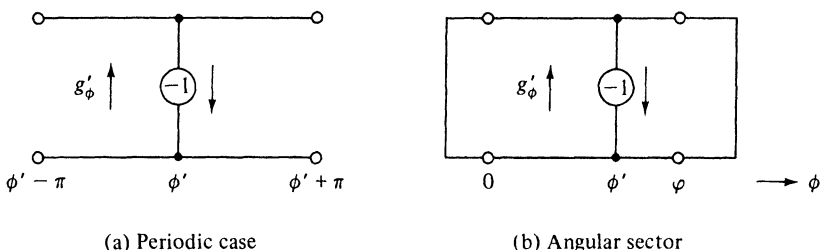


FIG. 3.4.12 E modes along z ($g'_\phi \rightarrow$ voltage).

[†] E - and H -mode designations are with respect to the z axis. The E -mode problem along z is actually an H -mode problem along the transmission coordinate ϕ since $E_\phi \equiv 0$, thereby corresponding to the designation in Eq. (3.3.4).

3.4.13(a) are exact duals of one another, thereby yielding the previous result $g'_\phi = g''_\phi$ for the periodic case. Perfectly conducting boundaries at the endpoints of the sectoral region give rise to the short-circuit terminations shown in Figs. 3.4.12(b) and 3.4.13(b). From Eq. (47), the ϕ -independent propagation constant on the angular transmission lines is given by $\sqrt{\lambda}$ and a characteristic impedance (admittance) for the H -mode (E -mode) problems can be chosen proportional to $\sqrt{\lambda}$ [see Eqs. (3.2.97), (3.2.98), (3.3.4) and the footnote on p. 000]. The voltage-current solutions on these transmission lines can therefore be taken directly from Sec. 2.4.

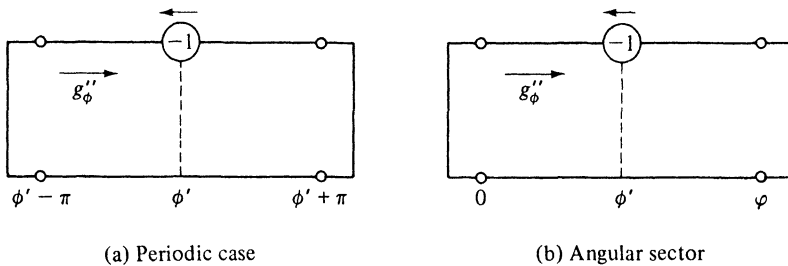


FIG. 3.4.13 H modes along z ($g''_\phi \rightarrow$ current).

The solution for the network problems in Figs. 3.4.12 and 3.4.13 can be expressed in terms of the traveling-wave representation in Eq. (2.4.29d) (with $z_0 = 0$) appropriate to a point-source-excited, terminated transmission line extending from $\phi = 0$ to $\phi = \varphi$:†

$$g_\phi(\phi, \phi'; \lambda) = \frac{(e^{j\mu\phi_-} + \overleftarrow{\Gamma} e^{-j\mu\phi_-})(e^{j\mu(\varphi-\phi_>)} + \overrightarrow{\Gamma} e^{-j\mu(\varphi-\phi_>)})}{2j\mu(e^{j\mu\varphi} - \overleftarrow{\Gamma} \overrightarrow{\Gamma} e^{-j\mu\varphi})} \quad (51)$$

where $\overleftarrow{\Gamma}$ and $\overrightarrow{\Gamma}$ are the reflection coefficients at the left and right endpoints, respectively [see Eq. (2.4.6) for relation between $\overrightarrow{\Gamma}(0)$ and $\overleftarrow{\Gamma}$], and $\mu = \sqrt{\lambda}$. To have g'_ϕ vanish at $\phi = 0, \varphi$, as in Fig. 3.4.12(b), it is required that $\overrightarrow{\Gamma} = \overleftarrow{\Gamma} = -1$, whence

$$g'_\phi(\phi, \phi'; \lambda) = \frac{\sin \mu\phi_- \sin \mu(\varphi - \phi_>)}{\mu \sin \mu\varphi} \quad (51a)$$

while the vanishing of $dg''_\phi/d\phi$ at the endpoints in Fig. 3.4.13(b) requires $\overrightarrow{\Gamma} = \overleftarrow{\Gamma} = 1$, whence

$$g''_\phi(\phi, \phi'; \lambda) = \frac{\cos \mu\phi_- \cos \mu(\varphi - \phi_>)}{-\mu \sin \mu\varphi}. \quad (51b)$$

†In this section μ is a complex parameter and is not to be confused with the same symbol used elsewhere for the permeability.

For the periodic case, one notes from Fig. 3.4.13(a) that the symmetric network can be short-circuit bisected at ϕ' . Assume for the moment that $\phi' = 0$. The resulting problem is then identical with that in Fig. 3.4.13(b), provided that the source (of strength $-\frac{1}{2}$ because of the bisection) is moved to $\phi' = 0$, and that φ is set equal to π . Displacement of the origin to ϕ' merely implies that ϕ is replaced by $\phi - \phi'$. Finally, from symmetry considerations, the same response holds in the region $\phi < \phi'$, whence $\phi - \phi'$ can be replaced by $|\phi - \phi'|$ to yield an expression valid in the entire interval $|\phi - \phi'| < \pi$. Therefore, twice the angular Green's function for the periodic case is deduced from Eq. (51) on writing $\vec{\Gamma} = \overleftarrow{\Gamma} = 1$, $\varphi = \pi$, $\phi_< = 0$, $\phi_> \rightarrow |\phi - \phi'|$, whence

$$g_\phi(\phi, \phi'; \lambda) = -\frac{\cos \mu [\pi - |\phi - \phi'|]}{2\mu \sin \mu\pi}. \quad (51c)$$

The Green's function solution in Eq. (51) is more general than that required for the problems discussed above since it applies also when the reflection coefficients $\vec{\Gamma}$ have a value different from +1 or -1. In fact, if one employs instead of the simple boundary conditions in Eqs. (48)–(50) the more general “impedance condition”

$$\frac{d}{d\phi} g_\phi = \pm jc_{1,2} g_\phi \quad \text{at } \phi = \begin{cases} 0 \\ \varphi \end{cases}, \quad (52)$$

where c_1 and c_2 are constants independent of ϕ and μ , one finds that Eq. (51) also represents the solution in this case provided that the following values for the reflection coefficients are employed:

$$\overleftarrow{\Gamma} = \frac{\mu - c_1}{\mu + c_1}, \quad \vec{\Gamma} = \frac{\mu - c_2}{\mu + c_2}. \quad (53)$$

Upon recalling that μ represents the characteristic impedance (admittance) for the H -mode (E -mode) problems, one notes that the voltage (current) reflection coefficients in Eqs. (53) have precisely the form (2.4.12), with $c_{1,2}$ representing the terminal impedances (admittances) (for passive terminations, $\operatorname{Re} c_{1,2} \geq 0$). The boundary condition (52) is utilized in Sec. 6.6 for analysis of diffraction by a wedge with a variable surface impedance.

For the above terminations, one verifies readily that g_ϕ is an even function of μ (i.e., a regular function of λ near $\lambda = 0$), and hence no special care need be taken in the definition of $\sqrt{\lambda}$. The only singularities are simple poles located at the zeros of the denominator of Eq. (51) (with the possible exception of $\mu = 0$). At infinity in the complex λ plane,

$$|g_\phi| \sim \frac{e^{-|\operatorname{Im} \mu| |\phi - \phi'|}}{2|\mu|}, \quad \text{as } |\operatorname{Im} \mu| \rightarrow \infty. \quad (54)$$

The representation in Eq. (51) is directly suited to the development of the image formulation described previously. The Green's function $g_\phi^\infty(\phi, \phi'; \mu)$ on an “infinite” (bilaterally matched) angular line is obtained upon letting $\vec{\Gamma} = 0$.

Since complex μ corresponds to a dissipative line, in which the response is required to decay away from the source, Eq. (51) (for $\Gamma = 0$) is valid only when $\text{Im } \mu < 0$. Conversely, since g_ϕ is an even function of μ , upon changing μ into $-\mu$ in Eq. (51), one derives a limiting form valid when $\text{Im } \mu > 0$, so

$$g_\phi^\infty(\phi, \phi'; \mu) = \frac{e^{\mp j\mu|\phi - \phi'|}}{\pm 2j\mu}, \quad \text{Im } \mu \leq 0. \quad (55)$$

Unlike g_ϕ , g_ϕ^∞ is not an even function of μ and is, in fact, discontinuous across the real μ axis. Hence, viewed as a function of $\lambda = \mu^2$, g_ϕ^∞ possesses a first-order branch point singularity at $\lambda = 0$, with branch cut along the positive real x axis [the top sheets in Eq. (55) are defined by $\text{Im } \sqrt{\lambda} \leq 0$]. Its behavior as $|\text{Im } \mu| \rightarrow \infty$ is identical with that of g_ϕ in Eq. (54). Upon employing the convergent power-series expansion†

$$\frac{1}{e^{j\mu\varphi} - \overleftarrow{\Gamma}\overrightarrow{\Gamma}e^{-j\mu\varphi}} = \sum_{n=1}^{\infty} (\overleftarrow{\Gamma}\overrightarrow{\Gamma})^n e^{-j(2n+1)\mu\varphi}, \quad \text{Im } \mu < 0, \quad (56)$$

in Eq. (51) and rearranging terms, one may write

$$\begin{aligned} g_\phi(\phi, \phi'; \lambda) = & g_\phi^\infty(\phi, \phi') + \sum_{n=1}^{\infty} (\overleftarrow{\Gamma}\overrightarrow{\Gamma})^n g_\phi^\infty(\phi, 2n\varphi - \phi') \\ & + \sum_{n=1}^{\infty} (\overleftarrow{\Gamma}\overrightarrow{\Gamma})^n [g_\phi^\infty(\phi, 2n\varphi + \phi') + g_\phi^\infty(\phi, -2n\varphi + \phi')] \\ & + \sum_{n=0}^{\infty} \overrightarrow{\Gamma}^n \overleftarrow{\Gamma}^{n+1} g_\phi^\infty(\phi, -2n\varphi - \phi'), \quad \text{Im } \mu < 0, \end{aligned} \quad (57)$$

with g_ϕ^∞ given in Eq. (55), and $\overleftarrow{\Gamma}$, $\overrightarrow{\Gamma}$ defined as in Eq. (53). On replacing μ by $-\mu$ in Eq. (57), one obtains a series representation valid when $\text{Im } \mu > 0$.

Equation (57) comprises contributions that can be interpreted as arising from a set of sources located at the points

$$\begin{aligned} \phi &= 2n\varphi - \phi', \quad n = 0, \pm 1, \pm 2, \dots \\ \phi &= 2n\varphi + \phi', \quad n = \pm 1, \pm 2, \dots \end{aligned} \quad (58)$$

on an infinitely extended transmission line. Only the actual source at $\phi = \phi'$ is situated in the physical angular domain $0 \leq (\phi, \phi') \leq \varphi$; all the other (image) sources lie outside this range. The amplitude of a given image source is identical with that of the corresponding multiply reflected wave; with each reflection at $\phi = 0$ and $\phi = \varphi$, a reflected wave acquires an amplitude factor $\overleftarrow{\Gamma}$ and $\overrightarrow{\Gamma}$, respectively. Hence, image 1, arising from the first reflection at $\phi = 0$, has an amplitude $\overleftarrow{\Gamma}$; image $1'$, arising from the first reflection at $\phi = \varphi$, has an amplitude $\overrightarrow{\Gamma}$; image 2, arising from the second reflection at $\phi = 0$, has an amplitude $\overleftarrow{\Gamma}\overrightarrow{\Gamma}$; etc. The angular coordinate ϕ in Fig. 3.4.14 has been plotted along a straight-line scale which makes the meaning of the extended non-periodic angular domain $-\infty < (\phi, \phi') < \infty$ unambiguous. If ϕ is plotted on its con-

†It is assumed that $|\overleftarrow{\Gamma}\overrightarrow{\Gamma}|e^{-2|\text{Im } \mu|\varphi} < 1$.

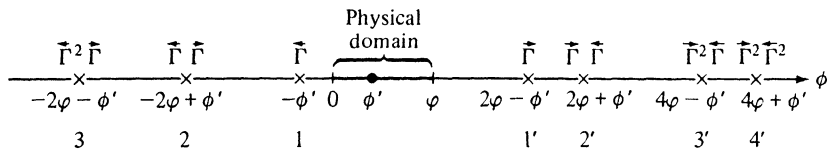


FIG. 3.4.14 Image representation for reflecting terminations at $\phi = 0, \varphi$.

ventional circular cylindrical coordinate scale whereon an increment of 2π corresponds to a complete circuit, it is necessary to view the ϕ domain as a complex Riemann surface^{7,8} having an infinite number of sheets [Fig. 3.4.11(c)]; the passage out of the physical domain $0 \leq \phi \leq \varphi$ into the image region then proceeds via branch cuts introduced along the lines $\phi = 0$ and $\phi = \varphi$. However, the extension of ϕ into a complex Riemann surface is not essential if all subsequent considerations are confined to the physical range $0 \leq (\phi, \phi') \leq \varphi$, over which Eq. (57) is defined unambiguously. In this instance, one interprets the image contributions as multiply reflected waves between the boundaries $\phi = 0, \varphi$. Although we shall adopt this latter, simpler interpretation to avoid the necessity of defining ϕ in a multisheeted complex plane, the equivalent image formulation schematized in Fig. 3.4.14 may be kept in mind as a simple schematization of the multiple reflection process.

If the terminations at $\phi = 0, \varphi$ comprise short or open circuits (i.e., $\Gamma = \pm 1$), Eqs. (57) simplify and can be written more compactly as

$$g_\phi(\phi, \phi'; \lambda) = \sum_{n=-\infty}^{\infty} g_\phi^\infty(\phi, 2n\varphi + \phi') \pm \sum_{n=-\infty}^{\infty} g_\phi^\infty(\phi, 2n\varphi - \phi'), \quad (59)$$

where the upper and lower signs correspond to $\tilde{\Gamma} = \tilde{\Gamma} = +1$ and $\tilde{\Gamma} = \tilde{\Gamma} = -1$, respectively. For the periodic case, one obtains in view of the remarks preceding Eq. (51c):

$$g_\phi(\phi, \phi'; \lambda) = \sum_{n=-\infty}^{\infty} g_\phi^\infty(\phi - \phi', 2n\pi) = \sum_{n=-\infty}^{\infty} g_\phi^\infty(\phi, 2n\pi + \phi'), \quad (60)$$

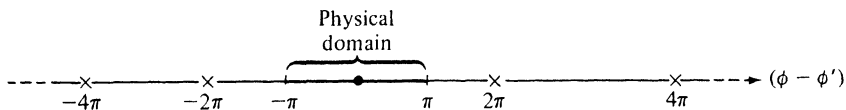


FIG. 3.4.15 Image representation for periodic case.

with an image representation as shown in Fig. 3.4.15. Equations (59) and (60) are used in Secs. 6.5 and 6.7 for an angular transmission analysis of high-frequency diffraction by a perfectly conducting wedge and cylinder, respectively.

Completeness relations for the domain $0 \leq \phi \leq \varphi$, with the boundary conditions of Eqs. (51a)–(51c), have already been given in Eqs. (3.2.47), (3.2.48), and (3.2.50). For the impedance boundary condition in Eq. (52), with $c_2 = 0$

for convenience, one finds that g_ϕ in Eq. (51) has simple singularities at $\mu = \xi$, where

$$\cot \xi \varphi = -\frac{j\xi}{c_1}. \quad (61)$$

If the surface impedance parameter is reactive so that $c_1 = j\gamma$, with $\gamma > 0$, then Eq. (61) has a discrete infinity of real roots ξ_1, ξ_2, \dots , and a single imaginary root $\xi_0 = j\eta$, η real, satisfying $\coth \eta \varphi = \eta/\gamma$; these roots may be determined from the graphical construction in Fig. 3.4.16. Then from Eq. (3.3.11),

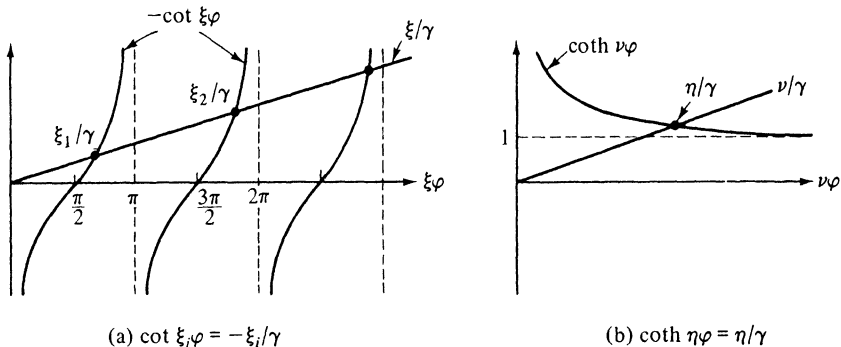


FIG. 3.4.16 Graphical solution of Eq. (61), with $c_1 = j\gamma$, $\gamma > 0$.

$$\delta(\phi - \phi') = \begin{cases} -\frac{1}{2\pi j} \oint g_\phi(\phi, \phi'; \lambda) d\lambda, \\ \sum_q \psi_q(\phi)\psi_q(\phi') + \psi_0(\phi)\psi_0(\phi')U(\gamma), \end{cases} \quad (62a)$$

$$(62b)$$

where $U(\gamma) = 1$ or 0 when $\gamma > 0$ or $\gamma < 0$, respectively, and

$$\psi_q(\phi) = \left[\frac{2}{\phi[1 - (\sin^2 \xi_i \phi)/\gamma \phi]} \right]^{1/2} \cos [\xi_i(\phi - \phi)], \quad q \equiv \xi_i > 0, \quad (62c)$$

$$\psi_0(\phi) = \left[\frac{2}{\phi[1 + (\sinh^2 \eta \phi)/\gamma \phi]} \right]^{1/2} \cosh [\eta(\phi - \phi)], \quad \eta > 0. \quad (62d)$$

The eigenfunctions $\psi_q(\phi)$ in Eq. (62c) are oscillatory in the interval $0 \leq \phi \leq \varphi$, while $\psi_0(\phi)$ in Eq. (62d) decays away from the reactive boundary at $\phi = 0$ and is therefore analogous to the surface-wave modes in Eq. (17b). The occurrence of only a single surface-wave mode is attributable to the assumption at $\phi = 0$ of a surface impedance that idealizes an implied medium in $\phi < 0$; in the analogous problem shown in Fig. 3.4.1(a), the medium in $x < 0$ is exhibited explicitly. It should be emphasized that constancy of the parameters $c_{1,2}$ does not imply constancy of surface impedance on the angular boundaries $\phi = 0, \varphi$ since the cylindrical (ρ, ϕ, z) coordinate system is curvilinear. This aspect is explored in detail in Sec. 6.6.

Spherical regions

Two-dimensional eigenvalue problems in the (θ, ϕ) cross section transverse to the radial coordinate r in a spherical coordinate system are defined by the differential equations (2.6.2) and (2.6.3). For separable boundary conditions [i.e., in regions bounded by plane surfaces $\phi = \text{constant}$ and (or) conical surfaces $\theta = \text{constant}$], the two-dimensional eigenvalue problems may be reduced to two one-dimensional eigenvalue problems:

$$\left(\frac{d^2}{d\phi^2} + q^2 \right) \Phi_q(\phi) = 0, \quad \left. \begin{aligned} \Phi_q \\ \frac{\partial \psi_q}{\partial \phi} \end{aligned} \right\} = 0 \quad \text{at } \phi = 0, \varphi \quad (63a)$$

$$\left(\frac{d}{d\theta} \sin \theta \frac{d}{d\theta} - \frac{q^2}{\sin \theta} + p(p+1) \sin \theta \right) \Psi_p^q(\theta) = 0, \quad \left. \begin{aligned} \Psi_p^q \\ \frac{\partial \psi_p^q}{\partial \theta} \end{aligned} \right\} = 0 \quad \text{at } \theta = \theta_{1,2}, \quad (63b)$$

where the product solutions $\Phi_i(p) = \Phi_q(\phi)\Phi_p^q(\theta)$ and $\psi_i(p) = \psi_q(\phi)\psi_p^q(\theta)$ have been introduced, and where $p(p+1) = k_{ii}^2$. Since Eqs. (63a) and (3.2.46a) are identical, the eigenvalue and characteristic Green's function problems for the azimuthal (ϕ) domain are the same as in cylindrical geometry. For the θ domain $\theta_1 \leq \theta \leq \theta_2$, comparison of Eqs. (63b) and (3.3.1) yields the characteristic Green's function problem:

$$\left(\frac{d}{d\theta} \sin \theta \frac{d}{d\theta} - \frac{q^2}{\sin \theta} + \lambda \sin \theta \right) g_\theta(\theta, \theta'; q^2, \lambda) = -\delta(\theta - \theta'), \quad (64)$$

where q is a fixed parameter which, in spherical boundary-value problems, represents the azimuthal eigenvalue [see Eq. (63a)]. On replacing x by θ , comparison with Eq. (3.3.1) shows that the θ transmission line is non-uniform, since the parameters $p(\theta) = w(\theta) = \sin \theta$, $q(\theta) = q^2/\sin \theta$ are θ dependent. For an angularly unbounded spherical region, the endpoints of the θ interval are $\theta_1 = 0$ and $\theta_2 = \pi$; $\theta_1 = 0, 0 < \theta_2 < \pi$ represents a single cone at $\theta = \theta_2$, while $0 < \theta_1 < \theta_2 < \pi$ defines cones at $\theta = \theta_1, \theta_2$, respectively. The boundary conditions for electromagnetic E - and H -mode problems with respect to the radial direction, distinguished by primes and double primes, respectively, are [see Eqs. (2.6.2) and (2.6.3)]

$$g'_\theta(\theta, \theta'; q^2; \lambda) = 0 \quad \text{at } \theta = \theta_{1,2} \quad (E \text{ modes}), \quad (64a)$$

$$\frac{d}{d\theta} g''_\theta(\theta, \theta'; q^2; \lambda) = 0 \quad \text{at } \theta = \theta_{1,2} \quad (H \text{ modes}). \quad (64b)$$

Note $\theta = 0, \pi$ are “limit point” singularities of the differential operator in Eq. (63). If these points terminate the θ interval, a sufficient boundary condition is

$$g_\theta \text{ finite at } \theta_1 = 0 \text{ and (or) } \theta_2 = \pi. \quad (64c)$$

These angular boundary-value problems may be schematized as in Fig. 3.4.11.

The various $g_\theta(\theta, \theta'; q^2; \lambda)$ may be constructed from the linearly independent solutions of the homogeneous equation (64). Since $\lambda = v(v + 1)$ is a complex parameter and q may also be non-real (see discussion on alternative representations, Sec. 3.3c), the classical Legendre polynomials are inadequate to describe this more general situation. Instead, it is best to express the associated Legendre functions as special cases of hypergeometric functions, the theory of which is well advanced. It may be shown that $P_v^{-q}(\cos \theta)$ and $P_v^{-q}[\cos(\pi - \theta)] \equiv P_v^{-q}(-\cos \theta)$ are linearly independent solutions of the associated Legendre equation and are related to the hypergeometric function $F(a, \beta; \gamma; z)$ as follows⁹:

$$\begin{aligned} P_v^{-q}(\cos \theta) &= \frac{1}{\Gamma(1+q)} \tan^q\left(\frac{\theta}{2}\right) F\left(-v, v+1; 1+q; \sin^2 \frac{\theta}{2}\right) \\ &= P_{-v-1}^{-q}(\cos \theta), \end{aligned} \quad (65a)$$

$$P_v^{-q}(-\cos \theta) = \frac{1}{\Gamma(1+q)} \cot^q\left(\frac{\theta}{2}\right) F\left(-v, v+1; 1+q; \cos^2 \frac{\theta}{2}\right), \quad (65b)$$

where $\Gamma(x)$ is the gamma function and v and q are arbitrary. Some properties of the hypergeometric function are given in Sec. 3.6b. Important for the present discussion is the relation

$$F(a, b; c; 0) = 1, \quad (65c)$$

which permits the study of the behavior of $P_v^{-q}(\pm \cos \theta)$ near the singular points $\theta = 0, \pi$. It is also useful to recall that

$$\begin{aligned} F(a, b; c; z) &= \frac{\Gamma(c)\Gamma(c-a-b)}{\Gamma(c-a)\Gamma(c-b)} F(a, b; a+b-c+1; 1-z) \\ &+ (1-z)^{c-a-b} \frac{\Gamma(c)\Gamma(a+b-c)}{\Gamma(a)\Gamma(b)} F(c-a, c-b; c-a-b+1; 1-z), \end{aligned} \quad (65d)$$

which relation permits study of the behavior of the hypergeometric function near $z = 1$. If $\operatorname{Re} q > 0$, then $P_v^{-q}(\cos \theta)$ and $P_v^{-q}(-\cos \theta)$ are bounded at $\theta = 0$ and $\theta = \pi$, respectively, but not at the opposite endpoint. We shall also have occasion to employ the Wronskian

$$\begin{aligned} P_v^{-q}(\cos \theta) \frac{d}{d\theta} P_v^{-q}(-\cos \theta) - P_v^{-q}(-\cos \theta) \frac{d}{d\theta} P_v^{-q}(\cos \theta) \\ = \frac{2}{\pi} \frac{\sin(v-q)\pi}{\sin \theta} \frac{\Gamma(v-q+1)}{\Gamma(v+q+1)} \\ = -\frac{2}{\sin \theta \Gamma(q-v)\Gamma(v+q+1)}; \end{aligned} \quad (66a)$$

the asymptotic formula

$$\begin{aligned} P_v^{-q}(\cos \theta) &\sim \sqrt{\frac{2}{\pi \sin \theta}} \frac{\Gamma(v - q + 1)}{\Gamma(v + \frac{3}{2})} \cos \left[\left(v + \frac{1}{2} \right) \theta - \frac{\pi}{4} - \frac{q\pi}{2} \right] \\ &\times \left[1 + O\left(\frac{1}{v}\right) \right], \end{aligned} \quad (66b)$$

valid when $|v| \gg |q|$, $|\arg v| < \pi$, $|v| \sin \theta \gg 1$; the Stirling approximation

$$\Gamma(v + \alpha) \sim \sqrt{\frac{2\pi}{v}} \left(\frac{v}{e} \right)^v v^\alpha, \quad |v| \rightarrow \infty, |\arg v| < \pi, \alpha > 0; \quad (66c)$$

and the relation

$$F(a, b; c; z) \sim 1 + O\left(\frac{1}{c}\right), \quad c \rightarrow \infty. \quad (66d)$$

Like the azimuthal Green's function g_ϕ defined in Eq. (47), g_θ may be synthesized in terms of images on an infinitely extended θ transmission line. As noted earlier, such a representation is useful for analysis of high-frequency diffraction by conical and spherical obstacles. We illustrate the procedure for the domain bounded by $\theta_1 = 0$ and $\theta_2 \equiv \theta_0 < \pi$ since closed-form expressions for g'_θ or g''_θ , analogous to Eq. (51), then have a relatively simple form. By Eq. (3.3.14) and Eqs. (64)–(66), the desired solution can be written in terms of the Green's function $g_\theta^0(\theta, \theta'; q^2; \lambda)$ for the interval $0 \leq \theta \leq \pi$, plus a correction term. Thus, g_θ^0 is given by

$$\begin{aligned} g_\theta^0(\theta, \theta'; q^2; \lambda) &= -\frac{\pi}{2} \frac{\Gamma(v + q + 1)}{\Gamma(v - q + 1) \sin(v - q)\pi} P_v^{-q}(\cos \theta_-) P_v^{-q}(-\cos \theta_+), \\ 0 \leq \theta' &\leq \pi, \end{aligned} \quad (67)$$

with $\lambda = v(v + 1)$, $\text{Im } \lambda \neq 0$, and $\text{Re } q > 0$. Then, for E modes,

$$\begin{aligned} g'_\theta(\theta, \theta'; q^2; \lambda) &= g_\theta^0(\theta, \theta'; q^2; \lambda) \\ &+ \frac{\pi}{2} P_v^{-q}(\cos \theta) P_v^{-q}(\cos \theta') \frac{\Gamma(v + q + 1) P_v^{-q}(-\cos \theta_0)}{\Gamma(v - q + 1) P_v^{-q}(\cos \theta_0) \sin(v - q)\pi}, \end{aligned} \quad (68)$$

and, for H modes,

$$\begin{aligned} g''_\theta(\theta, \theta'; q^2; \lambda) &= g_\theta^0(\theta, \theta'; q^2; \lambda) \\ &+ \frac{\pi}{2} P_v^{-q}(\cos \theta) P_v^{-q}(\cos \theta') \frac{\Gamma(v + q + 1) (d/d\theta_0) P_v^{-q}(-\cos \theta_0)}{\Gamma(v - q + 1) (d/d\theta_0) P_v^{-q}(\cos \theta_0) \sin(v - q)\pi}. \end{aligned} \quad (69)$$

For positive real q , one verifies that g_θ^0 , g'_θ , and g''_θ behave asymptotically as

$$|g_\theta(\theta, \theta'; q^2; \lambda)| \rightarrow \frac{1}{|v| \sqrt{\sin \theta \sin \theta'}} e^{-|\text{Im } v||\theta - \theta'|}, \quad |v| \rightarrow \infty, \quad (70)$$

whence the characteristic Green's functions decay at infinity in the complex λ plane. Since $\lambda = v(v + 1) = (v + \frac{1}{2})^2 - \frac{1}{4}$, and $(\sin \pi z)\Gamma(z)\Gamma(1 - z) = \pi$, one observes that g_θ^0 , g'_θ , and g''_θ are even functions of $(v + \frac{1}{2})$.

To obtain traveling-wave solutions on a bilaterally matched θ transmission line, it is necessary to introduce traveling-wave functions instead of the standing-wave functions $P_v^{-q}(\pm \cos \theta)$ [see Eq. (66b)]. The traveling-wave functions $E_q^{(1,2)}(\xi, \theta)$ for arbitrary v and q are defined as follows[†]:

$$E_q^{(1,2)}(\xi, \theta) = \pm \frac{j}{\sin(v - q)\pi} [P_v^{-q}(-\cos \theta) - e^{\pm j(v-q)\pi} P_v^{-q}(\cos \theta)], \quad (71)$$

$$= E_q^{(1,2)}(\xi, \pi - \theta) e^{\pm j(v-q)\pi}, \quad \xi = v + \frac{1}{2}, \quad (71a)$$

whence

$$P_v^{-q}(\cos \theta) = \frac{1}{2} [E_q^{(1)}(\xi, \theta) + E_q^{(2)}(\xi, \theta)]. \quad (71b)$$

The relation in Eq. (71a) is evident from the definition (71). On use of hypergeometric function representations for $P_v^{-q}(\pm \cos \theta)$, one may show that¹⁰

$$E_q^{(1,2)}(\xi, \theta) = \sqrt{\frac{2}{\pi \sin \theta}} \frac{\Gamma(\xi + \frac{1}{2} - q)}{\Gamma(\xi + 1)} e^{\pm j(\xi\theta - q\pi/2 - \pi/4)} R_q^{(1,2)}(\xi, \theta), \quad (72)$$

where

$$R_q^{(1,2)}(\xi, \theta) = \begin{cases} F\left(\frac{1}{2} + q, \frac{1}{2} - q; \xi + 1; \frac{e^{\pm j\theta}}{\pm 2j \sin \theta}\right), \\ (1 - e^{\pm j2\theta})^{(1/2)-q} F\left(\frac{1}{2} - q, \xi + \frac{1}{2} - q; \xi + 1; e^{\pm j2\theta}\right). \end{cases} \quad (72a)$$

$$(1 - e^{\pm j2\theta})^{(1/2)-q} F\left(\frac{1}{2} - q, \xi + \frac{1}{2} - q; \xi + 1; e^{\pm j2\theta}\right). \quad (72b)$$

Equation (72b) follows from Eq. (72a) via the transformation

$$F\left(a, b; c; \frac{z}{1-z}\right) = (1-z)^b F(b, c-a; c; z). \quad (72c)$$

The traveling-wave character (for large $\xi \sin \theta$) of the functions $E_q^{(1,2)}(\xi, \theta)$ becomes evident from Eq. (72) on use of the asymptotic formula (66d), which yields

$$R_q^{(1,2)}(\xi, \theta) \sim 1, \quad |\xi| \rightarrow \infty, \quad \sin \theta \neq 0. \quad (72d)$$

The characteristic Green's functions in Eqs. (68) and (69) can now be represented in terms of multiply reflected traveling waves if one utilizes Eq. (71b) and the power-series expansion [note analogy with Eq. (56)]

$$\frac{1}{1 + b_q(\xi, \theta)} = \sum_{n=0}^{\infty} [-b_q(\xi, \theta)]^n, \quad (73)$$

where, for $\text{Im } \xi > 0$,

$$b_q(\xi, \theta_0) = \frac{L E_q^{(1)}(\xi, \theta_0)}{L E_q^{(2)}(\xi, \theta_0)} \equiv -e^{j(2\xi\theta_0 - q\pi - \pi/2)} f_{\xi q}(\theta_0), \quad (73a)$$

with $L \equiv 1$ for the E -mode case in Eq. (68), and $L \equiv d/d\theta_0$ for the H -mode case in Eq. (69). Thus, one finds

[†]In the present discussion, j is the imaginary unit and does not refer to a particular harmonic time dependence.

$$g_\theta(\theta, \theta'; q^2; \xi^2 - \frac{1}{4}) = \left[\frac{\Gamma(\xi + q + \frac{1}{2})\Gamma(\xi - q + \frac{1}{2})}{\xi\Gamma^2(\xi)} \right] \frac{1}{\sqrt{\sin \theta \sin \theta'}} \left\{ \quad \right\}, \quad (74)$$

where

$$\begin{aligned} \left\{ \quad \right\} &= g_\theta^\infty(\theta, \theta') R_q^{(2)}(\theta_<) R_q^{(1)}(\theta_>) \\ &+ \sum_{n=1}^{\infty} \overleftarrow{\Gamma}^{n-1} \vec{\Gamma}^n g_\theta^\infty(\theta, 2n\theta_0 - \theta') f_{\xi q}^n R_q^{(2)}(\xi, \theta) R_q^{(2)}(\xi, \theta') \\ &+ \sum_{n=1}^{\infty} (\overleftarrow{\Gamma} \vec{\Gamma})^n f_{\xi q}^n [g_\theta^\infty(\theta, -2n\theta_0 + \theta') R_q^{(1)}(\xi, \theta) R_q^{(2)}(\xi, \theta')] \\ &\quad + g_\theta^\infty(\theta, 2n\theta_0 + \theta') R_q^{(2)}(\xi, \theta) R_q^{(1)}(\xi, \theta')] \\ &+ \sum_{n=0}^{\infty} \overleftarrow{\Gamma}^{n+1} \vec{\Gamma}^n f_{\xi q}^n g_\theta^\infty(\theta, -2n\theta_0 - \theta') R_q^{(1)}(\xi, \theta) R_q^{(1)}(\xi, \theta'), \end{aligned} \quad (74a)$$

$$g_\theta^\infty(\theta, \theta') = \frac{e^{j\xi|\theta-\theta'|}}{-2j\xi}, \quad \overleftarrow{\Gamma} = e^{-j(q+1/2)n}, \quad \vec{\Gamma} = \begin{cases} -1 & \text{for } g'_\theta, \\ +1 & \text{for } g''_\theta. \end{cases} \quad (74b)$$

Equation (74) is valid when $\text{Im } \xi > 0$; since g_θ is an even function of ξ [see remarks following Eq. (70)], a series representation for $\text{Im } \xi < 0$ is obtained on replacing ξ by $-\xi$.

The series in Eq. (74a) has been written in a manner that permits direct identification with corresponding terms in the azimuthally traveling-wave expansion (57). Recalling Eq. (72d) and recognizing from Eq. (73a) that for $\sin \theta, \sin \theta', \sin \theta_0 \neq 0$,

$$f_{\xi q} \sim 1 + O\left(\frac{1}{\xi}\right), \quad |\xi| \rightarrow \infty, \quad (75)$$

one finds that the large ξ asymptotic behavior of Eq. (74a) coincides with Eq. (57), whence the image representation in Fig. 3.4.14 applies directly. $\overleftarrow{\Gamma}$ in Eq. (74b) expresses the effective reflection coefficient at the singular endpoint $\theta = 0$, while $\vec{\Gamma}$ accounts for reflection at $\theta = \theta_0$. Since the large- ξ value of the term in brackets in Eq. (74) equals unity, the asymptotic Green's function in θ space differs from that in ϕ space only through the factor $[\sin \theta \sin \theta']^{-1/2}$. g_θ^∞ represents the asymptotic form of the Green's function on a bilaterally matched θ transmission line (i.e., when $\overleftarrow{\Gamma} = \vec{\Gamma} = 0$). For arbitrary ξ values, the image representation retains its validity, but it is no longer possible to represent the propagation process in terms of waves traveling solely along $+\theta$ and $-\theta$. Thus, the first term in Eq. (74a) [with Eq. (74)] yields the exact Green's function in an angularly matched (i.e., infinitely extended) θ space, but the presence of the functions $R_q^{(2)}(\theta_<)$ and $R_q^{(1)}(\theta_>)$ distorts the purely traveling wave character of $g_\theta^\infty(\theta, \theta')$.

Completeness relations involving eigenfunctions that satisfy the differential equation (63b) are obtained directly on use of Eq. (3.3.11) and the appropriate

characteristic Green's function. The results are summarized below, with $\lambda_p = p(p + 1)$ denoting the eigenvalues while $\Phi_p^q(\theta)$ and $\psi_p^q(\theta)$ represent the *E*- and *H*-mode eigenfunctions, respectively.

$$0 \leq \theta \leq \pi$$

The characteristic Green's function g_θ^0 for the complete θ interval between 0 and π is given in Eq. (67). As noted after Eq. (70), g_θ^0 is an even function of $v + \frac{1}{2}$ and hence contains no branch-point singularities in the complex $\lambda = v(v + 1)$ plane. $\Gamma(w)$ has no zeros and has simple poles with residues $(-1)^n/n!$ at $w = -n$, $n = 0, 1, 2, \dots$, while the Legendre functions $P_{v+q}^{-q}(\pm \cos \theta)$ are regular in any finite part of the complex v plane. Thus, the singularities of g_θ^0 are simple poles located at

$$\lambda_p = p(p + 1), \quad p + \frac{1}{2} = \pm(q + n + \frac{1}{2}), \quad n = 0, 1, 2, \dots \quad (76)$$

From Eq. (3.3.11), on substitution of Eq. (67) and a residue evaluation,

$$\frac{\delta(\theta - \theta')}{\sin \theta'} = \frac{1}{2} \sum_{n=0}^{\infty} [2(n + q + 1)] \frac{\Gamma(n + 2q + 1)}{n!} P_{n+q}^{-q}(\cos \theta) P_{n+q}^{-q}(\cos \theta'), \quad (77)$$

so the normalized scalar eigenfunctions $\Phi_p^q(\theta)$ and $\psi_p^q(\theta)$ for the *E*- and *H*-mode problems, respectively, are identical and are given by

$$\Phi_p^q(\theta) = \psi_p^q(\theta) = \left\{ \frac{[2(n + q + 1)\Gamma(n + 2q + 1)]}{2n!} \right\}^{1/2} P_{n+q}^{-q}(\cos \theta), \quad n = 0, 1, 2, \dots \quad (77a)$$

When $q = m$ is an integer, one may employ the relation⁹

$$P_v^{-m}(x) = (-1)^m \frac{\Gamma(v - m + 1)}{\Gamma(v + m + 1)} P_v^m(x) \quad (78)$$

to reduce Eq. (77) to

$$\frac{\delta(\theta - \theta')}{\sin \theta'} = \frac{1}{2} \sum_{n=m}^{\infty} (2n + 1) \frac{(n - m)!}{(n + m)!} P_n^m(\cos \theta) P_n^m(\cos \theta'), \quad (79)$$

where $P_n^m(\cos \theta)$ is the conventional Legendre polynomial which vanishes identically when $n < m$. The eigenfunctions are now

$$\Phi_p^q(\theta) = \psi_p^q(\theta) = \left[\frac{(n + \frac{1}{2})(n - m)!}{(n + m)!} \right]^{1/2} P_n^m(\cos \theta), \quad n - m = 0, 1, 2, \dots, \quad (79a)$$

where

$$P_n(\cos \theta) = \frac{1}{2^n n!} \frac{d^n}{dz^n} (z^2 - 1)^n \Big|_{z=\cos \theta},$$

$$P_n^m(\cos \theta) = (-1)^m \sin^m \theta \frac{d^m}{dz^m} P_n(z) \Big|_{z=\cos \theta}, \quad (79b)$$

or, for special choices of n and m ,

$$\begin{aligned} P_0(\cos \theta) &= 1, \quad P_1(\cos \theta) = \cos \theta, \\ P_2(\cos \theta) &= \frac{1}{2}(3 \cos^2 \theta - 1) = \frac{1}{4}(3 \cos 2\theta + 1), \text{ etc.,} \\ P_1^!(\cos \theta) &= -\sin \theta, \quad P_2^!(\cos \theta) = -\frac{3}{2} \sin 2\theta, \\ P_2^2(\cos \theta) &= \frac{3}{2}(1 - \cos 2\theta), \quad \text{etc.} \end{aligned} \quad (79c)$$

Also, the following relations are useful when n and m are positive integers:

$$\begin{aligned} P_n^m(0) &= 0 = \int_0^\pi P_n^m(\cos \theta) d\theta, \quad n + m \text{ odd,} \\ \frac{d}{d\theta} P_n^m(\cos \theta) \Big|_{\theta=\pi/2} &= 0 = \int_0^\pi P_n^m(\cos \theta) \cos \theta d\theta, \quad n + m \text{ even} \\ \frac{d}{d\theta} P_n^m(\cos \theta) \Big|_{\theta=0,\pi} &= \frac{P_n^m(\cos \theta)}{\sin \theta} \Big|_{\theta=0,\pi} = 0, \quad m > 1, \\ \frac{d}{d\theta} P_n^1(\cos \theta) \Big|_{\theta=0} &= \frac{P_n^1(\cos \theta)}{\sin \theta} \Big|_{\theta=0} = -\frac{n(n+1)}{2}. \end{aligned} \quad (79d)$$

$$0 \leq \theta_1 \leq \theta \leq \theta_2$$

E modes

g'_θ in Eq. (68) is an even function of $v + \frac{1}{2}$ and thus exhibits pole singularities only. The poles are simple and are located at

$$\lambda_p = p(p+1), \quad \text{where } P_p^{-q}(\cos \theta_0) = 0. \quad (80)$$

No poles arise when $v - q$ equals an integer since under these conditions, $P_v^{-q}(-x) = (-1)^{v-q} P_v^{-q}(x)$; a similar relation obtains when $v + q + 1$ is an integer (note: $P_v^{-q} \equiv P_{-v-1}^{-q}$). The weighted delta function then has the spectral representation

$$\begin{aligned} \frac{\delta(\theta - \theta')}{\sin \theta'} &= -\frac{\pi}{2} \sum_{p>0} (2p+1) \frac{\Gamma(p+q+1)}{\Gamma(p-q+1)} \\ &\times \frac{P_p^{-q}(-\cos \theta_0)}{[\sin(p-q)\pi][(\partial/\partial p)P_p^{-q}(\cos \theta_0)]} P_p^{-q}(\cos \theta) P_p^{-q}(\cos \theta'), \end{aligned} \quad (81)$$

and the orthonormal eigenfunctions are

$$\Phi_p^q(\theta) = \left[-\frac{\pi(2p+1)\Gamma(p+q+1)P_p^{-q}(-\cos \theta_0)}{2\Gamma(p-q+1)\sin(p-q)\pi[(\partial/\partial p)P_p^{-q}(\cos \theta_0)]} \right]^{1/2} P_p^{-q}(\cos \theta), \quad (81a)$$

where p is any positive zero of $P_p^{-q}(\cos \theta_0)$.

H modes

g''_θ in Eq. (69) is an even function of $v + \frac{1}{2}$ and exhibits pole singularities only. The poles are simple and are located at

$$\lambda_p = p(p+1), \quad \text{where } \frac{d}{d\theta_0} P_p^{-q}(\cos \theta_0) = 0. \quad (82)$$

The weighted delta function has the spectral representation

$$\begin{aligned} \frac{\delta(\theta - \theta')}{\sin \theta'} &= \frac{1}{2} \csc^2 \left(\frac{\theta_0}{2} \right) \delta_{q_0} \\ &- \frac{\pi}{2} \sum_{p>0} (2p+1) \frac{\Gamma(p+q+1)}{\Gamma(p-q+1)} \\ &\times \frac{(d/d\theta_0) P_p^{-q}(-\cos \theta_0)}{\sin(p-q)\pi[(\partial^2/\partial p \partial \theta_0) P_p^{-q}(\cos \theta_0)]} P_p^{-q}(\cos \theta) P_p^{-q}(\cos \theta') \end{aligned} \quad (83)$$

where $\delta_{\alpha\beta} = 0$, $\alpha \neq \beta$, and $\delta_{\alpha\alpha} = 1$; the orthonormal eigenfunctions are

$$\psi_p^q(\theta) = \left[\frac{-\pi(2p+1)\Gamma(p+q+1)[(d/d\theta_0)P_p^{-q}(-\cos \theta_0)]}{2\Gamma(p-q+1)[\sin(p-q)\pi](\partial^2/\partial p \partial \theta_0)P_p^{-q}(\cos \theta_0)]} \right]^{1/2} P_p^{-q}(\cos \theta), \quad p > 0, \quad q \neq 0. \quad (83a)$$

When $q = 0$, $\lambda_p = 0$ is an eigenvalue, and the constant term $2^{-1/2} \csc(\theta_0/2)$ must be included. In this instance, the functions $P_p^{-q}(x)$ reduce to the ordinary Legendre functions $P_p^0(x) \equiv P_p(x)$.

$$0 \leq \theta_1 \leq \theta \leq \theta_2 < \pi$$

E modes

The E-mode characteristic Green's function $g_\theta(\theta, \theta'; q^2; \lambda)$ which vanishes at $\theta = \theta_{1,2}$, may be expressed in the form

$$g'_\theta(\theta, \theta'; q^2; \lambda) = \frac{\pi}{2} \frac{C(v, q; \theta_<, \theta_1)C(v, q; \theta_>, \theta_2)\Gamma(v+q+1)}{[\sin(v-q)\pi]\Gamma(v-q+1)C(v, q; \theta_2, \theta_1)}, \quad (84)$$

where

$$C(v, q; \alpha, \beta) = P_v^{-q}(\cos \alpha)P_v^{-q}(-\cos \beta) - P_v^{-q}(-\cos \alpha)P_v^{-q}(\cos \beta). \quad (84a)$$

The behavior at $|\lambda| \rightarrow \infty$ is still specified by Eq. (70), and the singularities of g'_θ are simple poles located at

$$\lambda_p = p(p+1), \quad \text{where} \quad C(p, q; \theta_2, \theta_1) = 0. \quad (85)$$

Then

$$\begin{aligned} \frac{\delta(\theta - \theta')}{\sin \theta'} &= \frac{\pi}{2} \sum_p \frac{(2p+1)\Gamma(p+q+1)}{[\sin(p-q)\pi]\Gamma(p-q+1)} \frac{P_p^{-q}(\cos \theta_1)}{P_p^{-q}(\cos \theta_2)} \\ &\times \frac{C(p, q; \theta, \theta_2)C(p, q; \theta', \theta_2)}{(\partial/\partial p)C(p, q; \theta_1, \theta_2)}, \end{aligned} \quad (86)$$

and

$$\Phi_p^q(\theta) = \left[\frac{\pi(2p+1)\Gamma(p+q+1)P_p^{-q}(\cos \theta_1)}{2[\sin(p-q)\pi]\Gamma(p-q+1)P_p^{-q}(\cos \theta_2)[(\partial/\partial p)C(p, q; \theta_1, \theta_2)]} \right]^{1/2} \times C(p, q; \theta, \theta_2). \quad (86a)$$

H mode

$$g''_0(\theta, \theta'; q^2; \lambda) = \frac{\pi}{2} \frac{B(v, q; \theta_<, \theta_1)B(v, q; \theta_>, \theta_2)\Gamma(v + q + 1)}{[\sin(v - q)\pi]\Gamma(v - q + 1)[(\partial/\partial\theta_2)B(v, q; \theta_2, \theta_1)]}, \quad (87)$$

where

$$B(v, q; \alpha, \beta) = P_v^{-q}(\cos \alpha) \frac{d}{d\beta} P_v^{-q}(-\cos \beta) - P_v^{-q}(-\cos \alpha) \frac{d}{d\beta} P_v^{-q}(\cos \beta). \quad (87a)$$

Simple poles are located at

$$\lambda_p = p(p + 1), \quad \text{where} \quad \frac{\partial}{\partial\theta_2} B(p, q; \theta_2, \theta_1) = 0. \quad (88)$$

The delta-function representation is

$$\begin{aligned} \frac{\delta(\theta - \theta')}{\sin \theta'} &= \frac{1}{2} \csc\left(\frac{\theta_2 - \theta_1}{2}\right) \csc\left(\frac{\theta_2 + \theta_1}{2}\right) \delta_{q0} \\ &\quad - \frac{\pi}{2} \sum_p (2p + 1) \frac{\Gamma(p + q + 1)[(d/d\theta_1)P_p^{-q}(\cos \theta_1)]}{[\sin(p - q)\pi]\Gamma(p - q + 1)[(d/d\theta_2)P_p^{-q}(\cos \theta_2)]} \\ &\quad \times \frac{B(p, q; \theta, \theta_2)B(p, q; \theta', \theta_2)}{[(\partial^2/\partial p \partial\theta_2)B(p, q; \theta_2, \theta_1)]} \end{aligned} \quad (89)$$

whence for $q \neq 0$ and $p > 0$,

$$\begin{aligned} \psi_p^q(\theta) &= \left[-\frac{\pi(2p + 1)\Gamma(p + q + 1)[(d/d\theta_1)P_p^{-q}(\cos \theta_1)]}{2[\sin(p - q)\pi]\Gamma(p - q + 1)(d/d\theta_2)P_p^{-q}(\cos \theta_2)} \right]^{1/2} \\ &\quad \times \frac{B(p, q; \theta, \theta_2)}{[(\partial^2/\partial p \partial\theta_2)B(p, q; \theta_2, \theta_1)]^{1/2}} \end{aligned} \quad (89a)$$

When $q = 0$, the constant term

$$2^{-1/2} \left[\csc\left(\frac{\theta_2 - \theta_1}{2}\right) \csc\left(\frac{\theta_2 + \theta_1}{2}\right) \right]^{1/2}$$

must be included.

Equations (86) or (89) lend themselves to the study of various special cases. First, one may derive the results in Eqs. (81) and (83) by letting $\theta_1 \rightarrow 0$. Next, consider the symmetrical case $\theta_2 = \pi - \theta_1$. In this instance, the transcendental equation (85) may be separated into

$$\begin{aligned} 0 &= C(p, q; \pi - \theta_1, \theta_1) \\ &= [P_p^{-q}(\cos \theta_1) + P_p^{-q}(-\cos \theta_1)][P_p^{-q}(\cos \theta_1) - P_p^{-q}(-\cos \theta_1)], \end{aligned} \quad (90)$$

so that the eigenvalues occur in two sets p' and p'' corresponding to the vanishing of the first and second factors, respectively. It may be verified that the modes described by p' and p'' possess even or odd symmetry about the bisecting plane $\theta = \pi/2$ so that a source problem in a symmetrical biconical region may be decomposed into two separate simpler problems arising from

even and odd excitation about the symmetry plane. Analogous considerations apply to the H -mode case.

While the mode functions described above are complete for the representation of scalar functions, azimuthally symmetric vector fields may contain in addition a TEM mode that must be derived separately.

3.4c Radial Transmission Lines

Because of the non-uniformity of successive cross sections transverse to the radial direction, radial transmission problems in cylindrical and spherical geometries involve non-uniform transmission lines, as noted in Sec. 2.7 for the spherical case. Although vector separability into E and H modes with respect to the radial direction is possible for spherical geometries, it is generally not possible for electromagnetic fields in cylindrical geometries; nevertheless, cylindrical regions may be viewed as waveguides in the direction parallel to the cylinder axis. Radial transmission is then relevant for alternative representations of the z -separated solution (see Secs. 3.3a and 6.2). Since the radial problem in spherical coordinates, as specified by Eq. (2.7.2), is related to that in cylindrical coordinates in Eq. (3.2.46b) by the transformation in Eqs. (3.5.1) and (3.5.2) [see also Eq. (2.7.3a)], results for the cylindrical case are readily obtained from the spherical transmission-line analysis in Sec. 2.7.

The radial characteristic Green's-function problem in cylindrical regions is defined as follows [see Eqs. (3.2.46b) and (3.3.1)] :

$$\left(\frac{d}{d\rho} \rho \frac{d}{d\rho} + \tau\rho - \frac{\lambda}{\rho} \right) g_\rho(\rho, \rho'; \tau, \lambda) = -\delta(\rho - \rho'), \quad (91)$$

subject to the boundary conditions

$$g'_\rho(\rho, \rho'; \tau, \lambda) = 0 \quad \text{at } \rho = \rho_{1,2}, \quad (91a)$$

$$\frac{dg''_\rho(\rho, \rho'; \tau, \lambda)}{d\rho} = 0 \quad \text{at } \rho = \rho_{1,2}, \quad (91b)$$

for E modes (single primes) and H modes (double primes), respectively. When $\rho_1 = 0$, the boundary condition at the origin is replaced by a finiteness requirement [see also Eq. (2.7.7)], while an unbounded domain $\rho_2 \rightarrow \infty$ requires imposition of a radiation condition. The eigenvalue problems associated with the characteristic Green's functions g_ρ in Eqs. (91) differ according to whether λ or τ is the characteristic parameter. In a z -transmission representation of three-dimensional Green's functions involving the eigenfunctions $\Phi_q(\phi)$ or $\Psi_q(\phi)$ in Eq. (3.2.46a) [see also Sec. 3.3c], $\lambda = q^2$ is prescribed from the angular eigenvalue problem and τ is the characteristic parameter for the radial domain. On the other hand, in a ϕ -transmission representation of two- or three-dimensional Green's functions, τ is prescribed and λ is the characteristic parameter [see Secs. 3.3c and 6.2b; for two-dimensional problems, $\tau = k^2$, while for the three-dimensional case, $\tau = (k^2 - \gamma^2)$, where γ is the eigenvalue for the z -dependent eigenfunctions]. Mode spectra and completeness relations for various radial

domains, required for the z -transmission representation, have already been given in Sec. 3.2c. It follows from Eqs. (2.7.1-2) (with $\mu, \epsilon = \text{constant}$, $k^2 \rightarrow \tau$, $k_{ii}^2 \rightarrow \lambda$) and from Eqs. (91) that the characteristic Green's functions $g_r(r, r'; \tau, \lambda)$ and $g_\rho(\rho, \rho'; \tau, \lambda)$ for the spherical and cylindrical geometries, respectively, are related as follows :

$$g_\rho(\rho, \rho'; \tau, \lambda) = \frac{1}{\sqrt{rr'}} g_r(r, r'; \tau, \lambda + \frac{i}{4}) \Big|_{\substack{r=r' \\ r'=r}}, \quad (92)$$

where for the E -mode case,

$$g'_r = \frac{i\zeta}{k} Y'_i(r, r'); \quad k^2 \rightarrow \tau, \quad k_{ii}^2 \rightarrow \lambda, \quad (92a)$$

and, for H -mode case,

$$g''_r = \frac{i}{k\zeta} Z''_i(r, r'), \quad k^2 \rightarrow \tau, \quad k_{ii}^2 \rightarrow \lambda, \quad (92b)$$

with $Y'_i(r, r')$ and $Z''_i(r, r')$ denoting the modal Green's functions in Sec. 2.7, and $\zeta = \sqrt{\mu/\epsilon}$.

For the unbounded radial domain $0 < \rho < \infty$ wherein the E -and H -mode solutions coincide, one has from Eqs. (92), (2.7.11), and (2.7.3a) (with $j \rightarrow -i$),†

$$g_\rho(\rho, \rho'; \tau, \lambda) = \frac{\pi i}{2} J_\nu(\sqrt{\tau} \rho_-) H_\nu^{(1)}(\sqrt{\tau} \rho_+), \quad \nu = \sqrt{\lambda}, \quad 0 < \frac{\rho}{\rho'} < \infty. \quad (93)$$

If $\nu = q > 0$ is prescribed, then τ is the characteristic variable and g_ρ possesses a branch-point singularity at $\tau = 0$ in the complex τ plane. It then follows from Eq. (3.2.70b) that the condition $\text{Im } \sqrt{\tau} > 0$ must be imposed in order for g_ρ to decay as $\rho \rightarrow \infty$. By choosing a branch cut along the positive real τ axis and defining $0 < \arg \tau < 2\pi$, one may enforce $\text{Im } \sqrt{\tau} > 0$ on the entire top sheet, the “spectral” sheet, of the complex τ plane. From Eq. (3.3.11) and the change of variable $\xi = \sqrt{\tau}$, one obtains the spectral representation of $\delta(\rho - \rho')/\rho'$ in Eq. (3.2.72), which can be written in the alternative forms in Eqs. (3.2.68) or (3.2.62).

When τ is prescribed and λ is the characteristic variable, a different spectral representation is derived ; as noted earlier, $\sqrt{\tau} = k$ for angular transmission formulations of z -independent two-dimensional Green's functions (see Sec. 6.2). g_ρ now has a branch-point singularity at $\lambda = 0$ in the complex λ plane. The Hankel function of the first kind (with $\text{Im } k > 0$ for small dissipation) satisfies the radiation condition at $\rho \rightarrow \infty$ for fields with time dependence $\exp(-i\omega t)$. To enforce finiteness at $\rho = 0$, it is necessary to impose $\text{Re } \nu > 0$ since $J_\nu(k\rho) \sim (k\rho)^\nu$ as $\rho \rightarrow 0$; by drawing the branch cut along the negative real axis as in Fig. 17(a) and defining $-\pi < \arg \lambda < \pi$ with $\nu = \sqrt{\lambda}$, one has $\text{Re } \nu > 0$

†For the discussion of characteristic Green's functions, j or i merely denotes the imaginary unit; however, subsequent results apply directly to radiation problems with time dependence $\exp(-i\omega t)$.

on the spectral sheet of the complex λ plane. Since g_ρ behaves like $(\rho_-/\rho_>)^{\sqrt{\lambda}}$ as $\lambda \rightarrow \infty$ [see Eqs. (2.7.4b)], the characteristic Green's function decays at infinity on the spectral sheet, thereby providing the basis for application of Eq. (3.3.11). Comparison of Eqs. (3.3.1) and (91) shows that the weight function w equals $-1/\rho$, whence one obtains as the desired completeness relation in the domain $0 < (\rho, \rho') < \infty$ [note that the imaginary unit j in Eq. (3.3.11) is replaced by i in the present discussion] :

$$\rho' \delta(\rho - \rho') = \frac{1}{2\pi i} \oint_C g_\rho(\rho, \rho'; k^2, \lambda) d\lambda \quad (94a)$$

$$= \frac{1}{2} \int_{-i\infty}^{i\infty} v J_v(k\rho_-) H_v^{(1)}(k\rho_>) dv = \frac{1}{2} \int_{-i\infty}^{i\infty} v J_v(k\rho) H_v^{(1)}(k\rho') dv \quad (94b)$$

$$= \frac{1}{4} \int_{-i\infty}^{i\infty} v H_v^{(1)}(k\rho) H_v^{(1)}(k\rho') dv \quad (94c)$$

$$= \frac{1}{4} \int_0^{i\infty} v(1 - e^{i2v\pi}) H_v^{(1)}(k\rho) H_v^{(1)}(k\rho') dv \quad (94d)$$

$$= \sum_p \Phi_p(k\rho) \bar{\Phi}_p(k\rho'), \quad 0 < \frac{\rho}{\rho'} < \infty, \quad (94e)$$

where C is the integration contour in Fig. 3.4.17(a). Equation (94c) follows from Eq. (94b) on use of the relations

$$J_v(x) = \frac{1}{2} [H_v^{(1)}(x) + H_v^{(2)}(x)], \quad H_{-v}^{(1,2)}(x) = e^{\pm iv\pi} H_v^{(1,2)}(x), \quad (94f)$$

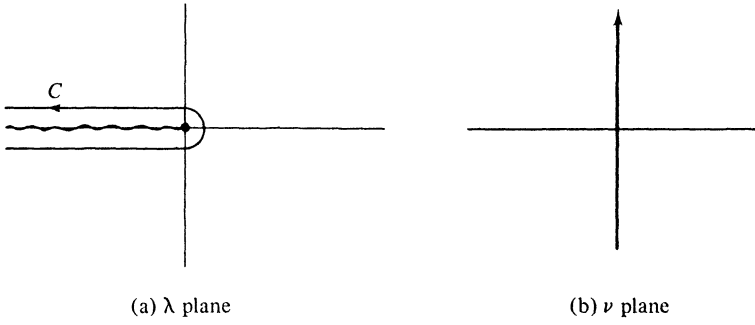


FIG. 3.4.17 Integration paths and singularities.

whence $v H_v^{(2)}(x) H_v^{(1)}(y)$ is an odd function of v that does not contribute to the integral along the imaginary v axis. The symmetrical form of Eq. (94c) justifies suppression of ρ_- and $\rho_>$ in the second of Eqs. (94b). The representation theorem contained in Eqs. (94) gives rise to the Kontorovitch-Lebedev transform pair¹¹

$$f(\rho) = \frac{1}{4} \int_{-i\infty}^{i\infty} v H_v^{(1)}(k\rho) F(v) dv, \quad F(v) = \int_0^\infty \frac{1}{\rho} f(\rho) H_v^{(1)}(k\rho) d\rho, \quad (95)$$

the convergence properties of which are discussed in connection with Eqs. (6.

3.1). From the generic representation in Eq. (94e), one may identify on comparison with Eqs. (94b)–(94d) the orthonormal radial eigenfunctions $\Phi_p(k\rho)$, the adjoint functions $\bar{\Phi}_p(k\rho)$ [see Eq. (94b)], and the meaning of Σ_p .

When the radial domain extends from $\rho = a$ to $\rho = \infty$, boundary conditions at $\rho = a$ must be included. For generality, we assume that

$$\frac{dg_\rho}{d\rho} = -ik\bar{C}g_\rho, \quad \text{at } \rho = a, \quad \bar{C} = \text{constant}, \quad (96)$$

from which follow the special cases in Eqs. (91a) ($\bar{C} = \infty$) and (91b) ($\bar{C} = 0$). As noted in Sec. 6.7a, \bar{C} may be related to the surface impedance on a cylindrical scatterer with radius a . The solution for g_ρ satisfying Eq. (96) and the radiation condition at infinity (for $\text{Im } k > 0$) is now given by [see also Eq. (2.7.14)]

$$g_\rho(\rho, \rho'; k^2; \lambda) = \frac{\pi i}{2} \left[J_v(k\rho_<) - \frac{b(v)}{d(v)} H_v^{(1)}(k\rho_<) \right] H_v^{(1)}(k\rho_>), \quad v = \sqrt{\lambda}, \quad (97)$$

where $a \leq (\rho, \rho') < \infty$ and

$$b(v) = J'_v(ka) + i\bar{C}J_v(ka), \quad d(v) = H_v'^{(1)}(ka) + i\bar{C}H_v^{(1)}(ka), \quad (97a)$$

with the prime denoting the derivative with respect to the argument. One may verify on use of Eq. (94f) that g_ρ in Eq. (97) is an even function of v , so $\lambda = 0$ is a regular point in the complex λ plane. g_ρ decays as $\lambda \rightarrow \infty$ [see Eqs. (6.7.14) et seq.] and has complex pole singularities v_p defined by the transcendental equation

$$d(v_p) = 0, \quad (97b)$$

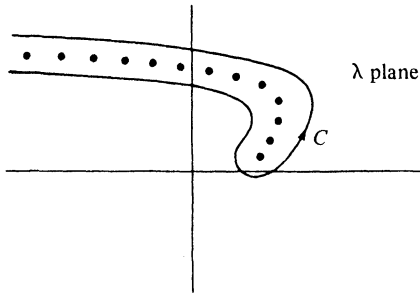
located in the first and third quadrants of the complex v plane (see Sec. 6.A5 for the special cases $\bar{C} = 0$ or $\bar{C} = \infty$); the pole locations $\lambda_p = v_p^2$ in the complex λ plane are shown in Fig. 3.4.18. Equation (3.3.11) then yields the completeness relation¹²:

$$\rho' \delta(\rho - \rho') = \frac{1}{2\pi i} \oint_C g_\rho(\rho, \rho'; k^2, \lambda) d\lambda, \quad (98a)$$

$$= -\pi i \sum_p \left[\frac{v_p b(v_p)}{\frac{d}{dv} d(v)} \right]_{v_p} H_{v_p}^{(1)}(k\rho) H_{v_p}^{(1)}(k\rho'), \quad (98b)$$

$$= \sum_p \Phi_p(k\rho) \Phi_p(k\rho'), \quad a \leq \frac{\rho}{\rho'} < \infty. \quad (98c)$$

Equation (97) may also be used to derive a spectral theorem for the case where $v = q > 0$ is prescribed and $k^2 \rightarrow \tau$ is the characteristic parameter. One may verify that g_ρ possesses a branch point at $\tau = 0$ in the complex τ plane and that the condition $\text{Im } \sqrt{\tau} > 0$ must be imposed to satisfy the radiation condition at infinity [see discussion following Eq. (93)]. For the special cases $\bar{C} = 0$ and $\bar{C} = \infty$, no pole singularities [i.e., zeros of $H_q^{(1)}(\sqrt{\tau}a)$ or $H_q'^{(1)}(\sqrt{\tau}a)$] exist on the spectral sheet $0 < \arg \tau < 2\pi$ [see discussion preceding Eq. (5.9.12)].

FIG. 3.4.18 Singularities of g_ρ in complex λ plane.

By considerations analogous to those mentioned earlier, one then obtains the following completeness relations in the domain $a \leq (\rho, \rho') < \infty$ [see also Eqs. (3.4.24)]:

$$\frac{\delta(\rho - \rho')}{\rho'} = - \frac{1}{2\pi i} \oint_C g_\rho(\rho, \rho'; \tau, q^2) d\tau \quad (99a)$$

$$= \int_0^\infty \Phi_\xi(\rho) \Phi_\xi^*(\rho') d\xi, \quad \bar{C} = \infty, \quad (99b)$$

$$= \int_0^\infty \Psi_\xi(\rho) \Psi_\xi^*(\rho') d\xi, \quad \bar{C} = 0, \quad (99c)$$

where

$$\Phi_\xi(\rho) = \sqrt{\xi} \left[J_q(\xi\rho) - \frac{J_q(\xi a)}{H_q^{(1)}(\xi a)} H_q^{(1)}(\xi\rho) \right], \quad (99d)$$

$$\Psi_\xi(\rho) = \sqrt{\xi} \left[J_q(\xi\rho) - \frac{J'_q(\xi a)}{H_q^{(1)}(\xi a)} H_q^{(1)}(\xi\rho) \right]. \quad (99e)$$

C is a contour enclosing the branch cut along the positive real λ axis, and $\xi = \sqrt{\tau}$. It may be noted that the normalized eigenfunctions in Eqs. (99d) and (99e) are obtainable from those for the interval $0 < \rho < \infty$ in Eq. (3.2.62) on adding to the latter a solution of the homogeneous equation (91) so as to satisfy the boundary conditions $\Phi_\xi(a) = 0$ and $d\Psi_\xi(\rho)/d\rho|_{\rho=a} = 0$, respectively.

The corresponding characteristic Green's functions and completeness relations for the radial domain in spherical regions follow from the preceding results for cylindrical regions and from Eq. (92). In particular, for the unbounded domain $0 < (r, r') < \infty$:

$$r'^2 \delta(r - r') = \frac{1}{2\pi i} \oint_C g_r(r, r'; \lambda) d\lambda \quad (100a)$$

$$= \frac{1}{2\pi k} \int_{-(1/2)-i\infty}^{-(1/2)+i\infty} j_\nu(kr_<) h_\nu^{(1)}(kr_>) (2\nu + 1) dv \quad (100b)$$

$$= \frac{1}{4\pi k} \int_{-(1/2)-i\infty}^{-(1/2)+i\infty} h_\nu^{(1)}(kr) h_\nu^{(1)}(kr') (2\nu + 1) dv, \quad (100c)$$

which formulas are a restatement of the Kontorovitch–Lebedev transform theorem in Eqs. (94) in terms of spherical Bessel functions as defined in Eq. (2.7.3a). Similarly, for the domain $a < r < \infty$ with a perfectly conducting surface located at $r = a$, the H -mode Green's function in Eq. (2.7.12a) yields [see Eq. (98b) with $\bar{C} = \infty$]

$$r'^2\delta(r - r') = \sum_s (2s + 1) \frac{h_s^{(1)}(kr)h_s^{(1)}(kr')j_s(ka)}{ik[(\partial/\partial s)h_s^{(1)}(ka)]}, \quad h_s^{(1)}(ka) = 0, \quad (101a)$$

while the spectrum corresponding to the E -mode Green's function in Eq. (2.7.12b) leads to

$$r'^2\delta(r - r') = \sum_\sigma (2\sigma + 1) \frac{h_\sigma^{(1)}(kr)h_\sigma^{(1)}(kr')j'_\sigma(ka)}{ik[(\partial/\partial \sigma)h_\sigma^{(1)}(ka)]}, \quad h_\sigma^{(1)}(ka) = 0. \quad (101b)$$

In these relations $\text{Im } k \geq 0$, thereby making the results applicable to problems with $\exp(-i\omega t)$ dependence. For $\exp(+j\omega t)$ dependence, one replaces $h_a^{(1)}$ by $h_a^{(2)}$ throughout and lets $i \rightarrow -j$ in Eqs. (101).

3.5 APPROXIMATE METHODS FOR SOLVING THE NON-UNIFORM TRANSMISSION-LINE EQUATIONS

As presented in Chapter 2, the solution of field problems by modal analysis and synthesis requires knowledge of the eigenfunctions transverse to a chosen transmission coordinate, and of the modal amplitudes along that coordinate. By the characteristic Green's function method of Sec. 3.3a, eigenvalue and transmission-line problems are shown to be closely related, whence solution of separable multidimensional field problems rests essentially on the ability to solve one-dimensional transmission-line equations. These equations are of the Sturm–Liouville type and admit solutions in terms of known functions only for special forms of the x -dependent parameters p , q , and w in Eqs. (3.3.1) or (3.3.18). It is therefore relevant to discuss approximation or perturbation procedures that can be applied to more general parameter variations. If the parameters vary “slowly” over a distance interval equal to the local wavelength, the WKB approximation furnishes an unperturbed solution with a broad range of validity. For rapid variations, one must resort to special functions that approximate the desired one as closely as possible in the interval in question. While application of these methods, as described below, is successful in many cases of practical interest, the detailed calculation of the Green's functions or eigenfunctions for specific medium variations must frequently be accomplished by numerical means.

The Sturm–Liouville equation (3.3.18) may be reduced to a standard form by renormalization of the c, s solutions (3.3.18a) into modified \hat{c}, \hat{s} solutions defined by

$$\begin{Bmatrix} c(x, x_0) \\ s(x, x_0) \end{Bmatrix} = \frac{1}{\sqrt{p}} \begin{Bmatrix} \hat{c}(x, x_0) \\ \hat{s}(x, x_0) \end{Bmatrix} \quad (1)$$

whence

$$\left[\frac{d^2}{dx^2} + \gamma(x) \right] \begin{Bmatrix} \hat{c}(x, x_0) \\ \hat{s}(x, x_0) \end{Bmatrix} = 0, \quad (2)$$

where

$$\gamma(x) = -\frac{q(x)}{p(x)} + \frac{\lambda w(x)}{p(x)} - \frac{1}{\sqrt{p(x)}} \frac{d^2}{dx^2} \sqrt{p(x)}. \quad (2a)$$

For convenience, one chooses as initial conditions:

$$\begin{aligned} \hat{c}(x_0, x_0) &= 1, & \hat{s}(x_0, x_0) &= 0, \\ \hat{c}'(x_0, x_0) &= 0, & \hat{s}'(x_0, x_0) &= 1, \end{aligned} \quad (2b)$$

whence the functions c and s derived therefrom differ in general from those defined by Eqs. (3.3.18). When applied to propagation in an inhomogeneous medium, as in Eqs. (3.2.98) and (3.2.99), one has $p(x) = 1/\mu(x)$ for H modes along x (i.e., fields with $E_x \equiv 0$), and $p(x) = 1/\epsilon(x)$ for E modes along x .† If the medium is a variable dielectric $\epsilon(x)$ with constant permeability μ , the H -mode functions c, s are identical with \hat{c} and \hat{s} ; similarly, Eq. (3.3.18) reduces to the standard form for E modes in a medium with constant ϵ . Moreover, for the planar stratification considered in these examples, $w = p$, so the form of the functions c and s for arbitrary λ can be inferred from that for $\lambda = 0$ upon replacing $\gamma(x)|_{\lambda=0}$ by $(\gamma + \lambda)$. Since \hat{c} and \hat{s} are linearly independent solutions of Eq. (2), as verified from the non-vanishing of the Wronskian $\hat{c}\hat{s}' - \hat{s}\hat{c}'$ in Eq. (2b), a linear superposition of \hat{c} and \hat{s} may be employed to satisfy initial conditions of a type more general than those in Eq. (2b).

In the first approximation method to be described, Eq. (2) is rephrased as a Fredholm integral equation, with the kernel chosen to be as “small” as possible in order to yield a rapidly convergent iterative solution.

3.5a Integral Equation Formulation

Suppose that for given $\gamma(x)$, Eq. (2) has no known solution but that a solution is known for some other function $\zeta(x)$ which is chosen so that it resembles $\gamma(x)$ over the interval $x_1 \leq x \leq x_2$ [see Sec. 3.5b for a method of choosing

†In an inhomogeneous dielectric where $\epsilon = \epsilon(x)$ and $\mu = \text{constant}$, $\sqrt{\gamma(x)} = \omega \sqrt{\mu \epsilon(x)}$ represents the actual wavenumber descriptive of an H -mode field. For an E mode, $\sqrt{\gamma(x)} = \left[\omega^2 \mu \epsilon(x) - \sqrt{\epsilon(x)} \frac{d^2}{dx^2} \frac{1}{\sqrt{\epsilon(x)}} \right]^{1/2}$ represents an *effective* wavenumber [see also Eq. (2.3.45)]. Substantial differences in the propagation characteristics of the two wave types may arise when $\epsilon(x)$ varies rapidly or vanishes at some point in the interval. Dual considerations apply when $\mu = \mu(x)$ and ϵ is constant.

$\zeta(x)$. We construct the Green's function $G(x, x')$ that satisfies the differential equation

$$\left[\frac{d^2}{dx^2} + \zeta(x) \right] G(x, x') = -\delta(x - x'), \quad x_1 \leq (x, x') \leq x_2, \quad (3)$$

with as yet unspecified boundary conditions. Then from the one-dimensional form of Green's theorem of the second kind,[†] applied to the functions $G(x, x')$ and $u(x) = \hat{c}$ or \hat{s} , one derives the integral equation

$$\begin{aligned} u(x) &= \left[G(x', x) \frac{du(x')}{dx'} - u(x') \frac{d}{dx'} G(x', x) \right]_{x'=x_1}^{x'=x_2} \\ &\quad + \int_{x_1}^{x_2} [\gamma(x') - \zeta(x')] G(x', x) u(x') dx'. \end{aligned} \quad (4)$$

If $\gamma(x) \simeq \zeta(x)$ over the interval in question, the integral on the right-hand side of Eq. (4) is expected to be small and can be regarded as a correction to the unperturbed contribution in the first term. This highlights the importance of a proper choice of $\zeta(x)$, to be described in Sec. 3.5b. If $\gamma \equiv \zeta$ over one or more subintervals $x_3 \leq x \leq x_4$, where $x_3 > x_1$ and $x_4 < x_2$, then these ranges are excluded from the integration in the correction integral.

Initial conditions on u are specified at some point x_1 . The perturbation method of solution will be simplified if the Green's function satisfies the boundary condition

$$G(x', x) = \frac{d}{dx'} G(x', x) = 0, \quad x' > x, \quad (5)$$

whence Eq. (4) reduces to

$$\begin{aligned} u(x) &= \left\{ u(x_1) \frac{d}{dx_1} G(x_1, x) - G(x_1, x) \frac{du(x_1)}{dx_1} \right\} \\ &\quad + \int_{x_1}^x [\gamma(x') - \zeta(x')] G(x', x) u(x') dx', \end{aligned} \quad (6)$$

a Fredholm integral equation of the second kind, with a variable upper limit (Volterra integral equation).¹³ If $g_1(x)$ and $g_2(x)$ denote any two linearly independent solutions of the homogeneous equation (3),

$$\left[\frac{d^2}{dx^2} + \zeta(x) \right] g_{1,2}(x) = 0, \quad (7)$$

then it is verified that[‡]

$$\begin{aligned} &\overline{\int_{x_1}^{x_2} \left[u(x') \frac{d^2}{dx'^2} G(x', x) - G(x', x) \frac{d^2}{dx'^2} u(x') \right] dx'} \\ &= \left[u(x') \frac{d}{dx'} G(x', x) - G(x', x) \frac{d}{dx'} u(x') \right]_{x_1}^{x_2}. \end{aligned}$$

[†]See Eq. (3.3.14a), from which one subtracts the homogeneous solution $\vec{V}(x)\vec{V}(x')/(-pW)$ in order to satisfy the boundary condition (5). We have here utilized the fact that two Green's functions satisfying the same differential equation, but different boundary conditions, differ only by a solution of the homogeneous equation.

$$G(x', x) = \begin{cases} \frac{g_2(x')g_1(x) - g_1(x')g_2(x)}{W(g_1, g_2)}, & x_1 \leq x' \leq x, \\ 0, & x' > x. \end{cases} \quad (8)$$

$W(g_1, g_2)$ represents the Wronskian $(g_1 g'_2 - g_2 g'_1)$, where the prime on $g_{1,2}$ denotes the derivative with respect to the argument. Thus, one finds for $\hat{c}(x, x_1)$

$$\hat{c}(x, x_1) = \frac{d}{dx_1} G(x_1, x) + \int_{x_1}^x [\gamma(x') - \zeta(x')] G(x', x) \hat{c}(x', x_1) dx', \quad (9a)$$

while

$$\hat{s}(x, x_1) = -G(x_1, x) + \int_{x_1}^x [\gamma(x') - \zeta(x')] G(x', x) \hat{s}(x', x_1) dx'. \quad (9b)$$

For suitable kernels, these integral equations can be solved by the method of successive approximations. Let $u_0(x)$ denote the expression inside the braces on the right-hand side of Eq. (6); it constitutes the zeroth-order approximation to $u(x)$. Substitution of $u_0(x')$ for $u(x')$ in the integral yields the first approximation $u_1(x)$; substitution of $u_1(x')$ for $u(x')$ yields the second approximation $u_2(x)$; etc. Thus, the solution for $u(x)$ can be expressed in the form of a series,

$$u(x) = \sum_{n=0}^{\infty} u_n(x), \quad (10a)$$

$$u_n(x) = \int_{x_1}^x [\gamma(x') - \zeta(x')] G(x', x) u_{n-1}(x') dx', \quad n \geq 1. \quad (10b)$$

If γ , ζ , and G are (real) continuous functions of x in the interval $x_1 \leq x \leq x_2$ [if γ and ζ are piecewise continuous, the determination of $u(x)$ above is carried out separately in each interval segment wherein γ and ζ are continuous], then $u(x)$ is a real continuous function in the interval. Let the absolute value of $u_0(x)$ in the interval be smaller than some positive number N , and assume also that $|\gamma - \zeta|G| \leq M$ in the interval, where M is a positive number. Then, if $K(x', x)$ denotes the kernel $(\gamma - \zeta)G$,

$$|u_n(x)| = \left| \int_{x_1}^x dx' K(x', x) \int_{x_1}^{x'_1} dx'_1 K(x'_1, x') \int_{x_1}^{x'_2} \cdots dx'_{\alpha} \int_{x_1}^{x'_{\alpha}} dx'_{\beta} K(x'_{\beta}, x'_{\alpha}) u_0(x'_{\beta}) \right|, \quad (11)$$

where $\alpha = n - 2$, $x'_0 \equiv x'$, $x'_{-1} \equiv x$. In view of the above-mentioned inequalities, the absolute value of the last integral is bounded by $NM(x'_{\alpha} - x_1)$, that of the last two integrals by $(NM^2/2!)(x'_{\alpha-1} - x_1)^2$, and, finally,

$$|u_n(x)| \leq \frac{NM^n}{n!} (x - x_1)^n, \quad (12)$$

for all x in the interval $x_1 \leq x \leq x_2$. Hence, if $|K|$ is bounded in the interval, the series (10a) converges uniformly. The rapidity of convergence depends on the smallness of M (i.e., on $|\gamma - \zeta|$). If the function $\gamma(x)$ in Eq. (2) is well approximated by $\zeta(x)$ in Eq. (3), the first correction $u_1(x)$ may be sufficiently ac-

curate in furnishing an acceptable solution for $u(x)$. The inequality $\sum_{n=0}^{\infty} |u_n| \leq N \exp [M(x - x_1)]$ derived from (12) illustrates that convergence of the method depends not only on M but also on the boundedness of the interval $x - x_1$.

In many scattering problems, especially those involving unbounded geometrical cross sections, the inhomogeneity is confined to a finite region in space; in the exterior, the medium is homogeneous. Under these circumstances, the perturbed and unperturbed wave functions should be chosen to satisfy identical boundary conditions at the endpoints of the region, and it is convenient to employ an alternative formulation. Suppose that we wish to determine the Green's function $\hat{g}(x, x')$ associated with Eq. (2),

$$\left[\frac{d^2}{dx^2} + \gamma(x) \right] \hat{g}(x, x') = -\delta(x - x'), \quad (13)$$

subject to the boundary conditions

$$\frac{d\hat{g}}{dx} + \hat{\alpha}_{1,2}\hat{g} = 0 \quad \text{at } x_{1,2}, \quad (13a)$$

where $\hat{\alpha}_{1,2}$ are constants that may be complex [thereby admitting a radiation condition if $x_1 \rightarrow -\infty$ and (or) $x_2 \rightarrow \infty$]. Upon writing Eq. (13) as

$$\left[\frac{d^2}{dx^2} + \zeta(x) \right] \hat{g}(x, x') = \left[\zeta(x) - \gamma(x) \right] \hat{g}(x, x') - \delta(x - x'), \quad (14)$$

and treating the right-hand side of (14) as a "known" inhomogeneous term $Q(x, x')$, one may construct the solution for \hat{g} in terms of the unperturbed Green's function G by multiplying Eq. (3) by $-Q(x', x'')$ and integrating over x' :

$$\hat{g}(x, x'') = G(x, x'') - \int_{x_1}^{x_2} [\zeta(x') - \gamma(x')] G(x, x') \hat{g}(x', x'') dx'. \quad (15)$$

The absence of endpoint contributions in this (Fredholm) integral equation of the second kind for \hat{g} implies that G must satisfy the boundary condition (13a). The solution of the integral equation can again be found by an iteration procedure. However, since the integration limits are fixed, the resulting series converges under more restrictive conditions. A convergent series for any continuous (and therefore bounded) K can be obtained by the more general, but more cumbersome, method of Fredholm determinants.¹³

The Green's function G in the present case differs from that in Eq. (8) and is given via Eq. (3.3.14) by

$$G(x, x') = \frac{g_1(x_-)g_2(x_+)}{-W}, \quad W = g_1g'_2 - g_2g'_1, \quad (16)$$

where g_2 and g_1 now denote solutions of the homogeneous equation (7) that satisfy the boundary conditions (13a) at x_2 and x_1 , respectively. \hat{g} can similarly be written as

$$\hat{g}(x, x') = \frac{\hat{g}_1(x_-)\hat{g}_2(x_+)}{-\hat{W}}, \quad \hat{W} = \hat{g}_1\hat{g}'_2 - \hat{g}_2\hat{g}'_1, \quad (17)$$

where \hat{g}_2 and \hat{g}_1 are solutions of the homogeneous equation (13) [or of Eq. (2)] and satisfy the boundary conditions (13a) at x_2 and x_1 , respectively. Upon substituting these expressions into Eq. (15), one obtains, for $x < x''$,

$$\begin{aligned} \hat{g}(x, x'') = & \frac{g_1(x)g_2(x'')}{-\hat{W}} - \frac{g_2(x)\hat{g}_2(x'')}{W\hat{W}} \int_{x_1}^x [\zeta(x') - \gamma(x')] g_1(x') \hat{g}_1(x') dx' \\ & - \frac{g_1(x)\hat{g}_2(x'')}{W\hat{W}} \int_x^{x''} [\zeta(x') - \gamma(x')] g_2(x') \hat{g}_1(x') dx' \\ & - \frac{g_1(x)\hat{g}_1(x'')}{W\hat{W}} \int_{x''}^{x_1} [\zeta(x') - \gamma(x')] g_2(x') \hat{g}_2(x') dx', \end{aligned} \quad (18a)$$

while, for $x'' < x$,

$$\begin{aligned} \hat{g}(x, x'') = & \frac{g_2(x)g_1(x'')}{-\hat{W}} - \frac{g_1(x)\hat{g}_2(x'')}{W\hat{W}} \int_{x_1}^{x''} [\zeta(x') - \gamma(x')] g_1(x') \hat{g}_1(x') dx' \\ & - \frac{g_2(x)\hat{g}_1(x'')}{W\hat{W}} \int_{x''}^x [\zeta(x') - \gamma(x')] g_1(x') \hat{g}_2(x') dx' \\ & - \frac{g_2(x)\hat{g}_1(x'')}{W\hat{W}} \int_x^{x_1} [\zeta(x') - \gamma(x')] g_2(x') \hat{g}_2(x') dx'. \end{aligned} \quad (18b)$$

Suppose now that $x'' = x_1$. Then Eqs. (17) and (18b) yield

$$\hat{g}_2(x) = C_2 g_2(x) + \frac{g_2(x)}{W} \int_{x_1}^x (\zeta - \gamma) g_1 \hat{g}_2 dx' + \frac{g_1(x)}{W} \int_x^{x_1} (\zeta - \gamma) g_2 \hat{g}_2 dx', \quad (19)$$

where the constant C_2 is given by

$$C_2 = \frac{g_1(x_1)}{W} \frac{\hat{W}}{\hat{g}_1(x_1)} = \frac{\hat{g}_2 \hat{g}'_1 / \hat{g}_1 - \hat{g}'_2}{g_2 g'_1 / g_1 - g'_2} \Big|_{x_1} = \frac{\alpha_1 \hat{g}_2(x_1) + \hat{g}'_2(x_1)}{\alpha_1 g_2(x_1) + g'_2(x_1)}. \quad (19a)$$

The last expression in Eq. (19a) results upon imposition of the boundary condition $g'_1(x_1) + \alpha_1 g_1(x_1) = 0$, and similarly for \hat{g}_1 . Equation (19) represents an integral equation for the wave function \hat{g}_2 that satisfies the homogeneous equation (13) and the required boundary conditions at x_2 . Since we are interested only in the functional form of \hat{g}_2 , and the integral equation is linear, we may put $C_2 = 1$. If $\zeta \approx \gamma$ for $x_1 < x < x_3 < x_2$, the contribution from the first integral is negligible in this range and one finds that

$$\hat{g}_2(x) = g_2(x) + \frac{g_1(x)}{W} \int_{x_1}^{x_1} (\zeta - \gamma) g_2 \hat{g}_2 dx', \quad x_1 \leq x \leq x_3. \quad (20)$$

This formulation is useful for scattering problems (with $x_1 \rightarrow -\infty$, $x_2 \rightarrow \infty$) wherein one seeks to assess the influence on the scattered field of a deviation

of the medium parameter $\gamma(x)$ from its unperturbed value $\zeta(x)$ for which the solution g_2 is known. To a first approximation, one finds, from Eq. (20),

$$\hat{g}_2(x) \cong g_2(x) + g_1(x) \left\{ \frac{1}{W} \int_{x_1}^{x_2} [\zeta(x') - \gamma(x')] g_2^2(x') dx' \right\} \quad (21)$$

for observation points $x < x_3$. Similarly, if $\zeta \approx \gamma$ for $x_4 < x \leq x_2$, one has, from Eq. (19),

$$\hat{g}_2(x) = g_2(x) \left\{ 1 + \frac{1}{W} \int_{x_1}^{x_2} [\zeta(x') - \gamma(x')] g_1(x') \hat{g}_2(x') dx' \right\}, \quad x_4 < x. \quad (22)$$

To a first approximation, $\hat{g}_2(x')$ in the integral is replaced by $g_2(x')$.

Equation (21) yields the correction to the wave reflected from the inhomogeneity described by $\zeta - \gamma$, while Eq. (22) shows the perturbation of the transmitted wave. As an illustration, let us consider an infinite medium ($x_1 \rightarrow -\infty$, $x_2 \rightarrow \infty$) with a variable permittivity $\epsilon(x)$ that approaches the constant value ϵ_0 as $x \rightarrow \pm\infty$, or in terms of (13), a medium for which

$$\gamma(x) = k_0^2, \quad x \rightarrow \pm\infty, \quad (23a)$$

where k_0 is the propagation constant corresponding to ϵ_0 . We choose as the unperturbed problem

$$\zeta(x) = k_0^2, \quad -\infty < x < \infty. \quad (23b)$$

The unperturbed solution $g_2(x)$ which satisfies the radiation condition at $x_2 = \infty$ is given by†

$$g_2(x) = e^{ik_0 x} \quad (e^{-i\omega t} \text{ dependence}), \quad (24a)$$

while the corresponding solution for $x_1 = -\infty$ is

$$g_1(x) = e^{-ik_0 x}. \quad (24b)$$

Thus, $W = 2ik_0$, and from Eqs. (20) and (22),‡

$$\hat{g}_2(x) = e^{ik_0 x} + \bar{\Gamma} e^{-ik_0 x}, \quad \bar{\Gamma} = \frac{1}{2ik_0} \int_{-\infty}^{\infty} [k_0^2 - \gamma(x')] e^{ik_0 x'} \hat{g}_2(x') dx', \quad x \rightarrow -\infty, \quad (25a)$$

$$\hat{g}_2(x) = T e^{ik_0 x}, \quad T = 1 + \frac{1}{2ik_0} \int_{-\infty}^{\infty} [k_0^2 - \gamma(x')] e^{-ik_0 x'} \hat{g}_2(x') dx', \quad x \rightarrow +\infty. \quad (25b)$$

$\bar{\Gamma}$ in Eq. (25a) represents the plane-wave reflection coefficient of the inhomogeneous medium, while T in Eq. (25b) is the transmission coefficient. To a first approximation, the Born approximation,¹⁴ one has for a slightly inhomogeneous medium,

† In applications to wave propagation throughout this section, the time dependence is $\exp(-i\omega t)$.

‡ To avoid confusion with the gamma function $\Gamma(x)$, the reflection coefficient in this section is denoted by $\bar{\Gamma}$.

$$\bar{\Gamma} \cong \frac{1}{2ik_0} \int_{-\infty}^{\infty} [k_0^2 - \gamma(x')] e^{i2k_0x'} dx', \quad (26a)$$

$$T \cong 1 + \frac{1}{2ik_0} \int_{-\infty}^{\infty} [k_0^2 - \gamma(x')] dx', \quad (26b)$$

where it is implied that $(k_0^2 - \gamma)$ is integrable over the infinite interval.

Since $\hat{g}_2(x)$ plays the role of a voltage V (or current I) on a non-uniform transmission line (see Figs. 3.3.1 and 3.3.2), the constancy of real power flow on a non-dissipative line (k_0, γ real) implies that

$$\operatorname{Re}(VI^*) = \operatorname{Re} \left[\frac{-1}{ik_x^*(x)Z^*(x)} V(x) \frac{dV^*(x)}{dx} \right] = \text{constant}, \quad (26c)$$

where k_x and Z are the propagation constant and characteristic impedance, respectively [see Eqs. (3.3.2)]. Application of Eq. (26c) to Eqs. (25) yields the conservation condition

$$1 - |\bar{\Gamma}|^2 = |T|^2, \quad (26d)$$

satisfied by the magnitudes of the reflection and transmission coefficients. Because k_0 and γ are real, T in Eq. (26b) has a magnitude greater than unity, so that this approximation does not satisfy the conservation-of-energy requirement. This is not surprising since, to a first order of approximation, $1 + i\alpha = (1 - i\alpha)^{-1}$, where α is a small quantity, and the two results are equivalent to $O(\alpha)$. If one writes $T = (1 - i\alpha)^{-1}$, where $i\alpha$ represents the second term on the right-hand side of Eq. (26b), the resulting expression satisfies $|T| < 1$. These considerations highlight the fact that approximate results obtained by a perturbation method do not necessarily obey all the conditions satisfied by the exact solution.

For an alternative derivation of T and $\bar{\Gamma}$, consider Eq. (4) with the Green's function $G(x', x)$ now chosen so that Eq. (5) is satisfied when $x > x'$. One obtains instead of Eq. (6),

$$u(x) = \left\{ G(x_2, x) \frac{du(x_2)}{dx_2} - u(x_2) \frac{d}{dx_2} G(x_2, x) \right\} + \int_x^{x_2} [\gamma - \zeta] G(x', x) u(x') dx', \quad (27a)$$

with $G(x', x)$ given by the negative of the first expression in Eq. (8). If $x_2 \rightarrow \infty$ and we choose for $u(x_2)$ the solution that behaves like $T \exp(i k_0 x_2)$, where T is a constant, then via Eqs. (23), (24), and (27a),

$$u(x) = T e^{ik_0 x} + \frac{e^{ik_0 x}}{2ik_0} \int_x^{\infty} (\gamma - \zeta) e^{-ik_0 x'} u(x') dx' - \frac{e^{-ik_0 x}}{2ik_0} \int_x^{\infty} (\gamma - \zeta) e^{ik_0 x'} u(x') dx', \quad (27b)$$

whence, for the first-order approximation as $x \rightarrow -\infty$,

$$u(x) \cong e^{ik_0 x} \left[1 + \frac{1}{2ik_0} \int_{-\infty}^{\infty} (\gamma - \zeta) dx' \right] T - e^{-ik_0 x} \left[\frac{T}{2ik_0} \int_{-\infty}^{\infty} (\gamma - \zeta) e^{i2k_0 x'} dx' \right]. \quad (28)$$

For a unit amplitude incident wave, the coefficient of $\exp(ik_0x)$ is set equal to unity and the resulting expression for T , with $\zeta = k_0^2$, is equal to the complex conjugate of the reciprocal of Eq. (26b); as observed above, they agree to first order. The coefficient of the $\exp(-ik_0x)$ term is equal to the reflection coefficient $\bar{\Gamma}$ and agrees to first order with that in Eq. (26a).

3.5b The Comparison Equation

The success of the method described in the preceding section rests upon the ability to choose a comparison function $\zeta(x)$ so that the difference function $[\gamma(x) - \zeta(x)]$ is small. The idea of "smallness" is to be defined more precisely in this section, and it will be convenient to exhibit explicitly a large positive parameter Ω with respect to which an asymptotic solution of Eq. (2) may be found. For example, if Ω is the free-space wavenumber k_0 , the largeness of Ω describes short wavelength propagation phenomena for which the medium parameters appear to be slowly varying. Thus, we assume that

$$\begin{aligned}\gamma(x) &= \Omega^2[\alpha_0(x) + \alpha_1(x, \Omega)] \equiv \Omega^2\alpha(x, \Omega), \\ \zeta(x) &= \Omega^2[\beta_0(x) + \beta_1(x, \Omega)] \equiv \Omega^2\beta(x, \Omega),\end{aligned}\quad (29)$$

where $\alpha_1(x, \Omega)$ and $\beta_1(x, \Omega)$ are functions of x and Ω that tend to zero as $\Omega \rightarrow \infty$.

To facilitate the determination of ζ or β , it is convenient to transform the differential equation (7) so that the resulting $\zeta(x)$ involves an arbitrary transformation function $\varphi(x)$ chosen so as to make $\zeta(x)$ a good comparison function.¹⁵⁻¹⁷ To this purpose, assume that

$$\left[\frac{d^2}{d\xi^2} + \Omega^2 \bar{\beta}(\xi, \Omega) \right] \bar{g}(\xi) = 0 \quad (30)$$

defines known solutions $\bar{g}(\xi)$ and introduce a variable x via

$$\xi = \varphi(x), \quad \text{i.e., } d\xi = \varphi'(x) dx, \quad (31)$$

where the prime denotes differentiation with respect to x . With

$$\bar{g}(\xi) = \sqrt{\varphi'} g(x), \quad (32)$$

substitution of Eqs. (31) and (32) into Eq. (30) yields

$$\left[\frac{d^2}{dx^2} + \Omega^2 \beta(x, \Omega) \right] g(x) = 0, \quad (33)$$

where

$$\beta(x, \Omega) = \bar{\beta}(\varphi, \Omega) \varphi'^2 + \frac{1}{2\Omega^2} \{ \varphi, x \}, \quad (33a)$$

$\{ \varphi, x \}$ being the Schwarzian derivative of φ such that

$$\{ \varphi, x \} = \frac{\varphi'''}{\varphi'} - \frac{3}{2} \left(\frac{\varphi''}{\varphi'} \right)^2 = -2\sqrt{\varphi'} \frac{d^2}{dx^2} \frac{1}{\sqrt{\varphi'}}. \quad (33b)$$

Since the solutions of Eq. (30) are assumed to be known, the solutions of Eq. (33) are likewise known for any function $\varphi(x)$ that is thrice differentiable and has $\varphi' \neq 0$ in the interval $x_2 - x_1$.

It is now recognized that for large Ω , Eq. (33) resembles the desired equation

$$\left[\frac{d^2}{dx^2} + \Omega^2 \alpha(x, \Omega) \right] \hat{g}(x) = 0, \quad (34)$$

if $\varphi(x)$ is chosen so that

$$\varphi'^2 \bar{\beta}_0(\varphi) = \alpha_0(x), \quad \text{i.e., } \int_{\varphi_1}^{\varphi} \sqrt{\bar{\beta}_0(\varphi)} d\varphi = \int_{x_1}^x \sqrt{\alpha_0(x)} dx, \quad (35)$$

where $\bar{\beta}_0(\varphi) = \lim_{\Omega \rightarrow \infty} \bar{\beta}(\varphi, \Omega)$. This choice assures that the dominant terms in Eqs. (33) and (34) are identical and that the difference function $\zeta - \gamma$ is small compared to γ [i.e., $(\zeta - \gamma)/\gamma \rightarrow 0$ as $\Omega \rightarrow \infty$]. Thus, an approximate solution for \hat{g} is given by

$$\hat{g}(x) \approx g(x) = \frac{\bar{g}[\varphi(x)]}{\sqrt{d\varphi(x)/dx}}. \quad (36)$$

where

$$\varphi(x) = \int_{x_0}^x \sqrt{\frac{\alpha_0(\eta)}{\bar{\beta}_0[\varphi(\eta)]}} d\eta. \quad (36a)$$

Since $\varphi'(x)$ and $1/\varphi'(x)$ are to remain bounded in the interval, the comparison function $\bar{\beta}_0[\varphi(x)]$ must be chosen so that its zeros and poles occur at the same locations as those of the given function $\alpha_0(x)$.[†] Whether $g(x)$ in Eq. (36) is, in fact, a good approximation to $\hat{g}(x)$ can be assessed by examining the order of magnitude of the correction terms via the integral equation procedure in Sec. 3.4a. Although it is difficult to make a general statement,¹⁸ one observes that $\{\varphi, x\}$ in Eq. (33b) is small when $\varphi'(x)$ is a slowly varying function over the x interval under consideration; Eq. (36) may then be expected to apply. The previously mentioned matching of the singularities and zeros of $\alpha(x, \Omega)$ plays an important role in this connection.

3.5c Various Comparison Functions

$\alpha_0(x)$ has no zeros or poles (WKB solution)

As an illustration, let us suppose that $\alpha(x, \Omega) \equiv \alpha_0(x)$ has no zeros and is analytic in the interval under consideration (see Fig. 3.5.1). $\bar{\beta}$ may then be chosen as a constant,[‡] $\bar{\beta} = 1$, whence $\bar{g}(\xi) = \exp(\pm i\Omega\xi)$. Equation (36) yields

[†] Analogous considerations enter into the asymptotic evaluation of integrals where a given unknown integral is compared to a known and simpler one having a similar integrand in the vicinity of the stationary points (Sec. 4.1).

[‡] A better approximation may be obtained by choosing a comparison function which provides a “better fit” than $\beta = \text{constant}$ (e.g., a piecewise linear or a parabolic profile; see also Sec. 3.6b).

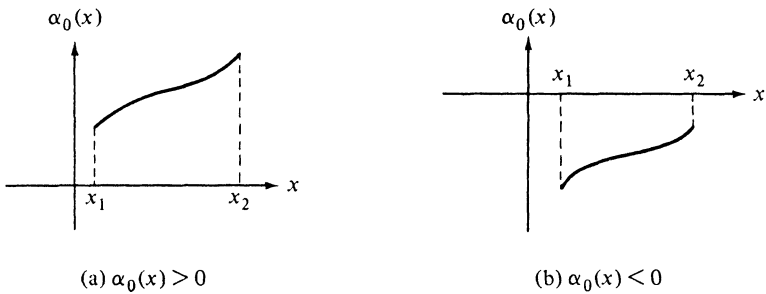


FIG. 3.5.1 Profiles without zeros or singularities.

$$\hat{g}(x) \cong g(x) = \frac{\exp\left[\pm i\Omega \int_{x_0}^x \sqrt{\alpha_0(\eta)} d\eta\right]}{\sqrt[4]{\alpha_0(x)}}, \quad \Omega \rightarrow \infty, \quad (37)$$

where x_0 is arbitrary. We choose $\arg \alpha_0(x) = 0$ if $\alpha_0(x) > 0$, $\arg \alpha_0(x) = \pi$ if $\alpha_0(x) < 0$, and take the principal value of all roots. This form of $\hat{g}(x)$ represents the *WKB approximation*, and satisfies *exactly* the differential equation (33), with $\tilde{\beta} = 1$, $\varphi' = \sqrt{\alpha_0}$; moreover,

$$\gamma(x) - \zeta(x) = -\frac{1}{2\Omega^2} \{\varphi, x\}. \quad (38)$$

The Green's function $G(x', x)$ of Eq. (8) becomes

$$G(x', x) = \frac{\sin \int_x^{x'} \sqrt{\gamma(\eta)} d\eta}{\sqrt[4]{\alpha_0(x)\alpha_0(x')} \Omega}, \quad \gamma = \Omega^2 \alpha_0. \quad (39a)$$

The Green's function in Eq. (16) can be constructed in a similar manner. For an unbounded region, α_0 is positive, and for a time dependence $\exp(-i\omega t)$, the positive and negative signs in Eq. (37) distinguish outgoing wave solutions at $x = +\infty$ and $x = -\infty$, respectively (Ω represents the wavenumber k_0). Thus, from Eq. (16),

$$G(x, x') = \frac{\exp\left[i\Omega \int_{x_-}^{x_>} \sqrt{\alpha_0(\eta)} d\eta\right]}{-2i\Omega[\alpha_0(x)\alpha_0(x')]^{1/4}}. \quad (39b)$$

On the other hand, if the region is bounded at $x = d$, and if $g = 0$ at $x = d$, the solution g_1 (which satisfies the boundary condition at $x = d$) is of the form

$$g_1(x) = \frac{\sin \left[\Omega \int_d^x \sqrt{\alpha_0(\eta)} d\eta \right]}{[\alpha_0(x)]^{1/4}}, \quad (39c)$$

while g_2 remains as in Eq. (37) (with $x_0 = d$, for convenience). Thus,

$$G(x, x') = \frac{\exp\left[i\Omega \int_{x_-}^{x_>} \sqrt{\alpha_0(\eta)} d\eta\right]}{-2i\Omega[\alpha_0(x)\alpha_0(x')]^{1/4}} - \frac{\exp\left[i\Omega \left\{ \int_d^x + \int_d^{x'} \right\} \sqrt{\alpha_0(\eta)} d\eta\right]}{-2i\Omega[\alpha_0(x)\alpha_0(x')]^{1/4}}, \quad (39d)$$

which formulation exhibits directly the breakup into incident and reflected waves; the factor (-1) multiplying the second term represents the reflection coefficient at the boundary. If $\alpha_0(x_0) = 0$ and $\alpha_0(x) \geq 0$ when $x \geq x_0$, the solution g_1 that remains bounded for $x < x_0$ is given below in Eq. (47a); it has the same form as in Eq. (39c) except that $d = x_0$ and a phase shift of $\pi/4$ is added to the sine argument. Thus, for $x, x' > x_0$,

$$G(x, x') = \frac{\exp \left[i\Omega \int_{x_0}^{x'} \sqrt{\alpha_0(\eta)} d\eta \right]}{-2i\Omega[\alpha_0(x)\alpha_0(x')]^{1/4}} + e^{-i\pi/2} \frac{\exp \left[i\Omega \left\{ \int_{x_0}^x + \int_{x_0}^{x'} \right\} \sqrt{\alpha_0(\eta)} d\eta \right]}{-2i\Omega[\alpha_0(x)\alpha_0(x')]^{1/4}}. \quad (39e)$$

In this instance, the effective reflection coefficient at the turning point† x_0 is $-i$. The formulas in Eqs. (37)–(39) evidently fail when α_0 has a zero in the interval. The continuation of a given form of the solution in Eq. (37) from positive to negative values of $\alpha_0(x)$ requires the knowledge of appropriate connection formulas, which are also discussed below [see Eqs. (47)].

$\alpha_0(x)$ has a simple zero

If $\alpha(x, \Omega) \equiv \alpha_0(x)$ is analytic in the interval and has a simple zero, conveniently chosen at $x = 0$ (see Fig. 3.5.2), the simplest comparison function is $\bar{\beta}(\xi, \Omega) \equiv \bar{\beta}_0(\xi) = \xi = \varphi(x)$, with $\varphi(0) = 0$. From Eq. (35),

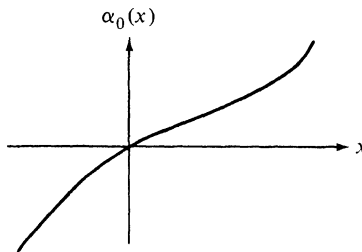


FIG. 3.5.2 Profile with simple zero.

$$\alpha_0^{1/2} = \varphi' \varphi^{1/2} = \frac{2}{3} \frac{d}{dx} \varphi^{3/2}, \quad (40)$$

so

$$\varphi(x) = \left[\frac{3}{2} \int_0^x \sqrt{\alpha_0(\eta)} d\eta \right]^{2/3}, \quad (41)$$

where the condition $\varphi(0) = 0$ has been utilized in determining the lower integration limit. To resolve the ambiguity introduced by $\sqrt{\alpha_0(x)}$ we draw a branch cut from zero to $-\infty$ along the negative real axis in the complex x plane and define $\arg \alpha_0(x) = 0$ when x is positive real. When $\arg x$ increases by π , x is located on the upper shore of the cut and

†If $\alpha_0(x)$ has a zero at x_0 , this point is called a “turning point” of the differential equation (34).

$$\int_0^{|x| e^{in}} \sqrt{\alpha_0(\eta)} d\eta = e^{in} \int_0^{|x|} \sqrt{\alpha_0(\zeta e^{in})} d\zeta = e^{i3\pi/2} \int_0^{|x|} |\sqrt{\alpha_0(\zeta)}| d\zeta, \quad x < 0, \quad (42a)$$

so

$$\varphi(x) \geq 0 \quad \text{when } x \geq 0. \quad (42b)$$

The solution of the differential equation

$$\left(\frac{d^2}{d\xi^2} + \Omega^2 \xi \right) \bar{g}(\xi) = 0 \quad (43)$$

is given by

$$\bar{g}(\xi) = \frac{\text{Ai}}{\text{Bi}}(-\Omega^{2/3} \xi), \quad (44)$$

where $\text{Ai}(\sigma)$ and $\text{Bi}(\sigma)$ are the Airy functions, whose properties are discussed in detail in Secs. 4.2e and 6.A5. Thus, from Eq. (36),

$$\hat{g}(x) \approx g(x) = \left[\frac{3}{2} \int_0^x \sqrt{\alpha_0(\eta)} d\eta \right]^{1/6} [\alpha_0(x)]^{-1/4} \text{Ai} \left\{ - \left[\frac{3}{2} \Omega \int_0^x \sqrt{\alpha_0(\eta)} d\eta \right]^{2/3} \right\}, \quad (45)$$

with the principal value taken in all roots. Since $\text{Ai}(\sigma)$ and $\text{Bi}(\sigma)$ are single-valued functions of σ , $\arg \sigma$ may be taken as $\pm\pi$ when $\sigma < 0$.

Since $\alpha_0(x) \sim x$ near $x = 0$, it follows that $\varphi(x) \sim x$ near $x = 0$ so that the expression for $\hat{g}(0)$ exists. For $|x|$ sufficiently large so that $\Omega^{2/3}|\varphi| \gg 1$, one may employ the asymptotic formulas (see Sec. 4.2e),

$$\text{Ai}(-\sigma) \sim \begin{cases} \frac{1}{\sqrt{\pi} \sigma^{1/4}} \sin \left(\frac{2}{3} \sigma^{3/2} + \frac{\pi}{4} \right), & \sigma \rightarrow +\infty, \\ \frac{1}{2\sqrt{\pi} (-\sigma)^{1/4}} e^{-(2/3)(-\sigma)^{3/2}}, & -\sigma \rightarrow +\infty \end{cases} \quad (46a)$$

$$\text{Bi}(-\sigma) \sim \begin{cases} \frac{1}{\sqrt{\pi} \sigma^{1/4}} \cos \left(\frac{2}{3} \sigma^{3/2} + \frac{\pi}{4} \right), & \sigma \rightarrow +\infty, \\ \frac{1}{\sqrt{\pi} (-\sigma)^{1/4}} e^{(2/3)(-\sigma)^{3/2}}, & -\sigma \rightarrow +\infty, \end{cases} \quad (46b)$$

to reduce the Ai part of the expression for $\hat{g}(x)$ in Eq. (45) for $x > 0$ to

$$\hat{g}(x) \approx \frac{1}{\sqrt{\pi}} \frac{1}{[\alpha_0(x)]^{1/4} \Omega^{1/6}} \sin \left[\Omega \int_0^x \sqrt{\alpha_0(\eta)} d\eta + \frac{\pi}{4} \right], \quad \Omega^{2/3} \varphi \gg 1, \quad (47)$$

and similarly for the Bi part. Thus, if the right-hand side of Eq. (45) is multiplied by $\Omega^{1/6}$, the resulting expression can be made to go smoothly from $x = 0$ to $|x|$ large, coinciding in the latter range with the WKB formula in Eq. (37). We then obtain the previously mentioned connection relations for the WKB formulas when the differential equation has a simple turning point. Application of Eqs. (46) to the general solution $\hat{g}(x)$ in Eq. (45) comprising both the Ai and Bi functions in the combination $[C_1 \text{Ai} + C_2 \text{Bi}]$ yields, to within irrelevant constants,

$$\hat{g}(x) \cong \begin{cases} \frac{1}{\sqrt[4]{\alpha_0(x)}} \left\{ C_1 \sin \left[\Omega \psi(x) + \frac{\pi}{4} \right] + C_2 \cos \left[\Omega \psi(x) + \frac{\pi}{4} \right] \right\}, & \alpha_0(x) > 0, \\ \frac{1}{\sqrt[4]{|\alpha_0(x)|}} \left\{ \frac{C_1}{2} e^{-\alpha |\psi(x)|} + C_2 e^{\alpha |\psi(x)|} \right\}, & \alpha_0(x) < 0, \end{cases} \quad (47a)$$

where

$$\psi(x) = \int_0^x \sqrt{\alpha_0(\eta)} d\eta, \quad (47b)$$

and $C_{1,2}$ are arbitrary constants that are determined from the boundary conditions. For example, if the region extends to $\pm\infty$, the requirement of a bounded solution leads to $C_2 = 0$; the corresponding physical phenomenon involves propagating waves in the region $x > 0$ which are totally reflected in the vicinity of $x = 0$. Since the argument of the Airy functions in Eq. (45) is positive when $x < 0$, Ai yields an exponentially decaying, and Bi an exponentially increasing, solution for $x < 0$. Upon multiplication by $\Omega^{1/6}$, these results can be made to coincide with the corresponding WKB solutions in Eq. (37).

To construct the Green's function in Eq. (16) we select solutions $g_1(x)$ and $g_2(x)$ that satisfy boundary conditions at the endpoints $x = x_1$ and $x = x_2 > x_1$, respectively. Let us suppose that the region is infinitely extended (i.e., $x_1 = -\infty$ and $x_2 = +\infty$) and that $\alpha_0(x)$ approaches the value of unity as $x \rightarrow +\infty$. Since a source placed at the point x' radiates fields which are bounded at $x \rightarrow \pm\infty$, the Ai function must be chosen for $g_1(x)$. To satisfy a radiation condition at $x = +\infty$, the wave function $g_2(x)$ must vary like $\exp(+i\Omega x)$ and therefore involves via Eqs. (46) both the Ai and Bi functions. Thus,

$$g_1(x) = \frac{1}{[\alpha_0(x)]^{1/4}} [Y(x)]^{1/6} \text{Ai}[-(\Omega Y)^{2/3}], \quad Y(x) = \frac{3}{2} \int_0^x \sqrt{\alpha_0(\eta)} d\eta, \quad (48a)$$

$$g_2(x) = \frac{1}{[\alpha_0(x)]^{1/4}} Y^{1/6} \{ \text{Ai}[-(\Omega Y)^{2/3}] - i \text{Bi}[-(\Omega Y)^{2/3}] \}, \quad (48b)$$

where the values of $Y(x)$ and $[\alpha_0(x)]^{1/4}$ for $x \geq 0$ have been defined in Eqs. (42). From the asymptotic form of $\text{Ai}(z)$ and $\text{Bi}(z)$ in Eqs. (46) as $z \rightarrow \infty$, one finds for the Wronskian

$$\text{Ai}(z) \frac{d}{dz} \text{Bi}(z) - \text{Bi}(z) \frac{d}{dz} \text{Ai}(z) = \frac{1}{\pi}, \quad (49)$$

whence for the functions in Eqs. (48),

$$W(g_1, g_2) = \frac{i}{\pi} \left(\frac{2}{3} \right)^{1/3}. \quad (50)$$

$\alpha_0(x)$ has two neighboring simple zeros

If $\alpha(x, \Omega) = \alpha_0(x)$ has isolated simple zeros (see Fig. 3.5.3), the asymptotic approximation of $\hat{g}(x)$ as $\Omega \rightarrow \infty$ can be constructed by a combination of the WKB- and Airy-function formulations. The WKB approximation is valid in those regions where $\alpha_0(x) \neq 0$, and the Airy-function approximation is used

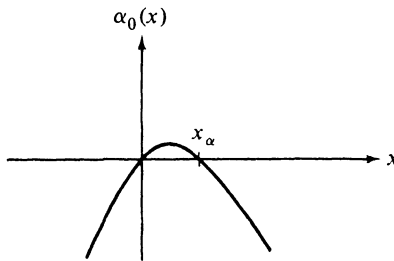


FIG. 3.5.3 Profile with two simple zeros.

to match smoothly through each turning point region $\alpha_0(x) \approx 0$. However, if two simple zeros of $\alpha_0(x)$ located at $x = 0$ and $x = x_\alpha$, respectively, tend to coalesce, the expression in Eq. (45) loses its validity and diverges as $x_\alpha \rightarrow 0$. The simplest comparison function when $\alpha_0(x)$ has two adjacent zeros is

$$\tilde{\beta}(\xi, \Omega) \equiv \tilde{\beta}_0(\xi) = (a^2 - \xi^2), \quad (51)$$

with no loss in generality incurred by the symmetrical location of the zeros at $\xi = \pm a$. To ensure that these zeros in the ξ plane correspond to those at $x = 0, x_\alpha$ in the x plane, we return to Eq. (35):

$$\int_0^x \sqrt{\alpha_0(x)} dx = \int_{-a}^a \sqrt{\tilde{\beta}_0(\varphi)} d\varphi = \frac{1}{2} \left\{ \varphi \sqrt{a^2 - \varphi^2} + a^2 \sin^{-1} \frac{\varphi}{a} + \frac{a^2 \pi}{2} \right\}. \quad (52a)$$

The choice of the lower integration limits implies the correspondence of $\varphi = -a$ and $x = 0$. To enforce that $\varphi = a$ when $x = x_\alpha$, set

$$\int_0^{x_\alpha} \sqrt{\alpha_0(x)} dx = \int_{-a}^a \sqrt{\tilde{\beta}_0(\varphi)} d\varphi = \frac{\pi a^2}{2}, \quad (52b)$$

which equation serves to determine the value of a .^{19,20}

The solution of the differential equation

$$\left[\frac{d^2}{d\xi^2} + \Omega^2(a^2 - \xi^2) \right] \tilde{g}(\xi) = 0 \quad (53)$$

is given by Weber's parabolic cylinder functions

$$\tilde{g}(\xi) = D_v(\pm \sqrt{2\Omega} \xi), \quad v = \frac{1}{2}(\Omega a^2 - 1). \quad (54)$$

When $\xi \not\simeq \pm a$, these functions have the asymptotic approximation

$$D_v(\sqrt{2\Omega} \xi) \sim \frac{e^{-\Omega a^2(\tau+1/4)}}{[2\Omega(\xi^2 - a^2)]^{1/4} (\Omega a^2/2)^{-\Omega a^2/4}} \left[1 + O\left(\frac{1}{\Omega a^2}\right) \right],$$

$$|\arg(\xi \sqrt{\Omega})| \leq \frac{\pi}{2}, \quad (55a)$$

$$a^2 \tau = a^2 \int_1^{\xi/a} \sqrt{t^2 - 1} dt = \frac{\xi}{2} \sqrt{\xi^2 - a^2} - \frac{a^2}{2} \ln \left[\frac{\xi}{a} + \sqrt{\left(\frac{\xi}{a} \right)^2 - 1} \right], \quad (55b)$$

where the latter expression constitutes the analytic continuation of the right-hand side of Eq. (52a) to the range ($\xi = \phi$) $> a$. This result is nothing but the WKB approximation in Eq. (37), normalized so that the function $D_v(z)$ reduces to the large argument form $z^v \exp(-z^2/4)$ as $|z/v| \rightarrow \infty$.²¹ Alternatively, when $\pi/2 \leq \arg(\xi\sqrt{\Omega}) \leq \pi$, one may utilize the large z behavior

$$D_v(z) \sim e^{-z^2/4} z^v \left[1 + O\left(\frac{1}{z}\right) \right] - \frac{\sqrt{2\pi}}{\Gamma(-v)} e^{vni} \frac{e^{z^2/4}}{z^{v+1}} \left[1 + O\left(\frac{1}{z}\right) \right], \quad (56)$$

to select the proper WKB approximation in this range. In the vicinity of the turning points $\xi = a$ or $\xi = -a$, one may employ the Airy-function approximation in the preceding section, and only when $a \rightarrow 0$ is it necessary to retain the parabolic cylinder function intact. The various asymptotic representations for $D_v(z)$ for large (and possibly complex) values of v and z have been discussed in detail by Olver.²²

$\alpha_0(x)$ has a simple pole

If $\alpha(x, \Omega) = \alpha_0(x)$ has a simple pole at $x = 0$ (see Fig. 3.5.4), the simplest comparison function is†

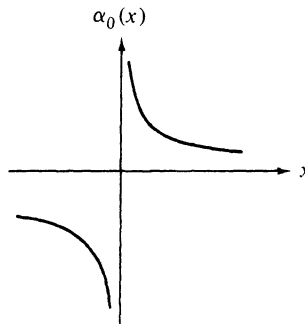


FIG. 3.5.4 Profile with simple pole.

$$\bar{\beta}(\xi, \Omega) = \frac{1}{\xi}, \quad (57)$$

which yields the following solutions of Eq. (30):

$$\bar{g}(\xi) = \sqrt{\xi} H_1^{(1,2)}(2\Omega\sqrt{\xi}). \quad (58)$$

Despite the singularity of $\bar{\beta}$, the solution $\bar{g}(\xi)$ is bounded at $\xi = 0$. Since $\bar{\beta}_0(\phi) = 1/\phi$, one obtains, from Eq. (35),

$$\frac{d\phi}{\sqrt{\phi}} = \sqrt{\alpha_0(x)} dx, \quad (59)$$

or, upon integration,

†A related comparison function is $\bar{\beta}(\xi, \Omega) = (1/\xi) - [(1 - v^2)/4\xi^2\Omega^2]$, which leads to the solutions $\bar{g}(\xi) = \sqrt{\xi} H_v^{(1,2)}(2\Omega\sqrt{\xi})$. This comparison function has a double pole at $\xi = 0$ and a simple zero at $(1 - v^2)/4\Omega^2$.

$$\varphi(x) = \frac{1}{4} \left[\int_0^x \sqrt{\alpha_0(\eta)} d\eta \right]^2. \quad (60)$$

Thus, from Eq. (36),

$$\hat{g}(x) \approx g(x) = \left[\frac{\int_0^x \sqrt{\alpha_0(\eta)} d\eta}{\sqrt{\alpha_0(x)}} \right]^{1/2} H_1^{(1,2)} \left[\Omega \int_0^x \sqrt{\alpha_0(\eta)} d\eta \right]. \quad (61)$$

For $x \not\asymp 0$, one may employ the asymptotic formula for the Hankel function,

$$H_1^{(1,2)}(z) \sim \sqrt{\frac{2}{\pi z}} e^{\pm i(z - 3\pi/4)}, \quad |z| \gg 1, \quad -\pi < \arg z < \pi. \quad (61a)$$

If Eq. (61) is multiplied by $\Omega^{1/2}$, the resulting expression transforms smoothly into the WKB approximation (37), apart from x and Ω independent factors.

To determine the appropriate continuation of $\xi = \varphi(x)$ around the singularity at $\xi = 0$, the permissible range of $\arg \xi$ must be specified. If $\bar{\beta}(\xi, \Omega)$ represents the dielectric constant in the medium and slight loss is assumed, then $\text{Im } \bar{\beta}(\xi, \Omega) \geq 0$ [for a time dependence $\exp(-i\omega t)$]. The function $\bar{\beta} = 1/\xi$ may be replaced by $\bar{\beta} = 1/(\xi - i\delta)$, where δ is a small positive constant, so that the singularity is located above the real ξ axis. As $\delta \rightarrow 0$, the path along which ξ varies must be indented below the pole, whence $\arg \xi$ changes from zero to $-\pi$ as ξ passes through zero. Thus, $0 \geq \arg \sqrt{\xi} \geq -\pi/2$; hence $\arg \sqrt{\xi} = -\pi/2$ when $\xi < 0$. To obtain a solution that decays when $\xi < 0$, it is necessary [see Eq. (61a)] to select the $H_1^{(2)}$ function in Eq. (61). Since $\arg \sqrt{\xi} = 0$ when $\xi > 0$, this function represents a wave traveling in the $-\xi$ direction [for the assumed $\exp(-i\omega t)$ dependence], i.e., a wave incident from $\xi = +\infty$. The absence of an $H_1^{(1)}$ contribution implies that there is no reflected wave, and the incident wave is “completely absorbed” by the singularity, although the medium itself is assumed to be lossless. For a possible physical realization of this result, see Reference 23.

$\alpha_0(x)$ has neighboring simple pole and simple zero

The confluent hypergeometric function of Whittaker, $W_{l,m}(z)$, which satisfies the differential equation

$$\frac{d^2 W_{l,m}}{dz^2} + \left(-\frac{1}{4} + \frac{l}{z} - \frac{m^2 - \frac{1}{4}}{z^2} \right) W_{l,m} = 0, \quad (62)$$

may serve as the prototype for a general class of comparison functions. For example, the previously mentioned parabolic cylinder function $D_v(z)$ may be derived from $W_{l,m}(z)$ via the relation

$$D_v(z) = 2^{(2v+1)/4} z^{-1/2} W_{l,m} \left(\frac{z^2}{2} \right), \quad l = \frac{2v+1}{4}, \quad m = -\frac{1}{4}. \quad (63)$$

Of particular interest is the case $m = \pm \frac{1}{2}$, in which instance the coefficient $[(l/z) - \frac{1}{4}]$ has a simple pole at $z = 0$ and a simple zero at $z = 4l$. In the notation of the present chapter, the following comparison function is appropriate when $\alpha(x, \Omega) = \alpha_0(x)$ has a simple pole and an adjacent simple zero:

$$\left[\frac{d^2}{d\xi^2} + \Omega^2 \left(1 + \frac{a}{\xi} \right) \right] \bar{g}(\xi) = 0, \quad (64)$$

$$\bar{g}(\xi) = W_{-ia\Omega/2, 1/2}(i2\Omega\xi). \quad (64a)$$

The resulting profile is similar to that shown in Fig. 3.5.4, except that the branches are asymptotic to the line $\alpha_0(x) = 1$ at $|x| \rightarrow \infty$; the left branch crosses the x axis at $x = -a$. For a wave incident from the right, the singularity shields the turning point while the converse is true when the wave impinges from the left. The solution $W_{-l,m}(-z)$ is linearly independent of $W_{l,m}(z)$, and for large z , $W_{l,m}(z)$ has the asymptotic approximation

$$W_{l,m}(z) \sim e^{-z/2} z^l \left[1 + O\left(\frac{1}{z}\right) \right], \quad |\arg z| < \pi. \quad (65)$$

Detailed asymptotic formulas for various ranges of l , m , and z may be found in References 24 and 25.

An effective permittivity $\alpha(x)$ of the type described here arises in a plasma medium with linearly varying electron density, $(\omega_p/\omega)^2 = 1 + b\xi$, when an infinite static magnetic field is impressed along ξ [see Eq. (7.3.1) with $\epsilon = 1 - (\omega_p^2/\omega^2)$]. E modes in such a medium propagate according to Eqs. (7.2.7), which may be written in the form of Eq. (64), with \bar{g} representing the current.²⁶

3.5d Error Bounds on the Approximate Solutions

It can be shown that the expressions in Eqs. (37), (45), (54), and (61) represent the asymptotic approximations of the corresponding functions $\hat{g}(x)$ as $\Omega \rightarrow \infty$, i.e.,†

$$\hat{g}(x) \sim g(x)[1 + \epsilon(\Omega)], \quad \frac{d\hat{g}}{dx} \sim \frac{dg}{dx}[1 + \bar{\epsilon}(\Omega)], \quad (66)$$

where ϵ and $\bar{\epsilon}$ approach zero as $\Omega \rightarrow \infty$. While asymptotic estimates are very useful and usually sufficiently accurate to infer the basic physical behavior of the wave solution as $\Omega \rightarrow \infty$, it is desirable to have exact error bounds when detailed numerical calculations are involved. Estimates for various approximating functions have been supplied by Olver,²⁷ whose results for the WKB approximation are given below.

Let $\alpha(x, \Omega)$ be negative real, let $d^2\alpha/dx^2$ be a continuous function of x in the interval $a \leq x \leq b$ (which may be infinite), and let Ω be a positive parameter; then the differential equation (34) has solutions $\hat{g}_{1,2}$ such that

$$\hat{g}_{1,2}(x) = g_{1,2}(x)[1 + \Delta_{1,2}], \quad (67a)$$

$$g_{1,2}(x) = \frac{1}{\sqrt[4]{|\alpha(x, \Omega)|}} \exp \left[\pm \Omega \int_{x_0}^x \sqrt{|\alpha(\eta, \Omega)|} d\eta \right], \quad (67b)$$

†The derivation of formal asymptotic series involving higher-order terms in the WKB approximation is illustrated in Sec. 3.5e.

$$\frac{d}{dx} \hat{g}_{1,2}(x) = \pm \Omega^{\frac{1}{4}} \sqrt[4]{\alpha(x, \Omega)} \exp \left[\pm \Omega \int_{x_0}^x \sqrt{\alpha(\eta, \Omega)} d\eta \right] \left[1 + 2\chi_{1,2} \pm \frac{d\alpha/dx}{4\Omega|\alpha|^{3/2}} (1 + \Delta_{1,2}) \right], \quad (68)$$

where the magnitudes of $\Delta_{1,2}$ and $\chi_{1,2}$ are bounded by the numbers

$$|\Delta_{1,2}| \text{ or } |\chi_{1,2}| \leq \exp \left[\frac{1}{2\Omega} F_{1,2}(x, \Omega) \right] - 1, \quad (69a)$$

with

$$F_1(x, \Omega) = \int_a^x |\alpha(\eta, \Omega)|^{-1/4} \left| \frac{d^2}{d\eta^2} |\alpha(\eta, \Omega)|^{-1/4} \right| d\eta. \quad (69b)$$

F_2 is given by the same integral except that the interval of integration runs from x to b . $-a$ and (or) b may be infinite provided that the integrals $F_{1,2}$ converge. A somewhat weaker but more easily applied bound replaces Eq. (69a) by

$$|\Delta_{1,2}| \text{ or } |\chi_{1,2}| \leq \frac{F_{1,2}(x, \Omega)}{2\Omega - \frac{1}{2} F_{1,2}(x, \Omega)}, \quad (69c)$$

provided that $4\Omega > F_{1,2}$. This formulation makes evident the validity of Eq. (66).

If $\alpha(x, \Omega)$ is positive real, one has instead of the above,

$$\hat{g}_{1,2}(x) = g_{1,2}(x)(1 + \Delta_{1,2}), \quad (70a)$$

$$g_{1,2}(x) = \frac{1}{\sqrt[4]{\alpha(x, \Omega)}} \exp \left[\pm i\Omega \int_{x_0}^x \sqrt{\alpha(\eta, \Omega)} d\eta \right], \quad (70b)$$

$$\frac{d}{dx} \hat{g}_{1,2}(x) = \pm i\Omega^{\frac{1}{4}} \sqrt{\alpha(x, \Omega)} \exp \left[\pm i\Omega \int_{x_0}^x \sqrt{\alpha(\eta, \Omega)} d\eta \right] \left[1 + \chi_{1,2} \pm \frac{i d\alpha/dx}{4\Omega\alpha^{3/2}} (1 + \Delta_{1,2}) \right], \quad (71)$$

where $\Delta_1 = \Delta_2^*$, $\chi_1 = \chi_2^*$, and

$$|\Delta_{1,2}| \text{ or } |\chi_{1,2}| \leq \exp \left[\frac{1}{\Omega} F(x, \Omega) \right] - 1 \leq \frac{F(x, \Omega)}{\Omega - \frac{1}{2} F(x, \Omega)}, \quad (72a)$$

$$F(x, \Omega) = \left| \int_c^x [\alpha(\eta, \Omega)]^{-1/4} \left| \frac{d^2}{d\eta^2} [\alpha(\eta, \Omega)]^{-1/4} \right| d\eta \right|. \quad (72b)$$

c is an arbitrary point such that $a \leq c \leq b$. The interval (a, b) and the value of c may be infinite provided that the integral F converges. The second inequality in Eq. (72a) represents the weaker bound as in Eq. (69c). Uniform bounds valid in the entire interval $a \leq x \leq b$ are obtained upon replacing the lower and upper limits of integration in (69b) and (72b) by a and b , respectively. From Eqs. (69), $\Delta_1 = 0$ when $x = a$, so the function $\hat{g}_1(x)$ in Eq. (67a)

satisfies the boundary condition $\hat{g}_1(a) = g_1(a)$. The boundary conditions on the other functions or their derivatives are ascertained in a similar manner.

3.5e Corrections to the WKB Approximation

In Sec. 3.5c, appropriate comparison functions $g(x)$ are selected as a first asymptotic approximation to the desired function $\hat{g}(x)$ in Eq. (34). Corrections to the first approximation can then be obtained via the iteration procedure in Eq. (10a) based on the integral equations (9). Corrections can alternatively be derived directly from the differential equation. The latter procedure is illustrated here for the WKB approximation when $\alpha(x, \Omega) \equiv \alpha(x)$ is positive (i.e., it has no zeros in the interval under consideration).²⁸ It is convenient to start from the first-order, source-free transmission line equations (3.3.2) for H modes [for an $\exp(-i\omega t)$ dependence; i.e., $j \rightarrow -i$]:

$$\frac{d\hat{V}(x)}{dx} = i\omega\mu\hat{I}(x), \quad \frac{d\hat{I}(x)}{dx} = i\omega\epsilon(x)\hat{V}(x), \quad (73)$$

with constant permeability μ and x -dependent permittivity ϵ . Evidently,

$$\left[\frac{d^2}{dx^2} + \Omega^2 \alpha(x) \right] \hat{V}(x) = 0, \quad \Omega^2 = k_0^2 = \omega^2 \mu \epsilon_0, \quad \alpha(x) = \frac{\epsilon(x)}{\epsilon_0}, \quad (74)$$

so the voltage function $\hat{V}(x)$ can be identified with the wave function \hat{g} , while k_0 and $\epsilon(x)/\epsilon_0$ correspond to Ω and α , respectively ($\epsilon_0 = \text{constant}$).

The first approximation to $\hat{V}(x) \equiv \hat{g}(x)$ is given in Eq. (37). To derive corrections, assume that $\hat{V}(x)$ is represented by

$$\hat{V}(x) = [A(x)e^{i\Omega\psi(x)} - B(x)e^{-i\Omega\psi(x)}] \frac{1}{\sqrt[4]{\alpha(x)}}, \quad (75)$$

where $\psi(x)$ is the phase integral

$$\psi(x) = \int_{x_0}^x \sqrt{\alpha(\eta)} d\eta. \quad (75a)$$

$A(x)$ and $B(x)$ are slowly varying amplitude functions which are to be determined; if they are constant, Eq. (75) reduces to the WKB approximation. Similarly, let

$$\hat{I}(x) = \frac{\Omega}{\omega\mu} \sqrt[4]{\alpha(x)} [A(x)e^{i\Omega\psi(x)} + B(x)e^{-i\Omega\psi(x)}]. \quad (76)$$

Note that the expression for $\hat{I}(x)$ in Eq. (76) is the first-order asymptotic approximation to $(1/i\omega\mu)d\hat{V}/dx$ as $\Omega \rightarrow \infty$, with \hat{V} taken from Eq. (75). For a self-consistent determination of $A(x)$ and $B(x)$, substitute Eqs. (75) and (76) into Eqs. (73) to obtain

$$Ae^{i\Omega\psi} - Be^{-i\Omega\psi} = 4 \frac{\alpha}{\alpha'} [A'e^{i\Omega\psi} - B'e^{-i\Omega\psi}], \quad (77a)$$

$$Ae^{i\Omega\psi} + Be^{-i\Omega\psi} = -4 \frac{\alpha}{\alpha'} [A'e^{i\Omega\psi} + B'e^{-i\Omega\psi}], \quad (77b)$$

where a prime denotes the x derivative. Addition of these equations yields

$$B'(x) = -\frac{\alpha'(x)}{4\alpha(x)} e^{i2\Omega\psi(x)} A(x), \quad (78a)$$

while subtraction of the second from the first leads to

$$A'(x) = -\frac{\alpha'(x)}{4\alpha(x)} e^{-i2\Omega\psi(x)} B(x). \quad (78b)$$

Since $\psi(x)$ increases with x , the first term in Eq. (75) represents a wave traveling in the $+x$ direction while the second represents a wave traveling in the $-x$ direction. $A(x)$ and $B(x)$ are the corresponding wave amplitudes, and Eqs. (78) show that the variability of the medium parameter $\alpha(x)$ produces coupling between these two wave types. When α'/α is very small, the right-hand sides of Eqs. (78) can be set equal to zero and the resulting $A, B = \text{constant}$ yields the lowest-order approximation to $\hat{V}(x)$ and $\hat{I}(x) = (1/i\omega\mu)d\hat{V}/dx$; in this approximation, the waves traveling in the $+x$ and $-x$ directions are uncoupled.

Equations (78) can be solved by the method of successive approximations. They are first converted to coupled integral equations by integrating over x :

$$B(x) = B_0 + \int_{x_2}^x \delta_2(\xi) A(\xi) d\xi, \quad A(x) = A_0 + \int_{x_1}^x \delta_1(\xi) B(\xi) d\xi, \quad (79)$$

with

$$\delta_{1,2}(x) = -\frac{\alpha'}{4\alpha} e^{\mp i2\Omega\psi}, \quad (79a)$$

and $B(x_2) = B_0$, $A(x_1) = A_0$. B_0 , A_0 are arbitrary but specified, and $x_{1,2}$ are arbitrary points in the interval. Iteration of the two integrals then leads to the series

$$A(x) = \sum_{n=0}^{\infty} A_n(x), \quad B(x) = \sum_{n=0}^{\infty} B_n(x), \quad (80)$$

where $A_0(x) \equiv A_0$, $B_0(x) \equiv B_0$, and, for $n \geq 1$,

$$A_n(x) = \int_{x_1}^x \delta_1(\xi) B_{n-1}(\xi) d\xi, \quad B_n(x) = \int_{x_2}^x \delta_2(\xi) A_{n-1}(\xi) d\xi. \quad (81)$$

For conditions analogous to those discussed in connection with Eq. (10), these series are convergent.

Equations (81) have an important physical interpretation: they show that a zeroth-order wave traveling in the $+x$ direction gives rise to a first-order wave traveling in the $-x$ direction, which in turn generates a second-order wave in the $+x$ direction, etc. Thus, each term in the series (80) can be viewed as arising from continuous internal reflections caused by those portions in the inhomogeneous medium which lie between the observation point x and the points x_1 and x_2 where the amplitudes of the waves traveling in the positive and negative x directions, respectively, are assumed to be specified. This process is schematized in Fig. 3.5.5.

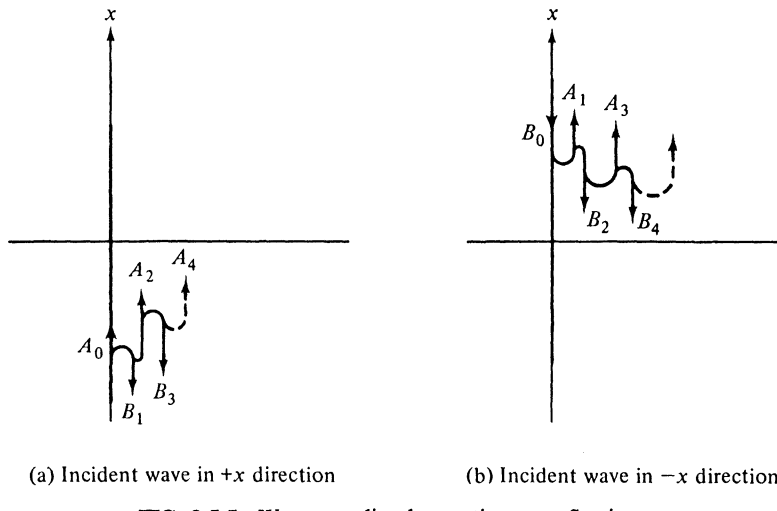


FIG. 3.5.5 Wave coupling by continuous reflection.

The lowest-order (WKB) approximation is adequate if $|A_1| \ll B_0$ or $|B_1| \ll A_0$. From Eq. (81),

$$|A_1| = \frac{|B_0|}{4} \left| \int_{x_1}^x \frac{\alpha'(\xi)}{\alpha(\xi)} e^{-i2\Omega\psi(\xi)} d\xi \right| = \frac{|B_0|}{8\Omega} \left| \int_{x_1}^x \frac{\alpha'(\xi)}{\alpha(\xi)\psi'(\xi)} \left[\frac{d}{d\xi} e^{-i2\Omega\psi(\xi)} \right] d\xi \right|, \quad (82)$$

where it has been assumed that $\psi'(x) = \sqrt{\alpha(x)}$ [see Eq. (75a)] does not vanish in the interval. Integration by parts yields

$$|A_1| = \frac{|B_0|}{8\Omega} \left| \frac{\alpha'(\xi)}{[\alpha(\xi)]^{3/2}} \right|_{x_1}^x + O\left(\frac{1}{\Omega^2}\right), \quad (83)$$

with the validity of the order estimate verified upon repeated integration by parts. Thus, A_1 is $O(1/\Omega)$ as $\Omega \rightarrow \infty$, thereby confirming the asymptotic validity of the WKB approximation (see Sec. 4.2b for a discussion of asymptotic expansions). That the maximum value of the first term in Eq. (83) provides a suitable bound for $|A_1|$ when Ω is large can be observed from the fact that the exponential in Eq. (82) is a very rapidly oscillating function while the remaining terms are slowly varying over a period of this oscillation; hence, if $\alpha(\xi)$ varies monotonically, the integral between the limits x_1 and x can be bounded by an integral over a half period, with the function $(\alpha'/\alpha\psi')_{\max}$ removed from within the integration sign. The resulting estimate

$$\left| \frac{\alpha'(x)}{\Omega[\alpha(x)]^{3/2}} \right|_{\max} \ll 1 \quad (84)$$

can thus be taken as a criterion for the validity of the WKB approximation $A(x) \approx A_0$ or $B(x) \approx B_0$ in a medium with monotonically varying properties.

The above formulation allows the voltage reflection coefficient $\bar{\Gamma}$ to be expressed as follows:

$$\bar{\Gamma} = -\frac{B(x)}{A(x)} e^{-i2\Omega\psi(x)} = -\frac{B_1(x) + B_3(x) + B_5(x) + \dots}{A_0 + A_2(x) + A_4(x) + \dots} e^{-i2\Omega\psi(x)}, \quad (85)$$

where it has been assumed that the incident wave travels along the $+x$ direction so that $B_0 \equiv 0$. From this condition it follows that $A(x)$ contains only even-order terms while $B(x)$ contains only odd-order terms. For large Ω , the reflection coefficient magnitude arising from internal reflections is given to a lowest order by $|B_1(x)/A_0|$, which in turn behaves like $|\alpha'/\Omega\alpha^{3/2}|$.

3.6 APPLICATION TO VARIOUS INHOMOGENEITY PROFILES

3.6a Reflection from a Continuous Transition

For illustration of the results in Sec. 3.5e, consider the profile in Fig. 3.6.1, where $\alpha(x) = \alpha_1$ when $x < x_\alpha$, $\alpha(x) = \alpha_2$ when $x > x_\beta$, and α_1 and α_2 are positive constants. $\alpha(x)$ is assumed to be analytic and monotonic in the region

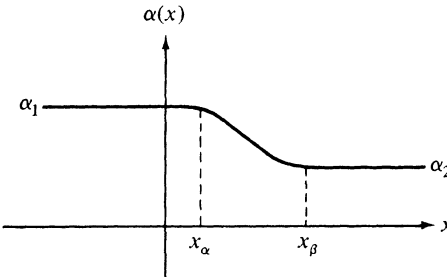


FIG. 3.6.1 Smooth transition.

$x_\alpha < x < x_\beta$. When a wave is incident from the left, the reflection coefficient $\bar{\Gamma}$ observed in the region $x < x_\alpha$ is given in the first approximation by [see Eqs. (3.5.85) and (3.5.81)]

$$\bar{\Gamma}(x) = -\frac{B_1(x)}{A_0} = \left[\frac{1}{4} \int_{x_2}^{x_\alpha} \frac{\alpha'(\xi)}{\alpha(\xi)} e^{i2\Omega\psi(\xi)} d\xi \right] e^{-i2\Omega\psi(x)}, \quad (1)$$

with the upper limit replaced by x_α since $\alpha' = 0$ when $x < x_\alpha$. If the phase reference is chosen so that $\psi(x_1) = 0$, then

$$\bar{\Gamma}(x_1) = \frac{1}{4} \int_{x_\beta}^{x_\alpha} \frac{\alpha'(\xi)}{\alpha(\xi)} e^{i2\Omega\psi(\xi)} d\xi. \quad (2)$$

The choice of the lower limit results from the requirement $B_1 = 0$ at $x = x_2$ in Eq. (3.5.81), whence the reference point x_2 is located in the region where the internal reflections tend to zero (i.e., $x_2 \geq x_\beta$); since $\alpha' = 0$ when $x > x_\beta$, the lower limit may be replaced by x_β . Physically, Eq. (2) implies that the first-order internal reflections are taken into account from the entire region of inhomogeneity lying to the right of the observation point.

The order of magnitude of the reflection coefficient depends on the smoothness of the junction of the inhomogeneous and homogeneous regions at $x = x_{\alpha,\beta}$, as can be verified by repeated integration by parts as in Eq. (3.5.82). If $\alpha(x)$ is continuous at $x_{\alpha,\beta}$ but $\alpha'(x)$ is not, then $\bar{\Gamma}$ is $O(1/\Omega)$; if $\alpha(x)$ and $\alpha'(x)$ are continuous at $x_{\alpha,\beta}$ but $\alpha''(x)$ is not, then $\bar{\Gamma}$ is $O(1/\Omega^2)$. In general, continuity of $\alpha(x)$ and its first N derivatives at $x_{\alpha,\beta}$ implies that $\bar{\Gamma}$ is $O(1/\Omega^{N+1})$. If $\alpha(x)$ is constant for $x < x_\alpha$ or $x > x_\beta$ (i.e., all its derivatives vanish identically in these regions), it is non-analytic when regarded in the entire interval $-\infty < x < \infty$, and thus the reflection coefficient is proportional to some finite inverse power of Ω determined by the order of the first discontinuous derivative. If $\alpha(x)$ is analytic in the entire interval (this requires that $x_\alpha \rightarrow -\infty$, $x_\beta \rightarrow \infty$), the reflection coefficient vanishes faster than any finite inverse power of Ω , as $\Omega \rightarrow \infty$, and is, in fact, exponentially small.

As an example of a smooth transition characterized by an analytic function of x , consider²⁹

$$\alpha(x) = \alpha_0 - a \tanh \frac{x}{b}, \quad (3)$$

where α_0 , a , and b are positive numbers, with $a \ll \alpha_0$. Since $|\tanh x| \leq 1$ in the interval $-\infty < x < \infty$, we have, to $O(a)$,

$$\sqrt{\alpha(x)} \cong \left(1 - \frac{a}{2\alpha_0} \tanh \frac{x}{b}\right) \sqrt{\alpha_0}, \quad (4a)$$

$$\frac{\alpha'}{\alpha} \cong -\frac{a}{b\alpha_0} \operatorname{sech}^2 \frac{x}{b}. \quad (4b)$$

Thus, from Eq. (1), with x_2 and x_α replaced by $+\infty$ and x , respectively,

$$\bar{\Gamma}(x) \cong \frac{-a}{4b\alpha_0} \int_{-\infty}^x \operatorname{sech}^2 \frac{\xi}{b} \exp \left[i2\Omega \int_x^\xi \sqrt{\alpha(\eta)} d\eta \right] d\xi, \quad (5)$$

which expression is to be evaluated for $x \rightarrow -\infty$. With Eq. (4a), the integral over η is elementary and yields

$$\frac{1}{\sqrt{\alpha_0}} \int_x^\xi \sqrt{\alpha(\eta)} d\eta = (\xi - x) - \frac{ab}{2\alpha_0} \left(\ln \cosh \frac{\xi}{b} - \ln \cosh \frac{x}{b} \right). \quad (6)$$

Since $|x|$ is very large, we may approximate $\cosh(x/b)$ by $\frac{1}{2} \exp(|x|/b)$, whence $\ln \cosh(x/b) \approx |x|/b - \ln 2$. Upon imposing the restriction

$$\Omega ab \ll 1, \quad (7)$$

and recognizing that the major contribution to the integral in Eq. (5) arises from the vicinity of $\xi = 0$, one may write

$$\bar{\Gamma}(x) \cong \frac{a}{4b\alpha_0} \exp \left[-i2\bar{\Omega} \left(1 + \frac{a}{2\alpha_0} \right) x \right] I \quad \text{as } x \rightarrow -\infty, \quad (8a)$$

where

$$I = \int_{-\infty}^{\infty} \operatorname{sech}^2 \frac{\xi}{b} e^{i2\bar{\Omega}\xi} d\xi, \quad \bar{\Omega} = \Omega \sqrt{\alpha_0}. \quad (8b)$$

To evaluate I , introduce the change of variable

$$t = e^{2\xi/b} \quad (9)$$

to transform Eq. (8b) into

$$I = 2b \int_0^\infty \frac{t^{ib\bar{\Omega}}}{(1+t)^2} dt = 2b \frac{\Gamma(1+ib\bar{\Omega})\Gamma(1-ib\bar{\Omega})}{\Gamma(2)}. \quad (10)$$

The expression in terms of the gamma functions results from the formula³⁰

$$\int_0^\infty \frac{t^z dt}{(1+t)^{w+1}} = \frac{\Gamma(1+z)\Gamma(w-z)}{\Gamma(w+1)}, \quad \operatorname{Re} w > \operatorname{Re} z > -1. \quad (11)$$

Since $\Gamma(2) = 1$, $\Gamma(z)\Gamma(1-z) = \pi/\sin \pi z$, and $\Gamma(z+1) = z\Gamma(z)$, one obtains

$$\Gamma(1+ib\bar{\Omega})\Gamma(1-ib\bar{\Omega}) = \frac{\pi}{i \sinh(\pi b\bar{\Omega})} \frac{\Gamma(1+ib\bar{\Omega})}{\Gamma(ib\bar{\Omega})} = \frac{\pi b\bar{\Omega}}{\sinh(\pi b\bar{\Omega})}, \quad (12)$$

and the reflection coefficient is given by

$$\bar{\Gamma}(x) \cong \frac{a}{2\alpha_0} \frac{\pi b\bar{\Omega}}{\sinh(\pi b\bar{\Omega})} \exp\left[-i2\bar{\Omega}\left(1 + \frac{a}{2\alpha_0}\right)x\right], \quad x \rightarrow -\infty. \quad (13)$$

This result, valid under the restriction in Eq. (7), demonstrates the previous assertion that the reflection coefficient vanishes exponentially when $\alpha(x)$ is analytic and Ω is large.

The x dependence of the reflection coefficient is the same as for a medium with constant $\alpha(x) = [\sqrt{\alpha_0} + (a/2\sqrt{\alpha_0})]^2 \approx (\alpha_0 + a)$ for $a \ll \alpha_0$. To within the approximations made,[†] this is the expected phase dependence since $\alpha(-\infty) = \alpha_0 + a$. If b is very small, the transition region, wherein $\alpha(x)$ changes from $(\alpha_0 + a)$ to $(\alpha_0 - a)$, is localized near $x = 0$, and the limiting case $b = 0$ corresponds to an abrupt transition. In this case, Eq. (13) yields

$$|\bar{\Gamma}(x)| \cong \frac{a}{2\alpha_0}, \quad b = 0, \quad (14)$$

which, upon evaluating to $O(a)$ the rigorous expression $[\sqrt{\alpha(-\infty)} - \sqrt{\alpha(\infty)}] \times [\sqrt{\alpha(-\infty)} + \sqrt{\alpha(\infty)}]^{-1}$, is easily seen to be the correct result.

The exact value of $|\bar{\Gamma}|$ for arbitrary a and b is given by the formula [see Eq. (33), with $v = 2a$, $\tau = 2/b$, $\alpha_0 = 1 + a$]

$$|\bar{\Gamma}| = \frac{\sinh[\pi b\bar{\Omega}(\sqrt{1+\bar{a}} - \sqrt{1-\bar{a}})/2]}{\sinh[\pi b\bar{\Omega}(\sqrt{1+\bar{a}} + \sqrt{1-\bar{a}})/2]}, \quad \bar{a} = \frac{a}{\alpha_0}, \quad \bar{\Omega} = \Omega\sqrt{\alpha_0}, \quad (15)$$

which reduces to Eq. (13) when $\bar{a} \ll 1$, $\Omega ab \ll 1$.

If the transition between two media with slightly different, constant values of α is confined to a small region wherein the phase factor in Eq. (2) is essentially constant, then

$$|\bar{\Gamma}(x_1)| \cong \left| \frac{1}{4} e^{i2\Omega\psi(x_\alpha)} \int_{x_\beta}^{x_\alpha} \left[\frac{d}{d\xi} \ln \alpha(\xi) \right] d\xi \right| = \left| \frac{1}{4} \ln \frac{\alpha_2}{\alpha_1} \right| \cong \frac{|\alpha_2 - \alpha_1|}{4\alpha_1}, \quad (16)$$

[†]The phase dependence is given more correctly by $e^{-i2\Omega\sqrt{\alpha_0+a}x}$.

where $|\alpha_2 - \alpha_1| \ll \alpha_1$. When applied to the special case in Eq. (3), one obtains the limiting value in Eq. (14).

3.6b The Epstein Solution for a Continuous Transition

For the specific $\alpha(x)$ in Eq. (3), $\hat{V}(x)$ in Eq. (3.5.74) can be expressed in closed form in terms of hypergeometric functions. This solution, given below, can also be employed as a comparison function in the determination of the scattering properties of other smooth transition profiles. It can be shown that Eq. (3.5.74), with

$$\alpha(x) \equiv \frac{\epsilon(x)}{\epsilon_0} = (1 + a) - a \tanh \frac{x}{b} = 1 + \frac{\nu}{1 + e^{\tau x}}, \quad \nu = 2a, \quad \tau = \frac{2}{b}, \quad (17)$$

where ν and τ are constant parameters, can be solved by^{31,32†}

$$\hat{V}_i(x) = \zeta^{(\gamma-1)/2} (1 - \zeta)^{(\alpha+\beta+1-\gamma)/2} u_i(\alpha, \beta; \gamma; \zeta), \quad \zeta = -e^{\tau x}. \quad (18)$$

While ν and τ may in general be complex, they will be assumed positive real in this section. The functions u_i are solutions of the hypergeometric equation:

$$\left\{ \zeta(1 - \zeta) \frac{d^2}{d\zeta^2} + [\gamma - (\alpha + \beta + 1)\zeta] \frac{d}{d\zeta} - \alpha\beta \right\} u_i(\alpha, \beta; \gamma; \zeta) = 0, \quad (19)$$

and

$$\begin{aligned} \alpha &= 1 + i \frac{\Omega}{\tau} (\sqrt{1 + \nu} - 1), & \beta &= 1 + i \frac{\Omega}{\tau} (\sqrt{1 + \nu} + 1), \\ \gamma &= 1 + \frac{2i\Omega}{\tau} \sqrt{1 + \nu}. \end{aligned} \quad (20)$$

From these definitions,

$$\begin{aligned} \alpha + 1 - \beta &= 1 - i \frac{2\Omega}{\tau}, & \alpha + 1 - \gamma &= 1 - i \frac{\Omega}{\tau} \left[\sqrt{1 + \nu} + 1 \right], \\ \gamma - \beta &= \frac{i\Omega}{\tau} \left[\sqrt{1 + \nu} - 1 \right], \end{aligned} \quad (20a)$$

The differential equation (19) has singular points at $\zeta = 0, 1, \infty$, near each of which its two independent solutions can be expressed in terms of convergent hypergeometric series. Near $\zeta = 0$, the appropriate solutions are

$$u_1 = F(\alpha, \beta; \gamma; \zeta), \quad (21a)$$

$$u_5 = \zeta^{1-\gamma} F(\alpha - \gamma + 1, \beta - \gamma + 1; 2 - \gamma; \zeta), \quad (21b)$$

where the hypergeometric series

$$F(\alpha, \beta; \gamma; \zeta) = 1 + \frac{\alpha\beta}{1!\gamma} \zeta + \frac{\alpha(\alpha+1)\beta(\beta+1)}{2!\gamma(\gamma+1)} \zeta^2 + \dots \quad (21c)$$

[†]The notation is the same as in H. Bateman et al., *Higher Transcendental Functions*, Vol. 1, McGraw-Hill Book Company, 1953. Note that the index α in u_i , etc., should not be confused with $\alpha(x) \equiv \epsilon(x)/\epsilon_0$.

converges inside the circle $|\zeta| < 1$. Near $\zeta = 1$, the pertinent functions are

$$u_2 = F(\alpha, \beta; \alpha + \beta - \gamma + 1; 1 - \zeta), \quad (22a)$$

$$u_6 = (1 - \zeta)^{\gamma-\alpha-\beta} F(\gamma - \alpha, \gamma - \beta; \gamma - \alpha - \beta + 1; 1 - \zeta), \quad (22b)$$

and, near $\zeta = \infty$,

$$u_3 = \frac{1}{(-\zeta)^2} F\left(\alpha, \alpha - \gamma + 1; \alpha - \beta + 1; \frac{1}{\zeta}\right), \quad -\zeta = \zeta e^{i\pi}, \quad (23a)$$

$$u_4 = \frac{1}{(-\zeta)^\beta} F\left(\beta, \beta - \gamma + 1; \beta - \alpha + 1; \frac{1}{\zeta}\right). \quad (23b)$$

While the various hypergeometric *series* converge only in the ranges $|\zeta| < 1$, $|1 - \zeta| < 1$, and $|\zeta| > 1$, respectively, the corresponding hypergeometric *functions* denoted by the same symbols can be continued analytically beyond the ranges of convergence of the series representations. Since the resulting two solutions in each set are linearly independent, they can be superposed (with appropriate constants) to represent any of the remaining functions. The ensuing formulas are called the “connection” or “circuit” relations for these functions, and the ones pertinent for the discussion herein are as follows:

$$u_1 = \frac{\Gamma(\gamma)\Gamma(\beta - \alpha)}{\Gamma(\gamma - \alpha)\Gamma(\beta)} u_3 + \frac{\Gamma(\gamma)\Gamma(\alpha - \beta)}{\Gamma(\gamma - \beta)\Gamma(\alpha)} u_4, \quad (24a)$$

$$u_5 = \frac{\Gamma(2 - \gamma)\Gamma(\beta - \alpha)e^{i\pi(1-\gamma)}}{\Gamma(1 - \alpha)\Gamma(\beta + 1 - \gamma)} u_3 + \frac{\Gamma(2 - \gamma)\Gamma(\alpha - \beta)e^{i\pi(1-\gamma)}}{\Gamma(1 - \beta)\Gamma(\alpha + 1 - \gamma)} u_4, \quad (24b)$$

$$u_3 = \frac{\Gamma(1 - \gamma)\Gamma(\alpha + 1 - \beta)}{\Gamma(1 - \beta)\Gamma(\alpha + 1 - \gamma)} u_1 - \frac{\Gamma(\gamma)\Gamma(1 - \gamma)\Gamma(\alpha + 1 - \beta)}{\Gamma(2 - \gamma)\Gamma(\gamma - \beta)\Gamma(\alpha)} e^{i\pi(\gamma-1)} u_5, \quad (25a)$$

$$u_4 = \frac{\Gamma(1 - \gamma)\Gamma(\beta + 1 - \alpha)}{\Gamma(1 - \alpha)\Gamma(\beta + 1 - \gamma)} u_1 - \frac{\Gamma(\gamma)\Gamma(1 - \gamma)\Gamma(\beta + 1 - \alpha)}{\Gamma(2 - \alpha)\Gamma(\gamma - \alpha)\Gamma(\beta)} e^{i\pi(\gamma-1)} u_5. \quad (25b)$$

The asymptotic behavior of the solutions $u_{3,4}$ at $x = \infty$ (i.e., $\zeta = -e^{ix} = -\infty$) is obtained directly from Eqs. (23) and the hypergeometric-series representation in Eq. (21c):

$$u_3 \sim (-\zeta)^{-\alpha}, \quad u_4 \sim (-\zeta)^{-\beta}, \quad x \rightarrow \infty, \quad (26a)$$

whence, from Eqs. (18) and (20),

$$\hat{V}_3(x) \sim e^{i\pi(\gamma-1)/2} e^{\tau x(\beta-\alpha)/2} = e^{i\pi(\gamma-1)/2} e^{i\Omega x}, \quad x \rightarrow \infty, \quad (26b)$$

$$\hat{V}_4(x) \sim e^{i\pi(\gamma-1)/2} e^{\tau x(\alpha-\beta)/2} = e^{i\pi(\gamma-1)/2} e^{-i\Omega x}, \quad x \rightarrow \infty. \quad (26c)$$

Thus, \hat{V}_3 and \hat{V}_4 represent, respectively, outgoing and incoming waves as $x \rightarrow \infty$. At $x \rightarrow -\infty$, the behavior of $u_{1,5}$ follows from Eqs. (21) as

$$u_1 \rightarrow 1, \quad u_5 \rightarrow \zeta^{1-\gamma}, \quad x \rightarrow -\infty, \quad (27a)$$

so

$$\hat{V}_1(x) \sim e^{i\pi(\gamma-1)/2} (e^{\tau x})^{(\gamma-1)/2} = e^{i\pi(\gamma-1)/2} e^{i\Omega\sqrt{1+\nu}x}, \quad x \rightarrow -\infty, \quad (27b)$$

$$\hat{V}_s(x) \sim e^{-i\pi(\gamma-1)/2} e^{-i\Omega\sqrt{1+\nu}x} \quad x \rightarrow -\infty. \quad (27c)$$

At $x = -\infty$, \hat{V}_1 and \hat{V}_s represent incoming and outgoing waves, respectively. It is noted from the above that the asymptotic wave character of the \hat{V}_i is contained entirely in the simple factors multiplying the hypergeometric functions, whence the latter serve as correction terms accounting for the medium inhomogeneity in the range of finite x . One observes also that the wave functions at $x = +\infty$ are those for a medium with $\epsilon(x)/\epsilon_0 = 1$, while those at $x = -\infty$ are appropriate to a medium with $\epsilon(x)/\epsilon_0 = 1 + \nu$, in accord with expectations from Eq. (17).

Let us suppose that a plane wave of unit amplitude is incident from $x = -\infty$ in the medium of Eq. (17), and that we seek the amplitude and phase of the reflected and transmitted waves. Since the transmitted wave must be outgoing at $x = +\infty$, it is necessary to choose the solution $\tilde{V}_3(x)$ whose properties as $x \rightarrow \infty$ [see Eq. (26b)] can be calculated directly from its hypergeometric-series representation. This hypergeometric series cannot be employed, however, to calculate the behavior of $\tilde{V}_3(x)$ at $x = -\infty$, and it is necessary to utilize the connection relation (25a) expressing u_3 in terms of u_1 and u_s , which latter functions can be evaluated near $x = -\infty$ from Eqs. (21). If $\tilde{V}_1(x)$ in Eq. (27b) is to represent an incident wave of unit amplitude, the expression in Eq. (18) must be multiplied by the factor $\exp[i\pi(1-\gamma)/2]$. Let

$$\tilde{V}_i(x) = \hat{V}_i(x) e^{i\pi(1-\gamma)/2}, \quad (28)$$

then, from Eq. (25a),

$$\begin{aligned} \tilde{V}_3(x) & \frac{\Gamma(1-\beta)\Gamma(\alpha+1-\gamma)}{\Gamma(1-\gamma)\Gamma(\alpha+1-\beta)} \\ &= \tilde{V}_1(x) - \tilde{V}_s(x) \frac{\Gamma(\gamma)\Gamma(1-\beta)\Gamma(\alpha+1-\gamma)}{\Gamma(2-\gamma)\Gamma(\gamma-\beta)\Gamma(\alpha)} e^{i\pi(\gamma-1)}. \end{aligned} \quad (29)$$

The right-hand side of this equation can be used to evaluate the wave function near $x = -\infty$, while the left-hand side is appropriate for $x = +\infty$. Since $\tilde{V}_1(-\infty) \sim \exp[i\Omega\sqrt{1+\nu}x]$, the second term on the right-hand side represents directly the reflected-wave contribution. If we write

$$\tilde{V}(-\infty) = e^{i\Omega\sqrt{1+\nu}x} + \bar{\Gamma}(-\infty) e^{-i\Omega\sqrt{1+\nu}x}, \quad (30a)$$

then the voltage reflection coefficient $\bar{\Gamma}(-\infty)$ is given by

$$\begin{aligned} \bar{\Gamma}(-\infty) &= -\frac{\Gamma(\gamma)\Gamma(1-\beta)\Gamma(\alpha+1-\gamma)}{\Gamma(2-\gamma)\Gamma(\gamma-\beta)\Gamma(\alpha)} = \frac{\Gamma(\gamma-1)}{\Gamma(1-\gamma)} \frac{\Gamma(1-\beta)\Gamma(\alpha+1-\gamma)}{\Gamma(\gamma-\beta)\Gamma(\alpha)} \end{aligned} \quad (30b)$$

$$\begin{aligned} &= \frac{\Gamma\left[\frac{i2\Omega}{\tau}\sqrt{1+\nu}\right]}{\Gamma\left[-\frac{i2\Omega}{\tau}\sqrt{1+\nu}\right]} \frac{\Gamma\left[-\frac{i\Omega}{\tau}(\sqrt{1+\nu}+1)\right]}{\Gamma\left[i\frac{\Omega}{\tau}(\sqrt{1+\nu}-1)\right]} \frac{\Gamma\left[1-i\frac{\Omega}{\tau}(\sqrt{1+\nu}+1)\right]}{\Gamma\left[1+i\frac{\Omega}{\tau}(\sqrt{1+\nu}-1)\right]}. \end{aligned} \quad (30c)$$

Similarly, if

$$\bar{V}(\infty) = T(\infty)e^{i\Omega x}, \quad (31a)$$

then the transmission coefficient T is obtained from the left-hand side of Eq. (29) as

$$\begin{aligned} T(\infty) &= \frac{\Gamma(1 - \beta)\Gamma(\alpha + 1 - \gamma)}{\Gamma(1 - \gamma)\Gamma(\alpha + 1 - \beta)} \\ &= \frac{\Gamma\left[-\frac{i\Omega}{\tau}(\sqrt{1 + \nu} + 1)\right]\Gamma\left[1 - i\frac{\Omega}{\tau}(\sqrt{1 + \nu} + 1)\right]}{\Gamma\left[-\frac{i2\Omega}{\tau}\sqrt{1 + \nu}\right]\Gamma\left[1 - i\frac{2\Omega}{\tau}\right]}. \end{aligned} \quad (31b)$$

The magnitude of the reflection coefficient can be expressed in a simple manner. Since $\Gamma(z)$ is real for real z , it follows from the Schwarz reflection principle³³ that $\Gamma(z^*) = \Gamma^*(z)$. Thus, the ratio of the first two gamma functions in Eq. (30c) has unit magnitude since Ω , ν , and τ are real. Also, from

$$\Gamma(z)\Gamma(1 - z) = \frac{\pi}{\sin \pi z}, \quad (32a)$$

it follows that for imaginary $z = ih$, h real,

$$|\Gamma(ih)\Gamma(1 + ih)| = |\Gamma(ih)\Gamma(1 - ih)| = \frac{\pi}{|\sinh \pi h|}. \quad (32b)$$

Thus, from Eq. (30c), the reflection coefficient is

$$|\bar{\Gamma}(-\infty)| = \frac{\sinh\left[\pi\frac{\Omega}{\tau}(\sqrt{1 + \nu} - 1)\right]}{\sinh\left[\pi\frac{\Omega}{\tau}(\sqrt{1 + \nu} + 1)\right]}. \quad (33)$$

The limiting cases of an abrupt transition ($\tau = \infty$) and of a very gradual transition (τ small) have been discussed in the preceding section.

The preceding considerations are appropriate for a plane wave propagating along the x direction, with no variation along y or z , and must be modified for oblique incidence. The simplest case arises when the wave in question is an H mode (i.e., $E_x \equiv 0$), in which case $p(x)$ in Eq. (3.5.2a) is equal to the (constant) permeability. For a plane-stratified medium, $w = p$, and the obliquity manifests itself through the appearance of the constant parameter λ in Eq. (3.5.2a). If Eq. (3.5.2) is written as

$$\left[\frac{d^2}{dx^2} + \Omega^2 \frac{\epsilon(x)}{\epsilon_0} - \xi^2 \right] \bar{V}_\xi(x) = 0, \quad (34)$$

with $\xi^2 = -\lambda$, then, from Eq. (17),

$$\Omega^2 \frac{\epsilon(x)}{\epsilon_0} - \xi^2 = (\Omega^2 - \xi^2) \left[1 + \frac{\nu\Omega^2/(\Omega^2 - \xi^2)}{1 + e^{\tau x}} \right]. \quad (35)$$

This equation is equivalent to Eq. (3.5.74), with Eq. (17), provided that one makes the following replacements:

$$\Omega \rightarrow \sqrt{\Omega^2 - \xi^2}, \quad v \rightarrow v \frac{\Omega^2}{\Omega^2 - \xi^2}, \quad (36)$$

from which the solutions $\tilde{V}_\xi(x)$ for $\xi \neq 0$ are obtainable at once from those for $\tilde{V}(x)$ above. In particular, the parameters α , β , and γ in Eqs. (20) are, for $\xi \neq 0$,

$$\alpha = 1 + \frac{i}{\tau} [\sqrt{\Omega^2(1+v) - \xi^2} - \sqrt{\Omega^2 - \xi^2}], \quad (37a)$$

$$\beta = 1 + \frac{i}{\tau} [\sqrt{\Omega^2(1+v) - \xi^2} + \sqrt{\Omega^2 - \xi^2}], \quad (37b)$$

$$\gamma = 1 + \frac{2i}{\tau} \sqrt{\Omega^2(1+v) - \xi^2}. \quad (37c)$$

To satisfy the radiation condition, all square roots are defined to have positive imaginary parts [see Eqs. (26) and (27)], and reduce to positive numbers when $\xi = 0$. These results, valid for arbitrary ξ , are required for the representation of the field of a concentrated source in Sec. 5.9d. For a plane wave whose propagation vector makes an angle θ with the positive x axis at $x \rightarrow \infty$, $\xi = \Omega \sin \theta$ and $-\pi/2 < \theta < \pi/2$.

The reflection coefficient magnitude in Eq. (33) is given for real $\xi \leq \Omega$ by

$$|\bar{\Gamma}(-\infty)| = \frac{\sinh \left\{ \frac{\pi}{\tau} [\sqrt{\Omega^2(1+v) - \xi^2} - \sqrt{\Omega^2 - \xi^2}] \right\}}{\sinh \left\{ \frac{\pi}{\tau} [\sqrt{\Omega^2(1+v) - \xi^2} + \sqrt{\Omega^2 - \xi^2}] \right\}}. \quad (38)$$

For a plane wave incident at an angle φ at $x = -\infty$, one has $\xi = \Omega \sqrt{1+v} \times \sin \varphi$, and Eq. (38) becomes

$$|\bar{\Gamma}(-\infty)| = \frac{\sinh \left\{ \frac{\pi \Omega}{\tau} [\sqrt{1+v} \cos \varphi - \sqrt{1-(1+v) \sin^2 \varphi}] \right\}}{\sinh \left\{ \frac{\pi \Omega}{\tau} [\sqrt{1+v} \cos \varphi + \sqrt{1-(1+v) \sin^2 \varphi}] \right\}}, \quad (39)$$

with the angle φ restricted so that $\varphi < \varphi_c$, where φ_c is the critical angle $\varphi_c = \sin^{-1} [(1+v)^{-1/2}]$. The reflection coefficient magnitude increases from its minimum value at $\varphi = 0$ to unity at $\varphi = \varphi_c$. Since the angle of refraction θ at $x = \infty$ is related to the angle of incidence at $x = -\infty$ via

$$\xi = \Omega \sqrt{1+v} \sin \varphi = \Omega \sin \theta, \quad \text{i.e., } \sin \theta = \sqrt{1+v} \sin \varphi, \quad (40)$$

one has $\theta = \pi/2$ when $\varphi = \varphi_c$. When $\varphi > \varphi_c$, the wave is totally reflected and it is to be expected that $|\bar{\Gamma}(-\infty)| = 1$. This can be verified from Eq. (30c) when modified in accord with Eq. (35) since for $(\pi/2) \geq \varphi > \varphi_c$, the gamma functions in the numerator are the complex conjugates of those in the denominator.

If the wave is incident from $x = +\infty$, it has to be outgoing at $x = -\infty$, and one must choose the solution \hat{V}_s [see Eq. (27c)] which is continued to $x =$

$\pm\infty$ via the connection relation in Eq. (24b). The incident wave is of unit amplitude if \tilde{V}_4 is the corresponding wave function; the resulting reflection and transmission coefficients are then given by

$$\begin{aligned}\bar{\Gamma}(\infty) &= \frac{\Gamma(1-\beta)\Gamma(\alpha+1-\gamma)\Gamma(\beta-\alpha)}{\Gamma(1-\alpha)\Gamma(\beta+1-\gamma)\Gamma(\alpha-\beta)}, \\ T(-\infty) &= \frac{\Gamma(1-\beta)\Gamma(\alpha+1-\gamma)}{\Gamma(2-\gamma)\Gamma(\alpha-\beta)},\end{aligned}\quad (41)$$

with α , β , and γ taken from Eqs. (37). In this case, with $\xi = \Omega \sin \theta$, $-\pi/2 \leq \theta \leq \pi/2$,

$$|\bar{\Gamma}(\infty)| = \frac{\sinh \left\{ \frac{\pi\Omega}{\tau} [\sqrt{\cos^2 \theta + \nu} - \cos \theta] \right\}}{\sinh \left\{ \frac{\pi\Omega}{\tau} [\sqrt{\cos^2 \theta + \nu} + \cos \theta] \right\}}. \quad (42)$$

The function $\alpha(x) = \epsilon(x)/\epsilon_0$ in Eq. (17) may be used as a comparison function for some other smooth transition profile for which no known solution of the differential equation (3.5.34) exists. If the problem of determining the unknown wave function is phrased as in Eq. (3.5.15), it is necessary to evaluate the Green's function in Eq. (3.5.16). To satisfy the boundary conditions (radiation condition) at $x = \pm\infty$, we choose $g_2(x) = \hat{V}_3(x)$ and $g_1(x) = \hat{V}_5(x)$. The Wronskian of these two solutions is a constant independent of x and can be evaluated at any convenient point, for example at $x = -\infty$. $\hat{V}_5(-\infty)$ is given in Eq. (27c). To calculate $\hat{V}_3(-\infty)$, it is necessary to employ the continuation formula (25a), which yields

$$\hat{V}_3(-\infty) = e^{i\pi(y-1)/2} [Ae^{i\Omega\sqrt{1+\nu}x} - Be^{-i\Omega\sqrt{1+\nu}x}], \quad (43)$$

where A and B denote the gamma-function factors multiplying u_1 and $-u_5 \exp[i\pi(y-1)]$, respectively, in Eq. (25a). Thus,

$$W(g_2, g_1) = \hat{V}_3 \frac{d\hat{V}_5}{dx} - \hat{V}_5 \frac{d\hat{V}_3}{dx} = -2i\Omega\sqrt{1+\nu} \frac{\Gamma(1-\gamma)\Gamma(\alpha+1-\beta)}{\Gamma(1-\beta)\Gamma(\alpha+1-\gamma)}, \quad (44)$$

which expression has been derived for $\xi = 0$ but is easily transformed to apply as well when $\xi \neq 0$ [see Eqs. (35) and (36)].

Hypergeometric functions can also be employed to solve the more general profile associated with an asymmetrical layer wherein $\alpha(x)$ in Fig. 3.6.1 has a minimum at x_β and approaches the value $\alpha_2 = \alpha(\infty) > \alpha(x_\beta)$, $\alpha_1 \neq \alpha_2$. The symmetrical layer or duct is included herein as the special case $\alpha_1 = \alpha_2$.

3.6c Dielectric Constant Profile with Simple Zero

To illustrate the use of the WKB and Airy function formulations for a profile having a simple zero, consider the example

$$\alpha(x, \Omega) = 1 - \frac{\mu^2 - \frac{1}{4}}{\Omega^2 x^2}, \quad (45)$$

where μ is a constant but may be complex.[†] If Ω denotes the wavenumber $k_0 = \omega/c$ in vacuum and μ^2 is positive and greater than $\frac{1}{4}$, the function $\alpha(x, \Omega)$ is of the form $[1 - (\omega_p^2/\omega^2)]$, which represents the permittivity of an ionized plasma model having an electron density distribution $N(x) \propto \omega_p^2(x)$ [see Eq. (1.5.20) with $\omega_c = 0$]. In most of the subsequent considerations, μ will be assumed positive and large enough so that $\mu^2 - \frac{1}{4} \approx \mu^2$. The simple zero of $\Omega^2\alpha(x)$ then occurs at $x \cong \mu/\Omega$; the singularity at $x = 0$ is of no interest for the present discussion and x is restricted to a range of positive values sufficiently far from the origin. Eq. (3.5.34), with Eq. (47), is solved exactly by the functions

$$\hat{g}(x) = \sqrt{\Omega x} C_\mu(\Omega x), \quad (46)$$

where C_μ is any linear combination of solutions of the Bessel equation.

If μ is small and Ω is very large, one may put $\alpha(x, \Omega) \approx 1$, so the resulting asymptotic approximation in Eq. (3.5.37) yields $\hat{g}(x) \sim \exp(\pm i\Omega x)$. If μ is large, this result still applies to observation points for which $\Omega x \gg \mu$. A more accurate description is obtained, however, upon retaining the complete expression in Eq. (45). By an elementary integration,

$$\int_{x_0}^x \sqrt{a(\eta)} d\eta \cong \int_{x_0}^x \cos \phi(\eta) d\eta = x \left[\cos \phi(x) + \left(\phi(x) - \frac{\pi}{2} \right) \sin \phi(x) \right], \quad (47)$$

where the approximation arises from $\mu^2 - \frac{1}{4} \approx \mu^2$, and

$$\sin \phi(x) = \frac{\mu}{\Omega x}, \quad \phi(x_0) \equiv \frac{\pi}{2}, \quad \mu < \Omega x. \quad (47a)$$

Similarly,

$$\int_x^{x_0} |\sqrt{a(\eta)}| d\eta \cong \int_x^{x_0} \sinh \bar{\phi}(\eta) d\eta = x [\bar{\phi}(x) \cosh \bar{\phi}(x) - \sinh \bar{\phi}(x)]. \quad (48)$$

with

$$\cosh \bar{\phi}(x) = \frac{\mu}{\Omega x}, \quad \bar{\phi}(x_0) = 0, \quad \mu > \Omega x. \quad (48a)$$

Equation (48) can be obtained from Eq. (47) by analytic continuation of $\phi(x)$ to a range of complex values $\phi(x) = \pi/2 - i\bar{\phi}(x)$, $\bar{\phi}(x) > 0$.

To identify the expression for $\hat{g}(x)$ in Eq. (3.5.37) with any one of the solutions of the Bessel equation, appropriate normalization factors must be included. For example, if the solution is known for $\Omega x \rightarrow \infty$, the required constants can be deduced from this limiting result. Since for $\Omega x \gg \mu$, the Hankel functions may be approximated as [see Eq. (5.3.13)]

$$\sqrt{\Omega x} H_\mu^{(1,2)}(\Omega x) \sim A^{(1,2)} e^{\pm i\Omega x}, \quad A^{(1,2)} = \sqrt{\frac{2}{\pi}} e^{\mp i(\mu\pi/2 + \pi/4)}, \quad (49)$$

one finds from Eqs. (3.5.37) and (47),

[†]Here μ is not to be confused with the same symbol used elsewhere for permeability.

$$\sqrt{\Omega x} H_{\mu}^{(1,2)}(\Omega x) \sim \sqrt{\frac{2}{\pi}} e^{\mp i\pi/4} \frac{\exp \{ \pm i\Omega x [\cos \phi + (\phi - (\pi/2)) \sin \phi] \}}{\sqrt{\cos \phi}}, \quad \mu < \Omega x. \quad (50a)$$

The constants in the range $\mu > \Omega x$ are now chosen in accord with Eq. (3.5.47a) and yield

$$\sqrt{\Omega x} H_{\mu}^{(1,2)}(\Omega x) \sim \mp i \sqrt{\frac{2}{\pi}} \frac{e^{\Omega x [\bar{\phi} \cosh \bar{\phi} - \sinh \bar{\phi}]}}{\sqrt{\sinh \bar{\phi}}}, \quad \mu > \Omega x. \quad (50b)$$

For the Bessel function, application of the formula $2J_{\mu}(y) = [H_{\mu}^{(1)}(y) + H_{\mu}^{(2)}(y)]$ yields

$$\sqrt{\Omega x} J_{\mu}(\Omega x) \sim \sqrt{\frac{2}{\pi \cos \phi}} \cos \left\{ \Omega x \left[\cos \phi + \left(\phi - \frac{\pi}{2} \right) \sin \phi \right] - \frac{\pi}{4} \right\}, \quad \mu < \Omega x, \quad (51a)$$

while, from Eq. (3.5.47b),

$$\sqrt{\Omega x} J_{\mu}(\Omega x) \sim \frac{1}{\sqrt{2\pi \sinh \bar{\phi}}} e^{-\Omega x [\bar{\phi} \cosh \bar{\phi} - \sinh \bar{\phi}]}, \quad \mu > \Omega x. \quad (51b)$$

Alternatively, the normalization factors could have been deduced from the known behavior of the functions when $\mu \gg \Omega x$. In this instance,

$$J_{\mu}(\Omega x) \sim \left(\frac{\Omega x}{2} \right)^{\mu} \frac{1}{\Gamma(\mu + 1)} \sim \frac{1}{\sqrt{2\pi\mu}} \left(\frac{e\Omega x}{2\mu} \right)^{\mu}, \quad (52a)$$

where we have employed the asymptotic formula [see Eq. (3.4.66c)],

$$\Gamma(\mu + 1) = \mu \Gamma(\mu) \sim \sqrt{2\pi\mu} \left(\frac{\mu}{e} \right)^{\mu}, \quad \mu \gg 1. \quad (52b)$$

Since for $\mu \gg \Omega x$,

$$\frac{\mu}{\Omega x} = \cosh \bar{\phi} \sim \sinh \bar{\phi} \sim \frac{e^{\bar{\phi}}}{2}, \quad \bar{\phi} \sim \ln \frac{2\mu}{\Omega x}, \quad (53)$$

one has

$$\frac{e^{\pm \Omega x (\bar{\phi} \cosh \bar{\phi} - \sinh \bar{\phi})}}{\sqrt{\sinh \bar{\phi}}} \sim \sqrt{\frac{\Omega x}{\mu}} \left(\frac{2\mu}{\Omega x e} \right)^{\pm \mu}. \quad (54)$$

Upon comparing Eqs. (54) and (52a), one finds that the decaying exponential must be chosen and that a factor $(2\pi)^{-1/2}$ must be included, whence the proper representation for the Bessel function is the one given in Eq. (51b). The appropriate form for the range $\mu < \Omega x$ is then obtained via Eq. (3.5.47a) and leads to Eq. (51a).

In the transition region $\mu \approx \Omega x$, it is necessary to employ the more elaborate formula (3.5.45). From a comparison of Eqs. (3.5.45), (3.5.47), and (51), one finds that the proper representation for the Bessel function near the turning point is

$$\sqrt{\Omega x} J_\mu(\Omega x) \sim \sqrt{\frac{2}{P}} [\tfrac{3}{2} \Omega x Q]^{1/6} \text{Ai}[-(\tfrac{3}{2} \Omega x Q)^{2/3}], \quad (55)$$

where

$$P = \cos \phi, \quad Q = \cos \phi + \left(\phi - \frac{\pi}{2} \right) \sin \phi, \quad \mu \leq \Omega x, \quad (55a)$$

$$P = i \sinh \bar{\phi}, \quad Q = e^{i3\pi/2} [\bar{\phi} \cosh \bar{\phi} - \sinh \bar{\phi}], \quad \mu \geq \Omega x. \quad (55b)$$

Expressions for the Hankel functions are deduced in a similar manner. The results obtained agree with those derived in Sec. 4.5a [see Eq. (4.5.33)] from the Sommerfeld integral representation of the cylinder function (see also Sec. 6.A).

A criterion delimiting the range of validity of the WKB approximation has been given in Eq. (3.5.84). For the present problem, with $\mu < \Omega x$, $\alpha \approx \cos^2 \phi$, and

$$\alpha'(x) \approx \frac{2\mu^2}{\Omega^2 x^3} = \frac{2}{x} \sin^2 \phi, \quad (56)$$

whence the required restriction in Eq. (3.5.84) is

$$\frac{2}{\mu} \tan^3 \phi \ll 1. \quad (57)$$

Since μ is assumed to be large, the condition is satisfied except when $\phi \rightarrow \pi/2$. Upon noting that

$$\mu \approx \Omega x, \quad \tan \phi \approx \sec \phi \approx \sqrt{\frac{\Omega x}{2(\Omega x - \mu)}}, \quad \text{as } \phi \rightarrow \frac{\pi}{2}, \quad (58)$$

and omitting irrelevant factors, one may rewrite the inequality as

$$(\Omega x - \mu) \gg (\Omega x)^{1/3}, \quad (59)$$

which agrees with the condition $\Omega^{2/3} \varphi \gg 1$ in Eq. (3.5.47). For $\mu > \Omega x$, the left-hand side of the inequality is replaced by its absolute value. Thus, Eqs. (50) and (51) are valid in this range but must be replaced by Eq. (55) or its equivalent when $|\Omega x - \mu| = O[(\Omega x)^{1/3}]$.

PROBLEMS

1. Use the free-space spectral representation in Eq. (3.2.40),

$$\delta(\mathbf{p} - \mathbf{p}') = \frac{1}{(2\pi)^2} \iint_{-\infty}^{\infty} e^{-j\xi(x-x') - j\eta(y-y')} d\xi d\eta, \quad (1)$$

where $-\infty < (x, x', y, y') < \infty$, to construct via the image principle *E*- and *H*-mode spectral representations for the half-space region $0 < (x, x') < \infty$, $-\infty < (y, y') < \infty$ [see Eqs. (3.2.38) and (3.2.39) and Fig. 3.2.4]. Repeat for the quarter-space region $0 < (x, x', y, y') < \infty$ [see Eqs. (3.2.32) and (3.2.33) and Fig. 3.2.3].

2. Utilizing the traveling wave formulation in Eqs. (3.3.28) and (3.3.29), show that the modal Green's function $Y(x, x')$ may be represented as [note that $Y(x, x')$ is the current in the network of Fig. 3.3.2; see also Eqs. (3.3.3)-(3.3.7)]:

$$Y(x, x') = \frac{\overleftarrow{I}(x_<, x_1) \overrightarrow{I}(x_>, x_2)}{\overleftrightarrow{\zeta}(x') \left[\frac{I^+(x') I^-(x')}{I^+(x_2) I^-(x_1)} - \vec{\Gamma}_I(x_2) \overleftarrow{\Gamma}_I(x_1) \frac{I^-(x') I^+(x')}{I^-(x_2) I^+(x_1)} \right]}, \quad (2)$$

where, with $\overleftrightarrow{\zeta} = \overrightarrow{\zeta} + \overleftarrow{\zeta}$,

$$\overleftarrow{I}(x, x_1) = \frac{I^-(x)}{I^-(x_1)} + \overleftarrow{\Gamma}_I(x_1) \frac{I^+(x)}{I^+(x_1)},$$

$$\overrightarrow{I}(x, x_2) = \frac{I^+(x)}{I^+(x_2)} + \vec{\Gamma}_I(x_2) \frac{I^-(x)}{I^-(x_2)}.$$

x_1 and x_2 are two conveniently chosen points in the x interval which, for example, coincide with the left and right termini of the region, respectively. Show that the formula reduces to Eq. (2.4.29c), with $x \rightarrow z$, when $x_1 = x_2 = x_0$ and when the transmission line is uniform [i.e., $I^\pm = \exp(\mp jkx)$]. Show that an analogous formula for $Z(x, x')$ is dual to the above with $\overrightarrow{I} \rightarrow \overrightarrow{V}$, etc.

3. By examining the input admittance in Eq. (3.3.21b) seen to the left from a finite point ρ in a region extending to the origin $\rho = 0$ in a cylindrical coordinate system, show that the boundary condition for the differential equation (3.2.46b) at $\rho = 0$ is of the limit point type; i.e., the boundary condition is independent of the termination at $\rho = 0$.
4. Calculate by the classical procedure the orthonormal H -mode eigenfunctions $\hat{\psi}_{v\beta}(x)$, $\hat{\psi}_{m\beta}(x)$, $\beta = 1, 2$, for the slab-loaded waveguide defined in Eqs. (3.4.13) and (3.4.14). Start from the general relation in Eq. (3.2.4) satisfied by any two eigenfunctions $f_m(x)$ and $f_n(x)$ with eigenvalues λ_m and λ_n ,

$$(\lambda_m - \lambda_n) \int_{x_1}^{x_2} w f_n^* f_m dx = \left[p \left(f_m \frac{df_n^*}{dx} - f_n^* \frac{df_m}{dx} \right) \right]_{x_1}^{x_2}. \quad (3)$$

When $n \neq m$, vanishing of the right-hand side in Eq. (3) via the boundary condition $p df_i/dx + \alpha_{1,2} f_i = 0$ at $x = x_{1,2}$, with $i = n, m$, implies the orthogonality of the mode set. To find the normalization constant when $n = m$, retain f_m as an eigenfunction with eigenvalue λ_m but treat λ_n as a variable parameter that approaches λ_m (since f_n still satisfies the differential equation (3.2.1), though not the boundary conditions, Eq. (3) remains valid). Evaluate the integral in Eq. (3) when $\lambda_n = \lambda_m$ by applying L'Hôpital's rule to the resulting indeterminate form [see Eqs. (3.2.55)].

5. To achieve a ϕ transmission formulation of a scattering problem in a spherical coordinate system (r, θ, ϕ) , the contour C_θ in Eq. (3.3.43b) is deformed about the singularities of $g_r(r, r'; \lambda_\theta)$ in the complex λ_θ plane. This specifies the λ_θ in terms of the radial eigenvalues, with λ_θ subsequently replaced by λ_r [for the radial domain $0 < r < \infty$, one has $\lambda_r = v_r(v_r + 1)$, $v_r = -\frac{1}{2} + iv_i$, v_i real; see Eq. (3.4.100b)]. The contour C_ϕ is then deformed about the singularities of $g_\theta(\theta, \theta'; \lambda_\phi; \lambda_r)$ in the complex λ_ϕ -plane. For the corresponding eigenvalue in the θ -domain, λ_ϕ replaced by $\hat{\lambda}_\theta$ plays the role of the eigenvalue, with λ_r remain-

ing a fixed parameter. These eigenfunctions may therefore be determined from a characteristic Green's function

$$\left(\frac{d}{d\theta} \sin \theta \frac{d}{d\theta} + v_r(v_r + 1) \sin \theta - \frac{\hat{\lambda}}{\sin \theta} \right) g_\theta(\theta, \theta'; \hat{\lambda}; \lambda_r) = -\delta(\theta - \theta'), \quad (4)$$

wherein v_r is assumed to be specified and $\hat{\lambda}$ is the characteristic parameter.

(a) Show that if λ_r is negative real ($v_r = -\frac{1}{2} + iv_i$, v_i real), then the eigenvalues $\hat{\lambda} = \hat{\lambda}_\mu$ are negative real. Assume this condition in the following.

(b) Show that the mode spectrum for the domain $0 \leq \theta \leq \pi$ is continuous and gives rise to the completeness relation

$$\begin{aligned} \sin \theta' \delta(\theta - \theta') &= \\ &- \frac{1}{2i} \int_{-i\infty}^{i\infty} \mu \frac{P_{v_r}^{-\mu}(\cos \theta) P_{v_r}^{-\mu}(-\cos \theta')}{[\Gamma(v_r - \mu + 1)/\Gamma(v_r + \mu + 1)] \sin(v_r - \mu)\pi} d\mu. \end{aligned} \quad (5)$$

(c) Show that the mode spectrum for the domain $0 < \theta_1 \leq \theta \leq \theta_2 < \pi$ is discrete and gives rise to the completeness relation

$$\begin{aligned} \sin \theta' \delta(\theta - \theta') &= \pi \sum_\mu \frac{\mu}{\sin \mu\pi} \frac{(d/d\theta_2) P_v^\mu(\cos \theta_2)}{(d/d\theta_1) P_v^\mu(\cos \theta_1)} \frac{A(v_r, \mu; \theta, \theta_1) A(v_r, \mu; \theta', \theta_1)}{(\partial^2/\partial\mu\partial\theta_2) A(v_r, \mu; \theta_2, \theta_1)}, \\ (6a) \end{aligned}$$

where μ is imaginary and is determined from a solution of the equation $(\partial/\partial\theta_2)A(v_r, \mu; \theta_2, \theta_1) = 0$, with

$$A(v, \mu; \varphi, \psi) \equiv P_v^\mu(\cos \varphi) \frac{d}{d\psi} P_v^{-\mu}(\cos \psi) - P_v^{-\mu}(\cos \varphi) \frac{d}{d\psi} P_v^\mu(\cos \psi). \quad (6b)$$

These eigenfunctions have vanishing derivatives at $\theta = \theta_{1,2}$.

(d) Repeat for eigenfunctions which vanish at $\theta_{1,2}$.

6. A half-space is bounded by an infinite perfectly conducting plane. In a coordinate system (I) whose z axis is perpendicular to the plane, the equation of the boundary may be described by $\theta = \pi/2$, whereas in a coordinate system (II) whose z -axis lies in the plane, the description is $\phi = 0, \pi$.

(a) Show that the normalized scalar mode functions in System I are:

$$\Phi_i(\theta, \phi) = \frac{1}{N_i} P_n^m(\cos \theta) \begin{cases} \cos m\phi \\ \sin m\phi \end{cases}, \quad (n+m) \text{ odd}, \quad (7a)$$

$$\Psi_i(\theta, \phi) = \frac{1}{N_i} P_n^m(\cos \theta) \begin{cases} \cos m\phi \\ \sin m\phi \end{cases}, \quad (n+m) \text{ even}, \quad (7b)$$

where $0 \leq \theta \leq \pi/2$, $0 \leq \phi \leq 2\pi$, n and m are positive integers (or zero), and

$$N_i^2 = \frac{2\pi}{\epsilon_m} \frac{1}{(2n+1)(n-m)!} (n+m)! \quad (7c)$$

with $\epsilon_m = 1$, $m = 0$, and $\epsilon_m = 2$, with $m \geq 1$.

(b) Show that the normalized scalar mode functions in System II are:

$$\Phi_i(\theta, \phi) = \frac{1}{N_i} P_n^m(\cos \theta) \sin m\phi, \quad 0 \leq \theta \leq \pi, 0 \leq \phi \leq \pi, \quad (8a)$$

$$\Psi_i(\theta, \phi) = \frac{1}{N_i} P_n^m(\cos \theta) \cos m\phi. \quad (8b)$$

7. (a) Use Eqs. (3.5.45) and the formula $D_v(-z) \sim (-z)^v \exp(-z^2/4)$ as $z \rightarrow \infty$ to derive the following uniform asymptotic representation for the parabolic cylinder function $D_v(-\sqrt{2\Omega}x)$, $2v = (\Omega a^2 - 1)$, valid for large Ω , and for all x in the interval $-\infty < x < a$:

$$D_v(-\sqrt{2\Omega}x) \sim \frac{2^{3/4}\pi^{1/2}}{\Omega^{1/12}} \left(\frac{\Omega a^2}{2e}\right)^{\Omega a^2/4} \frac{[\frac{3}{2}\psi(x)]^{1/6}}{[\alpha(x)]^{1/4}} \text{Ai}\{-[\frac{3}{2}\Omega\psi(x)]^{2/3}\}, \quad (9)$$

where $\psi(x) = \int_{-a}^x \sqrt{a^2 - \eta^2} d\eta$ and $\alpha(x) = a^2 - x^2$. Verify that this formula reduces to Eq. (3.5.55a) when $x \ll -a$.

- (b) Use Eq. (9) with $a \rightarrow \infty$ to derive an asymptotic representation valid for large v . By letting Ω take on complex values, show that the resulting formula may be written as

$$D_v(z) \sim \frac{1}{\sqrt[4]{2}} \left(\frac{-v}{e}\right)^{v/2} e^{-z\sqrt{-v}}, \quad |\arg(-v)| < \pi, |v| \rightarrow \infty. \quad (10)$$

8. A uniform plane wave with electric vector parallel to y is incident on an inhomogeneous slab with refractive index $n(x)$. The electric field satisfies the wave equation [see Eq. (1.7.41)]:

$$(\nabla^2 + k_0^2 n^2)E_y = 0. \quad (11)$$

- (a) If the profile is smooth and the inhomogeneity is confined to the interval $0 < x_1 < x < x_2$, show that the first-order reflection coefficient $\bar{\Gamma}(x)$ is given by [see Eq. (3.6.2)]:

$$\bar{\Gamma}(0) = \frac{1}{2} \int_{x_1}^{x_2} \frac{n(x)(dn/dx)}{n^2(x) - \sin^2 \theta} \left(\exp \left[i2k_0 \int_0^x \sqrt{n^2(\eta) - \sin^2 \theta} d\eta \right] \right) dx, \quad (12)$$

where θ is the angle of incidence with respect to the x axis ($\partial/\partial y = 0$).

- (b) If $n = 1 + \Delta$ in the interval, where Δ is very small, show that $\bar{\Gamma}(0)$ is given approximately by:

$$\bar{\Gamma}(0) \approx \frac{1}{2 \cos^2 \theta} \int_{x_1}^{x_2} \frac{d\Delta}{dx} e^{i2k_0 x \cos \theta} dx. \quad (13)$$

State the conditions for the validity of Eq. (13).

9. If the wave in Problem 8 is incident on an inhomogeneous dielectric slab bounded by plane interfaces at $x = 0$ and $x = d$, and if the field solutions inside the slab are assumed to have the form $E_y = \exp[(ik_0 \sin \theta)y]f_{\pm}(x)$, where $f_{\pm}(x)$ are two linearly independent solutions of the x -dependent part of the wave equation, derive exact expressions for the reflection coefficient $\bar{\Gamma}$ and transmission coefficient T .

10. Let $\hat{V}(x)$ satisfy the non-uniform wave equation,

$$\left[\frac{d^2}{dx^2} + \Omega^2 \alpha(x) \right] \hat{V}(x) = 0, \quad (14)$$

where Ω is a large positive parameter.

- (a) Assume that

$$\hat{V}(x) = e^{i\Omega\psi(x,\Omega)}, \quad (15)$$

and derive the differential equation satisfied by \hat{V} . Solve this equation by the method of successive approximations to derive an asymptotic expansion for $\hat{V}(x)$ in inverse powers of Ω .

(b) By an alternative procedure, assume that

$$\hat{V}(x) = \sum_{n=0}^{\infty} \frac{A_n(x)}{(i\Omega)^n} e^{i\Omega\psi(x)}, \quad (16)$$

where A_n and ψ are Ω -independent. Determine ψ and A_n and compare with the procedure in (a) [see also Eq. (1.7.16) and Problem 27 of Chapter 1]. Which procedure is more convenient for determining the asymptotic expansion of $\hat{V}(x)$?

11. The discussion of linear differential equations of higher order is systematized by expressing such equations as a system of first-order differential equations wherein the desired function and its derivatives appear as dependent variables. For example, show that the second-order differential equation (3.5.74) can be written equivalently as in Eq. (3.5.73) (see also Sec. 1.1d),

$$\frac{d}{dx} \Psi(x) = \mathcal{A}(x) \Psi(x), \quad (17)$$

where the wave vector Ψ and the matrix \mathcal{A} have the following representation,

$$\Psi(x) \rightarrow \begin{pmatrix} \hat{V}(x) \\ i\hat{l}(x) \end{pmatrix}, \quad \mathcal{A}(x) \rightarrow \begin{pmatrix} 0 & \omega\mu(x) \\ -\omega\epsilon(x) & 0 \end{pmatrix}. \quad (18)$$

For generality, assume both μ and ϵ to be x -dependent. The solution of Eq. (17) is to be effected subject to the initial condition

$$\Psi(x) = \Psi_0 \text{ at } x = x_0, \quad (19)$$

with the assumption that the $N \times N$ elements of the square matrix $\mathcal{A}(x)$ are real, single-valued, bounded, and integrable in an interval surrounding x_0 .

Show that if a matrix propagator (Green's function) $G(x, x_0)$ satisfies the equations

$$\frac{d}{dx} G(x, x_0) = \mathcal{A}(x) G(x, x_0) \text{ for } x \geq x_0, \quad G(x_0, x_0) = 1, \quad (20)$$

where $\mathbf{1}$ is the unit matrix, then the solution for $\Psi(x)$ is given by

$$\Psi(x) = G(x, x_0) \Psi_0, \quad \Psi_0 \equiv \Psi(x_0). \quad (21)$$

Show that Eq. (20) is solved by the ordered exponential having the series expansion

$$G(x, x_0) = \mathbf{1} + \int_{x_0}^x \mathcal{A}(\xi) d\xi + \int_{x_0}^x d\xi \mathcal{A}(\xi) \int_{x_0}^{\xi} \mathcal{A}(\xi_1) d\xi_1 + \dots \quad (22)$$

Construct the solution for $\Psi(x)$, and discuss the rate of convergence of the solution for various ranges of a parameter ω which may be contained in \mathcal{A} [see Eq. (18)].

12. To construct an alternative solution to the problem posed in Eqs. (17) and (19),[†] introduce via

[†]See H. B. Keller and J. B. Keller, "Exponential-Like Solutions of Systems of Linear Ordinary Differential Equations," *J. Soc. Indust. Appl. Math.*, **10** (1962), p. 246-259. Also I. Kay, "Some Remarks Concerning the Bremmer Series," *J. Math. Anal. Appl.*, **3** (1961), p. 40.

$$\Psi(x) = \mathcal{P}(x)W(x) \quad (23)$$

a non-singular transformation matrix $\mathcal{P}(x)$ chosen so that

$$\mathcal{L} = \mathcal{P}^{-1}\mathcal{A}\mathcal{P} \quad (24)$$

is a diagonal matrix.

(a) If a prime denotes the derivative with respect to x , show that

$$W' = (\mathcal{L} - \mathcal{P}^{-1}\mathcal{P}')W. \quad (25)$$

Show also that if a certain $\mathcal{P} = \mathcal{P}_1$ diagonalizes \mathcal{A} as in Eq. (24), then so does the matrix $\mathcal{P}_1\mathcal{D}$, where \mathcal{D} is a non-singular diagonal matrix. (\mathcal{D} may therefore be chosen to "normalize" the matrix \mathcal{P}_1 , and \mathcal{P} may be written in the form $\mathcal{P} = \mathcal{P}_1\mathcal{D}$.) If \mathcal{D} is to be chosen so that $\mathcal{P}^{-1}\mathcal{P}'$ in Eq. (25) has no diagonal terms, show that

$$\mathcal{D}(x) = \mathcal{D}_0 \exp \left[- \int_{x_0}^x \text{diag. } \mathcal{P}_1^{-1}(\xi) \mathcal{P}_1'(\xi) d\xi \right], \quad (26)$$

where \mathcal{D}_0 is a constant diagonal matrix and $\text{diag. } \mathcal{T}(x)$ denotes the diagonal part of $\mathcal{T}(x)$.

(b) If $\mathcal{A}(x)$ is slowly varying with x , show that W is given approximately by the traveling wave (exponential) solution

$$W(x) \cong \begin{pmatrix} e^{\int_{x_0}^x L_{11}(\xi) d\xi} & 0 \\ \ddots & \ddots \\ 0 & e^{\int_{x_0}^x L_{nn}(\xi) d\xi} \end{pmatrix} W(x_0), \quad (27)$$

where $L_{ii}(\xi)$ are the elements of the matrix $\mathcal{L}(\xi)$.

(c) Returning again to the general case, introduce into Eq. (25) the "traveling wave" transformation

$$W(x) = e^{\int_{x_0}^x \mathcal{L}(\xi) d\xi} Z(x). \quad (28)$$

and show that the wave vector $Z(x)$ is then given by the convergent series [see Eq. (22)]

$$Z(x) = G_M(x, x_0)W(x_0) = \left[1 + \int_{x_0}^x \mathcal{M}(\xi_1) d\xi_1 + \dots \right] W(x_0), \quad (29)$$

where

$$\mathcal{M}(\xi_1) = -e^{-\int_{x_0}^{\xi_1} \mathcal{L}(\xi) d\xi} \mathcal{P}^{-1}(\xi_1) \mathcal{P}'(\xi_1) e^{\int_{x_0}^{\xi_1} \mathcal{L}(\xi) d\xi} \quad (29a)$$

is small when the medium is slowly varying. Show that the resulting solution for $\Psi(x)$ is

$$\Psi(x) = \mathcal{P}(x) e^{\int_{x_0}^x \mathcal{L}(\xi) d\xi} G_M(x, x_0) \mathcal{P}^{-1}(x_0) \Psi_0, \quad (30)$$

where it is recalled that \mathcal{P} has been chosen so that $\text{diag. } \mathcal{P}^{-1}\mathcal{P}' = 0$. Compare this solution with the one in Eq. (23) and discuss its utility.

13. Apply the analysis in Problem 12 to the matrix \mathcal{A} in Eq. (18).

(a) Show that the eigenvalues of the matrix \mathcal{A} are $\pm ik$, $k = \omega\sqrt{\mu\epsilon}$; that a set of eigenvectors is $\begin{pmatrix} \pm i\zeta \\ 1 \end{pmatrix}$, $\zeta = \sqrt{\mu/\epsilon}$; and that a matrix \mathcal{P}_1 which diagonalizes \mathcal{A} is given by

$$\mathcal{P}_1 \rightarrow \begin{pmatrix} i\zeta(x) & -i\zeta(x) \\ 1 & 1 \end{pmatrix}. \quad (31)$$

Show also that to within a constant diagonal matrix, one has $\mathcal{D}(x) = 1\zeta^{-1/2}$, and

$$\mathcal{P}(x) \rightarrow \begin{pmatrix} i\zeta^{1/2} & -i\zeta^{1/2} \\ \zeta^{-1/2} & \zeta^{-1/2} \end{pmatrix}. \quad (32)$$

Then show that the solution for $\Psi(x)$ obtained by setting $\mathcal{M}(\zeta) \approx 0$ in Eq. (30) is given by:

$$\Psi(x) = \frac{1}{2} \begin{pmatrix} i\zeta^{1/2} & -i\zeta^{1/2} \\ \zeta^{-1/2} & \zeta^{-1/2} \end{pmatrix} \begin{pmatrix} e^{-i \int_{x_0}^x k(\xi) d\xi} & 0 \\ 0 & e^{i \int_{x_0}^x k(\xi) d\xi} \end{pmatrix} \begin{pmatrix} -i\zeta^{-1/2} & \zeta^{1/2} \\ i\zeta^{-1/2} & \zeta^{1/2} \end{pmatrix}_{x_0} \begin{pmatrix} \hat{V}_0 \\ i\hat{I}_0 \end{pmatrix}. \quad (33)$$

Compare this result with the WKB solution in Eqs. (3.5.75) and (3.5.76) (with $A, B = \text{constant}$).

(b) Consider the “matched” initial condition, $\hat{V}_0 = \zeta(x_0)\hat{I}_0$, and show that this implies $\hat{V}(x) = \zeta(x)\hat{I}(x)$ to a lowest order of approximation (WKB). By retaining the second term in the series representation of $G_M(x, x_0)$ in Eq. (30), derive a correction to the WKB result and show that it agrees with that obtained from Eq. (3.5.80).

R E F E R E N C E S

1. MORSE, P.M. and H. FESHBACH, *Methods of Theoretical Physics*, Sec. 6.3. New York: McGraw-Hill, 1953.
2. FRIEDMAN, B., *Principles and Techniques of Applied Mathematics*, p. 231. New York: John Wiley & Sons, 1956.
3. MAGNUS, W. and F. OBERHETTINGER, *Formulas and Theorems for the Special Functions of Mathematical Physics*, pp. 16-18, 136. New York: Chelsea Publishing Co., 1954.
4. FRIEDMAN, B., *Principles and Techniques of Applied Mathematics*, pp. 213-250. New York: John Wiley & Sons, 1956.
5. MARCUVITZ, N., “Field representations in spherically stratified regions,” *Comm. Pure and Appl. Math.* 4 (1951), pp. 263-315 (Secs. 3a and 5).
6. LORCH, E. R., *Spectral Theory*, Chapter 4. London: Oxford University Press, 1962. Also I. Stakgold, *Boundary Value Problems of Mathematical Physics*, Vol. I, Chapter 4. New York: Macmillan, 1967.
7. FRIEDLANDER, F. G., “Diffraction of pulses by a circular cylinder,” *Comm. Pure Appl. Math.* 7 (1954), pp. 705-732.
8. CLEMMOW, P.C., “Infinite integral transforms in diffraction theory,” *IRE Trans. on Antennas and Propagation*, AP-7 (1959), pp. S7-11.
9. MAGNUS, W. and F. OBERHETTINGER, *Formulas and Theorems for the Special Functions of Mathematical Physics*, pp. 1, 7, 9, 106, 112; Chapter 4. New York: Chelsea Publishing Co., 1954.

10. ERDELYI, A., W. MAGNUS, F. OBERHETTINGER, and F. TRICOMI, *Higher Transcendental Functions*, Vol. I, pp. 142-144. New York: McGraw-Hill, 1953.
11. KONTOROVITCH, M. J. and N. H. LEBEDEV, "On a method for solution of certain diffraction problems," *J. of Physics (Moscow)* **1** (1939), pp. 229-241.
12. SOMMERFELD, A., *Partial Differential Equations in Physics*, Sec. 20. New York: Academic Press, 1949.
13. WHITTAKER, E. T. and G. N. WATSON, *A Course of Modern Analysis*, Chapter XI. Cambridge, England: Cambridge University Press, 1952.
14. MORSE, P. M. and H. FESHBACH, *Methods of Theoretical Physics*, p. 1073. New York: McGraw-Hill, 1953.
15. LANGER, R. E., "The asymptotic solutions of ordinary linear differential equations of the second order, with special reference to turning points," *Trans. Am. Math. Soc.* **67** (1949), p. 461.
16. ERDELYI, A., "Asymptotic solutions of differential equations with transition points or singularities," *J. of Math. Phys.* **1** (1960), p. 16.
17. OLVER, F. W. J., "Uniform asymptotic expansions of solutions of linear second-order differential equations for large values of a parameter," *Phil. Trans. Roy. Soc. London*, **250A** (1958), p. 479.
18. PIKE, E.R., "On the related-equation method of asymptotic approximation (W. K. B. or A-A Method). 1. A proposed new existence theorem," *Quart. J. Mech. and Appl. Math.* **17** (1964), p. 105.
19. LANGER, R. E., "The asymptotic solution of a linear differential equation of the second order with two turning points," *Trans. Amer. Math. Soc.* **90** (1959), pp. 113-142.
20. KAZARINOFF, N. D., "Asymptotic theory of second order differential equations with two simple turning points," *Arch. for Rat. Mech. and Anal.* **2** (1958-1959), pp. 129-150.
21. MAGNUS, W. and F. OBERHETTINGER, *Formulas and Theorems for the Special Functions of Mathematical Physics*, p. 92. New York: Chelsea Publishing Co., 1954.
22. OLVER, F. W. J., "Uniform asymptotic expansions for Weber parabolic cylinder functions of large orders," *J. Res. NBS*, **63B** (1959), p. 131.
23. BUDDEN, K. G., *Radio Waves in the Ionosphere*, Sec. 21.13. Cambridge, England: Cambridge University Press, 1961.
24. ERDELYI, A. and C. A. SWANSON, "Asymptotic forms of Whittaker's Confluent Hypergeometric functions," *Memoirs of the Am. Math. Soc.*, No. 25, 1957.
25. SLATER, L.J., *Confluent Hypergeometric Functions*, Cambridge, England: Cambridge University Press, 1960.
26. BUDDEN, K. G., *Radio Waves in the Ionosphere*, Sec. 21.15. Cambridge, England: Cambridge University Press, 1961.
27. OLVER, F. W. J., "Error bounds for the Liouville-Green (or WKB) approximation," *Proc. Camb. Phil. Soc.* **57** (1961), pp. 790-810. F. W. J. OLVER, "Error

- bounds for first approximations in turning point problems," *J. Soc. Ind. Appl. Math.* **11** (1963), pp. 748-772. F. W. J. OLVER and F. STENGLER, "Error bounds for asymptotic solutions of second-order differential equations having an irregular singularity of arbitrary rank," *J. SIAM Numer. Anal.* **B2** (1965), pp. 244-249.
- 28. BREMNER, H., "The WKB approximation as the first term of a geometric-optical series," *Comm. Pure and Appl. Math.* **4** (1951), p. 105.
 - 29. RYDBECK, O. E. H., "On the propagation of waves in an inhomogeneous medium," *Trans. of Chalmers Univ. of Technology*, Gothenburg, Sweden, No. 74 (1948).
 - 30. MAGNUS, W. and F. OBERHETTINGER, *Formulas and Theorems for the Special Functions of Mathematical Physics*, p. 4. New York: Chelsea Publishing Co., 1954.
 - 31. EPSTEIN, P. S., "Reflection of waves in an inhomogeneous medium," *Proc. Natl. Acad. Sci. (USA)*, **16** (1930), p. 627.
 - 32. BREKHOVSKIKH, L. M., *Waves in Layered Media*, Secs. 14 and 16. New York: Academic Press (1960).
 - 33. COPSON, E. T., *Theory of Functions of a Complex Variable*, Sec. 8.4. London: Oxford University Press, 1935.